THIRD
INTERNATIONAL
CONFERENCE
ON

STABILITY OF SHIPS AND OCEAN VEHICLES

VOLUME II

STAB'86

22–26

September 1986

GDAŃSK–POLAND

STAB '86

MARIN

Maritiem Research Instituut Nederland
Haagsteeg 2 Postbus 28 6700 AA Wageningen

Third International Conference on Stability of Ships and Ocean Vehicles

22-26 September 1986
Gdańsk - Poland

Volume II

C O N T E N T S

Third International Conference on Stability of Ships and Ocean Vehicles, Gdańsk, Sept. 1986

STAB'86

SHIP MOTION SIMULATION IN A SEAWAY USING DETAILED HYDRODYNAMIC FORCE COEFFICIENTS

H. Böttcher

ABSTRACT

A model for simulating large amplitude ship motions in a seaway in 6 degrees of freedom is presented. It takes into account:

Froude-Kriloff forces and moments, using the actual waterline along the hull

Raditation and diffraction forces including memory effects and viscous effects especially at bilge keels

Autopilot settings, steering characteristics and propeller action and control

Forces and moments due to wind

Forces and moments due to internal fluid motion in tanks

After deriving rigid-body motion equations suitable for large motion amplitudes, methods for the determination of Froude-Kriloff forces based on previously determined tables are presented. A unique method is developed for the determination of hydrodynamic diffraction and radiation forces. It is based on higher-order differential equations relating relative motion between the water and the ship sections to the section forces.

1. INTRODUCTION

Our objective is simulating rolling motions of a ship in irregular seas with sufficient accuracy to be able to assess the safety against capsizing in a natural seaway compared to other ships without the need for model experiments. As rolling motion is coupled to some extent with all other ship motions, we think it necessary to use a simulation model for all 6 degrees of freedom of rigid-body motion. This model must include all of the major forces acting upon the ship, such as hydrostatic and hydrodynamic forces, rudder and propeller forces, forces due to wind, and forces due to internal fluid motion in tanks. Obviously the calculation of all these forces cannot be covered here. Particular attention will therefore only be given to setting up the equations of motion and calculating hydrodynamic forces.

2. COORDINATE SYSTEMS

We shall use two coordinate systems; one is fixed to the earth and points in it are described by the vector $\underline{\xi}$; the other is fixed to the ship, and points are described by the vector $\underline{x}$. Conversions between the two coordinate systems can be made by the following equation:

$$\underline{\xi} = T \cdot \underline{x} + \underline{\xi}_o \qquad (1)$$

T is a transformation matrix, which incorporates the rotation of the ship relative to the earth coordinate system, and $\underline{\xi}_o$ is the position of the ship coordinate system in the earth coordinate system.

The following conventions will be used in this paper: a vector will be denoted by an underscore; vectors in the earth coordinate system have an index ξ; vectors in the ship coordinate system are without index; an index G indicates, that a vector is expressed relative to the centre of gravity of the ship.

3. EQUATIONS OF MOTION

The momentum $\underline{b}_\xi$ can be written as:

$$\underline{b}_\xi = (\dot{T} \cdot \underline{x}_o + \dot{\underline{\xi}}_o) \cdot m \qquad (2)$$

where $\underline{x}_o$ are the coordinates of the centre of gravity and m is the ship's fixed mass. The time derivative of $\underline{b}_\xi$ is related to the

force $\underline{f}$ acting upon the ship by:

$$\dot{\underline{b}}_I = T \cdot \underline{f} \qquad (3)$$

A similar equation exists for the angular momentum with respect to the centre of gravity $\underline{h}_{oI}$:

$$\underline{h}_{oI} = T \cdot \Theta_o \cdot T^{-1} \cdot \underline{\omega} \qquad (4)$$

$$\dot{\underline{h}}_{oI} = T \cdot \underline{d} - (T \cdot \underline{x}_o) \times \dot{\underline{b}}_I \qquad (5)$$

Here $\underline{d}$ is the moment and Θ_o is a matrix containing the moments of inertia. $\underline{\omega}$ is a vector, the components of which are the three rotational velocities.

The equations for the momentum and the angular momentum (2 and 4), derivated by time, can be combined with equations 3 and 5 to yield:

$$(\dot{T} \cdot \underline{x}_o + \ddot{\underline{x}}_o) \cdot m = T \cdot \underline{f} \qquad (6)$$

$$(\dot{T} \cdot \Theta_o \cdot T^{-1} + T \cdot \Theta_o \cdot \dot{T}^{-1}) \underline{\omega} + T \cdot \Theta_o \cdot T^{-1} \cdot \dot{\underline{\omega}} =$$

$$T \cdot \underline{d} - (T \cdot \underline{x}_o) \times (\ddot{T} \cdot \underline{x}_o + \ddot{\underline{x}}_o) \cdot m \qquad (7)$$

These equations constitute a system of 6 equations for the accelerations in the 6 degrees of freedom.

These equations cannot be solved as they are, because the forces $\underline{f}$ and moments $\underline{d}$ contain terms depending on accelerations. We have to split up the forces and moments $\underline{f}$ and $\underline{d}$ into 2 parts, one containing accelerations, the other not:

$$\underline{f} = F_1 \cdot \ddot{\underline{x}}_o + F_2 \cdot \dot{\underline{\omega}} + \underline{f}_s \qquad (8)$$

$$\underline{d} = D_1 \cdot \ddot{\underline{x}}_o + D_2 \cdot \dot{\underline{\omega}} + \underline{d}_s \qquad (9)$$

F_1, F_2, D_1, and D_2 are 3x3-matrices. $\underline{f}_s$ and $\underline{d}_s$ contain all forces and moments which do not depend on accelerations.

4. FORCES AND MOMENTS

The following components of the forces and moments are included in the simulation model:

- Forces resulting from the ship's weight
- Froude-Kriloff forces
- Radiation and diffraction forces
- Propeller force
- Rudder forces
- Forces due to wind
- Forces due to internal fluid motions

The forces and moments due to internal fluid motions in tanks are treated in the conference paper by F. Petey. In the following I will restrict myself to dealing with the calculation of Froude-Kriloff and radiation and diffraction forces. The other forces are calculated according to normal practice. For the calculation of rudder forces I refer to a paper by Söding [1].

3.1 Froude-Kriloff Forces and Moments

Froude-Kriloff forces are those which would act on the ship if the water pressure was not disturbed by the ship's presence. To compute them approximately we do not use the actual pressure distribution. Instead we perform hydrostatic calculations up to a corrected waterline, approximated by a straight line in the section planes used for the calculation (Figure 1).

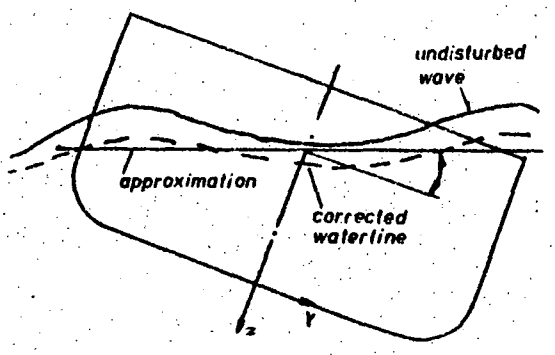

Figure 1:
Ship section, showing actual, corrected and approximated waterline

During the simulation the position and inclination of this effective waterline is calculated for a number of sections, and section area and righting moment are interpolated from a table, previously calculated for different depths of immersion and angles of inclination of the waterline.

3.2 Radiation and Diffraction Forces

The radiation and diffraction forces are determined as a function of relative motion between ship and water. A method similar to the strip method is used, which, however, takes account of non-linearities.

Let us first look at the two-dimensional flow around a partly submerged ship's section. In this case the pressure distribution can be determined by potential theory, the flow being represented by a distribution of time periodic sources and sinks satisfying the free surface condition. The relative motions between ship and water in the transverse and vertical directions and the section rotation are combined to a vector $\underline{u}_k$. A vector $\underline{f}_k$ is used to represent the section force and moment, which are obtained by integrating the pressure distribution along the section contour. The following differential equation describes the relationship between the force $\underline{f}_k$ and the motion $\underline{u}_k$ for time-harmonic motions:

$$\underline{f}_k = -\left(M\frac{d^2}{dt^2} + N\frac{d}{dt}\right)\cdot\underline{u}_k = -\frac{d}{dt}\left(M\cdot\dot{\underline{u}}_k + N\cdot\underline{u}_k\right) \qquad (10)$$

In this equation M is a 3x3-matrix of added mass, and N is a 3x3damping-matrix. The right part of the equation is equal to the middle part, if M and N are constant over time. However, we want to determine M and N as functions of the motion frequency and of the actual time dependent immersion of the section. Comparisons with experiments have shown that one can normally obtain good results using the right part of the equation. Only in those cases, where a rapid reduction of immersion, entailing flow separation, occurs, the middle part of the equation should be used.

An irregular seaway can be thought to consist of many regular waves of different frequencies. If the ship's response is a linear function of excitation,the response due to different regular waves can be calculated seperately and added to yield the total response (superposition). We cannot use superposition, though, because we want to include nonlinear wave and motion effects. It is therefore imperative to substitute added mass and damping, which depend on frequency, by quantities, which are independent of frequency. To that end we use a higher order differential equation to describe the relationship between motion and force:

$$\sum_{k=0}^{L} A_k\cdot\dot{\underline{u}}_k^{(k+1)} = \sum_{k=0}^{L} B_k\cdot\underline{f}_k^{(k)} \qquad (11)$$

A_k and B_k are 3x3-matrices depending on the immersed shape of the section but not on frequency. The superscripts denote time derivatives.

For time-harmonic motions of arbitrary frequency we want to express the same relationship by equations 10 and 11. It can be shown, that this is the case, if the following equation is valid for all frequencies ω:

$$\left[\sum_{k=0}^{L} B_k\cdot(i\omega)^k\right]^{-1}\cdot\sum_{k=0}^{L} A_k\cdot(i\omega)^k = -M(\omega) + \frac{i}{\omega}N(\omega) \qquad (12)$$

To illustrate the meaning of this rather abstract equation, I shall write it in another way for L = 3:

$$\frac{A_0 + A_1 i\omega + A_2(i\omega)^2 + A_3(i\omega)^3}{B_0 + B_1 i\omega + B_2(i\omega)^2 + B_3(i\omega)^3} = -M + \frac{i}{\omega}\cdot N$$

Thus A_k and B_k are the coefficients of a ratio-of-polynomials approximating M and N. A_k and B_k must be determined in such a way, that M and N are approximated with sufficient accuracy, while using as few coefficients as possible. Figures 2 and 3 show an example of added mass and damping for heaving motion compared to their approximation with L = 4.

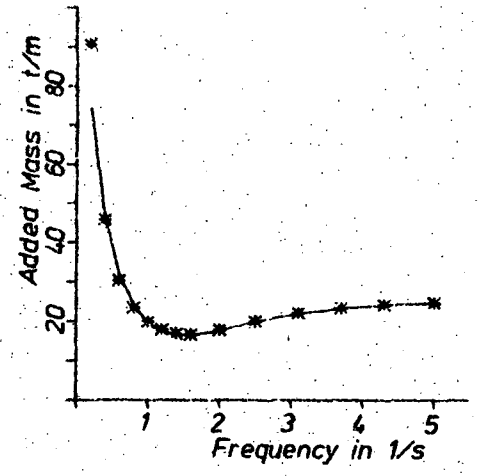

Figure 2:
Added mass for heaving motion
-- calculated by potential theory
* approximated by A and B for L = 4

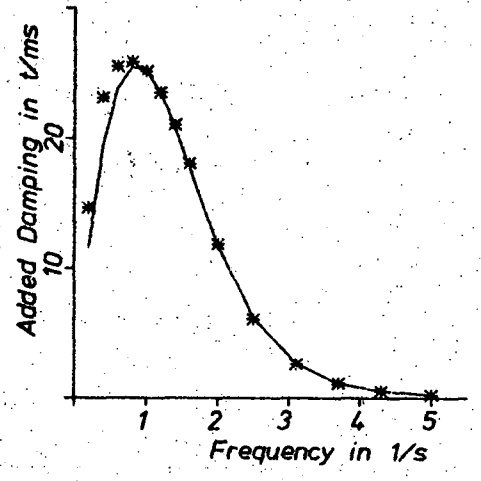

Figure 3:
Damping for heaving motion
-- calculated by potential theory
* approximated by A and B for L = 4

Matrices A_w and B_w will be calculated for a number of sections and for different depths of immersion and angles of inclination. During the simulation the matrices will be interpolated for the actual immersion.

With the matrices A and B we can calculate the forces due to the two-dimensional motion of a section. What we want, though, is to calculate the forces on a ship, i.e. a three-dimensional body. Therefore we must take into account the flow along the ship's length. This is done in analogy to the strip method. We treat each section separately, but substitute partial time derivatives by substantial derivatives:

$$\sum_{k=0}^{L} \left(\frac{\partial}{\partial t} - v\frac{\partial}{\partial x}\right)^{k+1} (A_w \cdot \dot{\underline{u}}_w) = \sum_{k=0}^{L} \left(\frac{\partial}{\partial t} - v\frac{\partial}{\partial x}\right)^{k} (B_w \cdot \underline{f}_w) \qquad (13)$$

v is the ship's speed.
By using this equation we include the effect of previous interaction between ship and water at sections ahead of the currently regarded section.

To solve this equation it is integrated substantially L times. A substantial integral is meant to be the inverse of a substantial derivative $(\partial/\partial t - v\partial/\partial x)$. It is indicated by a negative superscript.

$$\sum_{k=0}^{L} \left(\frac{\partial}{\partial t} - v\frac{\partial}{\partial x}\right)^{k+1-L} (A_w \cdot \dot{\underline{u}}_w) = \sum_{k=0}^{L} \left(\frac{\partial}{\partial t} - v\frac{\partial}{\partial x}\right)^{k-L} (B_w \cdot \underline{f}_w) \qquad (14)$$

The equation can be transformed to yield an expression for $\underline{f}_w$:

$$\underline{f}_w = B_L^{-1} \cdot \left(\sum_{k=0}^{L} (A_w \cdot \dot{\underline{u}}_w)^{(k+1-L)} - \sum_{k=0}^{L-1} (B_w \cdot \underline{f}_w)^{(k-L)}\right) \qquad (15)$$

For L = 2 this can be written as:

$$\underline{f}_w = B_2^{-1}\left((A_0 \cdot \dot{\underline{u}}_w)^{(-2)} + (A_1 \cdot \dot{\underline{u}}_w)^{(-1)} + (A_2 \cdot \dot{\underline{u}}_w)^{(0)} - (B_0 \cdot \underline{f}_w)^{(-2)} - (B_1 \cdot \underline{f}_w)^{(-1)}\right) \qquad (16)$$

On the right hand side of the equation there are a number of substantial integrals of $(A_w \cdot \dot{\underline{u}}_w)$ and $(B_w \cdot \underline{f}_w)$ (the terms with negative superscripts). These are calculated by numerical integration. Included in the term $(A_2 \cdot \underline{u}_w)^{(1)}$ is the acceleration $\ddot{\underline{u}}_w$. After transforming $\dot{\underline{u}}_w$ into the earth coordinate system and integrating $\underline{f}_w$ over the ships length expressions in the form of equations 8 and 9 can be found for the radiation and diffraction forces and moments. After adding all other forces and inserting these values into equations 6 and 7 we obtain a set of 6 simultaneous ordinary differential equations, which can be solved to yield the accelerations in the 6 degrees of freedom, which, in turn, are integrated numerically to yield the velocities and position of the ship.

5. FIRST RESULTS

Preparing the input data for our simulation program is a rather lengthy and difficult task, especially calculating the matrices A and B. At the moment we are developing methods to help us prepare the data in much less time than previously needed. So far, we have only done simulations using a limited set of data for one ship, with only 5 sections for the calculation of Froude-Kriloff and radiation and diffraction forces and 4 different depths of immersion.

Figures 4 and 5 show a comparison of transfer functions for heave and pitch calculated by simulation with results of strip method calculations for a ship in head waves. Agreement is fair for pitch, but less satisfactory for heave. We hope to obtain better results using much more detailed data.

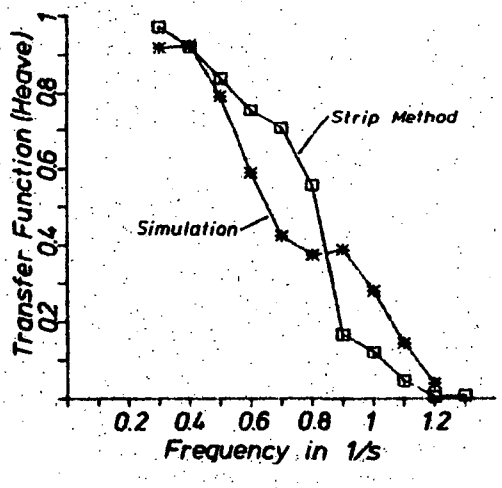

Figure 4:
Transfer functions for heaving motion for a ship in head waves, Fn = 0.18

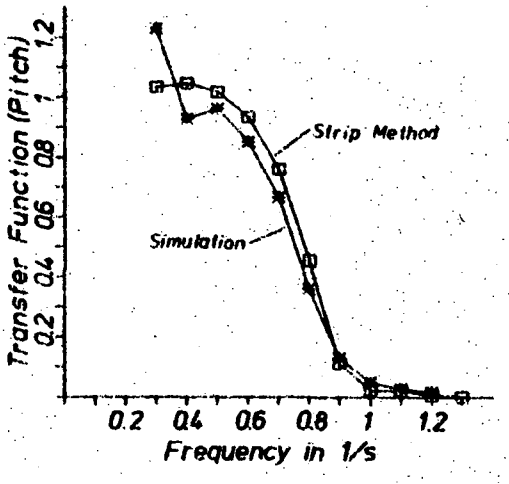

Figure 5:
Transfer functions for pitching motion for a ship in head waves, Fn = 0.18

REFERENCES

[1] H. Söding, Prediction of Ship Steering Capabilities, Schiffstechnik, Vol. 29, 1982

AUTHOR:

Harald Büttcher
Institut für Schiffbau
University of Hamburg
West Germany

Third International Conference on Stability of Ships and Ocean Vehicles, Gdańsk, Sept. 1986

STAB'86

FURTHER IMO ACTIVITIES IN THE DEVELOPMENT OF INTERNATIONAL REQUIREMENTS FOR THE STABILITY OF SHIPS

P. Plasse; A.A. Petrov

ABSTRACT

In the paper presented at the Second International Conference on Stability of Ships and Ocean Vehicles in Tokyo (STAB '82) a brief description of the work of the International Maritime Organization (IMO) in respect of development of international requirements and recommendations for intact and damage stability of various types of ships was given. The paper summarized the work of the Organization on the subject for the period 1962 - 1982. That work resulted in the formulating of such requirements for a wide range of ships which were included in IMO conventions, codes, guidelines and recommendations.

At present, new investigations and research programmes on intact stability employing the best available hydrodynamic, mathematical and computational techniques have deepened knowledge about a number of phenomena affecting stability of ships. It was, therefore, generally recognized that a scientific approach in development of future stability criteria should be adopted, based on the results of the study of such phenomena. Furthermore, some international requirements already developed within IMO still have areas where uniform interpretations of stability criteria are still to be developed.

This paper presents a brief account of work in respect of further development of intact and damage stability requirements carried out within IMO by its Sub-Committee on Stability and Load Lines and on Fishing Vessels Safety since 1982. Finally the paper will be expanded to outline in general the current work of the Sub-Committee on the subject.

1 PREAMBLE

With one of the main objectives to facilitate co-operation among governments on technical matters affecting international shipping in order to achieve the highest practical standards of maritime safety and navigation the International Maritime Organization since its inception took the task of developing the internationally agreed standards of stability and subdivision.

Based on statistical analyses of collated stability data for capsized ships and for ships with satisfactory stability, stability criteria for passenger and cargo ships and fishing vessels were elaborated as a first step. These criteria were used as a basis in further work on stability requirements for other types of ships, modification of which were made to take account of specific design and operation features. At present recommendations on intact stability are developed for the following types of ships:

- passenger ships
- cargo ships
- fishing vessels
- dynamically supported craft
- mobile offshore drilling units
- offshore supply vessels
- special purpose ships

Subdivision and damage stability requirements were first introduced for passenger ships in the 1948 SOLAS Convention and then readopted by the 1960 SOLAS Convention [1] and the 1974 SOLAS Convention [2]. Extensive work on development of subdivision and damage stability requirements for other types of ships has been continued until now. For their development different philosophies were accepted to take account of specific design features and conditions of operations of ships, e.g. in the case of oil and chemical tankers, and gas carriers the main idea was to provide the ship with the ability to remain afloat after damage in order to prevent massive spill of cargo and avoid pollution of the sea etc. At present, types of ships as indicated above and some others such as tankers, chemical tankers and gas carriers are provided with relevant subidivision and damage stability requirements which are stated in various conventions, codes, recommendations and guidelines.

The detailed description of IMO's activity in development of stability requirements until 1982 was reflected in the paper presented to the Second Conference on Stability of Ships and Ocean Vehicles held in Tokyo in 1982. With a view to further promoting the highest possible level of safety of ships being in balance with economic interests and design needs, IMO has continued the work on the stability through its Sub-Committee on Stability and Load Lines and on Fishing Vessels Safety. The following sections reflect the outcome of the work on the subject within that Sub-Committee.

2 NEW DEVELOPMENTS RELATING TO INTACT AND DAMAGE STABILITY

2.1 Intact and damage stability of special purpose ships

The Code of Safety for Special Purpose Ships [3] includes requirements for ships engaged in research, expeditions and surveys, ships for training of marine personnel, whale and fish factories not engaged in catching, etc. and carrying on board more than 12 special personnel including passengers. As special personnel are expected to be able bodied with a fair knowledge of the layout of a ship and have received some training in safety procedures and the handling of the ship's safety equipment, the special purpose ships on which they are carried need not be considered or treated as passenger ships. In developing the safety standards for this type of ship, account was taken of the number of special personnel being carried and the design and size of the ship.

The intact stability of special purpose ships under 100 metres in length should comply with the provisions specified in resolution A.167(ES.IV) [4] except that in respect to ships of design and characteristics similar to offshore supply vessels alternative criteria established for latter ships in the Guidelines for the Design and Construction of Offshore Supply Vessels [5] may be used where relaxation from requirements of minimum angle of heel at which the maximum righting arm occurs is compensated by increasing the corresponding area under the curve of righting levers up to that angle.

The intact stability of special purpose ships of 100 metres in length and over should be to the satisfaction of the administration.

The subdivision and damage stability of special purpose ships is mainly governed by the number of special personnel. In general, for ships carrying not more than 50 special personnel a single compartment, except machinery space, has to be assumed damaged and for ships carrying more than 50 but not more than 200 special personnel the damage should be assumed to occur anywhere in its length between transverse watertight bulkheads. For ships carrying more than 200 special personnel the subdivision and damage stability requirements for passenger ships carrying that number of passenger should apply.

2.2 Intact stability of pontoons

To provide sufficient safety for pontoons especially those engaged in ocean transportation, there was an agreement to develop internationally agreed requirements for intact stability of pontoons. Although some administrations use certain stability requirements at present there was no sufficient knowledge in order to set a single standard. Furthermore, there may be a need for operational experience including research data to cover special cargo handling operations especially in case of crane pontoons. As it was felt to be premature to develop a single criterion to be used for the assessment of intact stability of pontoons, Interim Guidelines on Intact Stability Requirements for Pontoons [6] were set up which included a compilation of the national practices of several countries.

These guidelines were issued for the information of the administrations concerned with the intact stability of pontoons and provide only general guidance and do not contain all specific requirements of those administrations whose criteria were included in the guidelines. The parameters in the various criteria are applicable to pontoons in unrestricted service. Less stringent requirements may be considered for pontoons in protected waters.

The guidelines also contain the provisions relating to the ways to present typical stability information and performance of calculations.

In general, for the purpose of guidelines, a pontoon is considered to be non self-propelled, normally unmanned, carrying only deck cargo and having no hatchways in the deck except small manholes closed with gasketed covers.

As to the national stability criteria for pontoons specified in the guidelines, the similarities of national practice are easily

identified. Differences may be necessary to take account of severity of service. It was an intention of the guidelines that the administration should use a criterion that best suits the design and modes of operation of the pontoon under consideration.

Further work is envisaged to be undertaken to establish a single criterion for intact stability of pontoons based on evaluation of criteria specified in the guidelines.

2.3 Stability of ships in breaking waves

The danger of the effect of breaking waves on safety of small ships is generally recognized, in particular for ships operating in coastal waters. The extension of range of stability, especially in the case of ships of less than 45 metres in length was believed to be a measure to prevent capsizing in breaking waves from the side. As a result of deliberations within the Sub-Committee it was recommended that administrations should consider addressing this effect in their national standards where ships are known to operate in waters subject to breaking waves of predictable frequency.

2.4 Weather criterion for passenger and cargo ships

The concept of weather criterion which takes account of the effect of a severe wind and rolling was introduced in stability requirements for such types of ships as fishing vessels, dynamically supported craft, MODU's. In pursuance of the task to improve adopted stability criteria for passenger and cargo ships specified in resolution A.167(ES.IV) the studies were undertaken with a view to developing a weather criterion for passenger and cargo ships. For this purpose a comparison of results obtained by applying criteria of resolution A.167(ES.IV) and the weather criterion according to various national methods of calculations to several ship types was carried out to produce a method of calculating the effect of wind and rolling.

Eventually, a draft weather criterion was proposed and test calculations were carried out. In general the calculations showed that the proposed criterion when used in conjunction with the requirements of resolution A.167(ES.IV) increased the stability requirements for ships with a large windage area.

The final recommendation on weather criterion [7] adopted by the Assembly in November 1985 which takes account of a severe wind and rolling is proposed for passenger and cargo ships of 24 metres in length and over. It supplements the stability requirements of resolution A.167(ES.IV) specified for ships of under 100 metres in length. As far as passenger and cargo ships of more than 100 metres in length are concerned the weather criterion should apply in addition to other appropriate stability criteria to the satisfaction of the administration.

The recommended weather criterion stipulates that under the specified weather conditions the stability of ships should be such as to withstand the combined effect of beam wind and rolling.

The weather criterion as adopted is given in the figure.

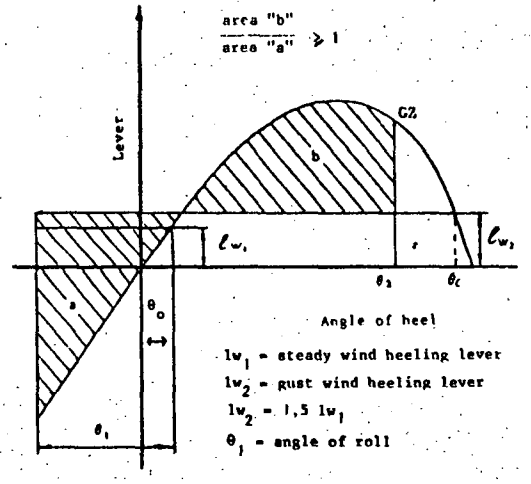

Figure

The criterion is applicable for each standard condition of loading and takes account of the free surface effect specified in appendix I to resolution A.167(ES.IV).

To avoid excessive resultant angles of heel when applying the weather criterion attention should be paid to the effect of steady wind. Although the value of angle of heel under action of steady wind is proposed to be limited to a certain angle to the satisfaction of the administration, as a guide a certain angle is suggested.

The present weather criterion, as developed for passenger ships and cargo ships is also recommended for application to fishing vessels of 45 metres in length and over in unrestricted service.

2.5 Information on the effect of flooding

In accordance with regulation II-1/23 of the 1974 SOLAS Convention as amended passenger ships shall be provided with damage control plans and a booklet containing information relating to the plans and arrangements for the correction of list due to flooding. Resolution A.515(13) adopted by the Assembly in 1983 contains inter alia draft regulation on damage control plans for dry cargo ships to be included in the future amendments to the 1974 SOLAS Convention. During the discussion within the Sub-Committee opinions were expressed that in addition to damage control plans damage stability information could be useful. The purpose of such information would be to enable the master to investigate the survival capability of the ship in the actual loading condition in the case of damage. However it was evident that in order to avoid misleading the master the information should not contain any specific instructions or recommendations.

In pursuance of this, Guidelines for the Preparation of Information on the Effect of Flooding to be provided to Masters of Dry Cargo Ships [8] were developed. These guidelines are intended for the use of adminstrations to the extent they consider necessary and for assistance to the master in exercising his judgement in case of serious flooding of the ship, to make him aware of the capabilities of the ship.

3 CURRENT WORK ON INTACT AND DAMAGE STABILITY

3.1 Improvement of stability criteria

Following the adoption in mid-70 of the long-term programme on improvement of stability criteria a review in recent years of theoretical work and analysis of the results of model tests carried out by countries concerning the capsizing phenomena made it possible to formulate an approach in respect of the further work on improvement of stability criteria and development of new stability criteria. It required to identify and define a few of the most dangerous situations of all possible situations which may occur during the life of a ship. The possible situations to be concentrated on in the work were defined as follows:

.1 ship in beam seas - severe wind and rolling including effect of shipping water on deck and other possible external forces;

.2 ship in following seas - pure loss of stability, parametric rolling and broaching including possible external forces such as water on deck etc.

For the above situations it is envisaged to develop mathematical models and perform systematic calculations upon which probabilistic stability criteria should be developed. For this purpose the results of analysis of casualty records and model tests should be taken into consideration.

The discussion within the Sub-Committee gave evidence that close international co-operation in research efforts would be more effective and would shorten the time to achieve the goal.

3.2 Stability of ships in following waves

Having finalized the development of the weather criterion for passenger and cargo ships, the Sub-Committee gave as a part of a long-term programme, further consideration to the subject of stability of ships in following waves. The opinion was expressed of the possibility of combining a new criterion for ships in following waves with the weather criterion.

To consider the capsizing of ships in following seas three modes leading to capsizing were identified to be analysed:

.1 pure loss of intact stability due to a wave crest located amidships;

.2 parametric rolling due to a periodic change in ship's stability in relation to wave frequency and ship's speed;

.3 broaching due to the loss of directional control with the waves overtaking the ship from the stern.

It was agreed to proceed with developing methods of analysis for each of these modes of capsizing followed by a detailed analysis. After each of the modes of a capsizing ship have been analysed efforts should be made to develop a single capsizing criterion or criteria.

Presently, the results of tests carried out by countries justify the recommendation that the still water righting arm curve is most suitable for a comparison in dealing with all types of dynamic phenomena.

3.3 Stability information for the master

The International Convention on Safety of Life at Sea, 1974 and the International Convention on Load Lines, 1966 [9] for passenger and cargo ships and the Torremolinos International

Convention on Safety of Fishing Vessels, 1977 [10] for fishing vessels provide provision to the effect that the master of the ship shall be supplied with information to enable him by rapid and simple processes to assess with ease and certainty the stability of a ship under varying conditions of service. This information shall be kept on board for ready access at all times and be subject to inspection with a view to keep it amended, if necessary.

Furthermore, the administrations were provided with guidance on the scope of data to be included in stability information. This guidance is contained in the annex to resolution A.167 (ES.IV) (for passenger and cargo ships) and resolution A.168 (ES.IV) [11] (for fishing vessels) which was later included in guidance on stability information contained in recommendation 4 of attachment 3 to the Final Act of the International Conference on Safety of Fishing Vessels, 1977. The application of these guidances and considerations of national practices on presentation of intact stability information proved the views that the information as outlined in the above documents providing the master with the most essential data should be simplified as much as possible so that the master can estimate with minimum expendure of time whether the stability of a ship is sufficient. To fulfil the task further work on information for the master on intact stability is envisaged to be undertaken by the Sub-Committee on the following:

.1 the table of contents of information desired for intact stability;

.2 method of special quick appraisal of intact stability of a ship suitable for inclusion in the stability information;

.3 the use of on-board computers for quick appraisal of stability by the master.

3.4 Standards of residual damage stability for passenger ships

Standards of residual damage stability have been defined for a number of types of ships in various codes and guidelines (oil and chemical tankers, gas carriers, offshore supply vessels, etc.) whereas such standards are not established for passenger ships. The experience of applying the provisions of regulation II-1/8 of the 1974 SOLAS Convention as amended revealed the need to develop a guidance for the administrations on a minimum acceptable standard of residual stability after damage for passenger ships.

A draft interpretation was developed specifying the stability criteria appropriate in determining the adequacy of the residual stability after damage. These criteria are given for both the intermediate and final stages of flooding after equalization. The discussion within the Sub-Committee demonstrated a wide range of opinions on the factors to be taken into account in the development of appropriate residual stability standards. The importance of any stability standard which may be adopted in relation to the economic and commercial design of passenger ships initiated the studies of the effect of various proposed criteria on typical ships. This would require to take into consideration the effect of the application of the proposed criteria on critical ship design, the need to relate the basic philosophy of passenger ship survival with the differing philosophies for other types of ships, effect of such factors as application of passenger distribution moment and one-sided lifeboat deployment etc. The results of investigations of the above are subject to further consideration within the Sub-Committee.

3.5 Damage stability of dry cargo ships

As it was mentioned the first internationally agreed damage stability requirements for passenger ships were introduced in the 1948 SOLAS Convention.

Since then the damage stability requirements for most types of ships have been developed and included in various conventions, codes and guidelines.

Due to other committments the Sub-Committee could only recently concentrate on the development of subdivision and damage stability requirements for dry cargo ships including ro-ro ships. The probabilistic concept of survival was taken as a basis for elaborating such requirements. The work to be undertaken by the Sub-Committee is to carry out sample calculations in accordance with the proposed draft probabilistic method for a range of ship types and sizes with a view to determining a preferred level of survival capability. This draft method proposes inter alia that the calculations should be made with the assumption that the ship is regarded as surviving flooding with certain probability if certain damage stability criteria, which are specified in the draft method, are met. For this purpose the work is also envisaged to be undertaken on factor "s" which evaluates the effect of freeboard, stability and heel in the final flooding condition.

REFERENCES

[1] International Conference on Safety of Life at Sea, 1960, including the International Convention for the Safety of Life at Sea, 1960*.

[2] International Conference on Safety of Life at Sea, 1974, including the International Convention for the Safety of Life at Sea, 1974 as amended in 1981 and 1983*.

[3] Code of Safety for Special Purpose Ships (resolution A.534(13))*.

[4] Recommendation on Intact Stability for Passenger and Cargo Ships under 100 Metres in Length (resolution A.167(ES.IV) as amended by resolution A.206(VII))*.

[5] Guidelines for the Design and Construction of Offshore Supply Vessels (resolution A.469 (XII))*.

[6] Interim Guidelines on Intact Stability Requirements for Pontoons (MSC/Circ.348).

[7] Recommendation on a Severe Wind and Rolling Criterion (Weather Criterion) for the Intact Stability of Passenger and Cargo Ships of 24 Metres in Length and Over (resolution A.562(14))*.

[8] Guidelines for the Preparation of Information on the Effect of Flooding to be Provided to Masters of Dry Cargo Ships (MSC/Circ.434).

[9] International Conference on Load Lines, 1966 including the International Convention on Load Lines, 1966*.

[10] International Conference on Safety of Fishing Vessels, 1977, including the Torremolinos International Convention for the Safety of Fishing Vessels, 1977*.

[11] Recommendation on Intact Stability of Fishing Vessels (resolution A.168(ES.IV))*.

---

* Available from the IMO Publications Section in English, French and Spanish.

The following internal IMO documents used as references can be examined at the IMO library:

Reports of the working group on intact stability:

SLF 28/WP.4, SLF 28/WP.4/Add.1, SLF 28/WP.4/Add.2, SLF 29/WP.7, SLF 30/WP.7, SLF 30/WP.7/Add.1.

Reports of the Sub-Committee on Stability and Load Lines and on Fishing Vessels Safety:

SLF 28/13, SLF 29/15, SLF 30/18.

4069Y

FERNANDO PLAZA, a Spanish national, graduated in naval architecture and marine engineering from the Superior Technical School at Madrid University. He then entered Lloyds Register of Shipping as a Ship Surveyor and after some years he joined the International Maritime Organization (IMO) in 1975. He is presently Head of the Sub-Division for Technology and Senior Deputy Director of the Maritime Safety Division of IMO.

ALEXANDER A. PETROV is a Technical Officer of the Maritime Safety Division of IMO (International Maritime Organization) and is the Secretary of the Sub-Committee on Stability and Load Lines and on Fishing Vessels Safety. He graduated in naval architecture in 1969 and started work as a naval architect at a shipyard in Leningrad. Before joining IMO in 1982, he held a position as a Senior Surveyor with the USSR Register of Shipping.

Third International Conference on Stability of Ships and Ocean Vehicles, Gdańsk, Sept. 1986 STAB'86

UTILIZATION OF PHOTOGRAMMETRY IN OBTAINING HULL OFFSETS FOR INTACT STABILITY CALCULATIONS

R. Latorre; A. Suda; C. Mugnier

ABSTRACT

The development of computer programs such as the Ship Hull Characteristics Program (SHCP) has automated the calculation of ship stability. Now the most time-consuming task is the development of a suitable table of hull offsets. The present paper describes the results from using a photogrammetry system to obtain the hull offsets of a large ship trawler.

When the hull plans are available it is fairly straightforward. But when the plans are not available, direct or indirect measurements to obtain the offsets are necessary. In this paper the use of optical imaging from overlapping photographs called "photogrammetry" is used to otain the offsets of a large Gulf of Mexico shrimp trawler hull for the stability calculations. The hydrostatic calculations results are summarized along with the results from the inclining experiment.

This system using a stereo planigraph allows the offsets to be easily obtained for the stability calculation.

INTRODUCTION

The development of computer programs such as the Ship Hull Characteristics Program (SHCP) has automated the calculation of ship stability. Now the most time-consuming task is the development of a suitable table of offsets.

When plans are available a digitizer table can be used. In the case of incomplete or missing plans, direct or indirect hull measurements are necessary. Even for small boats direct measurements can be difficult and time consuming. The use of optical imaging from overlapping photographs taken from different positions has been used for many years to produce accurate topographic maps. This technique called "Photogrammetry" has been proposed and used in a number of marine applications /1//2/. Since the photographs can "capture" any size vessel, photogrammetry is an extremely flexible technique.

On the Gulf Coast a large number of fishing vessels are outside the U. S. Coast Guard inspection. In many cases they are owner built and operated so the hull plans are incomplete. The vessels are often launched and operated without routine stability calculations. Fortunately the fishermen have gained enough experience that vessel capsize is a rare event when the vessels are operated in the Gulf of Mexico.

While these vessels are difficult to generalize, it nevertheless is worthwhile to document a sample vessel and perform the stability calculations. This led to the UNO-Shrimp Trawler Project outlined in Table 1.

TABLE 1. OUTLINE OF UNO SHRIMP TRAWLER PROJECT PHASE I

Phase I Characterization of Gulf Coast Shrimp Trawler Hull Form and Intact Stability

I-1 Selection of Shrimp Trawler for Study
I-2 Schedule of Personnel and Field Trip
I-3 Field Trip 4/2/85, Crown Point, Louisiana
  i) Docking of Trawler
  ii) Photograph of Trawler Hull
  iii) Inclining Experiment of Trawler
I-4 Analysis
  i) Inclining Experiment
  ii) Photogrammetry Photos
I-5 Development of Trawler Hull Offsets
I-6 SHCP Calculations

Project Team

R. Latorre, Project Manager
C. Mugnier, Photogrammetry
A. Suda, SHCP Calculations
Students: D. Rome; Selection of trawler, field trip details, inclining experiment
J. Gunter: Inclining experiment

Sponsor:
University of New Orleans, (UNO) Graduate Research Council Grant 7/84-7/85

TABLE 2 PARTICULARS OF SHIMP TRAWLER

Length Overall	72 ft
Length on waterline	70 ft
Beam maximum	24 ft
Beam on waterline	22.18 ft
Draft (no trim)	6 ft
Single Screw	
Displacement Δ	140 tons
Block coefficient C_B	0.544*
Waterplane coefficient C_{wp}	0.84*
KG	9.74 ft*

* Obtained from present analysis

2. Objectives of the Shrimp Trawler Project - Phase I

The main objectives of the shrimp trawler project were:

1. Select a Gulf Coast shrimp trawler for the study.
2. Obtain its hull offsets by photogrammetry.
3. Perform an inclining experiment on the trawler.
4. Perform the intact stability calculations using the SHCP computer program.

These objectives were the basis for the formation of the project team and the work summarized in Table 1. The students, in addition to providing manpower, were active in planning of the field trip.

Mr. Rome, who at the time of the project was a senior in the UNO-NAME program, arranged through family connections the agreement of a local fisherman to use his 72 ft - 140 ton shrimp trawler for the project. He also coordinated with the operator of a shipyard to arrange the hoisting out of the trawler and blocking for the photographs, as well as the supplies for the inclining experiment and insurance.

3. Shrimp Trawler

Table 2 summarizes the main particulars of the shrimp trawler. The fisherman prepared bulkhead drawings and sketches and built the vessel from steel plate several years ago. The plates were purchased from a local supplier and the vessel was welded in the yard behind his house next to the bayou. The bow section plates were formed by heating while the remainder of the hull was formed into a chine hull.

A trawler this size has capacity for trawling several weeks. The shrimp are taken from the trawl nets sorted on deck, iced and stored in the fish hold. Newer trawlers have been designed with refrigeration but when this vessel was built it was not commonplace. Since the trawl nets are suspended by two booms attached to the forward house, it is an easy matter to raise and lower the nets. This is one reason for the trawler

TABLE 3 UNO SHRIMP TRAWLER PROJECT
4/2/85 FIELD TRIP

Location: Crown Point, Louisiana

Schedule: 4/2/86

8:30	Leave New Orleans
9:45	Team arrives at Crown Point
10:30	Trawler arrives
12:00	Trawler is hauled out and set on blocks
	Total cost of hauling, blocking and returning boat to water: $ 630.00
13:00	Photogrammetry begins
16:00	Photogrammetry finished
17:00	Trawler in water
18:00	Trawler docks at owner's pier
18:15	Inclining experiment begins, draft marks tank sounding recorded, eleven 50 gallon drums loaded on trawler deck
22:30	Inclining experiment finished
24:00	Team returns to New Orleans

safety. When a bad storm comes up, the fisherman will lower the trawl nets over the sides to stabilize the vessel and ride out the storm.

4. Field Trip

Coordinating the fisherman's schedule with the University's spring recess, the field trip was scheduled for April 2,1985. This allowed several alternate days in case of rain. Fortunately the weather was clear and the field trip proceeded along the schedule outlined in Table 3.

The trawler was hauled out by a self propelled crane straddling the hull. Belts were run underneath the hull and the boat was lifted out and set on the blocks. The blocks were arranged in the yard to provide a full field vision to photograph the hull as shown in Fig. 2.

5. Photogrammetry

5.1 Analytical versus analog technique

The majority of literature on photogrammetric application to shipbuilding in the United States has been on the extremely precise methods of analytical photogrammetry /1//2/. (Typically, the accuracies obtained in a regular productive environment range from 1:80,000 to 1:250,000 of the object covered distance.) The problem with the use of these pure analytical techniques is that the personnel required are senior professional level photogrammetrists (less than 500 certified in U.S.). The approach used in this paper was the pure analogical technique using

TABLE 4 EQUIPMENT USED IN 4/2/85 SHRIMP TRAWLER FIELD TRIP AND ANALYSIS

I.	Photogrammetry Equipment
1.	Camera, Type K-22
2.	Lens, 15" focal length
3.	Photographic film, Kodak Super Aerographic
4.	Negative size for analysis, 5" x 7"
5.	Analyzer at University of New Orleans: Zeiss C-8 stereoplanigraph Universal stereoplotter
II.	Inclining Experiment
1.	Piano wire and washer
2.	Plumb
3.	Oil and bucket
4.	Eleven clean 50 gallon drums
5.	Hand trolley

a Universal stereoplotter (Ref. Table 4). In this project the use of an instrument of admittedly greater capital cost, allowed the personnel of more modest training to obtain the hull offsets. The practicality of the analog approach is that it is feasible to use personnel at a technician level who are comparatively easy to locate and employ. Thus for the trade-off with a one-time capital investment for the appropriate instrumentation (analog), the staffing considerations become realistically feasible for shipyards and other marine enterprises.

It should be noted that most (if not all) of the photogrammetric U. S. shipbuilding applications are currently performed by private consulting photogrammetrists of international reputation.

5.2 Procedure

Using the camera and other equipment in Table 4, a series of 10 overlapping photos were taken along a line 70 ft parallel to the trawler keel line as shown in Fig. 1. Additional photos of the bow and stern were made at points A and B respectively. A sample bow photo is shown in Fig. 2.

These photographs were processed and the negatives were analyzed on a Zeiss C-8 stereoplanigraph Universal stereoplotter.

The results of the analysis are shown in Figs. 3 and 4. Fig. 3 shows the shrimp trawler hull lines while Fig. 4 shows the perspective view of the trawler hull. As these figures indicate, the trawler hull has a simple form developed from welded flat plates.

6. Inclining Experiment

The U.S. Coast Guard has recommended /3/ that the range of pendulum movement be within $\theta = 3^{\circ}$. Initial estimates indicated that a total moment of 30 ft - ton (1 ton = 2240 lbs) would be required. In most boat yards a crane and inclining weights are available for this work.

Since the trawler inclining experiment was done at the owner's dock on the bayou a simple solution was adopted. Metal and plastic drums of 50 gallon capacity were used. Each empty drum weighs approximately 10 lbs and when filled with fresh water (8.3 lbs/gal) each drum weights 425 lbs. The drums are loaded onto the deck empty and shifted into position. Then they are filled until topped off to obtain the required heeling moment. They are dumped and moved empty until the experiment is finished.

Doing the inclining experiment at night (after 18:00) avoided the disturbances from the bayou boat traffic, so the tests were made in literally undisturbed water. Throughout the tests the trawler booms were upright without the nets (nets dry and stored).

The results of the inclining experiment are shown in Fig. 5. The data is for one station with a pendulum suspended from the trawler's rigging. In Fig. 5, with the exception of movement 6, the moment - tan θ results fall onto a straight line. At the dock the water depth was over 10 ft giving a good 4 ft clearance between the vessel bottom and mud.

Fig. 6 shows the location of the tanks in the hull. Soundings indicated that the free surface should be accounted for in the GM_T. Assuming tanks 1, 2, 3 and 4 are the only locations of free surface on the vessel the following corrections were made.

GM_{TO}	=	3.72 ft inclining experiment
TK 1	=	0.07 ft correction for free surface in Tank 1
TK 2	=	0.315 correction for free surface in Tank 2
TK 3-4	=	0.25 correction for free surface in Tanks 3-4
GM_T		4.355 ft

On another occasion the authors would like to do an inclining experiment with the booms and nets over the side to clarify the restoring moment during trawling.

7. SHCP Calculations

The trawler hull offsets obtained from the analysis of the stereo photographs (Figs. 3 and 4) were input into the SHCP Computer program and run on the University of New Orleans VAX 8600 cluster. For the present calculation eleven stations were used each with 4 points defining the hull section

7.1 Hydrostatic Results

The results of the SHCP hydrostatic calculations for no trim condition are plotted in Fig. 7. The range of draft $\leq T \leq 8$ was selected for future studies of the safety of the trawler during various stages of operation. For the present studies the conditions at the inclining experiment T = 6 ft no trim will be assumed. At T = 6 ft. the

TABLE 5. COMPARISON OF TAWLER INTACT STABILITY WITH VARIOUS CRITERIA [4]

Criteria	Notes	Formula	Satisfied
I GM_T Criteria	GM_T = 4.35 ft		
IMCO		$GM_T \geq$ 1.148 ft	Yes
JAPAN	a) Seiner	GM_R =((B/23.0) + 0.8858)) = 1.93	Yes
		or	
		GM_R =((L_{WL}/20) + 0.8858) = 1.47	Yes
	b) Fishing Vessel B $\geq$ 23 ft	GM_R = ((B/3.28 -7.0)/12.0 + .4) x 3.28 = 1.4	
		or	
		GM_R + (L_{WL}/3.28 - 4.2)/72.0 + .4) x 3.28 = 2.1	Yes
POLAND	Simplified	GM_R = D (0.105 - .706 F/B + 0.083 B/0 = 1.82	Yes
SOVIET	Simplified	GM_R = D (-0.47 - 0.35 F/B + 0.35 B/0) = 3.02	Yes
II. Dynamic Stability	Refer Fig. 8		
IMCO	Energy 0 - 30°	E 30° $\geq$ 10.3 ft - Deg (30.45 ft-Deg)	Yes
	Energy 0 - 40°	E 40° $\geq$ 16.9 ft-Deg (42.20 ft-Deg)	Yes
	Energy 30 - 40°	E 30-40° $\geq$ 5.6 ft-Deg (11.75 ft-Deg)	Yes
	GZ_{Max}	$GZ_{Max} \geq$ 0.656 ft (1.432 ft)	Yes
	Angle of GZ_{Max}	GZ_{Max} at $\theta \geq 30^0$ (θ = 30°)	Yes
	Down flooding	Insufficient data	

value of the transverse KM_T = 14.09 ft
Using KG = KM_T - GM_T, the value of
KG = 9.74 ft during the inclining experiment.

7.2 KN and GZ Curves

The SHCP program was run with zero pole height to obtain the value of KN using

GZ = KN-KG sinθ

the GZ curve corresponding to the trawler at 6 ft draft and KG = 9.74 was obtained. This is plotted in Fig. 8.

Referring to the GZ curve, the range of stability is 52° with GZ max = 1.43 ft at θ = 30°. The trawler intact stability is shown to comply with the various stability criteria in Table 5. In a future study the different trawler operating conditions will be analyzed to check if there is an operation situation which could be dangerous. However the present results indicate the vessel has more than adequate stability.

8. Discussion and Conclusions

This paper has summarized Phase I of the UNO-Shrimp Trawler project. In this phase the hull offsets were obtained by photogrammetry to make the hydrostatic and intact stability calculations.

The authors experience indicates that this procedure is relatively straight forward and could be used routinely for vessel stability calculations. The question of accuracy could not be addressed since the shrimp trawler was built without detailed plans. Experience has shown that an accuracy of 1/1000 ft. could be expected from the photogrammetry technique used in the project.

With such accuracy questionas as to the hull roughness, aging, as well as the hull construction, tolerance to the original lofting can be addressed.

The completion of Phase I leads to the following conclusions:

1. Photogrammetry represents an attractive technique for obtaining the hull offsets when the vessel can be docked and photographed.
2. A system has been demonstrated where photographs are used to obtain the hull offsets, and the hydrostatic calculations then performed.

Referring to the example shrimp trawler used in the study:

3. The inclining experiment indicated that the trawler GM_T is 4.35 ft.
4. From the hydrostatic calculations, the draft T = 6 ft, KM_T = 14.09 ft which gives KG = 9.74 ft.
5. Using the KN curve (Pole height = 0) from the intact stability calculation the GZ-θ curve in Fig. 8 was obtained.
6. Checks with various stability criteria indicate that the trawler has adequate intact stability.

These results provide a basis for future studies on the safety of Gulf Coast Shrimp Trawlers.

9. Acknowledgements

The authors are grateful to D. Rome and J. Gunter for their assistance in this project. The photogrammetric equipment was kindly loaned by Mr. Joseph Roberts, Southern Aerial Marine, Baton Rouge, La., who also was kind enough to develop the negatives and print positives of the trawler for analysis. The authors are grateful to Mr. A. DesClaire and his family for their cooperation and hospitality during the field trip as well as to the University of New Orleans Graduate Research Council for their support of Phase I project. Finally they are grateful to Mrs. Latapie for typing the manuscript.

10. References

[1] Kenefick, J. F., "Shipbuilding Application of Photogrammetry," Proceedings American Society of Photogrammetry, Semi-Annual Convention, Seattle, Washington, Sept. 1976.

[2] Kenefick, J. F., Hueto, D. A., "Photogrammetric Surveys of the COGNAC Jacket Structure," Marine Technology, Vol. 17, No. 3, July 1980, pp. 243-249.

[3] "Notes on Preparations and Procedures for Stability Tests, Navigation & Vessel Inspection Circular No. 1-67," Prepared by Merchant Marine Technical Division, Office of Merchant Marine Safety, U. S. Coast Guard Washington, D. C. 1967.

[4] Amy, J., Johnson, R., Miller, E., "Development of Intact Stability Criteria for Towing and Fishing Vessels," Transactions SNAME, 1976.

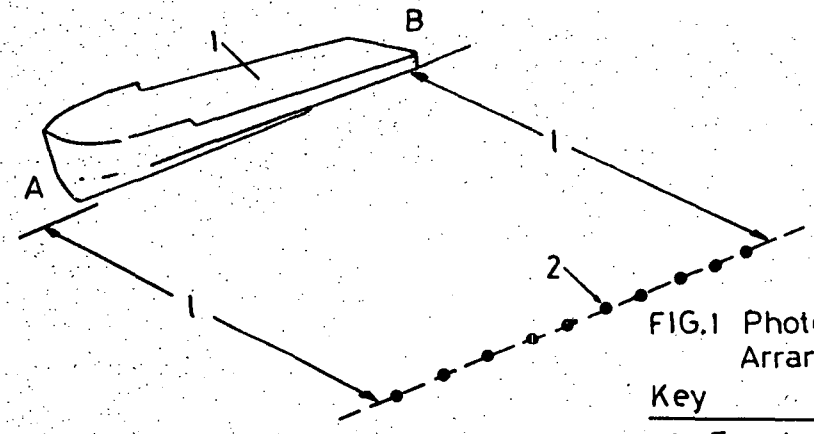

FIG.1 Photo Arrangement

Key

1 Trawler

2 Camera Position

l = 70 ft.

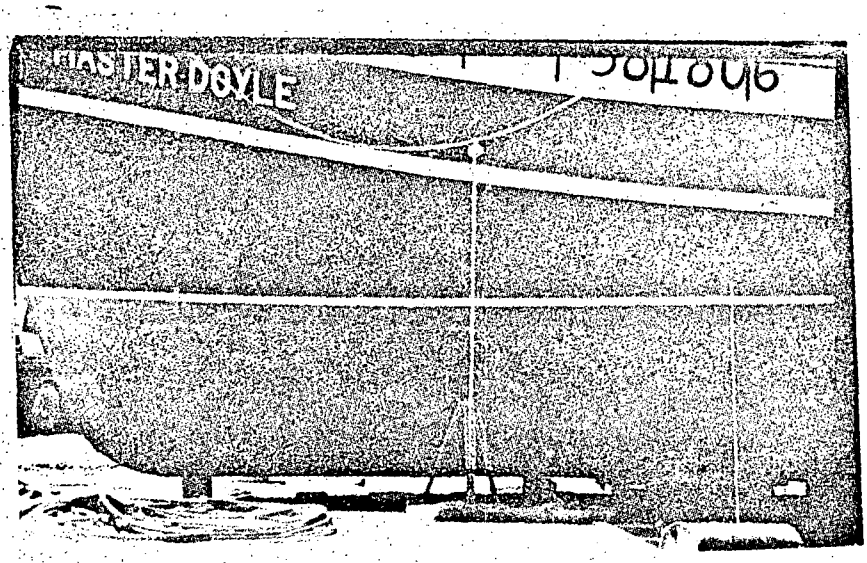

FIG. 2. Photograph of Shrimp Trawler Bow. Note Sighting Instruments Used in Calibration.

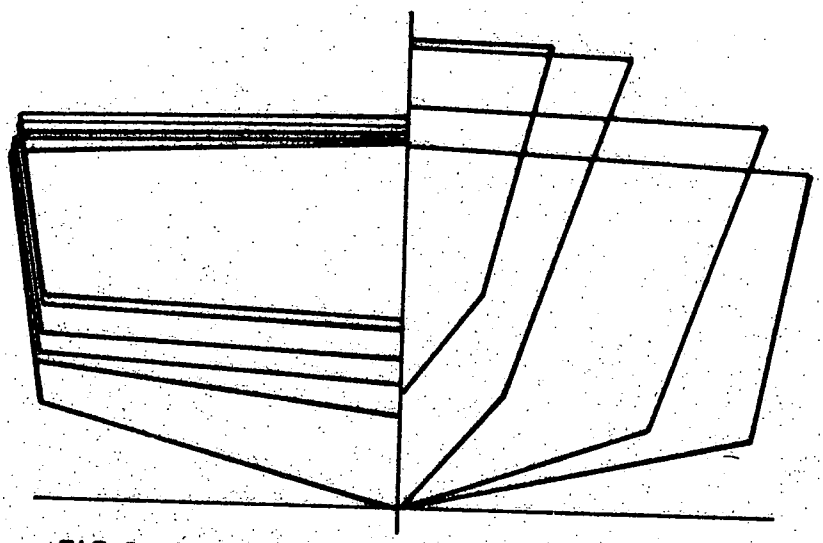

FIG. 3 SHRIMP TRAWLER LINES PLAN
UNO TRAWLER PROJECT

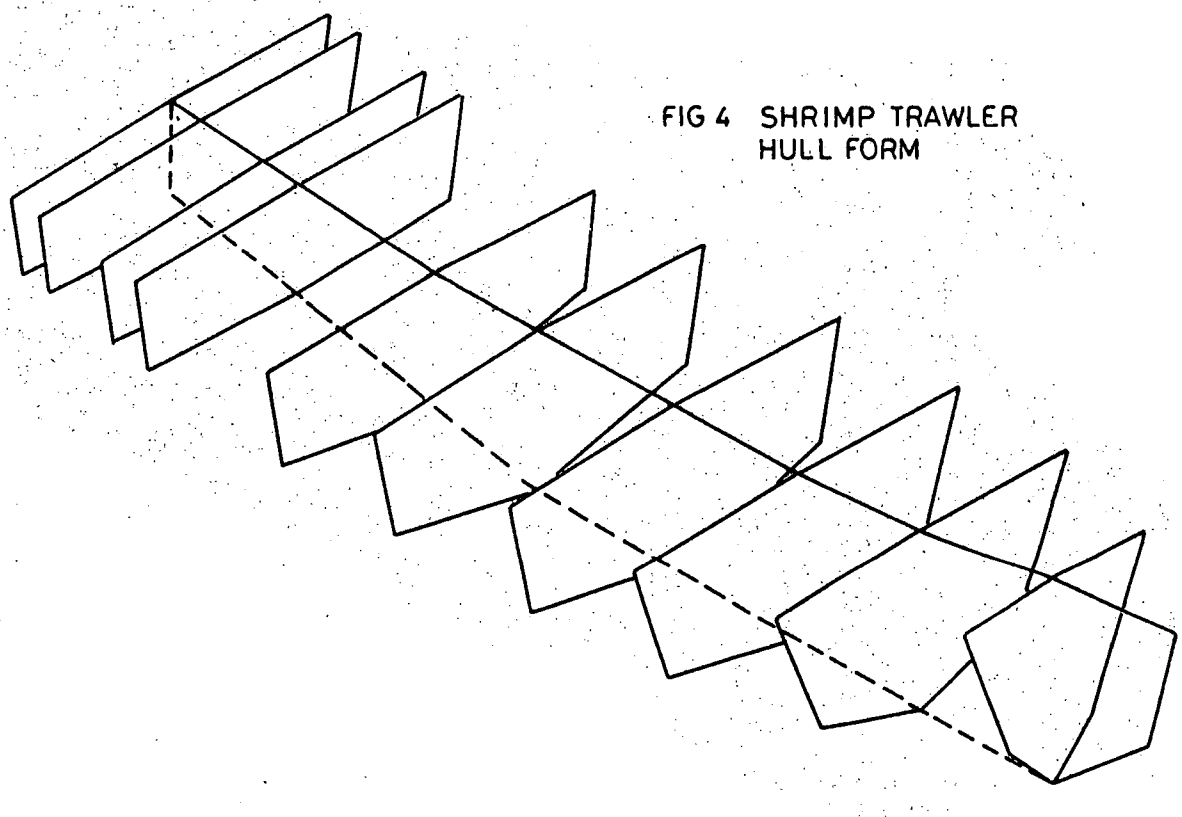

FIG 4 SHRIMP TRAWLER
HULL FORM

UNO SHRIMP TRAWLER PROJECT

FIG. 5 INCLINING EXPERIMENT 4/2/85

PENDULUM LENGTH l = 28 ft

$GM_{T_{exp}} = \frac{34.1 \text{ ft ton}}{143.3 \text{ t}(0.064)} = 3.72 \text{ ft}$

Free Surf. Correction = 0.635 ft

$GM_T = 4.35$ ft

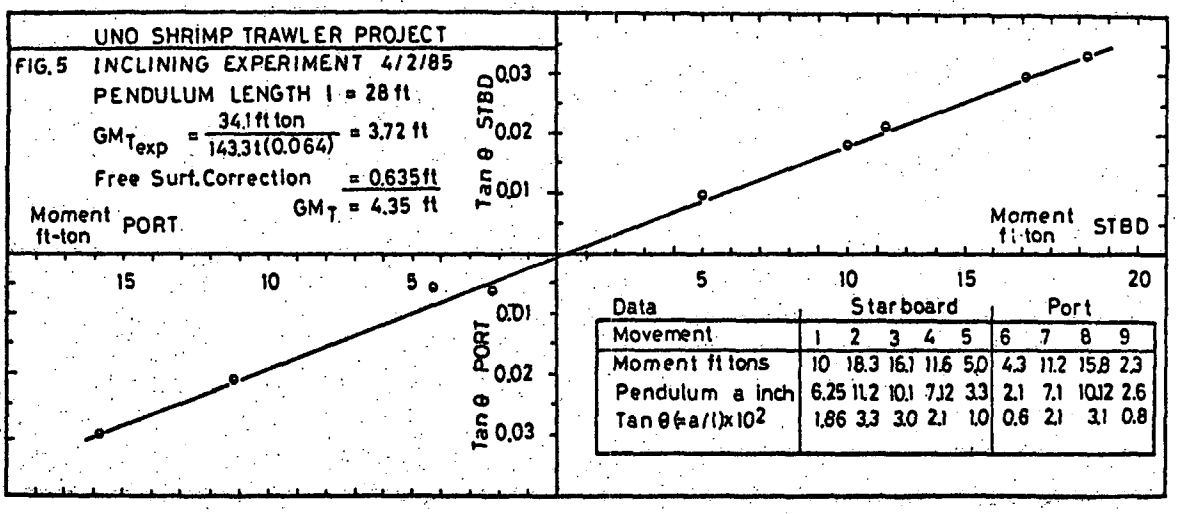

Data	Starboard					Port			
Movement	1	2	3	4	5	6	7	8	9
Moment ft tons	10	18.3	16.1	11.6	5.0	4.3	11.2	15.8	2.3
Pendulum a inch	6.25	11.2	10.1	7.12	3.3	2.1	7.1	10.12	2.6
Tan θ (=a/l) x 10^2	1.86	3.3	3.0	2.1	1.0	0.6	2.1	3.1	0.8

UNO SHRIMP TRAWLER PROJECT

FIG. 6 TANK ARRANGEMENT

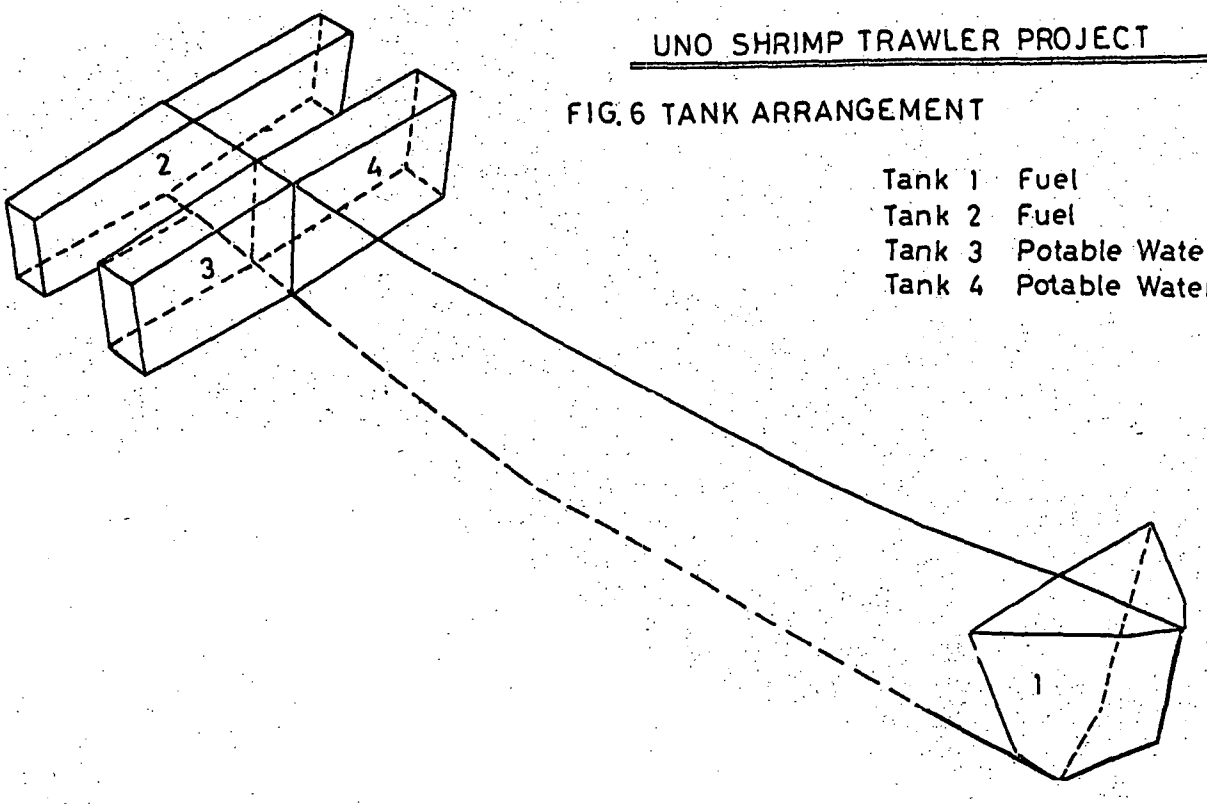

Tank 1 Fuel
Tank 2 Fuel
Tank 3 Potable Water
Tank 4 Potable Water

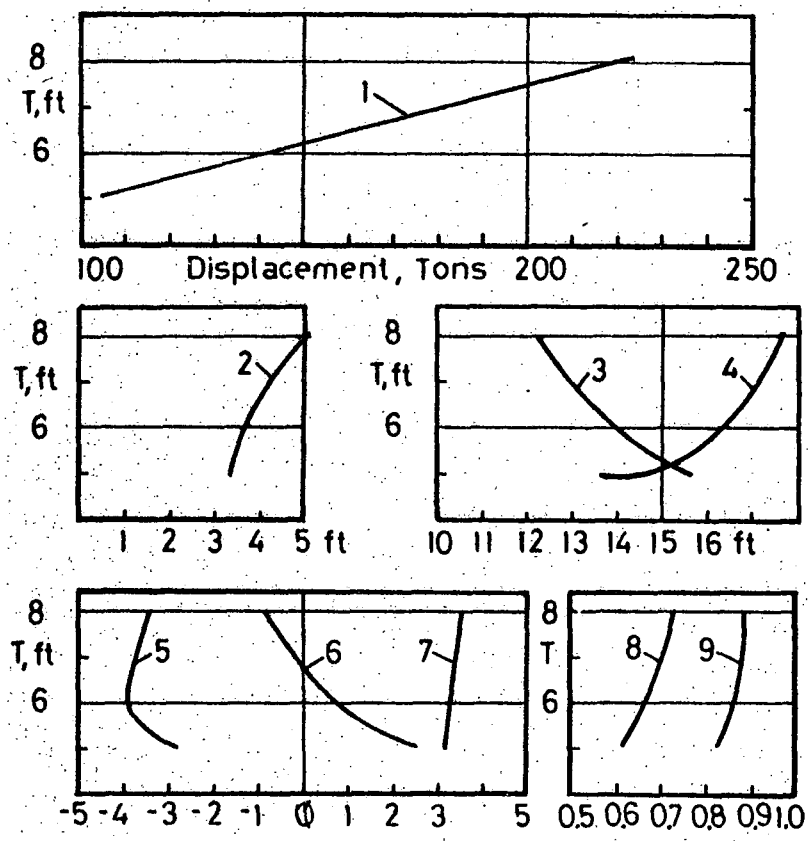

FIG.7 SHRIMP TRAWLER HYDROSTATICS
NO TRIM UNO TRAWLER PROJECT

KEY

1 DISPLACEMENT	4 MTI	7 TPI
2 KB	5 LCF	8 Cp
3 KM_T	6 LCB	9 C_{wp}

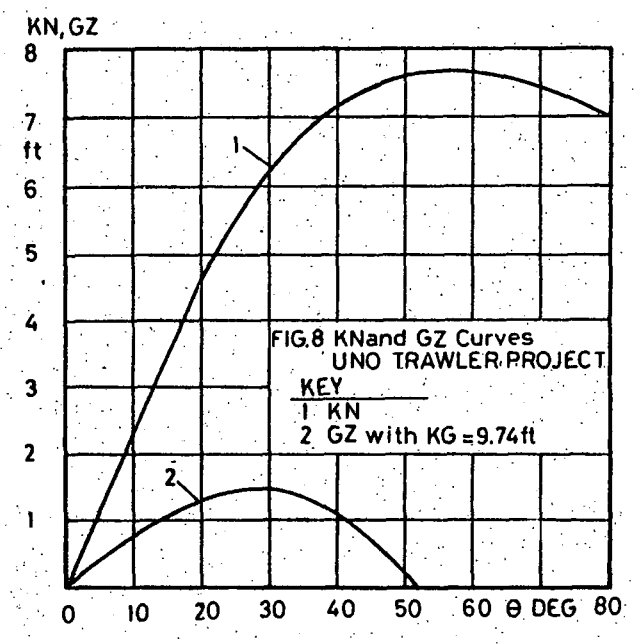

FIG.8 KNand GZ Curves
UNO TRAWLER PROJECT

KEY

1 KN
2 GZ with KG = 9.74ft

Third International Conference on Stability of Ships and Ocean Vehicles, Gdańsk, Sept. 1986

STAB'86

STABILITY AND EXTRACTION OF GROUNDED ICEBREAKERS

B.C. Nehrling; N.T. Tsai

ABSTRACT

Whenever large and powerful polar icebreakers are used for aggressive ramming there is the distinct possibility that the ship will be driven too far onto the ice field. As a consequence of being driven too far aground, the ship can become unstable and/or remain stranded. Consequently, it is important for naval architects to be able to predict the intact stability characteristics of a grounded icebreaker as well as the force needed to extract it. This paper presents a summary of the work involved in developing a computer model to provide these predictions. These theoretical predictions are shown to compare favorably with experimental data obtained through model testing.

1. INTRODUCTION

Ice breaking operations are conducted in a variety of ways depending upon such parameters as hull form, available power and ice conditions. One of the current trends in icebreaker design philosophy is to attempt to maximize the inherent advantages provided by forebody shape and weight while maintaining adequate stability and minimizing extraction difficulties. To help naval architects accomplish these objectives, the U.S. Coast Guard has been developing analytical methods to help predict the performance of various icebreaker designs. Design parameters such as bow stem angle, spread angle complement and friction coefficient have been introduced into a computer model in order to better predict the ramming and continuous icebreaking capability of a given hull form in terms of the standard ice thickness which is to be broken. This model has also been used to predict extraction requirements.

Procedures have also been developed to better evaluate the statical stability of an icebreaker after it has run aground onto thick ice. In 1985, these procedures and those of the previous model were revised and incorporated as one additional option of the general purpose Ship Hull Characteristics Program (SHCP).

In order to provide additional confidence in the predictions provided by this computer program, a series of tests were conducted in the stability basin of the U.S. Naval Academy's Hydromechanics Laboratory using two icebreaker models. The experimental results, when expanded to full scale values, showed good agreement with the computer's predictions.

2. ANALYTICAL METHODS

White [1,2] attempted to calculate an icebreaker's dynamic icebreaking capability by developing both a detailed mathematical model and a simplified implementation. To use the detailed mathematical model many characteristics of the ship and its environment must be known. However, by introducing certain simplifying expressions, the detail model can be converted into a simple program suitable for most preliminary design studies. These simplifying expressions were derived from the common geometric and kinematic relationships of a typical operational icebreaker. Characteristics such as length, beam, bow configuration, transverse and longitudinal metacentric heights, center of buoyancy, center of gravity, thrust and friction coefficients are used. With these simplifying expressions, the simple model may be used to calculate what standard ice thickness can be broken and the expected difficulty of extraction.

The difficulty of extraction is represented by an index defined as the ratio of the extraction thrust necessary to pull the ship off the ice to the available thrust. An index value of zero would mean that no extraction thrust was necessary. A negative value would indicated that the ship slides off the ice. An index value of +0.5 with an assumed static friction coefficient of 0.6 appears to be a reasonable upper limit for practical designs.

Another problem associated with icebreaking operations is that of maintaining adequate intact statical stability when the ship goes aground on an ice field. While the initial statical stability of an icebreaker is usually quite large due to a high transverse metacentric radius provided by a broad beam, this degree of stability rapidly decreases and can even become negative if the icebreaker is driven too far onto the ice during ramming operations. This problem becomes even more serious when topside icing and beam winds are present. A procedure to approximate the statical stability of a grounded icebreaker during design studies is explained in reference [3]. Basically this methodology considers a stranded icebreaker to be stable if, at any stem-to-ice contact position, the stern is above the water's surface, the transverse metacentric height is positive and a righting moment is present.

In conjunction with one of the Coast Guard's current design projects, namely that of a polar oceanographic research ship, the aforementioned models were merged together and installed as one additional option of the widely used SHCP. By utilizing the hydrostatic values computed by SHCP, many of the simplifying expressions and underlying approximations used in these models could be eliminated. For example, with the help of SHCP, values for the metacentric heights and longitudinal center of floatation can be easily calculated during each of the iterations needed to complete the grounded stability analysis.

To help illustrate this model, the Coast Guard's Polar class icebreaker will be analyzed. A rough body plan for this hull is shown in Fig. 1. Fig. 2 shows the effect of the stem-to-ice contact position on the icebreaker's righting arm. As can be seen from this figure, the stability of the ship steadily decreases as the aground position approaches the keel. Fig. 3 indicates that the effective transverse metacentric height is reduced and the trim angle increased as the aground

position once again approaches the keel. A typical plot of the index of extraction as a function of ramming speed is shown in Fig. 4. Other relevant parameters such as the vertical grounding force at the bow and the ship's effective center of gravity can be calculated and plotted for each stem-to-ice contact position. This ship's index of extraction difficulty is derived as follows. For any given ramming speed, the computer model determines the downward force exerted on the ice. This downward force is then used to determine the location of the stem-to-ice contact point. This position is then used to determine the bow stem angle which in turn enables the computer algorithm to calculate the index of extraction difficulty.

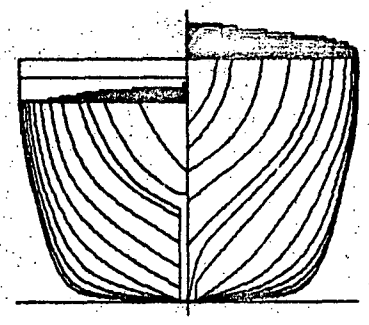

Figure 1 Polar Class Body Plan

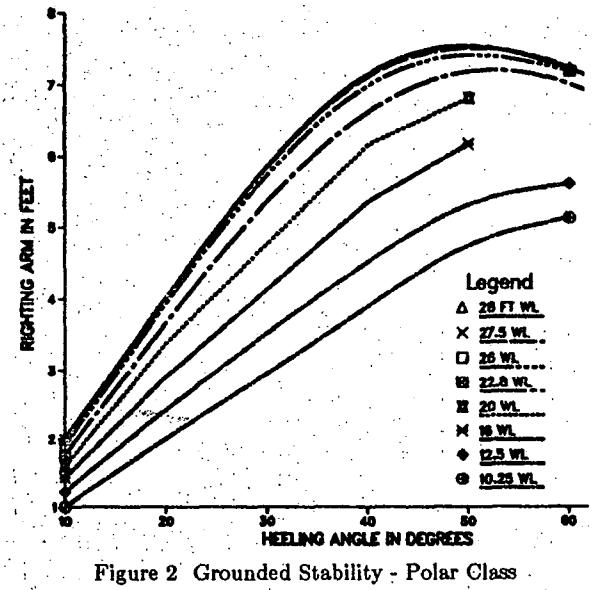

Figure 2 Grounded Stability - Polar Class

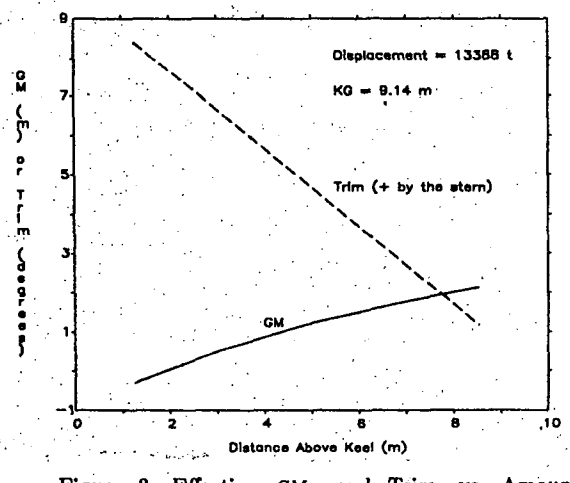

Figure 3 Effective GM_T and Trim vs. Amount Aground - Polar Class

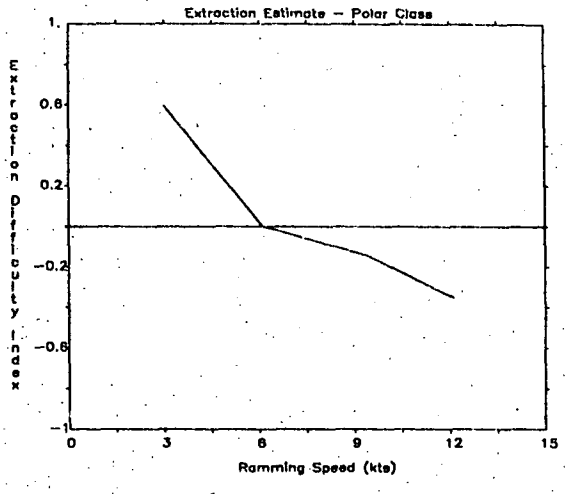

Figure 4 Extraction Estimate - Polar Class

3. EXPERIMENTAL PROGRAM

During the summer of 1985, a series of grounded stability experiments were conducted in the stability basin at the Naval Academy's Hydromechanics Laboratory for the Coast Guard. For these experiments, two scale models were used. One model was that of the USCG's Polar class icebreaker, while the other model was of a proposed polar oceanographic research ship [4].

3.1 Test Procedure

The experimental phase of this project can be summarized as follows:

[1] Each model was ballasted to the displacement (Δ) and trim specified by the Coast Guard.

[2] An inclining experiment was conducted to determine the vertical position of the center of gravity. Internal weights were then shifted vertically and the inclining experiment repeated until the vertical center of gravity (KG) specified by the Coast Guard for these stability experiments was obtained.

[3] For each model, a fully afloat intact statical stability curve at the required displacement and center of gravity was determined experimentally.

[4] Individually, the bow of each model was placed on the test apparatus. This apparatus was configured to represent an ice field that the ship could have conceivably run aground on. The model's righting moment, vertical grounding force and trim were measured as a function of heel angle for several stem-to-ice contact positions. Similar data was also gathered for one stem-to-ice contact point but with varying heights of exposed ice.

[5] The experimental results were expanded to full scale values and plotted for each ship. These plots clearly indicate the detrimental effect that being aground has on a ship's intact statical stability. They also clearly show that the farther aground the ship has run, the worse its stability becomes.

[6] For reasons of brevity, only the experimental results associated with the Polar class icebreaker will be described and discussed in this paper.

3.2 Model

Pertinent characteristics of the Polar class icebreaker (ship and model) are given in Table 1. A rough bodyplan for this hull is shown in Fig. 1. The model used in these stability tests was of wooden construction. It had previously been used for a variety of resistance experiments.

TABLE 1 - Polar Class Characteristics		
Characteristic	Ship	Model
LOA	121.62 m	253.4 cm
LBP	107.20 m	223.5 cm
Depth	14.33 m	29.6 cm
Draft	9.75 m	20.3 cm
Δ (note 1)	13388 t	117.94 kg
Trim	0	0
LCG	1.35 m fwd amidships	2.8 cm fwd amidships
KG	7.92 m	16.5 cm
GM_T (note 2)	3.62 m	7.5 cm
KM_T (note 3)	11.54 m	24.0 cm
Scale factor	1	48

Notes:

[1] Ship in salt water at 15 C (SHCP output). Model in fresh water at 20 C.

[2] Model's GM_T was derived from an inclining experiment.

[3] Ship's KM_T was obtained from SHCP output.

3.3 Inclining Experiments

The following procedure was used to determine the model's vertical center of gravity (*KG*).

[1] The model was ballasted to the required displacement and trim. Included aboard the model was a previously calibrated electronic inclinometer and a set of centerline weights which could be moved to either port or starboard a predetermined distance.

[2] The weights were shifted several times to both port and starboard to create known heeling moments. For each moment, the angle of heel was determined by converting the inclinometer's voltage to an angular value. Fig. 5 shows the acquired data and the least squares linear regression equation which best fits this experimental data. The slope of this linear equation along with model's displacement was used to compute the transverse metacentric height (GM_T).

$$GM_T = 1/(\Delta * SLOPE)$$

[3] The transverse metacentric height above the keel (KM_T) for each model was derived by scaling full scale hydrostatic data provided by the Coast Guard.

[4] The model's *KG* was found by subtracting GM_T from KM_T. Values for Δ, KM_T, GM_T, and *KG* for the Polar class icebreaker model are given in Table 1 along with equivalent values for the full scale ship.

3.4 Statical Stability Experiments

The following procedure was used to determine the model's fully afloat intact statical stability curve.

[1] The model was ballasted to the required displacement, vertical center of gravity and trim. Included aboard the model was a pair of previously calibrated electronic inclinometers and a large heeling ring. One inclinometer was positioned so as to measure heel while the other one measured trim. The heeling ring, connected by a cable to a winch, was used to produce a heeling moment. The heeling force was measured by means of a previously calibrated load cell. Fig. 6 is a schematic representation of how this equipment was configured. The model was slowly heeled over by cranking in on the winch. While it was heeling over the model developed a righting moment equivalent to the heeling moment.

$$(GZ * \Delta) = (HEELING\ FORCE * RING\ DIAMETER)$$

[3] The model was heeled over until the deck edge was immersed.

[4] Computed values of the model's righting arm were expanded to full scale. A plot of ship righting arm (*GZ*) as a function of heel angle for the Polar class is shown in Fig. 7. Also shown in this figure is the full scale GM_T that was determined during the inclining experiment.

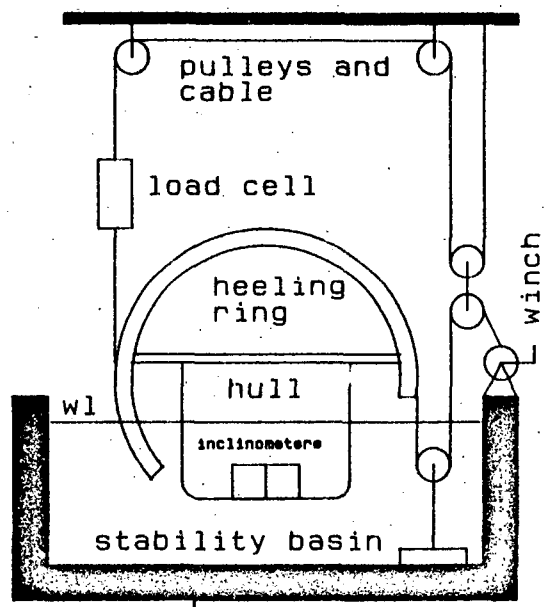

Fig. 6 Inclining Apparatus

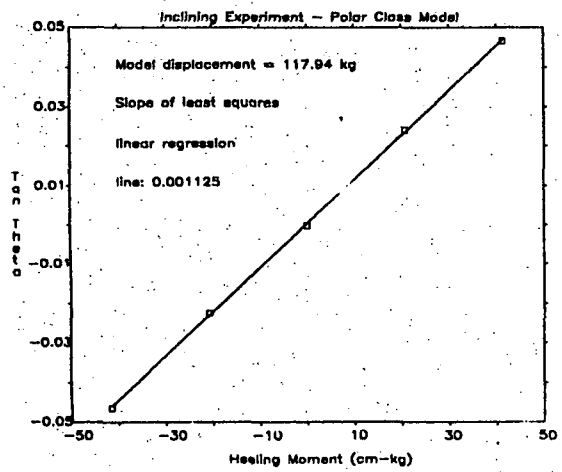

Figure 5

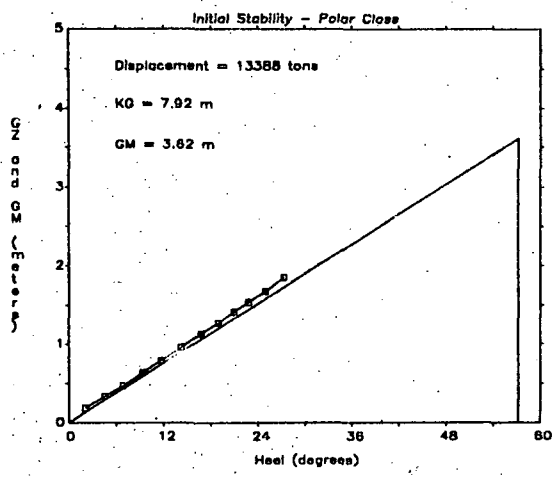

Figure 7

3.5 Grounding Experiments

The following procedure was used to determine, for the model under various conditions, the model's righting moment, the vertical grounding force at the bow and the angle of trim.

[1] The model was outfitted just as it had been for the freely afloat statical stability measurements.

[2] The stem of the model was placed on a horizontal metal bar simulating the edge of a rigid ice field. The downward force exerted on the metal bar by the hull was measured by means of a calibrated force block firmly anchored to the bottom of the stability basin. Fig. 8 shows this equipment. Fig. 9, a photo of the Polar class model, was taken during these grounding experiments.

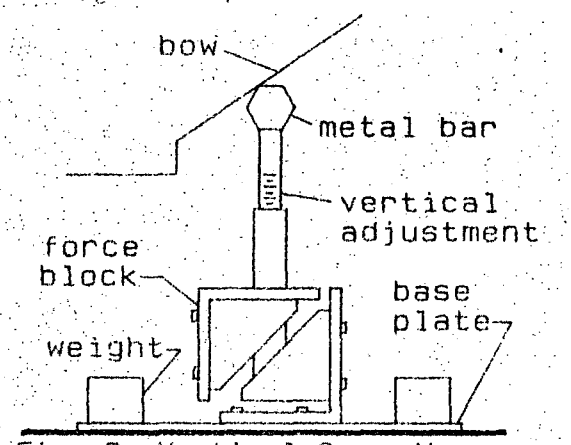

Fig. 8 Vertical Grounding Force Apparatus

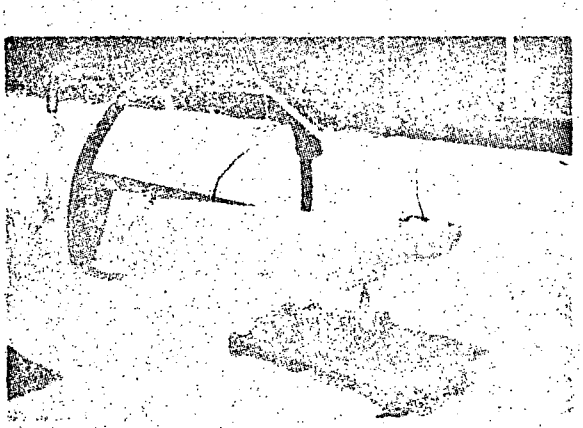

Figure 9 Testing the Polar Class Model

[3] The model was slowly heeled over using the winch, cable and heeling ring. At approximately 3 degree increments the voltage values from the inclinometers, load cell and force block were read and recorded. The model was heeled over until either the deck edge was submerged or the hull became almost unstable. The model was slowly released and several additional voltage readings were taken as it returned to the upright.

[4] For subsequent grounding experiments, the model was positioned with the hull progressively farther aground. Otherwise, the procedure and the data acquisition process was the same.

[5] The measured voltages from the two inclinometers, the load cell and the force block were converted to engineering units and then scaled up to ship values. Righting moment, force aground and trim have been plotted as a function of the angle of heel for various stem-to-ice contact positions. Figs. 10, 11 and 12 show this data for the Polar class icebreaker. Righting moment was plotted rather then righting arm since the ship's buoyant displacement, which is a function of the extent aground, was changing.

[6] During the aforementioned experiments the water level was even with the upper edge of the horizontal metal bar which was representing the ice field. In other words, the surface of the simulated ice field was flush with the surrounding water. A series of subsequent stability tests were conducted for one stem-to-ice contact point but with varying heights of exposed ice. Figs. 13, 14 and 15 show, for the Polar class, its righting moment, force aground and trim as a function of the angle of heel for three ice heights at a constant stem-to-ice contact location.

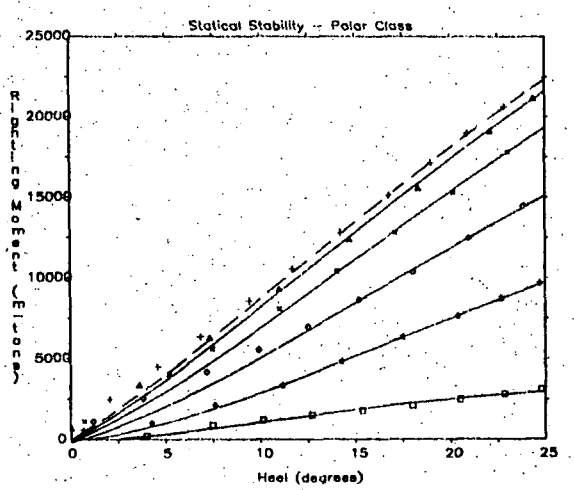

FIGURE 10 Statical Stability - Polar Class	
Raw Data Symbol	Ship Condition
	KG = 7.92 m
+ (dashed line)	Freely floating
Triangle	Aground 0.68 m fwd FP
X	Aground 4.51 m aft FP
Diamond	Aground 8.55 m aft FP
Star	Aground 11.45 m aft FP
Box	Aground 13.66 m aft FP

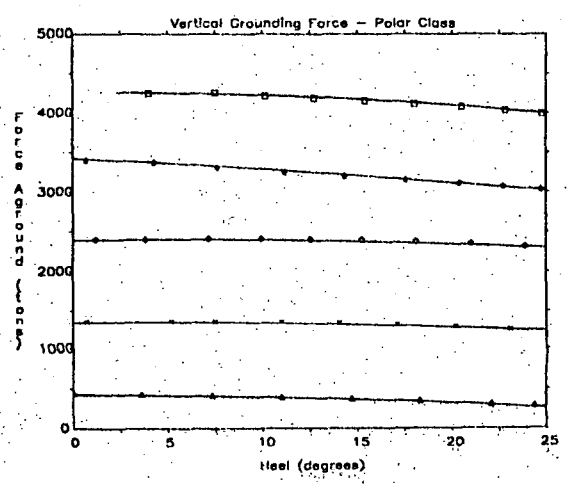

FIGURE 11 Vertical Grounding Force - Polar Class	
Raw Data Symbol	Ship Condition
	Initial Δ = 13388 t Initial KG = 7.02 m
Triangle	Aground 0.68 m fwd FP
X	Aground 4.51 m aft FP
Diamond	Aground 8.55 m aft FP
Star	Aground 11.45 m aft FP
Box	Aground 13.66 m aft FP

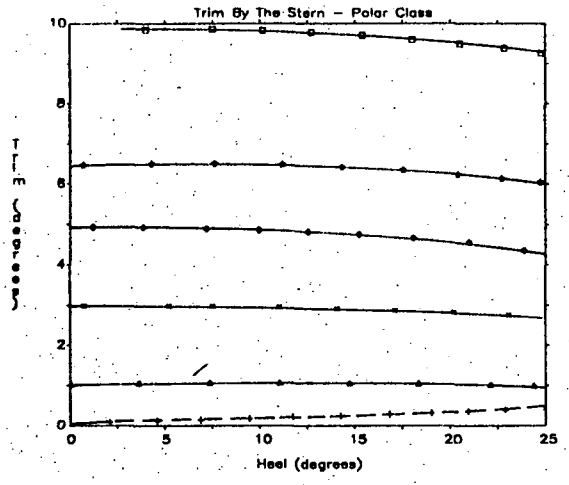

FIGURE 12 Trim By The Stern - Polar Class	
Raw Data Symbol	Ship Condition
+ (dashed line)	Freely floating
Triangle	Aground 0.68 m fwd FP
X	Aground 4.51 m aft FP
Diamond	Aground 8.55 m aft FP
Star	Aground 11.45 m aft FP
Box	Aground 13.66 m aft FP

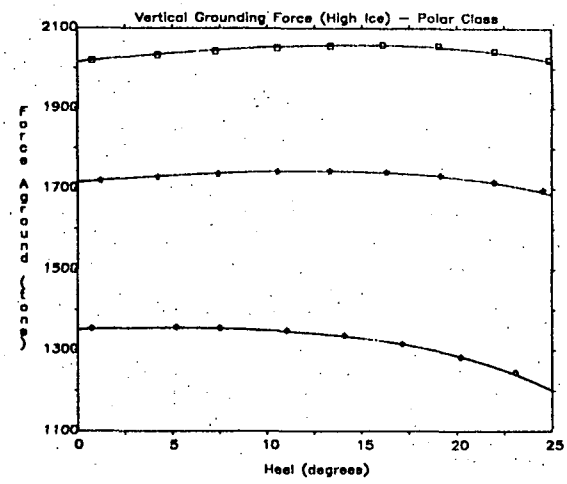

FIGURE 14 Vertical Grounding Force (High Ice) - Polar Class	
Raw Data Symbol	Ship Condition
	Initial Δ = 13388 t Initial KG = 7.92 m
Diamond	Aground 4.51 m aft FP with the ice 0.02 m above the water
Star	Aground 4.51 m aft FP with the ice 1.22 m above the water
Box	Aground 4.51 m aft FP with the ice 2.29 m above the water

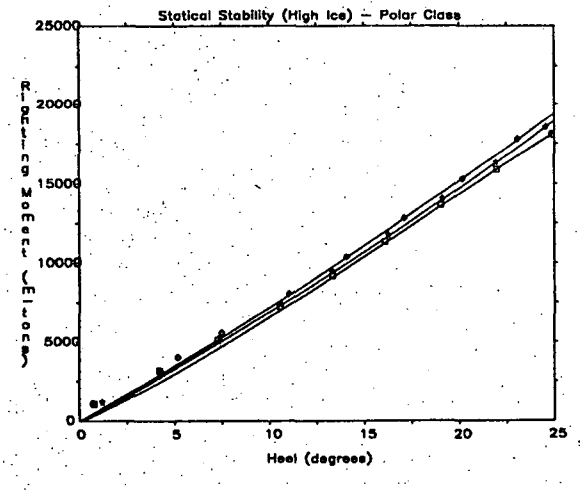

FIGURE 13 Statical Stability (High Ice) - Polar Class	
Raw Data Symbol	Ship Condition
	KG = 7.92 m
Diamond	Aground 4.51 m aft FP with the ice 0.02 m above the water
Star	Aground 4.51 m aft FP with the ice 1.22 m above the water
Box	Aground 4.51 m aft FP with the ice 2.29 m above the water

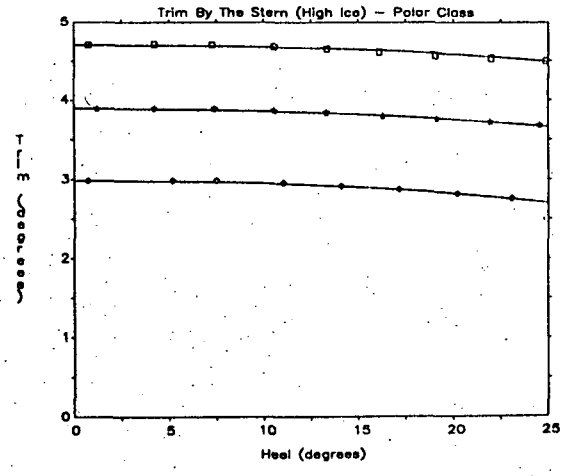

FIGURE 15 Trim By The Stern (High Ice) - Polar Class	
Raw Data Symbol	Ship Condition
Diamond	Aground 4.51 m aft FP with the ice 0.02 m above the water
Star	Aground 4.51 m aft FP with the ice 1.22 m above the water
Box	Aground 4.51 m aft FP with the ice 2.29 m above the water

4.0 COMPARING PREDICTIONS

One of the primary goals of this research project was to evaluate the validity of the computer's predictions. It is now possible to directly compare experimentally obtained and computer predicted values for statical stability, vertical grounding force and trim. These various comparisons, for the full scale Polar class hull form, are shown in Figs. 16, 17 and 18. In each case the independent parameter is angle of heel. The reason the maximum heel angle is so small is because the model was not outfitted with a watertight deck.

From an applied engineering standpoint there is an adequate level of correlation between the computer's predictions and the expanded experimental results. The quantitative magnitudes are in general agreement while the qualitative ranking is very good. Nevertheless, modifications to both the experimental process and the computer model are certainly warranted. However, the computer model, when used as an engineering design tool, does do a reasonable job of predicting the statical stability, vertical grounding force and trim of an icebreaker which has been driven up onto an ice field.

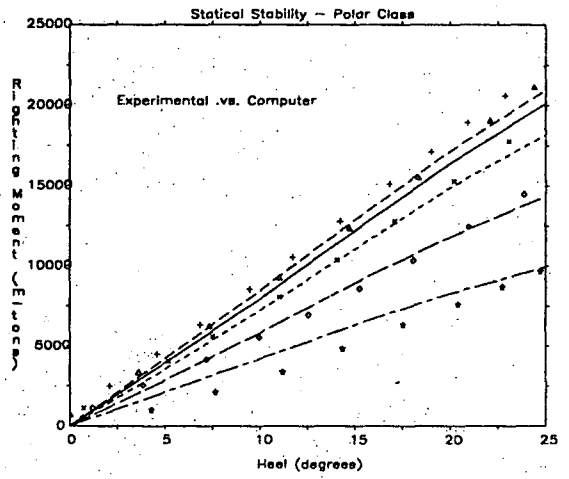

FIGURE 16
Statical Stability - Polar Class
Experimental .vs. Computer

Experimental Point	Computer Line	Ship Condition
		KG = 7.92 m
+	Short dash	Freely floating
Triangle	Solid	Aground 0.68 m fwd FP
X	Dotted	Aground 4.51 m aft FP
Diamond	Long dash	Aground 8.55 m aft FP
Star	Dot-dash	Aground 11.55 m aft FP

5.0 DISCUSSION and CONCLUSION

This series of experiments established the feasibility of experimentally predicting the stability characteristics of a ship aground at the bow. The applicable theory was substantiated and the anticipated trends were observed.

The inclining experiment produced data which, when plotted, was extremely linear. This expected linearity gave a high level of confidence to the computed GM_T value.

The fully afloat intact statical stability curve was fair and consistent through the measured range of heel angles. The slope, at small angles, compared very favorably to the previously determined GM_T value when plotted at one radian. Since the model was not outfitted with a watertight deck the range of heel angles was limited to the angle of imminent downflooding. This angle occurred shortly after the deck-at-edge became immersed.

The grounding experiments represented an innovative approach to measuring the loss of transverse stability which is known to occur when a ship runs aground. The experiments, though restricted to one particular case, namely, that of a ship having only stem-to-ice contact points, clearly showed that the ship's transverse stability deteriorated at an increasing rate as the ship was run farther and farther onto the ice. As expected, the farther each hull was driven onto the ice the greater the vertical grounding force and angle of trim became. For each grounding condition, the magnitude of these two parameters was reduced somewhat as the angle of heel increased.

For the initial set of tests the surface of the simulated ice field was flush with the surrounding water. A series of subsequent stability tests were conducted for one stem-to-ice contact point but with varying heights of exposed ice. As the height of the exposed ice increased stability decreased slightly while the vertical force aground and the angle of trim increased.

Even though the results of this project indicate an acceptable level of agreement between what was predicted analytically and what was measured experimentally, further validation is recommended. It would be very interesting to see this validation accomplished by using either a larger scale model or by conducting full scale icebreaker tests on the Great Lakes. In either case, by minimizing or eliminating the scale factor, some of the observed differences between the analytical and experimental results would certainly be accounted for.

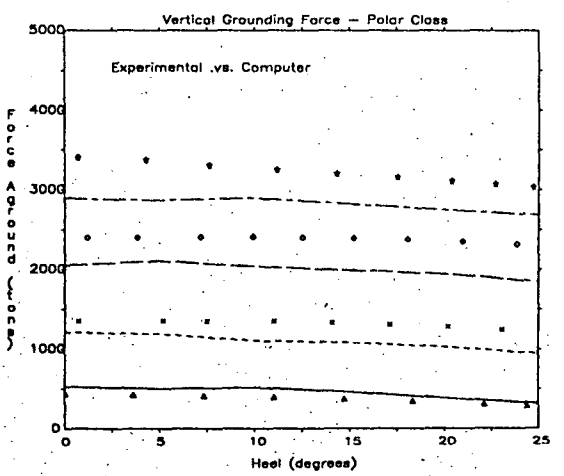

FIGURE 17
Vertical Grounding Force - Polar Class
Experimental .vs. Computer

Experimental Point	Computer Line	Ship Condition
		Initial Δ = 13388 t Initial KG = 7.92 m
Triangle	Solid	Aground 0.68 m fwd FP
X	Dotted	Aground 4.51 m aft FP
Diamond	Long dash	Aground 8.55 m aft FP
Star	Dot-dash	Aground 11.45 m aft FP

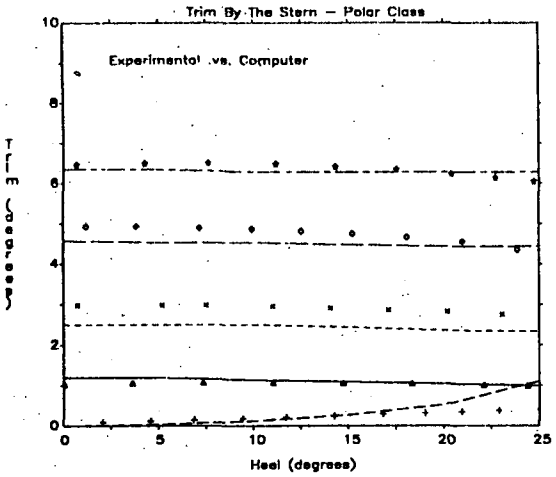

FIGURE 18 Trim By The Stern - Polar Class Experimental .vs. Computer		
Experimental Point	Computer Line	Ship Condition
+	Short dash	Freely floating
Triangle	Solid	Aground 0.68 m fwd FP
X	Dotted	Aground 4.51 m aft FP
Diamond	Long dash	Aground 8.55 m aft FP
Star	Dot-dash	Aground 11.45 m aft FP

ACKNOWLEDGEMENTS

The authors appreciate the support provided by the U.S. Coast Guard and the U.S. Naval Academy while conducting this research. In particular, the authors wish to thank Messrs. Haciski and Bagnell of the Coast Guard and Messrs. Hill, Enzinger and Bunker of the Naval Academy's Hydromechanics Laboratory. These five individuals contributed significantly to the success of this project.

REFERENCES

[1] White, R. M., "Dynamically Developed Force at the Bow of an Icebreaker", Ph.D. Thesis, Massachusetts Institute of Technology, 1965.

[2] White, R. M., "Prediction of Icebreaker Capability",Trans. RINA, vol. 112, 1970.

[3] Melberg, L. C., Lewis, J. W., Edwards, R. Y., Taylor, R. G. and Voelker, R. P., "The Design of Polar Icebreakers", Trans. SNAME Spring Meeting, Washington, D.C., April 1970.

[4] Nehrling, B. C. and Enzinger, S. W., "Grounded Stability Experiments on Polar Icebreakers", U.S. Naval Academy Report No. EW-13-86, March 1986.

Third International Conference on Stability of Ships and Ocean Vehicles, Gdańsk, Sept. 1986

STAB'86

DYNAMICAL STABILITY OF SUPPORT SHIP - DIVING BELL COMPLEX

P.A. Bogdanov; R.Z. Kishev

ABSTRACT

When investigating the interaction between the diving bell and the supporting ship, two basic problems arise, namely the determination of dynamic tensile force in the connecting line, which is directly connected with the diver's security, and the influence of the hanged load over the rolling motion and hence over the dynamical stability of the ship-bell complex.

The investigations in this report concern configurations with stern hoisters operating in low intensity beam seas. The dynamics of ship-bell complex is described in the frames of the linear hydrodynamic theory of ship motion for different mutual positions of the ship and the apparatus. The results from different experiments with similar configurations are summarized, and the presence of transient regimes is marked, during which the hydrodynamic heeling angle and tensile force in the rope increase several times in comparison with the static values. Schemes for evaluation of the complex stability are recommended with consideration of those phenomena and the extent of their influence on the exploitation restrictions is shown.

1. INTRODUCTION

As a result of the total expansion of human activity into the Ocean, the share of diving operations in port areas and open sea is constantly increasing. This activity is not new at all, but the new circumstances at which complicated undersea research, mounting and rescue operations are performed, the nonstandard diving and auxiliary equipment, the use of unspecialized or multipurpose support vessels, and last but not least - the wanted prolongation of operational period and hence the necessity for ensuring of damageless operation both in calm water and moderate waves - all these impose strong requirements to the structure and especially to the reliable dynamic characteristics of the complex, i.e. low amplitudes of motion, low dynamic loadings in the hoisting structure, increased dynamic stability. These requirements are purely operational as, because of the nonstandard character of the equipment and the operations, no particular classification rules exist, but only equalizational and not always proper and explicit estimations.

In most published investigations on hydrodynamic interaction between the ship and the hanged load, noteworthy examples of which are those of Berteaux (1) and Heller-Motherway (5), the basic attention is paid to the determination of the tensile force in the supporting line by reducing the problem to one degree of freedom spring mass system dynamics under harmonic excitation. In fact, the problem is much more complicated because of the presence of dynamic impulse loadings in the rope, which is directly connected to the security of divers, and because of the influence of the hanged load over the rolling motion characteristics and transverse stability. Here, an attempt is made for systematization of some theoretical and experimental results obtained at BSHC during the hydrodynamic investigations of some coastal ships used for supporting of rescue and diver operations.

2. FORMULATION OF THE MOTION PROBLEM

Consider the case of pure transverse motion of a ship equipped with stern-hoister for supporting diver apparatus, operating in small-amplitude regular beam seas. In addition, the ship is anchored in two points - with bow and stern anchors which are considered not to constrain the orbital movement but only the horizontal drift.

A standard set of reference frames is introduced according to Fig. 1, with GYZ - first movable (translational) coordinate system connected with the centre of gravity and GZ upwards, and O_{yz} - local coordinate system fixed to the top of

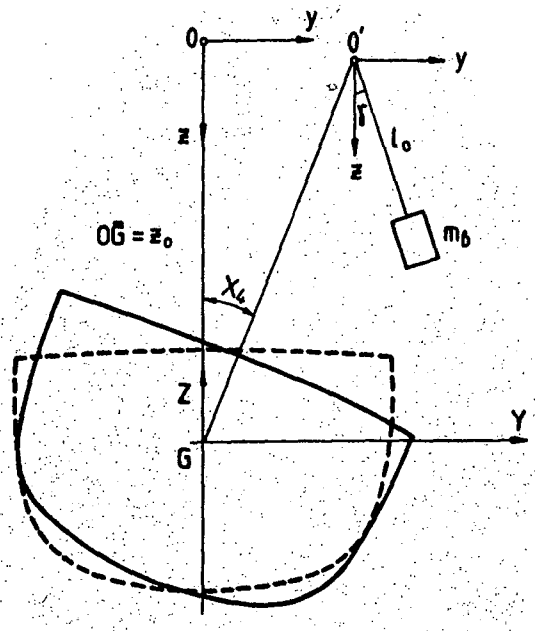

Fig. 1. Definition of coordinates

loading arm with 0_z pointed downwards.

In the course of work with the diver complex, 4 characteristic mutual positions can be distinguished as illustrated in Fig. 2:

A - apparatus loaded on deck;

B - apparatus hanged in air, acting as a pendulum load;

C - regime of transition through water surface;

D - apparatus deeply submerged.

When the diving bell is secured on deck, the ship motion may be described by the well known equations of motion, linearized at small excitation assumptions:

$$x_2 + 2\nu_2 x_2 = \xi_a \alpha_2 (\omega^2 \sin\omega t - 2\nu_2 \omega \cos\omega t) \quad (1)$$

$$x_3 + 2\nu_3 x_3 + n_3^2 x_3 = \xi_a \alpha_3 ((n_3^2 - m_3\omega^2)\cos\omega t - 2\nu_3 \omega \sin\omega t) \quad (2)$$

$$x_4 + 2\nu_4 x_4 + n_4^2 x_4 = \frac{2\pi}{\lambda} \xi_a x_4 n_4^2 \sin\omega t \quad (3)$$

where α_i-coefficients of exciting force reduction under ship body influence on wave motion;

n_i- natural motion frequency;

ν_i-nondimensional damping;

m_i-nondimensional added mass.

As can be seen from the above equations, the mutual influence between the three modes of motion is neglected because of smallness considerations described in detail in (2). As a result, the three equations become independent.

In the process of ship motion the point of hanging $O(0,z_o)$ will oscillate according to the law:

$$y = z_o \sin x_4 + x_2 \quad (4)$$

$$z = 2z_o - z_o \cos x_4 + x_3.$$

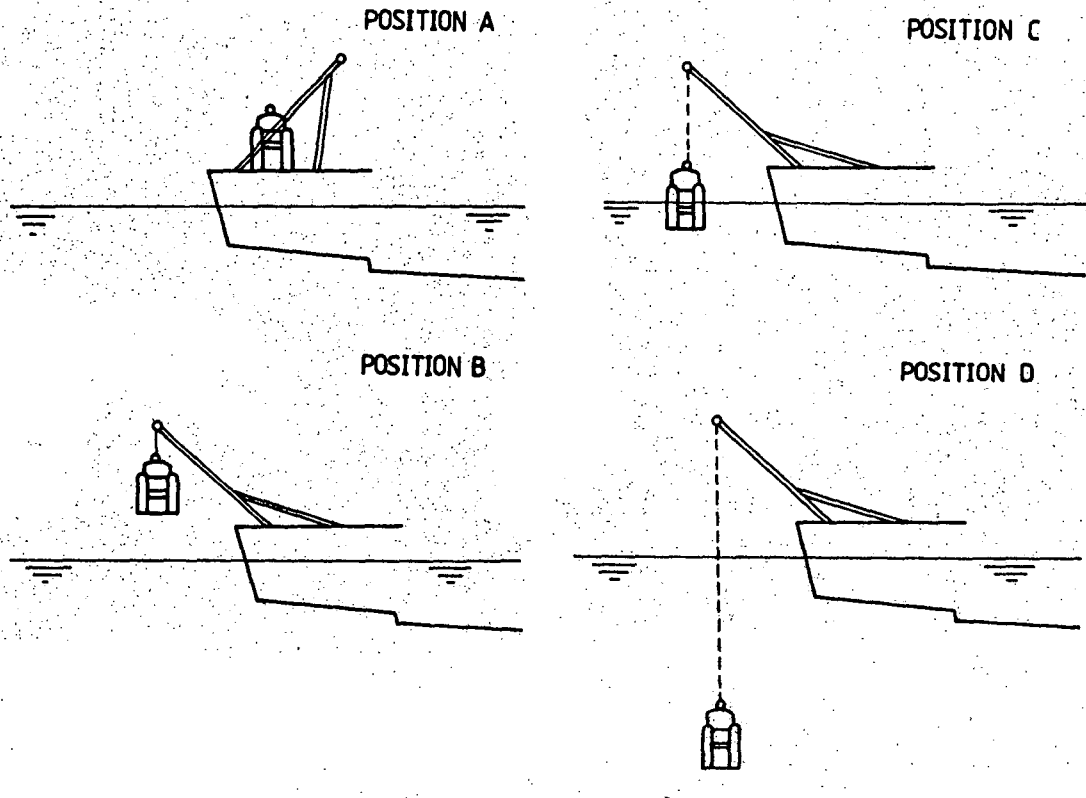

Fig. 2. Principle ship - bell configurations

When the apparatus is lifted in the air, as a result of the motion of the hanging point a kinematic excitation of the hanged load occurs, whose oscillation is described by the equations taken from (4) (see also Fig. 3a):

$$\gamma + \frac{1}{l_o}(y\cos\gamma + (g - z)\sin\gamma) = 0 \qquad (5)$$

$$-l_o\gamma^2 + y\sin\gamma - (g - z)\cos\gamma = -\frac{T_b}{m_b} \qquad (6)$$

The mass of the bell m_b is sufficiently small (1.5 - 2%D), hence the increase of the vertical force, acting on the ship (T_b-gm_b), is small and we can assume that the vertical motion is not influenced by the swinging of the load. The additional heeling moment is, consequently:

$$M_T = z_o T_b \sin(x_4 + \gamma^2) \qquad (7)$$

However, especially at great angles of inclination, this moment can reach up to 20% of the restoring moment and as a result, its influence should be taken into consideration in the roll motion equation (3), which becomes:

$$\ddot{x}_4 + 2\nu_4\dot{x}_4 + n_4^2 x_4 = \frac{2\pi}{\lambda}\xi_a\alpha_4 n_4^2 \sin\omega t + \frac{z_o T_b}{I_{44}+A_{44}}\sin(x_4 + \gamma) \qquad (8)$$

So, the behaviour of the ship-apparatus complex will be described by the mutual solving of the equations (1),(2), (4),(5),(6),(8).

When the bell is submerged into water, the interaction changes considerably. The flexibility of the rope in transverse direction and the hydrodynamic resistance of the apparatus give us grounds to accept that it will perform only vertical motions, equal to the motions of the hanging point and the line of the rope will pass always through the initial position of the coordinate centre.

According to Fig. 3b, the angle between the rope and the load mast will satisfy the condition

$$\frac{tg\gamma - 1}{tg\gamma + 1} = \frac{2}{2 + x_4}\,\frac{x_2 - z_o}{x_2 + z_o} \qquad (9)$$

in which the smallness of rolling motion angles is considered.

When the line lengthens during the submerging of the apparatus, the elasticity of the connection begins to influence considerably the formation of tensile force which,according to (1) and (3), may be expressed as:

$$T_b = pl_o + (gm_b - \gamma_w V_b) + \frac{2\pi}{\lambda}\alpha_z x_3 \qquad (10)$$

where α_z - amplitude reduction factor, depending on bell's inertia and damping and on the natural frequency of line's elastic vibrations as well.

According to the scheme of Fig. 3b, the additional heeling moment becomes:

$$M_T = z_o T_b \sin\gamma \qquad (11)$$

and the equation of rolling motion:

$$\ddot{x}_4 + 2\nu_4\dot{x}_4 + n_4^2 x_4 = \frac{2\pi}{\lambda}\xi_a\alpha_4 n_4^2 \sin\omega t + \frac{z_o T_b}{I_{44}+A_{44}}\sin\gamma \qquad (12)$$

where γ is evaluated according to equation (9).

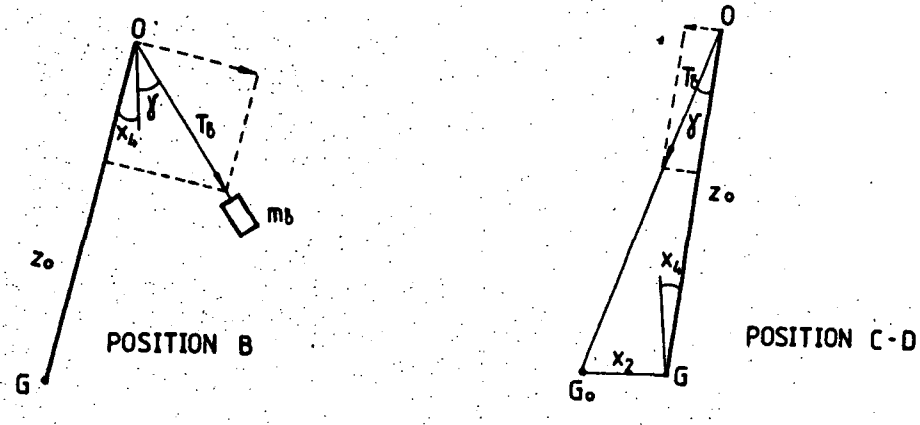

Fig. 3. Tension force orientation

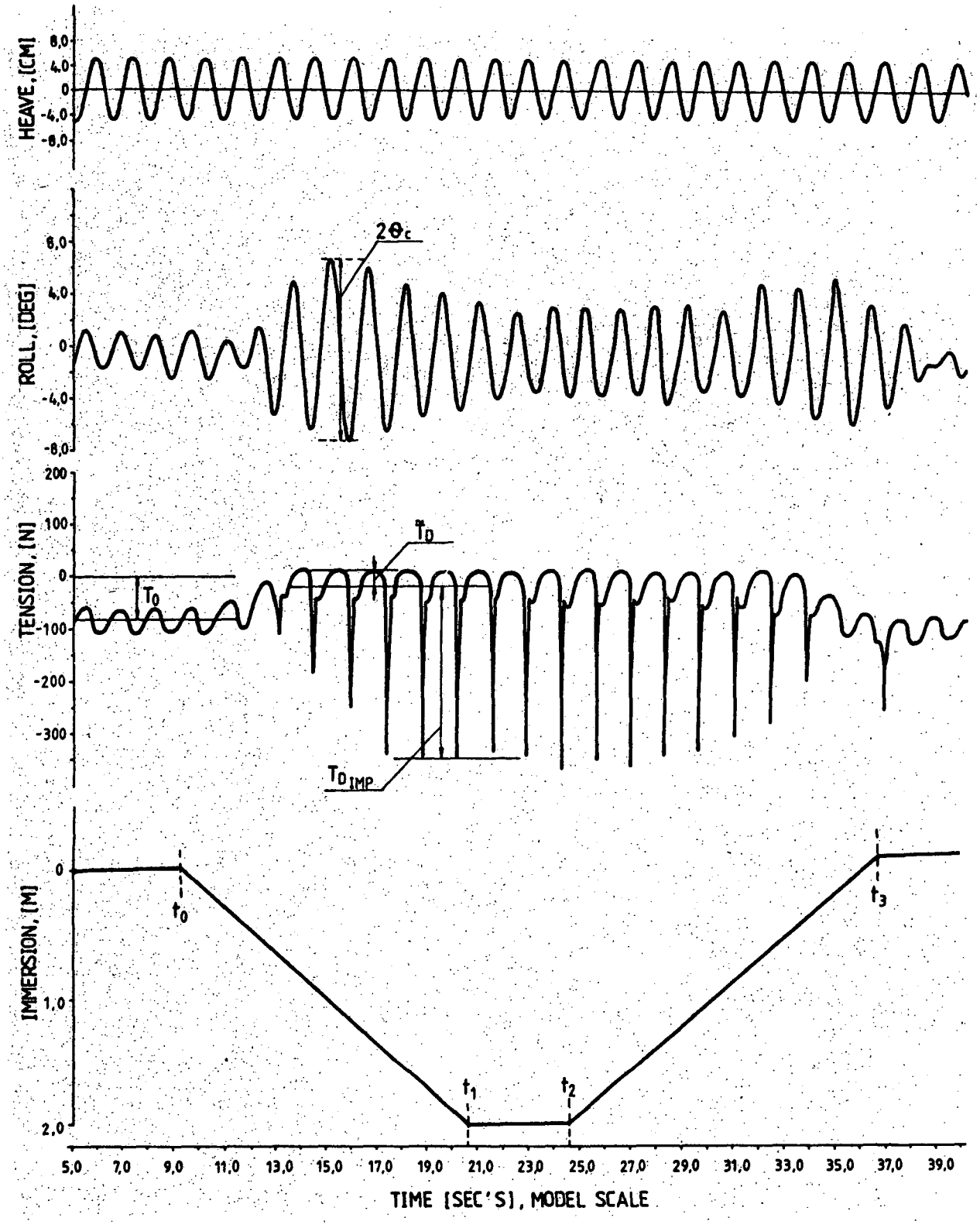

Fig. 4. Sample records of ship - bell complex responses in waves

In this case the dynamics of the complex is described by the set of equations (1),(2),(9) and (12).

The solving of both systems of differential equations for cases B and D according to the known numerical methods is not difficult. As can be seen, the solution is in the frames of harmonic excitation - harmonic reaction terms.

3. REVIEW OF EXPERIMENTAL RESULTS ON TENSION AND MOTION

During the last several years numerous tests were carried out (6) at BSHC for investigation of the interaction between the supporting ship and diving apparatus for different configurations of the complex, different ballast weights, different tests conditions (number of anchors and course angles), at regular and irregular seas, at fixed (quasisteady approach) and changeable depth of submergence. These parameters were not changed systematically as the tests were carried out separately at different times with large-scale models of existing or design projects under construction. Some general characteristics of the behaviour of ship - apparatus complex are presented in Fig. 4, summarizing the records of processes of vertical and rolling motion and the tension force in the connecting line, measured in regular waves with characteristics chosen in such a way that the reaction of the complex corresponds to the mean statistical values at irregular sea with intensity 3 Beaufort. The measurements are performed with constant speed of submerging, with stops in two positions - when the apparatus is on deck level (case B) and in operational position (case D). The moments of start and stop of the lift mechanism are denoted by t_0-t_3.

The results of the experiments may be summarized as follows:

3.1. Heave Motion

As is evident from Fig. 4, the vertical motion does not depend on the bell's position, which is in accordance with the theory. A complete illustration of this independence is given in Fig. 5, which summarizes the results of linear theory calculations and the measurements in irregular beam waves, taken at quasisteady apparatus positions corresponding to Fig. 2. The experimental transfer functions are directly obtained by dividing the rough linear spectra of motion and wave processes.

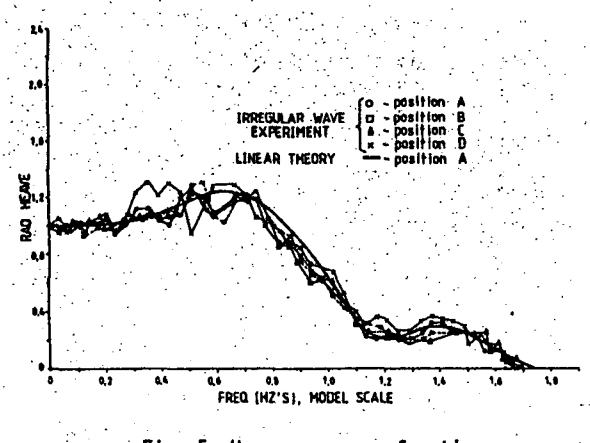

Fig. 5. Heave response function

3.2. Roll Motion

The ship dynamics in roll mode is more complicately connected with the apparatus's position.

The obvious relation between the mass of suspended load and rope length, on the one hand, and the ship roll natural frequency, on the other, may cause some amplification or, otherwise, reduction of roll amplitudes in position B compared with those in cruise position A. That, in fact, is one of general design as well as operational problems to solve by means of the set of equations (1)-(8).

Further, when the bell is submerged into the water, it begins to act as a damper as a result of both the body's resistance and the wave action. This leads to sudden increase of the heeling moment and of the rolling motion amplitude. This phenomenon, illustrated in Fig.4, is nonstationary and quickly slows down, as the results of quasisteady measurements show (Fig. 6 and Table 1), but it is this impulse increase of the rolling motion amplitude that may lead to loss of stability. To characterize this process, we use the relation:

$$K_\theta = \theta_c/\theta_A \qquad (13)$$

called rolling motion dynamics factor. An example of the dependence of K_θ on the wave intensity is shown in Fig. 7 as a result of experimental investigations because the nonstationarity of the process does not allow to obtain K_θ by harmonic excitation calculations in the frequency domain but requires modelling in time domain.

When deeply submerged in operational position, vertical wave action on the apparatus decreases and the motion process is steadying, which results in reducing of roll amplitudes down to their initial values, as shown in Table 1.

3.3. Line Tension

The tension in the rope strongly depends on the bell's position and is directly connected with the processes of motion. When the apparatus is lifted in air, the force in the rope fluctuates uniformly about the statical tension force $T=gm_b$ with amplitude T_B, which is not greater than 30% of T_o as shown in Table 2.

At passing through the free surface, the force begins to change independently and its mean value relatively decreases because of the lessening of apparatus weight during submerging.

However, as a result of the vertical ship motions and due to the bell's platform resistance, impulse tension forces appear. When reaching the ope-

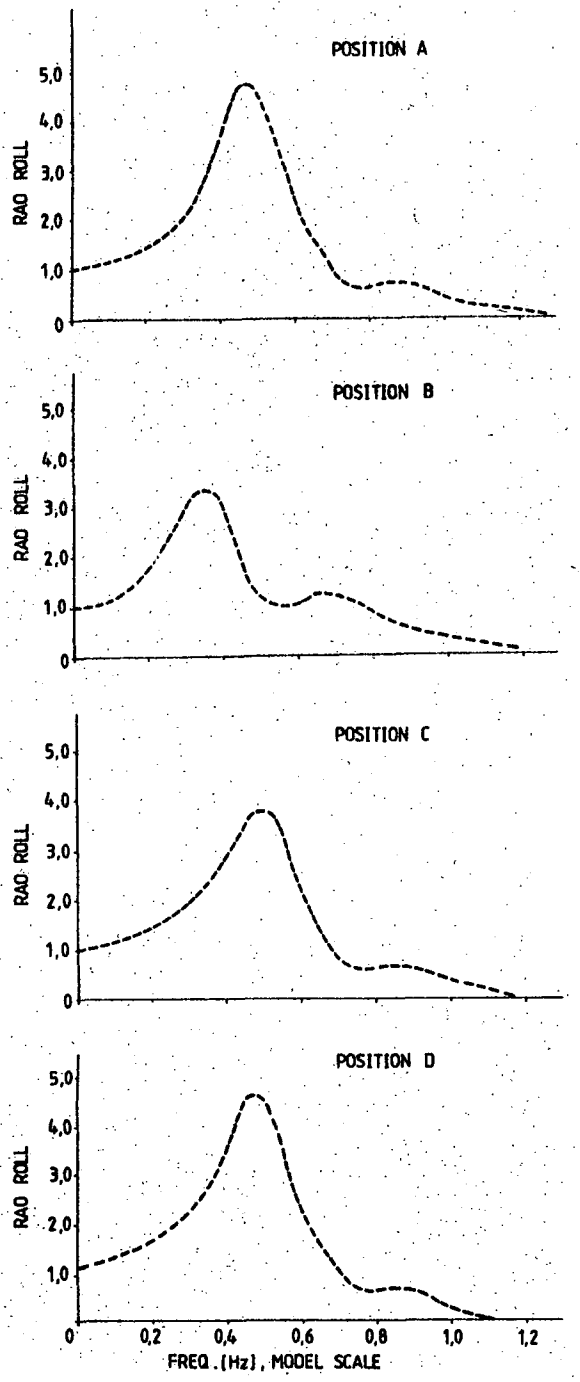

Fig. 6. Roll response functions at different bell positions

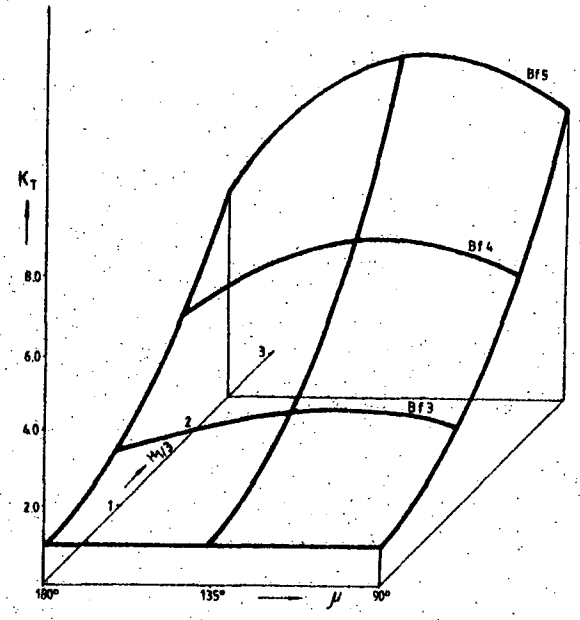

Fig. 7. Dynamical tension force amplification factor

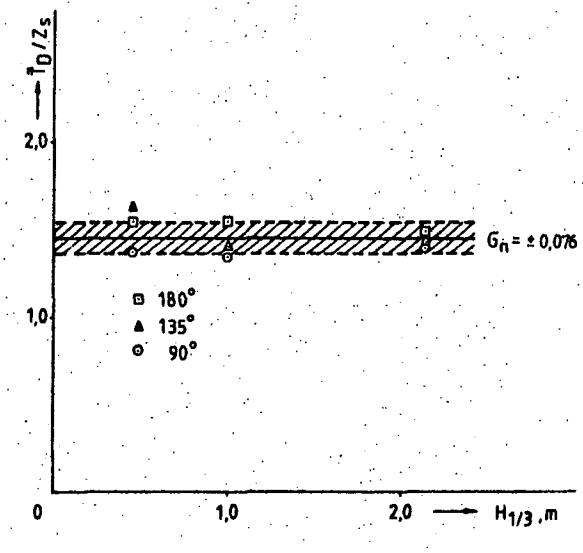

Fig. 8. Tension - motion ratio as a function of wave conditions

Table 1

Significant roll amplitudes at stationary bell positions, $\Theta_{1/3}$, deg				
Position	A	B	C	D
Bf 3	9.60	6.0	8.1	9.40
Bf 4	14.7	10.3	13.0	15.2
Bf 5	21.3	15.3	17.4	24.8

Table 2

Dynamical tension in position B, T_B/T_o, perc.		
Bf	Experiment, $m_b/M=1.6\%$	Theory, (eq.6)
2	15.8	17.2
3	24.8	21.1
4	29.3	26.7

ration position, the mean value of the force and of the shock impulses settles down. It is experimentally shown that their value - $T_{D_{IMP}}$ - is not influenced strongly by the depth of submerging but is several times greater than the static tension T_d. These impulses are of high frequency (about 7-8 ω) and according to the linear spectral theory are not considered when obtaining the mean low-frequency reaction T_D, which, as shown by equation (10) as well, is a linear function of the vertical displacement. This is illustrated in Fig. 8.

Similar to (13), a tension force dynamics factor may be introduced:

$$K_T = T_{MAX}/T_o, \qquad (14)$$

where T_{MAX} is obtained as $T_D + T_{D_{IMP}}$.

An example of the dependence of this factor on the wave amplitude and wave direction is shown in Fig. 9.

The pulling of the apparatus out of the water is characterized with the possibility of random single tension loading occurrence which may become equal to or greater than that in underwater position, as illustrated in Fig. 4.

4. STABILITY CONSIDERATIONS

The standard approach, recommended by the classification societies (8) for stability evaluation, consists in comparing the minimum capsizing moment at conventional motion amplitude - θ_m - with the exciting heeling moment:

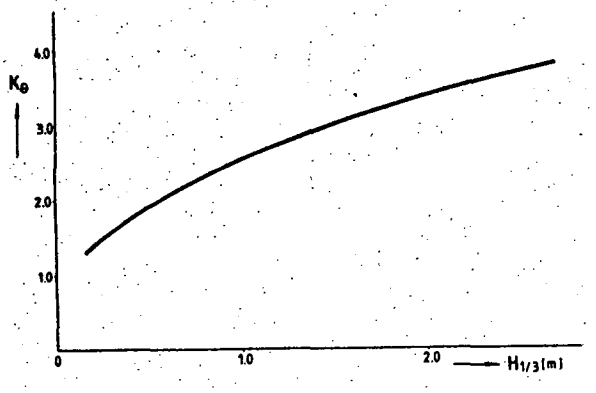

Fig. 9. Dynamical roll amplification factor

$$K = M_{MT}/M_v, \qquad (15)$$

where K is called basic siability criterion.

The determination of capsizing moment M_{MT} is illustrated in Fig. 10 for one of the investigated ships and the values of the design amplitude, the arm of dynamic stability and the basic criterion are given in Table 3. Comparing θ_m from Table 3 with the values of $\theta_{1/3}$ from Table 1, it may be concluded that the ship stability is ensured even at 5 Beaufort waves, when the standard requirements for admissible underwater operation conditions read 3 Beaufort. In addition, the ship satisfies all other classification requirements towards stability.

As was mentioned, however, at transient regimes the ship suffers from significantly greater motion angles and in operational position impulse line loading occurs. Both factors lead to aggravation of the stability, which may be evaluated in two ways:

- according to maximum dynamic heeling angle $\theta_c = K_\theta \cdot \theta_m$;
- according to impulse heeling moment as a function of the reference impulse velocity $V_I = 8z_s/\tau$.

The determination of the basic stability criterion according to the first method does not differ from the standard approach but the increased value of the reference angle leads to decreasing of the minimum capsizing moment and hence - to decreasing of the basic criterion, as shown in Table 3. In this case the limiting operation capability of the complex ship - bell is evaluated to be sea state 3 Beaufort.

The arm of the impulse heeling moment may be obtained directly from the diagram of dynamical stability if we have the value of impulse tension force and using equations (11) and (14). Another approach for determination of the arm d_{IMP} is recommended by Lugovsky (7):

$$d_{IMP} = \frac{V_I^2}{2g}(1 + A_{22})\, G\,(L,B,Z_g,Z_o), \qquad (16)$$

where A_{22} - sway added mass;
G - function of the hull geometry and hoister height.

Then the basic stability criterion is calculated as:

$$K = d_{MAX}/d_{IMP} - \Delta K, \qquad (17)$$

where d_{MAX} - dynamical stability arm corresponding to the statical stability diagram maximum;

ΔK - influence of the motion on the resulting heeling angle calculated at the steady value of roll angle θ_D.

The evaluations according to formula (17) are given in Table 3 from where it may be concluded that both approaches give comparable stability estimations which strongly decrease the limits of allowable exploitation conditions to not more than 3 Beaufort sea state.

Table 3

Evaluation of general stability criterion by different methods				
Approach		Conditional roll angle, θ_m	Overturning moment arm, d	General stability criterion, K
Register rules		24.0^0	0.11	2.09
Transitional roll angles approach	Bf 3	23.5^0	0.11	2.09
	Bf 4	49.4^0	0.03	0.58<1
Impulse loading approach	Bf 3	9.4^0	0.146	2.84
	Bf 4	15.2^0	0.048	0.93<1

5. CONCLUSIONS AND RECOMMENDATIONS

The comparison of the experimental results, obtained in dynamic mode of lowering and lifting of the bell with those from calculations and experiments at quasisteady approach, shows that the latter may be misleading in view of the values of maximum heeling angle for which the stability is evaluated. For theoretical investigations of the problem it is necessary to perform analysis in time domain. For engineering calculations the experimentally obtained dynamic coefficients for the maximum heeling- K_θ and impulse line loading - K_T, may be used taking into consideration their mutual connection with the geometric, inertia and dynamic characteristics of the ship - bell complex.

It is recommended that the evaluation of the dynamic stability for such configurations to be performed according to one of the proposed methods - with account of the maximum dynamic angle or of the impulse heeling moment as a function of the available experimental or design data. It may be considered that both methods give similar exploitation restrictions.

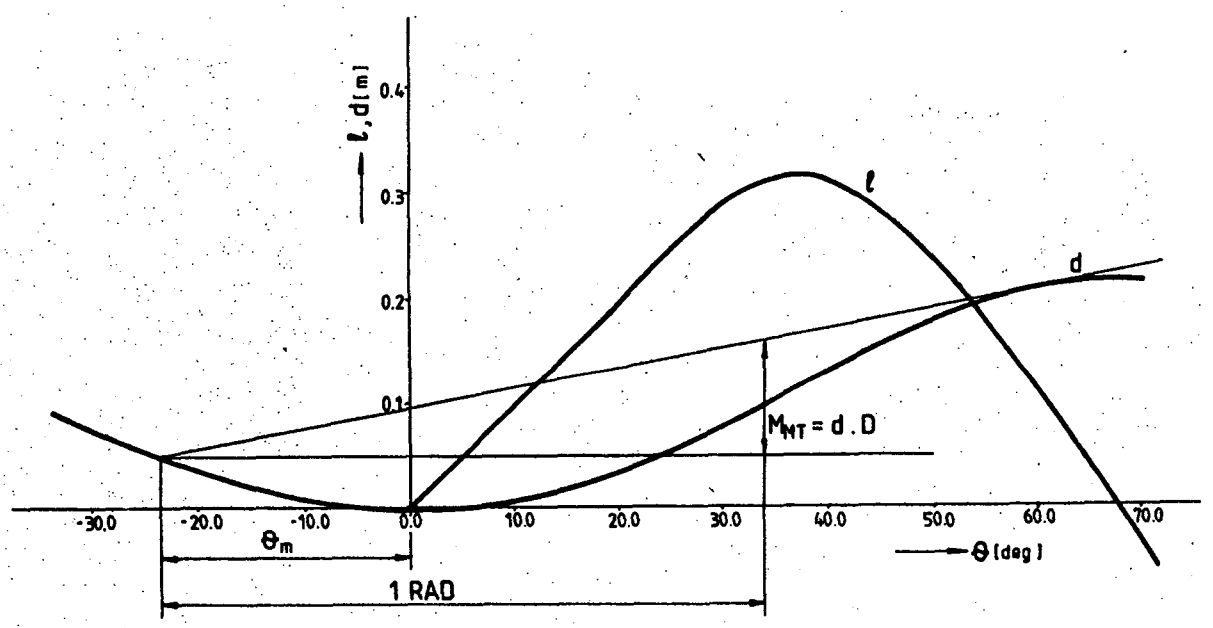

Fig. 10. Graphical evaluation of complex dynamical stability

NOMENCLATURE

B	- breadth of ship
d	- arm of dynamical stability
D	- weight displacement
g	- gravity accelerations
h_0	- initial metacentric height
$H_{1/3}$	- significant wave height
K	- basic stability criterion
K_θ	- dynamic coefficient of roll angle
K_T	- dynamic coefficient of line tension force
l	- arm of statical stability
l_0	- line length
L	- ship's length
m_b	- mass of the diving bell
M	- ship mass
M_T	- additional heeling moment from the tension in connecting line
M_ν	- heeling moment from wind action
M_{MT}	- minimum capsizing moment
p	- relative weight of the line
t_i	- moments of time expressing the passing of the bell through different basic positions at lowering and lifting
T_o	- static line loading
T_b	- general line force
$T_{A,B,C,D}$	- dynamic line force at every characteristic position
V_b	- volume displacement of apparatus
x_i	- modes of motion i = 2 - sway i = 3 - heave i = 4 - roll
z_o	- height of loading arm
z_s	- significant value of stern vertical motion
z_g	- vertical coordinate of the centre of gravity
γ	- angle between rope line and vertical axis
γ_w	- specific water weight
ξ_a	- amplitude of harmonic wave
$\theta_{A,B,C,D}$	- significant amplitudes of roll motion for characteristic positions of the apparatus
θ_m	- maximum design heeling angle
α_i	- correction coefficients
λ	- wave length
μ	- course angle
τ	- mean wave period
ω	- wave frequency

REFERENCES

1. Berteaux G. - Buoy Engineering, Leningrad, Sudostroenie Publ., 1979.

2. Boroday I., Netzvetaev Y. - Seakeeping of Ships, Leningrad, Sudostroenie Publ., 1982.

3. Cohen M. - An Experimental Analysis of the Dynamics of a Submerged Cradle in a Seaway, NEJ,vol. 92, No.1, 1980.

4. Gorshkov I., Machorin N. - Loads Transfer at Sea, Leningrad, Sudostroenie Publ., 1977.

5. Heller S., Motherway D. - Comparative Heave Dynamics of Two Unusual Ship Configurations for Recovery of Submersibles, NEJ, vol. 83, No.5, 1971.

6. Kishev R., Radev D., Botev J. - Model Investigation of Support Ship - Diving Bell Interaction in Waves, BSHC Internal Report, 1984.

7. Lugovsky V. - Ship Stability Regulations - Marine Transport Publ., Moscow, 1963.

8. Rules for Classification and Construction of Sea-Going Ships - Part IV - Stability, Bulgarian Register of Shipping, Varna, 1975.

Peter BOGDANOV, Dr., Honoured Scientist,
Director BSHC
Roumen KISHEV, Dr., Research Scientist
Bulgarian Ship Hydrodynamics Centre
9003 Varna, Bulgaria

Third International Conference on Stability of Ships and Ocean Vehicles, Gdańsk, Sept. 1986

STAB'86

APPLICATION OF CATASTROPHE THEORY TO NONLINEAR ROLLING MOTION OF SHIPS

R.L. Roy Choudhury; S.D. Nigam

ABSTRACT

The equation governing the nonlinear rolling motion [1] of a ship is solved by the method of averaging [4,5]. It is found that the respective amplitudes in the main and ultraharmonic resonance regions satisfy cubic equations while in the subharmonic case a quadratic equation with co-efficients depending on the parameters of the problem. These equations are studied by the methods of catastrophe theory and the domains of stability and instability are delineated in the control-parameter space. When a fifth degree term is included in the restoring moment, the amplitude satisfies an algebraic equation of seventh degree. This is also studied in the paper.

1. INTRODUCTION

The rolling amplitude of ships in waves is large compared to other modes of oscillation. The governing equation is nonlinear. The problem has been investigated extensively by model tests and also by analytical-numerical methods but the results are still far from being satisfactory. The difficulty is two fold: firstly, in developing a proper mathematical model and solving it analytically; secondly, in the presentation of the results in a unified way. For example, even after detailed numerical computations over a range of the values of the parameters occurring in the equation it is not possible to make general statements about the effect of varying certain parameters on the amplitude.

In this paper, the equation proposed by Cardo et al [1,2] is solved by the method of averaging [4,5] and the amplitude equation is discussed using the methods of Catastrophe Theory which makes a separate stability analysis unnecessary. The method is ideally suited for such problems and gives a unified picture of the way the amplitude varies with different parameters. The results obtained by this method are in complete agreement with those of Cardo et al in respect of main, subharmonic and ultraharmonic resonance. The equation for rolling after inclusion of fifth degree term in the restoring moment is also solved.

2. SOLUTIONS OF THE EQUATION OF ROLLING MOTION

The equation governing the rolling motion of a ship proposed by Cardo et al [1] in non-dimensional form is

$$\ddot{\theta}+(2\mu'+\delta_1'\theta^2)\dot{\theta}+\delta_2'\dot{\theta}^3+\omega_o^2\theta+\alpha_3'\theta^3 = A'\cos\omega t. \quad (1)$$

He has solved the equation with the Bogoliubov-Krylov-Mitropolsky asymptotic method.

In the present paper, the equation (1) is solved by the method of averaging [4,5]. We rewrite (1) as

$$\ddot{\theta}+\omega_o^2\theta = -\epsilon\left[(2\mu+\delta_1\theta^2)\dot{\theta}+\delta_2\dot{\theta}^3+\alpha_3\theta^3 - A\cos\omega t\right] \quad (2)$$

where ϵ is a small parameter. The equation (2) is expressed as

$$\dot{y} = -\omega_o^2\theta-\epsilon\left[(2\mu+\delta_1\theta^2)\dot{\theta}+\delta_2\dot{\theta}^3+\alpha_3\theta^3-A\cos\omega t\right], \quad y = \dot{\theta} \quad (3)$$

In the main resonance region we write

$$\omega_o^2 - \omega^2 = \epsilon\Omega \quad (4)$$

Since the solution in this region is

expected to be of frequency ω, the van der Pol's transformation

$$\begin{bmatrix} u \\ v \end{bmatrix} = \begin{bmatrix} \cos\omega t & -\omega^{-1}\sin\omega t \\ -\sin\omega t & -\omega^{-1}\cos\omega t \end{bmatrix} \begin{bmatrix} \theta \\ \dot{\theta} \end{bmatrix} \quad (5)$$

is appropriate and averaging is required to be carried out over $T = 2\pi/\omega$, [4]. Using (5), the equations (3) can be written as

$$\dot{u} = \frac{\epsilon}{8\omega}\left[-4\Omega v - 8\omega\mu u - (\delta_1\omega+3\delta_2\omega^3)(u^2+v^2)u - 3\alpha_3(u^2+v^2)v\right] + \epsilon\left\{A_1\cos 2\omega t + B_1\sin 2\omega t + A_2\cos 4\omega t + B_2\sin 4\omega t\right\} \quad (6a)$$

$$\dot{v} = \frac{\epsilon}{8\omega}\left[4\Omega u - 8\omega\mu v - (\delta_1\omega+3\delta_2\omega^3)(u^2+v^2)v + 3\alpha_3(u^2+v^2)u - 4A\right] + \epsilon\left\{C_1\cos 2\omega t + D_1\sin 2\omega t + C_2\cos 4\omega t + D_2\sin 4\omega t\right\} \quad (6b)$$

where A,B,C,D are functions of u,v and coefficients in (2). The associated autonomous averaged (to order ϵ) equations are

$$\dot{u} = \frac{\epsilon}{8\omega}\left[-4\Omega v - 8\omega\mu u - (\delta_1\omega+3\delta_2\omega^3)(u^2+v^2)u - 3\alpha_3(u^2+v^2)v\right] \quad (7a)$$

$$\dot{v} = \frac{\epsilon}{8\omega}\left[4\Omega u - 8\omega\mu v - (\delta_1\omega+3\delta_2\omega^3)(u^2+v^2)v + 3\alpha_3(u^2+v^2)u - 4A\right] \quad (7b)$$

Putting

$$u = \bar{x}\cos\phi, \quad v = \bar{x}\sin\phi \quad (8)$$

one obtains

$$\dot{\bar{x}} = \frac{\epsilon}{8\omega}\left[-8\omega\mu\bar{x} - (\delta_1\omega+3\delta_2\omega^3)\bar{x}^3 - 4A\sin\phi\right] \quad (9a)$$

$$\bar{x}\dot{\phi} = \frac{\epsilon}{8\omega}\left[4\Omega\bar{x} + 3\alpha_3\bar{x}^3 - 4A\cos\phi\right]. \quad (9b)$$

The constant solutions of (9a) and (9b) are obtained by setting $\dot{\bar{x}} = 0, \dot{\phi} = 0$. Then $\bar{x}$ and ϕ correspond to the amplitude and phase of the nearly periodic solution of (1), [5]. The equation for $R = \bar{x}^2$ is

$$m_1R^3+m_2R^2+m_3R+m_4 = 0, \quad (10)$$

where

$$m_1 = 9\alpha_3^2+\omega^2(\delta_1+3\delta_2\omega^2)^2 \quad (11)$$

$$m_2 = 24\alpha_3\Omega+16\omega^2\mu(\delta_1+3\delta_2\omega^2) \quad (12)$$

$$m_3 = 16\Omega^2+64\omega^2\mu^2 \quad (13)$$

$$m_4 = -16A^2 \quad (14)$$

The phase is given by

$$\tan\phi = -\left[8\omega\mu+(\delta_1\omega+3\delta_2\omega^3)\bar{x}^2\right]/(4\Omega+3\alpha_3\bar{x}^2). \quad (15)$$

The equations (10) and (15) agree with those given in [1]. By the substitution

$$R = y+h, \quad h = -m_2/3m_1 \quad (16)$$

(10) reduces to

$$y^3+dy+e = 0, \quad (17)$$

where

$$d = 3h^2+(2m_2h+m_3)/m_1 \quad (18)$$

$$e = h^3+(m_2h^2+m_3h+m_4)/m_1. \quad (19)$$

The results are discussed in the next Section.

In subharmonic resonance $\omega \approx 3\omega_o$, the solution of (1) is expected to be of the form, [4]

$$r\cos(\omega t/3+\phi_1)+B\cos\omega t, \quad (20)$$

where r and ϕ_1 are the amplitude and phase of the subharmonic component of the oscillation and

$$B = A/(\omega_o^2-\omega^2). \quad (21)$$

The van der Pol's transformation in this case is

$$\begin{bmatrix} u \\ v \end{bmatrix} = \begin{bmatrix} \cos\frac{\omega t}{3} & -\frac{3}{\omega}\sin\frac{\omega t}{3} \\ -\sin\frac{\omega t}{3} & -\frac{3}{\omega}\cos\frac{\omega t}{3} \end{bmatrix} \begin{bmatrix} \theta+B\cos\omega t \\ \dot{\theta}-\omega B\sin\omega t \end{bmatrix} \quad (22)$$

and the averaging is required to be carried out over $T = 6\pi/\omega$. Following the same procedure as in the previous case, the equation for the square of the amplitude $r^2 = x$ is ($u = r\cos\phi_1$, $v = r\sin\phi_1$),

$$(m_1^2+m_3^2)x^2+\left[2(m_1m_2+m_3m_4)-(m_5^2+m_6^2)\right]x + (m_2^2+m_4^2) = 0 \quad (23)$$

where m's are functions of the coefficients of (1) and B. The phase is given by

$$\tan 3\phi_1 = (P_1P_3-P_2P_4)/(P_1P_4+P_2P_3) \quad (24)$$

where

$$P_1 = (m_1r^2+m_2)r, \quad P_2 = (m_3r^2+m_4)r \quad (25)$$

$$P_3 = m_5r^2, \quad P_4 = m_6r^2.$$

The equations (23) and (24) agree with

those obtained by Cardo et al [1]. The equation (23) can be written as

$$x^2+ax+b = 0, \qquad (26)$$

where

$$a = m_8/m_7 \quad , b = m_9/m_7 \qquad (27)$$

$$m_7 = \frac{9}{16}\alpha_3^2 + \frac{\omega^2}{1296}(3\delta_1+\delta_2\omega^2)^2 \qquad (28)$$

$$m_8 = \frac{B^2}{16}\left[27\alpha_3^2 + \frac{\omega^2}{27}\{9(\delta_1+\delta_2\omega^2)^2 + 28\delta_1\delta_2\omega^2\}\right] + \frac{\alpha_3}{6}(9\omega_o^2-\omega^2) + \frac{\mu\omega^2}{27}(3\delta_1+\delta_2\omega^2) \qquad (29)$$

$$m_9 = \frac{B^4}{36}\left[81\alpha_3^2+\omega^2(\delta_1+3\delta_2\omega^2)^2\right] + \frac{B^2}{9}\left[3\alpha_3(9\omega_o^2-\omega^2) + 2\mu\omega^2(\delta_1+3\delta_2\omega^2) + \frac{1}{81}(9\omega_o^2-\omega^2)^2 + \frac{4}{9}\omega^2\mu^2\right]. \qquad (30)$$

The case of the ultraharmonic resonance $\omega_o \approx 3\omega$ can be solved by a transformation similar to (22) by replacing $\omega/3$ by 3ω and averaging over $T = 2\pi/\omega$. The equation for the determination of the amplitude of the ultraharmonic component has a form similar to (17). This case is not discussed in this paper.

A more refined version of (2) is considered by introducing a fifth degree term in the restoring moment:

$$\ddot{\theta}+\omega_o^2\theta = -\epsilon\left[(2\mu'+\delta_1'\theta^2)\dot{\theta}+\delta_2'\dot{\theta}^3+\alpha_3'\theta^3-A'\cos\omega t\right] - \epsilon^2\alpha_5'\theta^5. \qquad (31)$$

This equation is proposed in [1] but solutions are not given. Here we find its solution in the main resonance region $\omega \approx \omega_o$ by using the transformation (5). The averages of order ϵ for $\dot{u}$ and $\dot{v}$ are given by (7a) and (7b) respectively. The averages of order ϵ^2 are calculated by the method in [4]. The algebra is rather lengthy and is omitted. The equation for the square of the amplitude $r^2=R$, is

$$R^7+a_6R^6+a_5R^5+a_4R^4+a_3R^3+a_2R^2+a_1R-a_o=0. \qquad (32)$$

With $R = x+h$, $h = -a_6/7$ (32) becomes

$$x^7+ax^5+bx^4+cx^3+dx^2+ex+f = 0. \qquad (33)$$

The results are discussed in the next Section.

3. RESULTS

In the discussion of the results μ, δ_1, and δ_2 are assumed positive since they are damping coefficients.

3.1 Main Resonance of Equation (1)

The amplitude of (1) is $\bar{x} = (y+h)^{1/2}$, where y is obtained from (17) which is a Simple Cusp Catastrophe [6]. However in this case the manifold is restricted to $-h \leq y < \infty$, for $\bar{x}$ to be real. This results in a Constraint Cusp Catastrophe [3] whose geometry is shown in Fig. 1, obtained by truncating the manifold of the Simple Cusp by a plane y = -h and retaining the portion $y \geq -h$.

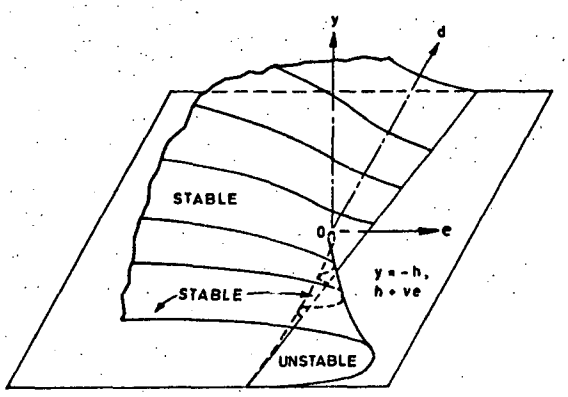

FIG.1-SECTION OF THE CATASTROPHE MANIFOLD OF THE POTENTIAL $\frac{1}{4}y^4 + \frac{1}{2}dy^2 + ey$ by $y=-h, h \cdot ve$

While the Simple Cusp is controlled by two parameters d and e, the constraint introduces an additional parameter h. The projection of the Simple Cusp on the d-e plane is shown in Fig. 2, the bifurcation lines being OA and OB. y jumps up to large values when the control point (d,e) crosses OB from right to left and jumps down from a peak value when this crosses OA from left to right (Fig. 2). Large positive h retains all the essential features of the simple cusp (Fig. 1); while truncation at y = -h, h<0, eliminates the line OB completely along with the origin O and retains only a portion of the line OA. Coming back to the solution of (1), an examination of (11) to (19) shows that

m_1 is always positive and hence the sign of h is opposite to that of m_2;

when α_3 is negative the peak amplitudes occur in the range of Λ positive and vice versa. Hence the large term $24\alpha_3\Lambda$ in m_2 is negative in this range of importance. The other positive term is much smaller at

least for the case α_3 negative. Hence m_2 is negative generally, and therefore h is large positive. It can become negative for the case α_3 positive.

Using (17) computations are carried out to find the maximum roll amplitudes for the ship 'Lucie Schulte' [2] . The results are plotted in Fig. 6, curve a, and they agree with those of Cardo.

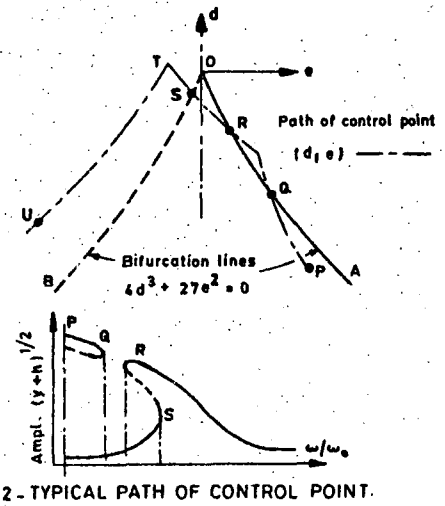

FIG. 2 - TYPICAL PATH OF CONTROL POINT. ω INCREASING (A = CONST.) AND ITS EFFECT ON AMPL. [EQN. (17)]

The path followed by the control point (d,e) with ω/ω_o increasing is schematically shown in Fig. 2 for the case A = 0.030, along with the response curve. The points Q,R,S where the path crosses the bifurcation lines are marked. The amplitude response shows a isolated region PQ of very large amplitude at very low ω/ω_o, which cannot be reached either with increasing or decreasing ω/ω_o. It is seen from the calculations that as the excitation amplitude is increased the points Q and R approach each other and coalesce when A is larger than 0.03 providing 'access' to the isolated region and results in the possibility of large amplitudes at low frequencies. This is also reported in[5]where it is mentioned that this causes the system to 'blow up', thus setting an upper limit of excitation amplitude for the system.

3.2 Subharmonic Oscillations of (1)

The square of the amplitude $r^2 = x$ is given by (26). Since $x \geq 0$, this equation represents a 'Constraint Fold Catastrophe' [3] ; its manifold is shown in Fig. 3, controlled by the two parameters a and b. Examination of (27) to (30) shows that m_7 is always positive and hence the signs of a and b are same as those of m_8 and m_9

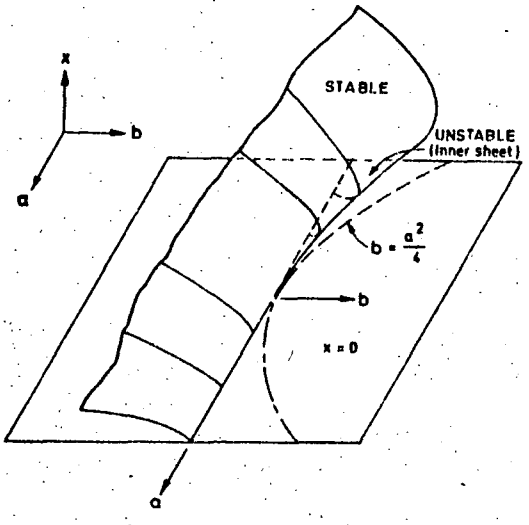

FIG. 3. CATASTROPHE MANIFOLD OF THE POTENTIAL $\frac{1}{3}x^3 + \frac{1}{2}ax^2 + bx$ (with constraint $x \geq 0$)

respectively. Further, $\alpha_3(9\omega_o^2 - \omega^2)$ is the only term which can be negative in m_8 and m_9. It is also observed that

m_9, in general, is positive because of the large positive terms in (30); m_8 can be negative either when

α_3 positive and $\omega \geq 3\omega_o$ or

α_3 negative and $\omega \leq 3\omega_o$.

Hence in general, a and b are positive and consequently x is zero, Fig. 3. Non zero amplitude is possible under the very restricted condition that m_8 be negative and in addition $b \leq a^2/4$; the threshold line being given by $b = a^2/4$. The value of B for any point on this line can be then calculated using (28),(29) and (30) and the threshold value of the excitation amplitude A is given by (21). It is also to be noted that along the fold line $b = a^2/4$, $x = -a/2$ and hence the amplitude $r = (-\frac{a}{2})^{1/2}$, $a < 0$.

a and b are calculated over a range of ω/ω_o for the two cases considered by Cardo et al [1] and they are given in Tables I and II. It is seen that b is slightly less than $a^2/4$ over the range of ω/ω_o indicating that the control points (a,b) are almost coincident with the

Table I - Calculated values of the coefficients (α_3 negative). ω_o = 1.0, A=0.2, α_3 = -1.75, μ= 0.005, δ_1 = 0.01, δ_2=0.01.

ω/ω_o	10^2a	10^3b	$10^3a^2/4$	Ampl.
2.40	-54.325	73.345	73.781	0.521
2.60	-37.562	35.094	35.273	0.433
2.80	-19.382	9.362	9.391	0.311
2.84	-15.578	6.059	6.067	0.279

projection of the fold line, but just within the area covered by the fold (Fig. 3). One unstable and one stable value of amplitude can occur in this region, the unstable value being always less than the stable one. In the vicinity of the fold line, the stable amplitudes can be approximated by those along the fold line and are shown in the Tables. These are in agreement with the results in [1]. As ω/ω_o tends to 3, the parameter a becomes positive and the subharmonic oscillations disappear.

Table II - Calculated values of coefficients (α_3 positive). ω_o = 1.0, A=0.2, α_3 = 4.00, μ= 0.005, δ_1 = 0.01, δ_2=0.01.

ω/ω_o	10^2a	10^3b	$10^3a^2/4$	Ampl.
3.12	- 5.282	0.695	0.698	0.163
3.20	- 9.044	2.036	2.045	0.213
3.40	-18.855	8.868	8.887	0.307
3.60	-29.248	21.363	21.387	0.382

3.3 Main Resonance of Equation (31)

The square of the amplitude, R=x+h, is obtained by solving (33). Equation(33) is the manifold of the Star Catastrophe, Fig. 4, taken from [7]. The upper part of this figure shows the order in which the extrema of the potential occur with increasing x and shows that the 'Star' manifold can be considered as being constructed by the apposition of two 'Simple Cusps' and a 'Swallowtail'. The lower part of the figure shows schematically the arrangement of the pleats of the manifold. The regions of minima and maxima on this surface correspond to the stable and unstable values of x and the fold lines are the bifurcation sets. As the six dimensional control point (a,b,c,d,e,f) moves, it can be 'covered' by three, two and one pleat or none giving rise respectively to 7,5 and 3 or one real root of x. Also it is important to note that among the sets of 7,5 or 3 roots, the maximum value corresponds to a minima of V followed alternately by maxima and minima and the least

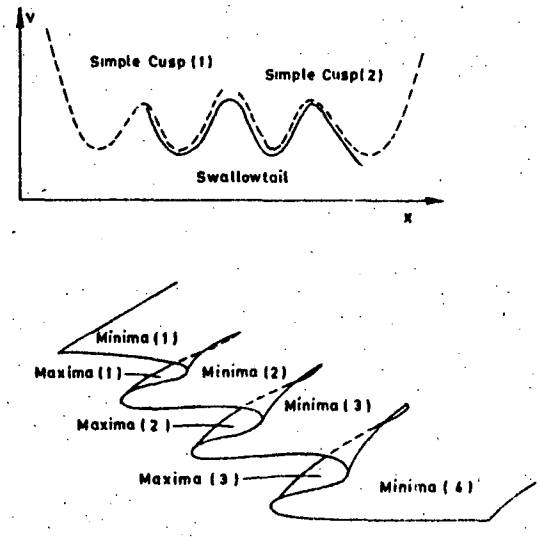

FIG. 4 - SCHEMATIC ORGANISATION OF THE STAR CATASTROPHE POTENTIAL. $V = \frac{1}{8}x^8 + \frac{a}{6}x^6 + \frac{b}{5}x^5 + \frac{c}{4}x^4 + \frac{d}{3}x^3 + \frac{e}{2}x^2 + fx$

value is again a minima. On the bifurcation lines the successive minima and maxima coalesce. When there is only one root it is a minima. These facts can be made use of to identify the stable and unstable solutions of (33), Fig. 5. There is a constraint in the solution of (33), namely, $x \geq -h$. This results in a constraint catastrophe as seen from the earlier discussion

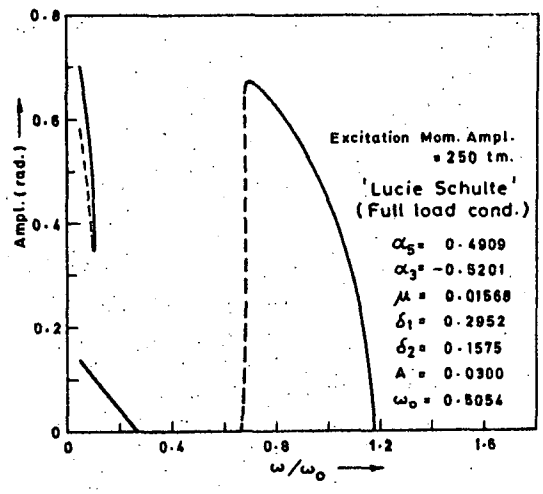

FIG.5 - AMPL. RESPONSE WITH α_5 IN RESTORING MOMENT.

of the solution of equation (1), necessitating the truncation of the manifold by the plane x = -h. From the many projections of the star catastrophe in [7], it can be generally said that only 3 or 1 root of x is likely to be met over a very large part of the parameter space.

Computations are carried out to find the maximum amplitude of roll of the ship 'Lucie Schulte', using equation (33) and

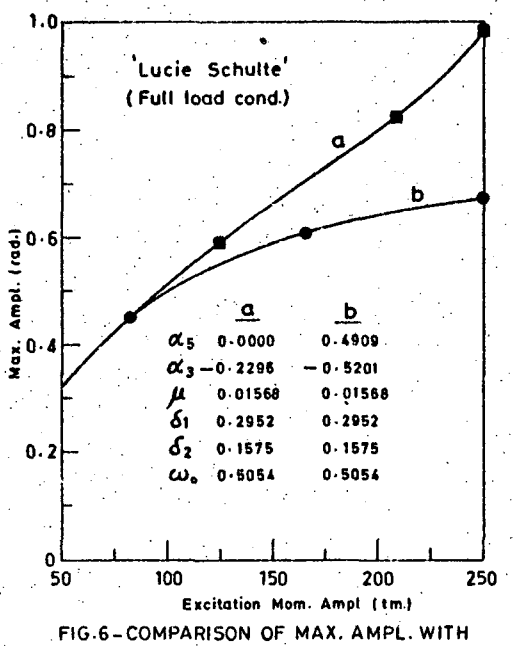

FIG.6-COMPARISON OF MAX. AMPL. WITH AND WITHOUT α_5 IN RESTORING MOM.

the results are presented in Fig. 6, curve b. The righting moment curve is generated from the data given in [2]. The coefficients α_3 and α_5 are determined by fitting a fifth degree odd polynomial to this curve. It shows an isolated region of large amplitude at low frequency, similar to the solution of (1), Fig. 2. The peak response is sharper, Fig. 5; the roll amplitudes are considerably lower, Fig. 6.

4. CONCLUSION

(i) Catastrophe manifolds related to the amplitude of rolling are presented in Figs. 1,2,3 and 4. They give a unified global picture of the domain of stability and instability in the control-parameter space. Thus, it is possible to see the effect of the variation of parameters on the nature of the solution.

(ii) Inclusion of the fifth degree term in the righting moment sharpen the peak response, Fig. 5; the maximum roll amplitudes are reduced considerably at higher values of the excitation amplitude A. However, the advantage progressively reduces to zero as the excitation level decreases, Fig. 6.

NOMENCLATURE

A	= Non-dim.. excitation amplitude.
B	= Amplitude of nonresonant component of response.
a,b,c, d,e,f	= Control parameters as defined.
θ	= Rolling angle.
α_3, α_5	= Non-dim. coefficients of the cubic & fifth degree terms in restoring moment.
μ, δ_1, δ_2	= Non-dim. damping coefficients.
ω_o, ω	= Non-dim. natural frequency of roll & excitation respectively.

REFERENCES

1. Cardo,A., Francescutto,A.,Nabergoj,R - Ultraharmonics and subharmonics in the rolling motion of a ship: Steady state solution, ISP,Vol.28, No.236,1981,pp234-251.

2. Cardo,A., Ceschia,M.,Francescutto,A. Nabergoj,R. - Effects of the angle-dependent damping on the rolling motion of ships in regular beam seas, ISP, Vol.27, No.310, 1980, pp.135-138.

3. Gilmore,R. - Catastrophe theory for scientists and engineers, John Wiley & Sons. 1981, pp.462-467.

4. Guckenheimer,J. and Holmes,P. - Nonlinear Oscillations, Dynamical systems and Bifurcations of vector fields, Springer Verlag, 1983, pp.167-184.

5. Holmes,P.J. and Rand,D.A. - The bifurcations of Duffing's equation: An application of catastrophe theory, J. of Sound and Vib., Vol.44, No.2, 1976, pp.237-253.

6. Poston,T and Stewart,I. - Catastrophe theory and its applications, Pitman, 1978, pp.172-180.

7. Woodcock,A.E.R. and Poston,T. - A geometrical study of the elementary catastrophes, Springer Verlag, 1974, pp.41 and 212.

R.L. ROY CHOUDHURY, Assistant Professor Naval Architecture,
S.D. NIGAM, Formerly Professor of Mathematics,
Indian Institute of Technology,
Madras 600036, India.

Third International Conference on Stability of Ships and Ocean Vehicles, Gdańsk, Sept. 1986

STAB'86

IMPROVED SAFETY BY APPLICATION OF SUBDIVISION AND MEANS OF FLOTATION FOR SMALL VESSELS

by

Emil Aall Dahle *) and Gunnar Nisja **)

ABSTRACT

In recent years, mainly based on work within IMO, national stability requirements have come into force. For special types of vessels, carrying passengers, or cargo that might cause damage to the environment, damage stability requirements are already in force through international conventions like SOLAS and MARPOL.

For larger cargo ships, damage stability standards can be adopted by the owner, thus reducing the freeboard. For small vessels, it is generally assumed that survivability after damage is difficult to obtain.

In the paper, recent Norwegian research on survivability of vessels of length 30-80 feet is covered. The design aspects to ensure a reasonable degree of survivability are dealt with. Emphasis is on subdivision and/or use of reserve buoyance provided by horizontal division, voids or hard foam in the upper parts of compartments.

The investigations have been carried out in collaboration with different firms and institutions. Some practical results are presented, mainly to point out that both intact and damaged stability standard for small crafts, which today is often in a regrettable state, can be improved by fairly moderate efforts, which can be evaluated at the design stage.

1. INTRODUCTION

Smaller vessels operate generally near to the coast. Consequently, they are subject to groundings. In many cases, the vessel will be broken up or founder, and improvement in vessel design is of little help.

However, if the vessel drifts off, after a grounding, it has often suffered a leak, and will often sink, capsize or both. The crew will, in some of these cases, have time to use the available means of evacuation. But in other cases, the sinking or capsize due to water ingress is so rapid that the crew perish.

In Norway, it is now required that all vessels above 10.35 m in length have to carry a life-saving suit for each crew-member.

However, practice has shown that even with a suit on, the danger of drowning in even moderately confused seas is present. It is therefore the opinion of the authors that efforts to obtain floatability and stability in damaged conditions can serve three purposes:

- avoid fast sinking and capsize in order to facilitate an orderly evacuation and provide time for sending distress signals.
- provide a fairly safe platform for survivors, also for those who might have donned a life-saving suit. From this platform, distress signals can be sent.
- protect the vessel and equipment onboard from being completely lost. This might lead to a reduction in the insurance-fee.

A more thorough discussion on the subject can be found in Dahle and Nisja (1), where also statistics is provided.

2. PRACTICAL DESIGN SOLUTIONS

In the following, practical solutions to obtain floatability and stability in damaged condition will be illustrated by 3 examples. In order to restrict the number of cases, the vessels will be presented as follows:

- floatability and stability without special means of flotation, loaded and ballast condition. All compartments damaged.
- as above, with selected design improvement implemented.

The lost buoyancy method is used in calculation of damaged stability.

2.1. Small coastal vessel A.

The first vessel is representative for a group of small multipurpose fishing vessels built in GRP operating in Norwegian coastal waters. The vessel was also dealt with by Dahle and Nisja (1).

The vessel will sink in both the ballast and the loaded condition without means of flotation, i.e. as built today. The vessel is shown in Fig. 1.

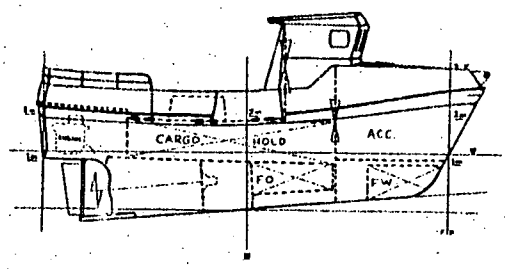

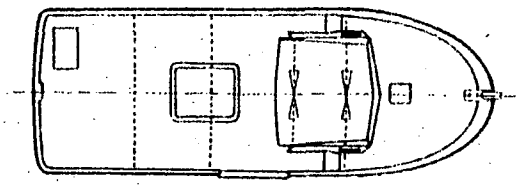

Length o.a.	:	9.15 m
Length p.p.	:	8.30 m
Breadth, moulded	:	3.20 m
Depth, moulded	:	1.65 m

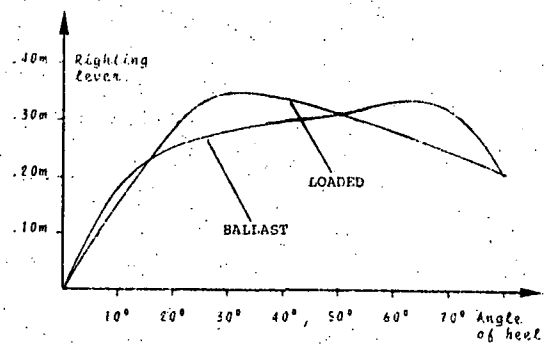

		Loaded	Ballast
Draft	:	1.29 m	1.08 m
VCG	:	1.45 m	1.54 m
GM	:	1.12 m	0.80 m
Displacement	:	10.8 m^3	6.40 m^3
Tonnage	:	10.0 GRT	
Cargo hold	:	7.00 m^3	
Fuel oil	:	0.70 m^3	
Fresh water	:	0.15 m^3	

Wheelhouse is not included in GZ.

Fig. 1. Vessel A. General arrangement, main dimensions and intact stability curves for ballast and loaded condition.

The most practical way of obtaining flotation for this vessel type is to:

- Insulate the hold and accommodation with hard foam.
- Insulate the upper part of said compartments.
- Supply the bulwark with hard foam where not taking up space needed.

This provides needed insulation in hold and accommodation, while only hard foam in bulwark adds to the building cost.

Amount of reserve buoyancy built into bulwark, cargo hold and engine room.

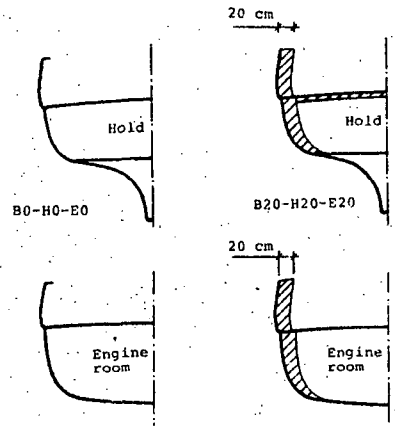

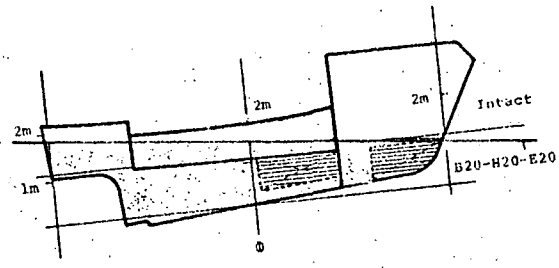

Compartment open to sea

Fuel oil and fresh water

B: Reserve buoyancy in bulwark
H: Reserve buoyancy in hold
E: Reserve buoyancy in engine room

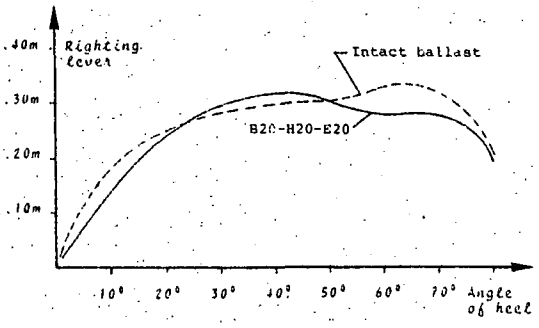

Penetrated	Cargo hold	Engine room
Permeability	0.95	0.85
Buoyancy	B0 - H0 - E0	B20-H20-E20
Floatability ?	No	Yes
Draft midships	—	1.51 m
Trim over length	—	-0.95 m
GM	—	0.69 m

Fig. 2. Vessel A. Accommodation, cargo hold and engine room penetrated. Stability and waterline after flooding. Valid for baliast and up to partly (50 %) loaded condition for fish and ice in hold.

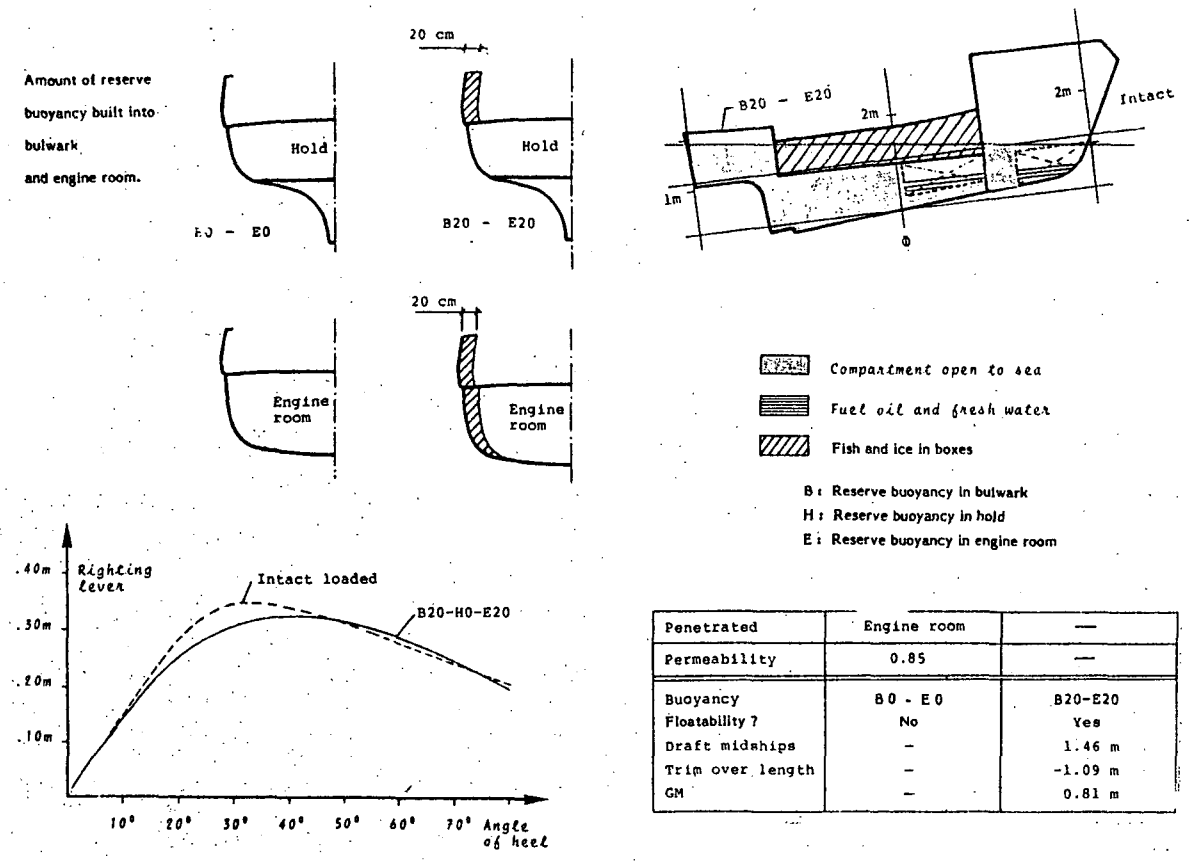

Penetrated	Engine room	—
Permeability	0.85	—
Buoyancy	B0 - E0	B20-E20
Floatability ?	No	Yes
Draft midships	–	1.46 m
Trim over length	–	-1.09 m
GM	–	0.81 m

Fig. 3. Vessel A. Engine room and accommodation penetrated. Stability and waterline after flooding. Loaded condition, 5 tons fish and ice in boxes.

The result of the investigation is evident from Fig. 2 and 3. The conclusions are:

- Providing means of flotation in the hull the vessel remains afloat and stable.
- The bulwark does not contribute to flotation in the damaged condition.
- The bulwark, if supplied with flotation, contributes significantly to damage stability, giving GZ comparable with the intact vessel.

2.2. Medium-sized fishing vessel B.

This vessel is built of wood with an aluminium superstructure above the main deck as shown in fig. 4. It is mainly intended for purse seining and long-lining. Thus, a leakage fore or aft will easily fill up the whole hull through the space between the internal and the external hull.

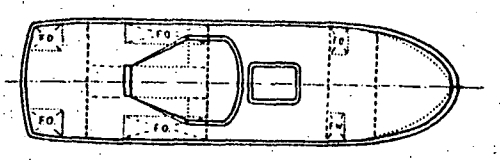

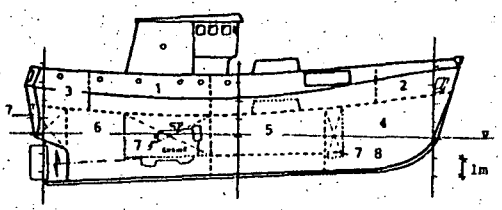

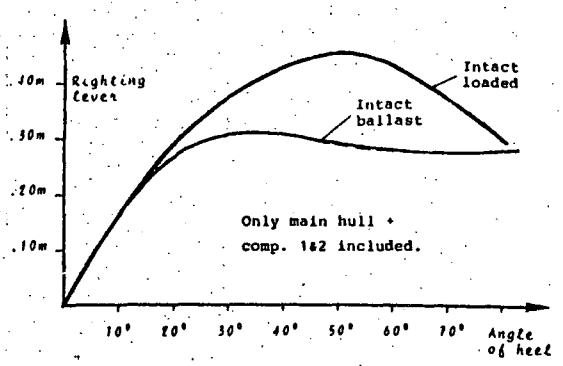

1 Accommodation	5 RSW-hold
2 Forecastle head	6 Engine room
3 Purse seine	7 Fuel oil
4 Store, fishing gear	8 Fresh water

Length o.a.	: 24.96 m	
Length p.p.	: 22.70 m	
Breath, moulded	: 6.86 m	
Depth, moulded	: 3.26 m	
	Loaded	Ballast
Draft	: 3.09 m	2.19 m
VCG	: 2.71 m	3.05 m
GM	: 1.02 m	0.92 m
Displacement	: 267.00 m^3	147.00 m^3
Tonnage	: 129.00 GRT	
RSW hold	: 108.00 m^3	
Fuel oil	: 20.20 m^3	
Fresh water	: 6.00 m^3	

Fig. 4. Vessel B. General arrangement, main dimensions and intact stability curves for ballast and loaded condition.

(Multi-purpose fishing vessel, wooden hull and aluminium superstructure above main-deck)

A practical way to improve the design is in this case to:

- Make the fish-hold watertight.
  This gives the vessel the opportunity to carry fish in refrigerated sea water (RSW), and will prevent leakage of water to other parts of the vessel if carrying fish in ice.
- Make a horizontal watertight division between hull and poop.
  This pre-supposes a watertight door leading to the engine room. This only implies to install an ordinary weathertight door that swings inward, so that the water pressure from below provides tightness.
- Make the forcastle watertight.
  This is normally the case today, if otherwise drain openings etc. are avoided.

The result is shown in Fig. 5 and 6.

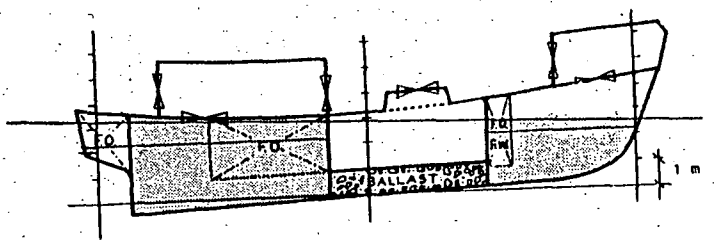

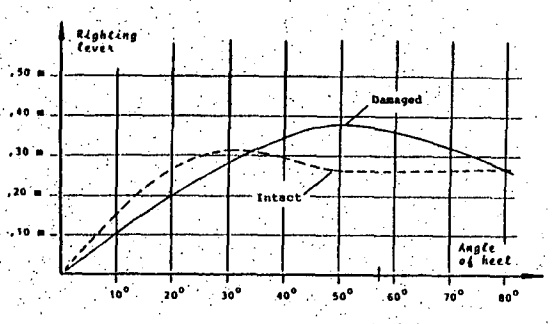

Penetrated	Store, fishing gear (4)	Void outside RSW-hold	Engine room (6)
Permeability	0.70	0.30	0.70
Watertight door/ hatch closed ?	Yes	No	
Floatability ?	Yes	Yes, but small trim or heeling might cause further flooding in superstructure	
Draft midship Trim over length GM	3.09 m - 0.58 m 0.60 m	3.09 m - 0.58 m 0.60 m	

Fig. 5. Vessel B. The whole internal structure except RSW-hold is penetrated. Stability and waterline after flooding. Ballast condition, 10 % fuel oil and fresh water.

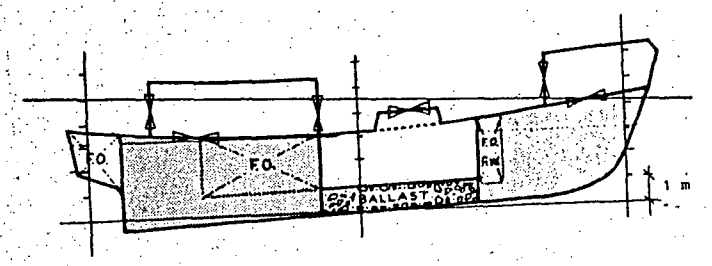

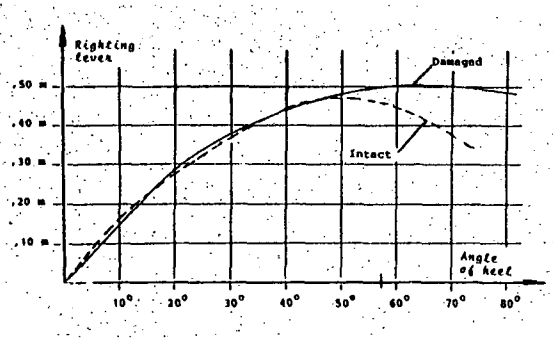

Penetrated	Store, fishing gear (4)	Void outside RSW-hold	Engine room (6)
Permeability	0.70	0.30	0.70
Watertight door/ hatch closed ?	Yes	No	
Floatability.	Yes, the damage is bounded by the hatch	No, the vessel will sink	
Draft midship Trim over length GM	4.88 m - 0.78 m 0.82 m	- - -	

Fig. 6. Vessel B. The whole internal structure except RSW-hold is penetrated. Stability and waterline after flooding. Loaded condition, fish in RSW and 100 % fuel oil and fresh water.

The result is:

- In the loaded condition, the vessel remains afloat and stable, but is strongly dependent on watertightness of the horizontally watertight forecastle and poop.
- Even in ballast condition in a moderate seaway in damaged condition the vessel will sink or capsize if doors/hatches are not closed.

2.3. Rescue vessel C.

The vessel was delivered in April 1986, and has been subject to extensive damage stability calculations by the authors. The vessel is selfrighting by use of 6.5 m^3 buoyancy on top of the wheelhouse.

The vessel is shown in Fig. 7. Only one loading condition is shown, as there are only small differences between them.

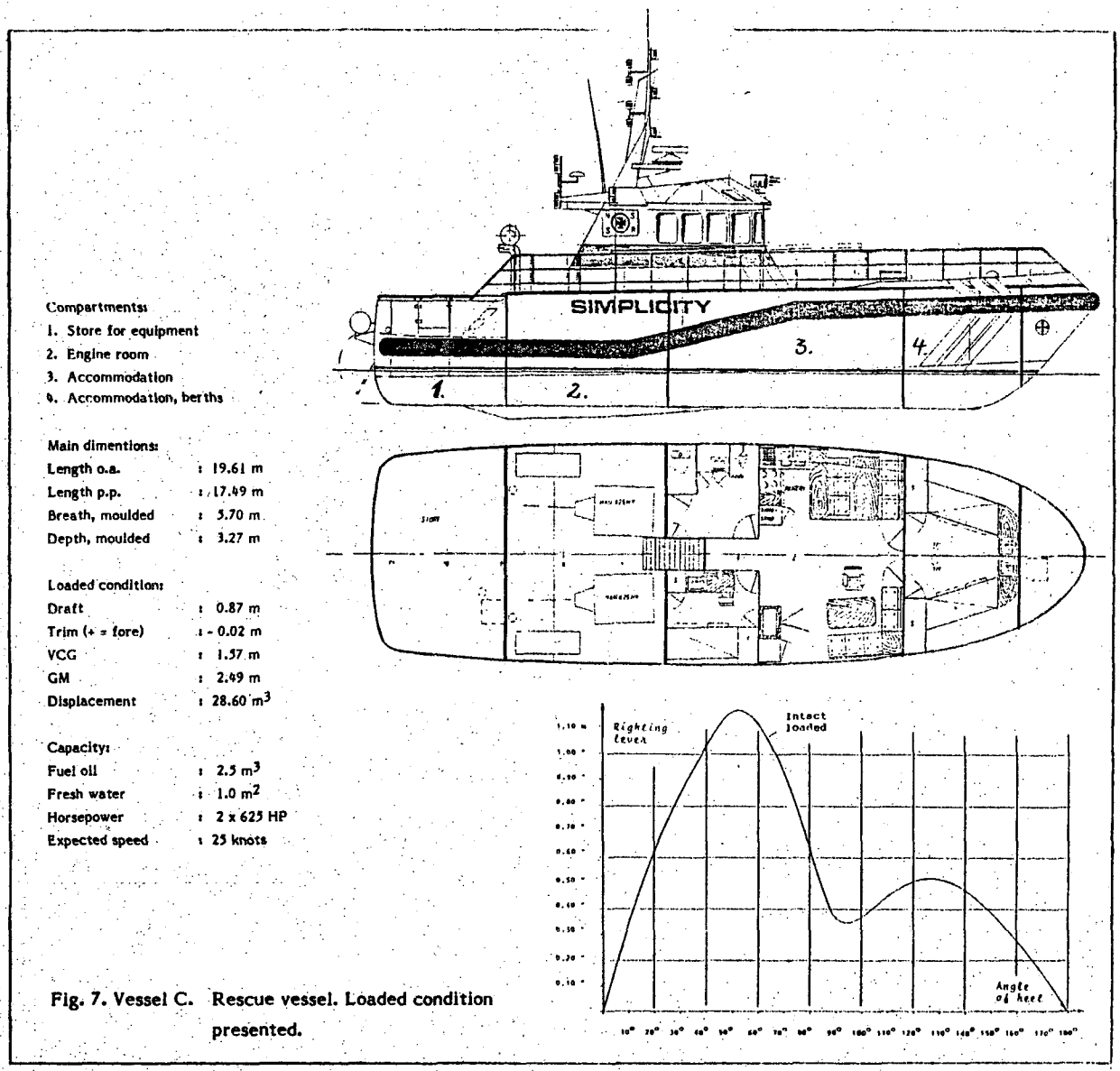

Fig. 7. Vessel C. Rescue vessel. Loaded condition presented.

Obviously, if built in ordinary GRP or metal, the vessel will sink if an extensive damage leads to ingress in all hull compartments.

This was one of the reasons for the decision of the Norwegian Rescue Service to design the hull in sandwich-built GRP.

The result is shown in Fig. 8.

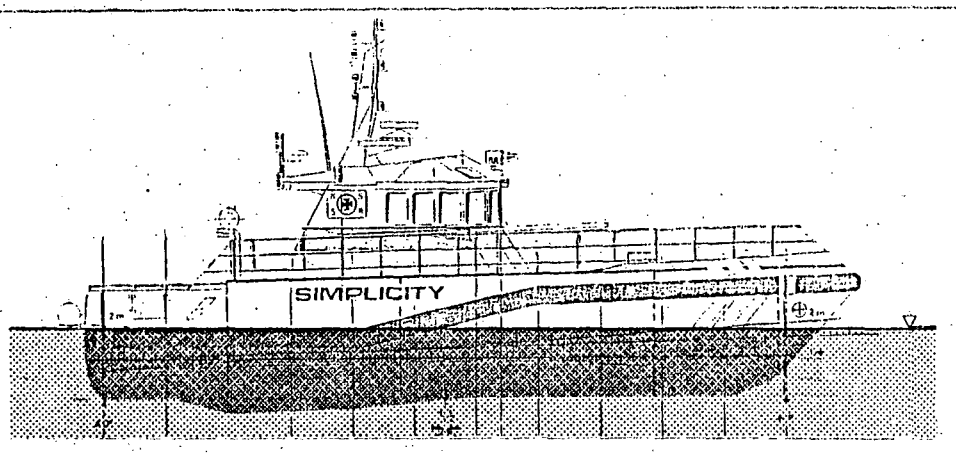

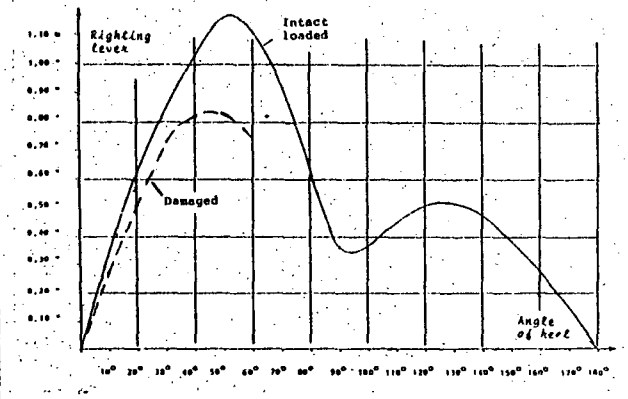

Penetrated	All compartments
Permeability	0.90
Watertight door/ hatch ?	No, water is free to flood any compartment
Floatability ?	Yes, due to the use of the sandwich method
Draft midtship Trim over length GM	1.73 m - 0.10 m 0.90 m

Fig. 8. Vessel C. All compartments penetrated. Stability and waterline after flooding. Loaded condition.

Clearly, the buoyancy and stability provided by the hull material with thickness of about 65-70 mm has completely changed the picture.

The vessel will now remain upright and stable for a maximum damage.

3. CONCLUSIONS

The Scandinavian Boat Standard (2) gives guidance on how to obtain floatability and stability for small, open vessel. The standard also gives advice on bulkheads for covered vessel.

However, especially for wooden vessels, a hull damage might easily lead to extended flooding.

In the paper, it is shown how various measures can be taken at the design stage to improve the safety. The measures should be practical, and might in some cases serve also other than pure safety purposes, i.e. provide needed insulation (Vessel A and C), or a practical fishhold (Vessel B), or lower the insurance-fee in general.

It is the opinion of the authors that smaller vessels, if remaining afloat after damage, will provide a relatively safe platform from which an orderly evacuation can take place. Alternativerly, the vessel can serve as a safe haven before rescue.

*) Dr.ing., Senior Principal Surveyor, DnV, Oslo, Norway.

**) MSc. Research Engineer, Division of Marine Systems Design, The Norwegian Institute of Technology, Trondheim, Norway.

REFERENCES:

(1) E. Dahle and G. Nisja, "Intact and damaged stability of small crafts with emphasis on design", Joint Int. Conf. on Design for safety in small craft. RINA, London, Feb. 1984.

(2) The Scandivavian Boat Standard. DnV 1983 (In Norwegian).

Third International Conference on Stability of Ships and Ocean Vehicles, Gdańsk, Sept. 1986

STAB'86

ON A MICRO COMPUTER BASED PASSIVE CONTROLLED ANTIROLL TANK SYSTEM

/SYSTEM SIMULATION AND FULL SCALE MEASUREMENTS/

Y. Terao; K. Minohara

ABSTRACT

The development of a new anti roll system of the passively controlled tank is presented in this paper. This system is widely applicable to any type of the ship , especially to rather small vessels.

As the core of the system , a micro computer is used.A valve in the channel between both wing tanks is governed by the micro computer with a specific program processing a newly developed phase control algorism.

In addition, the servo-mechanical forced oscillator is newly developed for the estimation of effectiveness of the system not dependent on the surrounding. The results of regular and irregular oscillation test with this forced oscillator and numerical simulation are given here.

In the end,full scale measurements at sea with 12-meter vessel proved the usefulness of the control system .

1. INTRODUCTION

To minimize roll motion is important because this is the most significant motion of the ship in the waves so it is closely related to human comfort and work efficiency on board.

Apart from the bilge keel which is commonly used as a major roll stabilization device, the roll stabilization is usually achieved by either passive or active device. Passive device such as passive tank use no energy to control the pump system. It is less costly but only a limited efficiency. One of the drawbacks in the passive tank system is that it may cause the vessel to roll heavily under a certain sea condition where a resultant rolling has a longer period than the inherent rolling period of the vessel.

On the contrary , active devices, such as active tank or fin stabilizers, provide high effectiveness . But active tank system needs an addition of drive power . This is not practicable in rather small vessels with minimal cost. It is well known that the fin stabilizer has a disadvantage.i.e., its efficiency decreases rapidly with speed reduction. The fin stabilizer is not a best solution when it is used for fishing boats or pleasure craft as they cruise at a slow speed most time at sea.

From above point of view , an intermediate method of these two stabilization devices is investigated here.

Rapid progress of micro processor technology in recent years made it quite easy to use digital control system for a wide variety of applications. Using digital control system , improvement of the passive tank efficiency and ship stability would be most interesting to naval architects . We evaluates the application of the passive tank control system. Use of high performance CPU and system sophistication is one thing. Each type of CPU has certain performance or economical features which determine its suitability for a specific application . Complex algorism or control sequence are not desirable because it requires more computing time and developing cost. We used an 8 bit CPU and developed simple and effective valve control algorism.

To operate the valve system , the information on ship motion and tank fluid is necessary . The signal available at sea contains a wide spectrum of noise which causes loss of reliability of the system so it must be reduced by the pretreatment. It

it must be useful and desirable if a sensor itself cancels or reduces noise component . In this system, we used a mean flow meter and obtained favorable results.

2.BENCH TEST

Using a newly developed servo mechanical oscillator system , regular and irregular oscillation tank tests were made. This oscillator system is not analog table system .[1]

2.1 Servo-mechanical Forced Oscillator

Servo-mechanical forced oscillator is operated by a position control servo motor. Rotating motion of the motor is converted to a reciprocating motion by a ball screw which is connected to a pinion gear. Taking the drive power from the pinion gear, the rack gear with a backlash adjuster turns on a rolling axis which generates swinging motion of the anti rolling tank model. Maximum swinging angle is 15°/ 1.5 Hz. The principal dimensions of the model tank are shown in Table 1 and front view of forced oscillator is shown in Photo.1

Table 1 Principal Dimensions of Model Tank

B_t	=	.80	m
L_t	=	.40	m
d_t	=	.065	m
L_d	=	.40	m
A_d	=	.022	m²

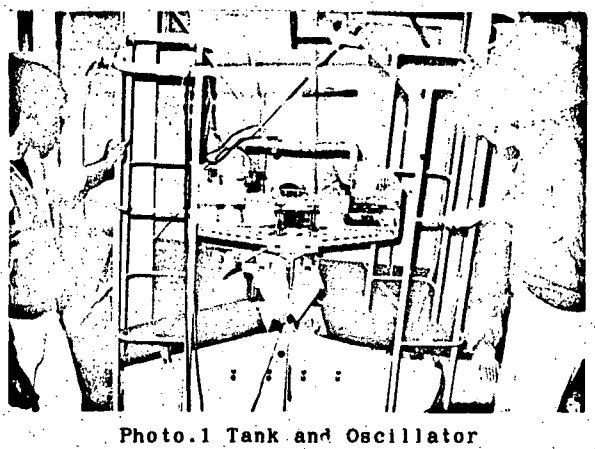

Photo.1 Tank and Oscillator

2.2 Measuring System

2.2.1 Sensor

Drag type flow meter was developed. The meter has a circular plate having a diameter of 10 mm , situated perpendicular to the flow and measures a drag force acting on the plate . The sensor measures a mean drag force acting as a low pass filter with sufficient immunity to noise .

2.2.2 Control and Measuring Diagram

Control and measuring diagram is shown in Fig. 1.

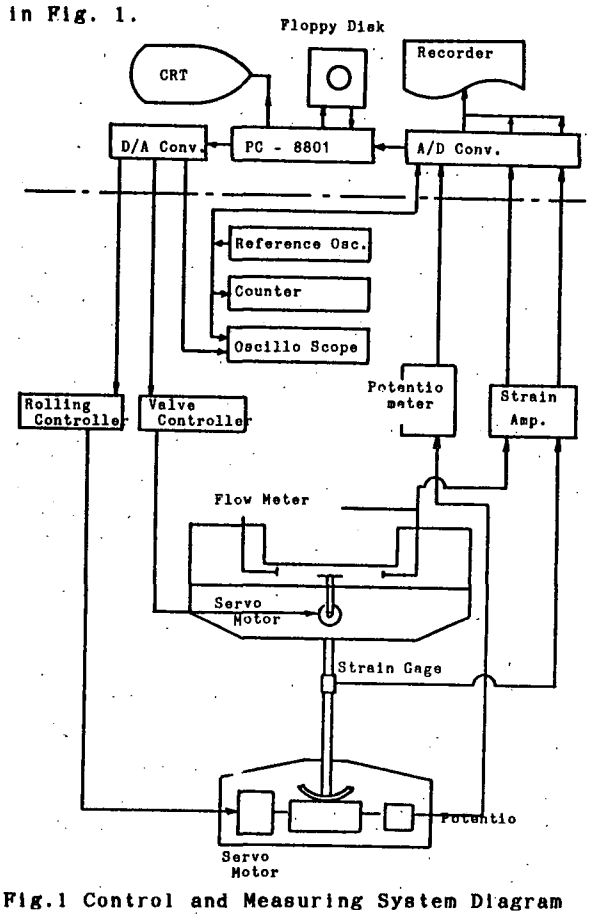

Fig.1 Control and Measuring System Diagram

Control signal for rolling angle is calculated and stored in RAM. The reference oscillator produces a frequency the 40 Hz trigger signal which is fed into micro computer through 12 bit A/D converter. Roll angle control signal is sent to the rolling controller in synchronism with a trigger. Data of the rolling angle ,rolling moment and velocity of the tank fluid are also fed to the micro computer at the same time through the A/D converter. Measured data are stored in RAM chip. Using these data ,the computer calculate a roll period and tank water period.

Simultaneously, the valve on / off control timing is also calculated. We named this process "NEW 1/2 SYSTEM". This is a phase control system which has a simple algorism. Details are described in 2.3 .

2.3 New Phase Control Diagram

Control diagram is shown in Fig.2 using PAD (Program Analysis Diagram). In the mechanical vibration theory , the principle of dynamic absorber is well known and widely used . Maximum damping or in this case , maximum roll reduction moment is obtained when the phase difference between rolling angle and fluid motion is equal to $\pi/2$ under which the roll angle is in phase of fluid velocity.

In the irregular seas, it is difficult to predict a next incoming wave or ship motion . But it may not make great error if we assume one half of next roll period is equal to the half roll period of last measurement. Based on this assumption , we developed algorism to match the both peak of roll angle and fluid velocity. When the tank's inherent cycle is faster than the roll period ,phase matching is possible using simple valve on / off control . As mentioned before ,a disadvantage of the passive tank lies in a rather longer period than the inherent rolling period of the vessel. Thus we can estimate that this valve control system can improve the passive tank system .

2.4 System Simulation

Relationship between the roll angle and tank fluid system is described in equation (1). We discuss the effectiveness of the anti roll tank by using simplified equation - pure roll motion and linear motion model . [2]

$$J_b\ddot{\phi} + B_b\dot{\phi} + K_b\phi + J_{st}\ddot{\psi} + K_t\psi = m_b \qquad (1)$$

If the fluid motion is fixed,we have the following equation

$$J_b\ddot{\phi} + B_b\dot{\phi} + K_b\phi = m_b' \qquad (2)$$

By subtracting (2) from (1), we get the following equation

$$J_{st}\ddot{\psi} + K_t\psi = -m_0\,\phi_0 \exp(i(\omega t - \delta)) \qquad (3)$$

In equation (3), out-of-phase component δ against ϕ concerns to a roll reduction moment. Generally speaking , B_t assumed to be small and m_b' to be in phase with ϕ , we can decompose the roll reduction moment using Fourier analysis to roll moment m_b and roll angle ϕ .

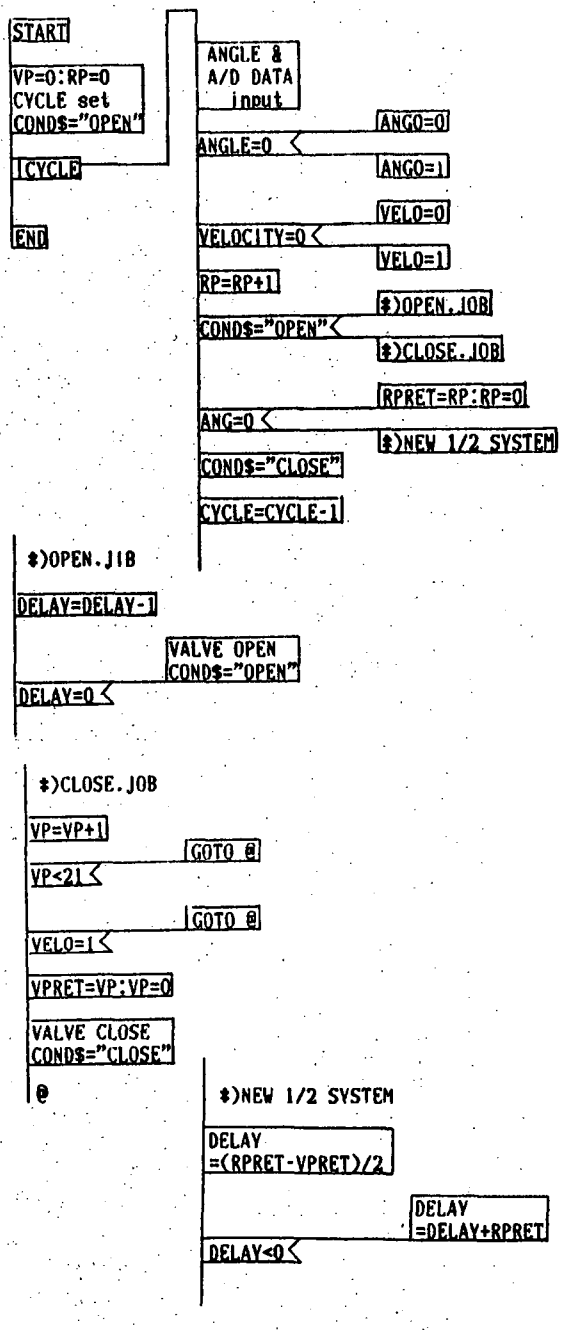

Fig.2 Control Process Diagram

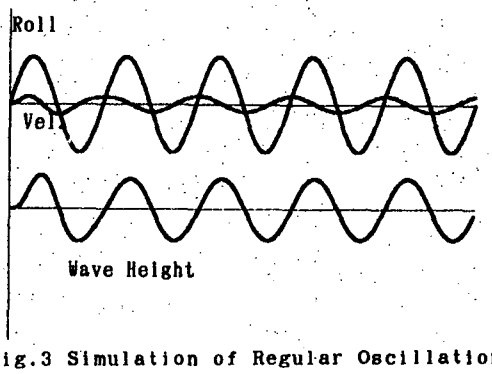

Fig.3 Simulation of Regular Oscillation

System simulation is shown in Figs 3 and 4 by using equation (3) and NEW

1/2 SYSTEM. Fig.3 shows a normal passive tank simulation test and Fig.4 shows the same tank with New 1/2 Method. From Fig.4 , we can see the rapid convergence of phase matching and greater wave height which means accumulating potential energy and accelerating fluid motion.

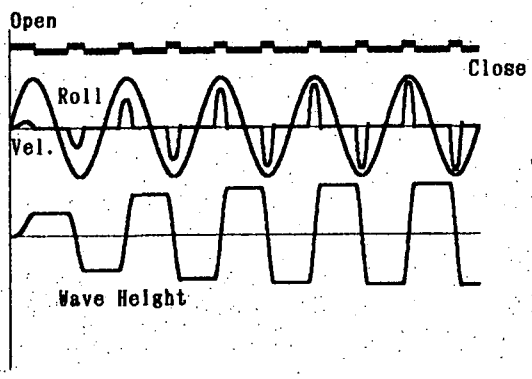

Fig.4 Simulation Test by NEW 1/2 SYSTEM

2.5 Results of Oscillation Test

2.5.1 Regular Oscillation Test

Regular oscillation test was made under 3 conditions with the valve opened , closed and under control .Results of these tests are shown in Fig.5 to Fig.7. Fig.5 shows Time history of test record with valve control condition . We can see close agreement of the peaks between roll angle and fluid velocity which is shown in Fig.4.

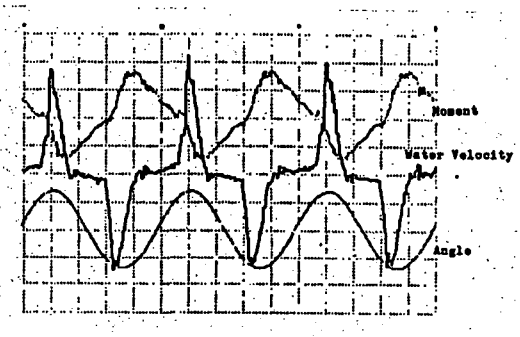

Fig.5 Time History of Tested Record

Phase shift between roll angle and moment is shown in Fig.6 . Fig 7 shows roll reduction moment. Horizontal axis is non dimensional by the tank natural circular frequency ω_t. From Fig.6 , we can see the desired phase lag up to e=1.5 when valve is controlled . In Fig.7 , roll reduction moment decreases as a roll angle increase . Such phenomenon can be explained as tank restoring term non-liniarity. From Fig.7 ,this system can be expected to have a high roll reduction efficiency when e is less than 1 (regular steady oscillation).

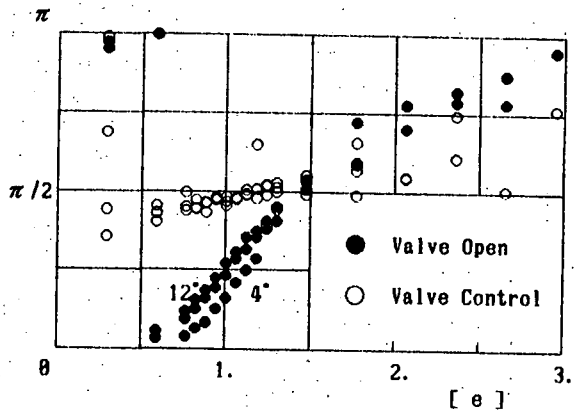

Fig.6 Phase Difference (Moment/Angle)

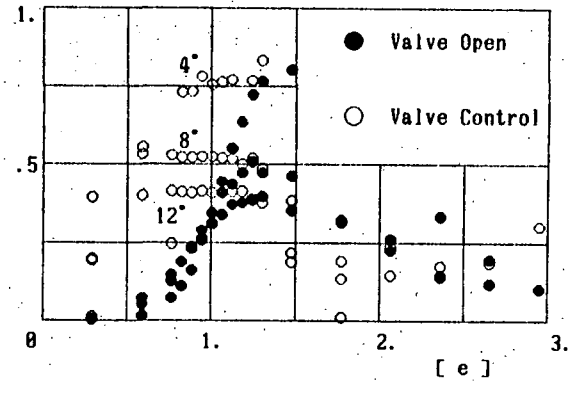

Fig.7 Roll Reduction Moment

2.5.2 Irregular Oscillation Test

To avoid too much load on the forced oscillator ,we imposed an irregular signal which has constant power spectrum of roll moment with fixed tank fluid motion , that is, valve shut condition. Signal sweep time is 102.4 sec. Fig.8 and Fig.9 show power spectrum of roll moment and roll angle respectively. Fig.10 shows time history of test record. Calculated transfer function $M_b(\omega)/\Phi(\omega)\cdot K_t$ real and imaginary part are shown in Fig.11 and Fig.12 respectively. The solid line is with the valve under control ,bold dotted line shows with the valve opened. From Fig.11,we can see the result of valve control is close to the valve shut condition which means this new control system has an advantage. The roll reduction efficiency is not affected by the circular oscillation frequency. On the contrary,we can see a difference between valve shut and open conditions. It is well

known that the double pendulum system has two peaks of its response which is due to this discrepancy.

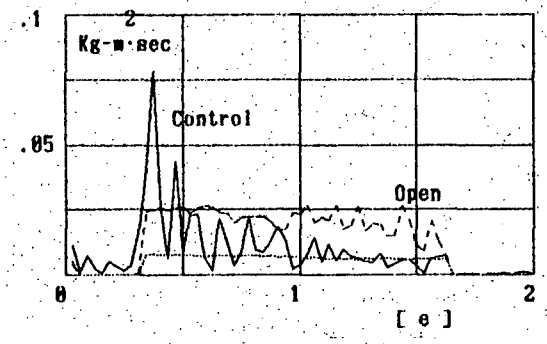

Fig.8 Power Spectrum of Roll Moment

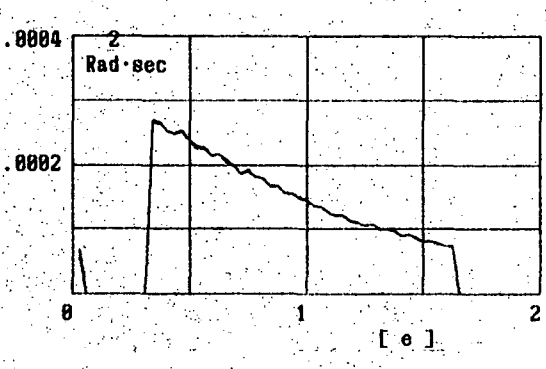

Fig.9 Power Spectrum of Roll Angle

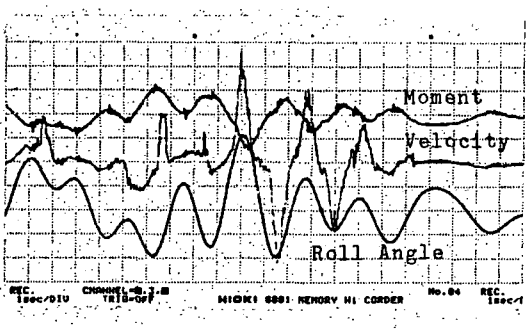

Fig.10 Time History of Test Record

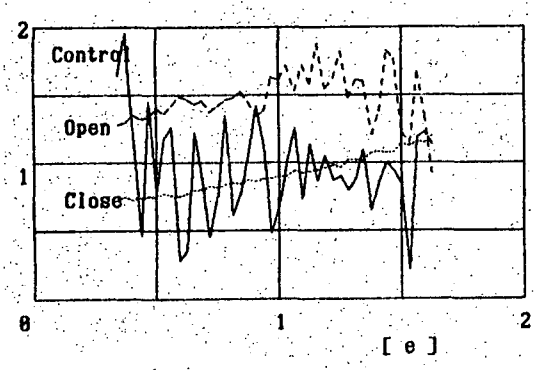

Fig.11 Transfer Function Real Part

In Fig.12 we can see the roll damping term. Damping of the valve control system is better than the valve open condition when e is equal or less than 1 . This tendency is shown in Fig.7 . It may be concluded that the new system is better than the ordinary passive tank system if circular rolling frequency is less than or equal to the tank's inherent frequency. In Fig.7, higher efficiency is observed even if e is up to 1.5 ,but in Fig.12 less efficiency is observed in this region . This must be a drawback of this new system .

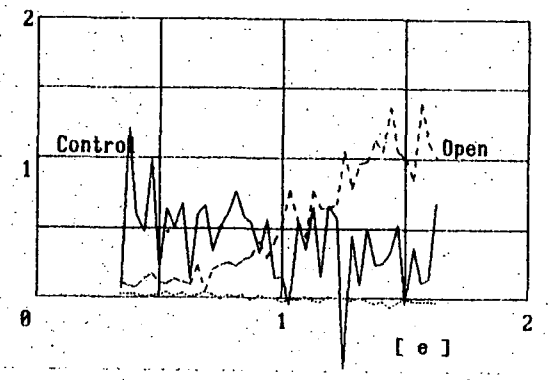

Fig.12 Transfer Function Imaginary Part

3. FULL SCALE TEST

3.1 Test Ship Fitted with Anti Roll Tank

The tank dimensions are shown in table 2. The dimensions are selected from parameter iteration to have minimum loss of GM and maximum efficiency. Tank's inherent period is set equal to ship's inherent roll period . Even if a problem arises in this control system , we will be able to ensure the improvement for the pure passive anti roll tank performance.

Table 2 Principal Dimensions of Tank

B_t	=	2.300 m
L_t	=	.500 m
d_t	=	.278 m
L_d	=	1.660 m
A_d	=	.08 m²

Principal dimensions of the test ship are shown in Table 3 . Hull section is deep V . At high or moderate speed ,the performance of the roll motion in the wave is excellent but operation at a reduced speed and at anchor is far from good.

Anti rolling tank is fitted in the deck house . Photo 2 shows the tank arrangement .

Table 3 Ship Principal Dimensions

L_{pp}	=	11.94 m
B	=	3.80 m
d	=	1.85 m
W (Full Load)	=	11.82 t
GM	=	1.466 m
KG	=	1.284 m
T	=	3.0 sec.

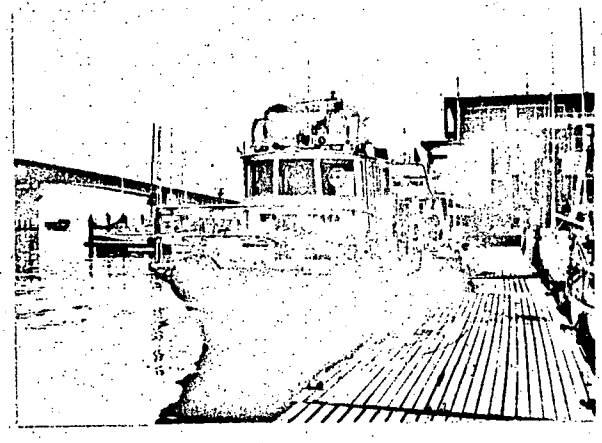

Photo.2 Test Ship Front View

In a sea trial ,the pendulum type roll angle detector and controller containing the same control system are used. The ship was set drifting freely and 3 valve conditions were tested. Incident wave was measured with a pressure type wave probe afloating with tied to a buoy .

3.2 Results of Full Scale Test

Fig.13 shows a record of full scale tests of valve control condition.Tank water height was measured by a mean wave probe.

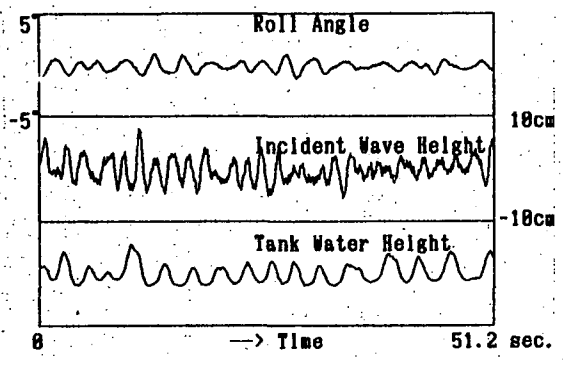

Fig.13 Time History of tested Record

Fig.14 shows transfer function amplitude where the solid line shows results of valve control condition. From this figure, we can conclude the valve control system is excellent .

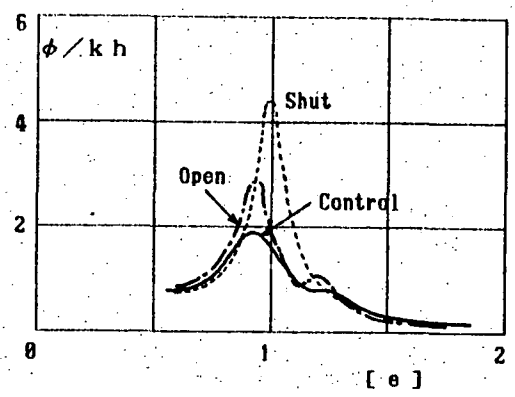

Fig.14 Transfer Function Amplitude

4.CONCLUSIONS

We propose a new control algorism for the passively controlled anti roll tank system . From regular and irregular oscillation tests with the model tank using newly developed oscillator , this tank system shows a high efficiency if circular rolling frequency is slower than the tank's inherent frequency . This was confirmed by the full scale test .

NOMENCLATURE

B_t : Tank breadth
L_t : Tank length
d_t : tank water depth
T : Inherent Roll period
J_b : Tank and fluid moment of inertia
B_b : Bench damping coefficient
K_b : Bench restoring coefficient
J_{st}: Tank coupling term
K_t : $\gamma \cdot \rho$
m_b : Forced moment
γ : Fluid specific weight
ρ : Tank free surface moment of gyration
ϕ : Bench and ship roll angle
ψ : Fluid displacement angle
L_d : Duct length
A_d : Duct area

REFERENCES

[1] John Bell, et al,"Activated and Passive Controlled Fluid Tank System for Ship Stabilization", SNAME vol.74,1966

[2] Zdybeg.T,"The Use of Bench Test Results for Calculating Roll Response of Tank Stabilized Ship", I.S.P.,vol.27,Apr., 1980,No.308.

Yutaka Terao:
Dr.Eng.,Assoc. Prof. of Univ. Tokai Department of Naval Architecture School of Marine Science & Technology

He graduated Yokohama National University, naval architecture ,in 1975
Master of Eng., 1977, Yokohama National University.
Doctor of Eng., 1980, Tokyo University

Kiyomi Minohara:
Director of Oceanological Instrument Division, Furuno Electric Co.,LTD.

He graduated in 1954,Osaka Electro Communication University

Third International Conference on Stability of Ships and Ocean Vehicles, Gdańsk, Sept. 1986

STAB'86

TOWARDS RATIONAL STABILITY CRITERIA FOR SEMISUBMERSIBLES - A PILOT STUDY

H.H. Chen; Y.S. Shin; J.L. Wilson

ABSTRACT

This paper summarizes the findings of the pilot study on the intact stability of twin-hull semisubmersibles mobile offshore drilling units (MODU's) that the American Bureau of Shipping (ABS) has undertaken in the past two years. The pilot study was aimed at obtaining a better understanding of the philosophy behind the current MODU stability criteria, to explore possible relationships between the dynamic behavior of the semisubmersibles and the underlying basis of the static stability criteria set forth in most rules and codes, and to find areas in need of further studies in order to achieve a better evaluation of stability using a rational approach.

This paper first presents the static stability of three typical semisubmersibles of 4-, 6- and 8-column units considered in the pilot study. Then, a brief discussion on the correlation of computed motions with model test results is given. Findings from calculations using a time-domain simulation are highlighted. Suggestions on some areas needed to be further studied are also included.

1. INTRODUCTION

The present intact stability criteria [1] for mobile offshore drilling units (MODU's) were initially introduced by the American Bureau of Shipping (ABS) in 1968. The criteria, derived on an empirical basis evolving from U.S. Navy ship criteria [2], call for a positive GM and specify a minimum ratio of 1.3 for the areas under the righting moment and the wind heeling moment curves. This criteria was widely recognized and adopted by the industry in ensuing years.

In recent years, some governmental agencies have imposed additional requirements [3] for the intact stability criteria, such as limited first and second intercept angles of heel, and a variety of new standards and criteria for MODU damage stability, including limited angles of heel and damaged area ratios (AR). Although these new rules have been directed toward enhancing MODU safety, there has not, however, been a supporting study demonstrating that the overall safety would be increased by these new rules. As a result, ABS has embarked upon a pilot study to investigate from first principles the intact stability of semisubmersible MODU's in seaways. The study was aimed at obtaining a better understanding of the underlying basis for intact stability criteria, exploring the relationships between the static stability requirements and the motions of the unit and investigating the effects of geometric and environmental parameters on the dynamic behaviour of the units.

This study includes (i) static stability characteristics of three semisubmersibles, (ii) correlation of calculated motions of the units with model test results; (iii) time-domain simulations of the units subjected to wind, waves and current, both alone and in combination; and (iv) correlations of MODU static stability and dynamic motion simulation. Figure 1 illustrates the scope of the work and procedure of the study.

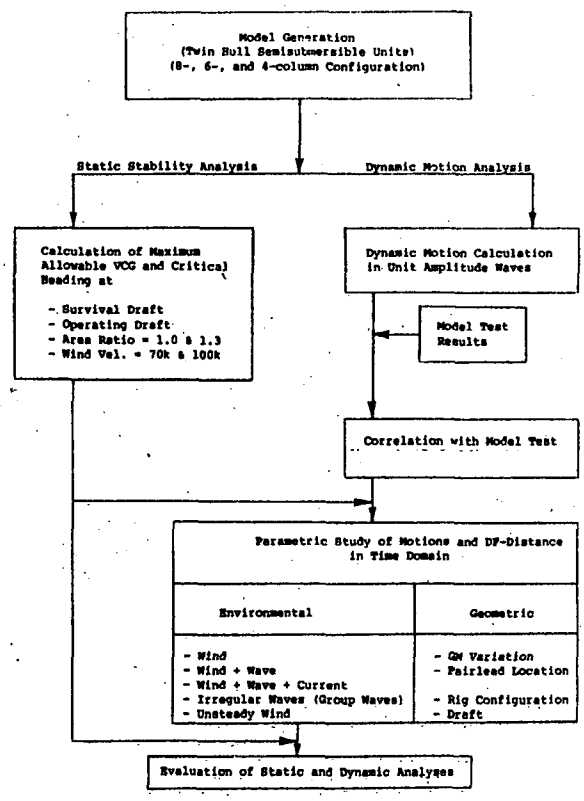

Fig. 1 Flow Diagram of Static Stability and Dynamic Motion Analyses

2. STATIC STABILITY

Three characteristic semisubmersibles of 4-, 6-, and 8-column were considered in the study. Figure 2 shows the schematic drawing of one of the units considered. For static stability calculations as well as the motions analysis which will be subsequently addressed, the three units were idealized by circular cylindrical sections as shown in Figure 3 (not in same scale). In the calculations, the decks and superstructures were assumed non-buoyant and were therefore not modelled. However, for wind force and wind moment calculations, the exact configuration above the waterline was taken into account.

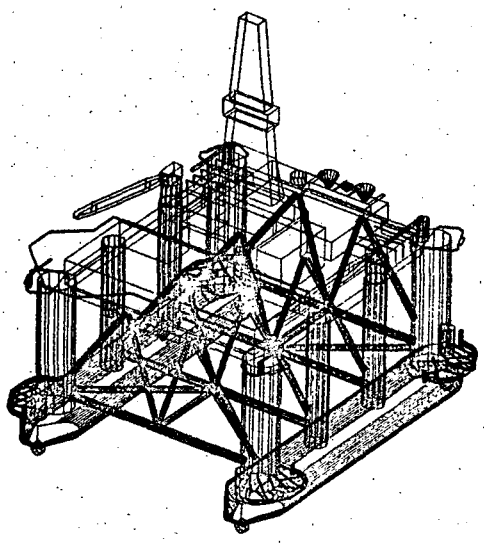

Fig. 2 Schematic Plot of 8-Column Rig

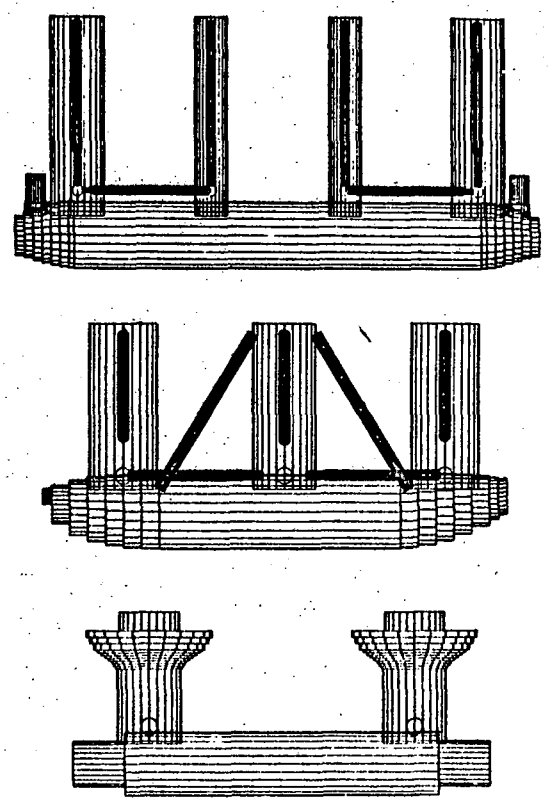

Fig. 3 Mathematical Models of the Three Units used for Static Stability and Motion Calculations

The static stability of a unit at a given draft was calculated for a specified range of heel angles and wind directions, for which the centers of buoyancy, the adjusted drafts and the trim angles were computed. The difference between the center of weight and the horizontal shifts of the center of buoyancy gives rise to the righting moment. When calculated for a range of heel angles, the righting moment curve is thus obtained.

The area ratio for a particular condition is calculated from the area under the righting moment curve up to the second intercept or downflooding (DF) angle, whichever is less, and the area under the wind heeling moment curve measured to the same angle. A desired area ratio can be calculated by varying the height of the center of gravity (KG) of the unit. When this calculation is carried out for a range of wind directions, an allowable KG value for each wind orientation can be obtained. The critical orientation is then determined by the allowable KG value that is the smallest for a given draft.

This static stability calculation was carried out for all three units at two drafts: survival and operating, and two area ratios: 1.0 and 1.3. The wind speeds used in calculating the wind forces and heeling moments were 100 and 70 knots, respectively. The minimum area ratio of 1.3 is the standard ABS Rule requirement for semisubmersibles. In this study, when the area ratio of 1.3 did not provide a positive GM, the allowable KG was lowered so that the additional requirement of positive GM was met. Shown in Figures 4, 5 and 6 are the resultant static stability curves at the required area ratios in the survival draft for the three units under consideration.

From the static stability calculation, findings indicate that a reduction of draft is accompanied by an increase of the maximum righting arm value and the range of positive arm. The increase in these values may be attributed to the emergence from the water surface of one end of a pontoon at the shallow survival draft condition, resulting in a greater lateral shift of the center of buoyancy and a large increase in righting

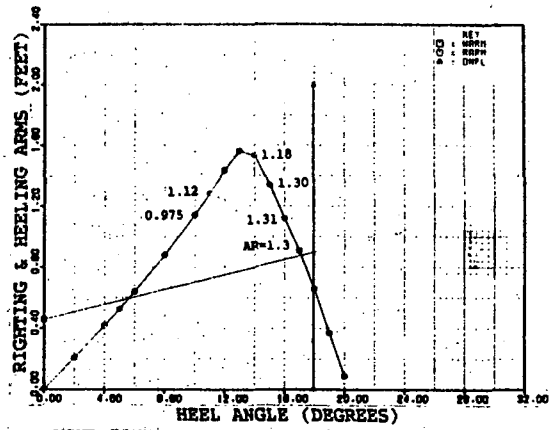

WIND=70KN, DRAFT=95', KG=63.549',
ORIEN.=-42.4°, AR=1.3, GM=6.03'

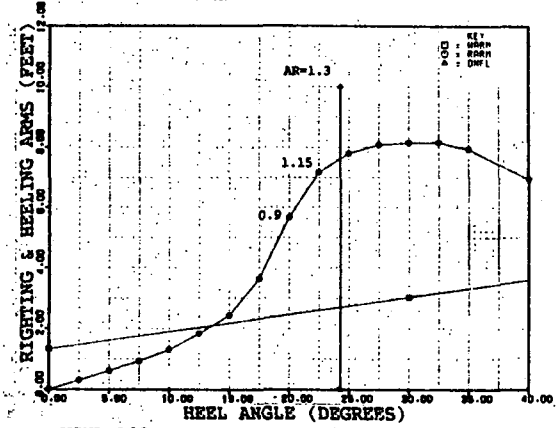

WIND=100KN, DRAFT=70', KG=61.207',
ORIEN.=-40.9°, AR=1.3, GM=7.01'

Fig. 4 Static Stability Curves for the 8-Column Rig (Operating and Survival Conditions)

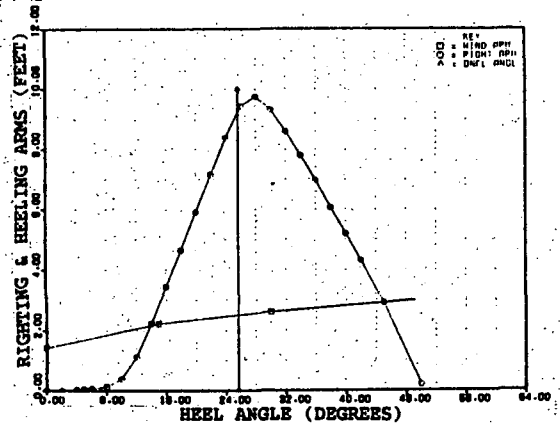

WIND=100KN, DRAFT=50', KG=68.0',
ORIEN.=+37.0°, AR=1.376, GM=0.0'

Fig. 5 Static Stability Curves for the 6-Column Rig (Survival Condition)

moment. Furthermore, the righting arm at the shallower draft condition increases more sharply than that for a deeper draft as the unit heels beyond a certain angle from its upright position. The sharp increase of the righting arm results in more nonlinear stability curve, with respect to

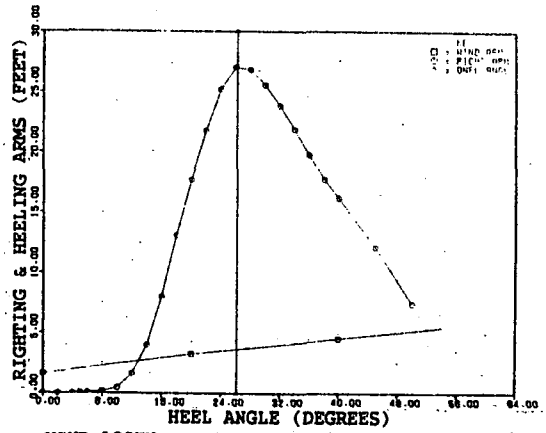

WIND=100KN, DRAFT=57.4', KG=77.60',
ORIEN.=-30.0°, AR=3.075, GM=0.0'

Fig. 6 Static Stability Curves for the 4-Column Rig (Survival Condition)

the heeling angle, in the range from zero to the maximum righting arm heeling angle. The effect of draft on the shape of the stability curve can be better illustrated by the 8-column unit when its stability curve at the 95 foot operating draft is compared to that of the 70 foot survival draft (top and bottom, respectively, of Figure 4).

The larger righting arm eitehr by increasing GM or by lowering draft implies that the unit would have a smaller static heeling angle (first intercept angle) in a steady wind. On the other hand, the increase of the righting arm tends to reduce the resonant period of rolling motion of the unit, in some cases, shifting it closer to the period of wave peak energy in a seaway. As a result, the dynamic rolling motion may be increased due to the increases in wave excitation and dynamic magnification. Thus, this is an indication that the overall stability of MODU's should be assessed by both the static characteristics and the dynamic motion of the unit using a realistic environmental condition of wind, waves and current.

3. MOTION CORRELATION

The correlation of calculated semisubmersible motions in waves with model test data was performed to verify and to calibrate the computational procedure with the appropriate hydrodynamic coefficients. In computing the motions of the unit, the semisubmersible was described as a space frame assembly of slender members as shown in Figure 3 for all the three units under consideration. The members of the unit were assumed to be widely separated, thus hydrodynamic interference between members was assumed to be negligible. The members were also

assumed to have small cross-sectional dimensions in comparison to the wave length, and the hydrodynamic forces were calculated using the Morison equation. In the correlation study, the added mass coefficient and the drag coefficient varied, in order to investigate the effects of the coefficients on the motion calculation. It has been found that for the wave period up to 24 seconds in full scale, the change of drag coefficient has little influence on the motions, except in the vicinity of the natural period of heaving motion. By changing the added mass coefficient, only the natural period of heave is altered, while the effects of added mass coefficient to other motions are not as noticeable. Shown in Figures 7 and 8 are the correlations for heave and roll of the 8-column unit.

Overall, good correlation of calculated and experimentally measured motions was achieved when an added mass coefficient of 1.90 and the drag coefficient of 0.75 were used in the analysis. Similar procedures were used for the 6- and 4-column units, producing satisfactory correlation.

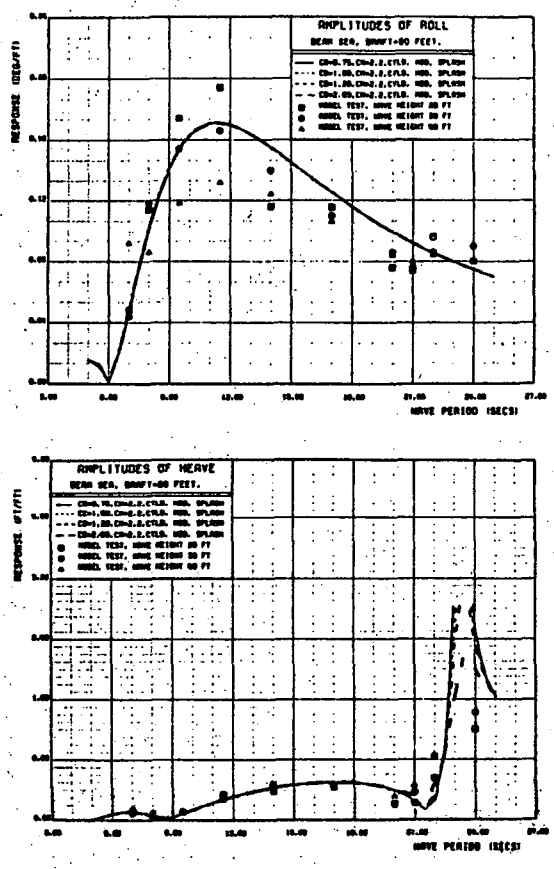

Fig. 7 Effects of Drag Coefficient on Roll and Heave Motions of the 8-Column Rig

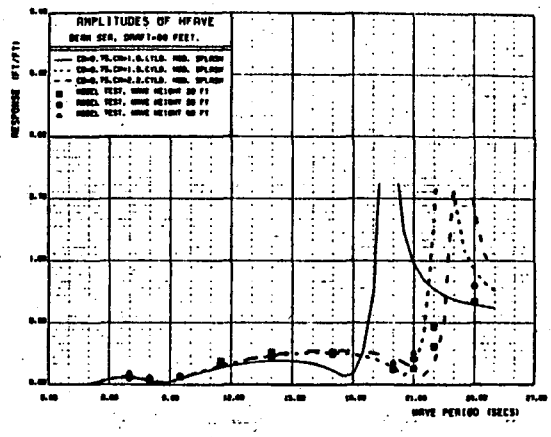

Fig. 8 Effects of Added Mass Coefficient on Heave Motion of the 8-Column Rig

4. DYNAMIC MOTION ANALYSIS

A nonlinear time domain simulation [4] was performed to analyze the response of the three semisubmersibles to waves and other external exciting forces such as wind, current and mooring using the idealized models in Figure 3. In the simulation, the nonlinearities due to viscous damping, mooring restoration and wave forces are taken into account. The motion in six degrees of freedom is computed at each time step. In addition the DF-distance, which represents the vertical distance between the DF-point and the instantaneous water surface, is also calculated. Some of the results from the dynamic motion analysis are given below.

4.1 Group Waves and Subharmonic Motion

The difference in the dynamic behavior of the three units in group waves were investigated in the study. For the three units, the effect of group waves causes greater heel and smaller DF-distance compared to irregular waves that were considered in the analysis. However, only the responses of the 8-column unit subjected to the group waves are shown here in Figure 9 for illustration. It should be noted that the wind is applied instantaneously to a full speed at the 232 seconds time step in the simulation.

In the condition of large amplitude waves, the time-domain simulation showed an unusually large nonlinear roll motion of the unit. This large nonlinear motion is subharmonic in nature and its response frequency is one-half the wave exciting frequency. This subharmonic motion is predominantly caused by nonlinear, time variant, restoration characteristics of a unit in waves under the conditions of low GM and shallow draft, e.g. Figure 10.

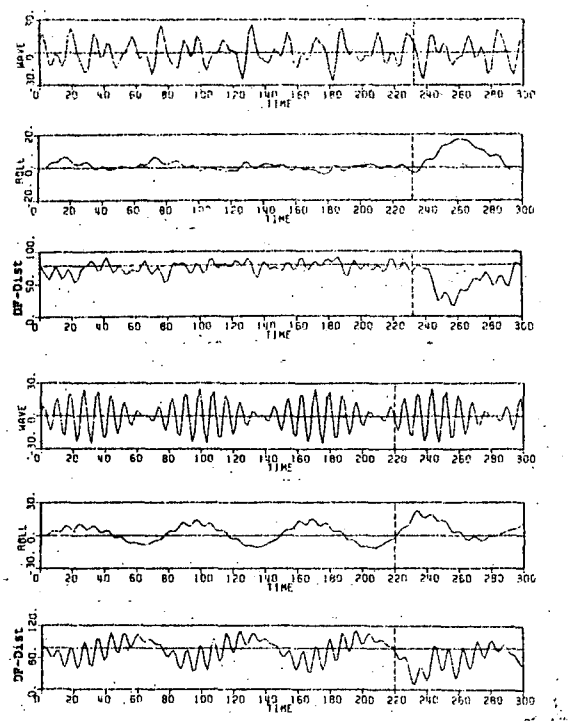

Fig. 9 *Responses of the 8-Column Rig subjected to Irregular and Group Waves with Wind*

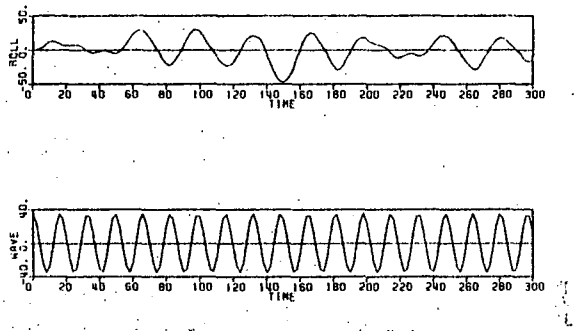

Fig. 10 Subharmonic Roll Response of Semi-submersible

4.2 Unsteady Wind Effect

A few preliminary calculations to study the effect of unsteady wind on platform motion were performed using the time domain simulation for the 8-column unit. The wind forces used in this analysis were assumed to be proportional to the square of the instantaneous wind velocity consisting of the sum of a mean wind and a time varying component. The steady wind heel component was computed based on the exposed area and a 100 knot wind. The time dependent component was simulated by using the Simiu-Leigh wind spectrum. The rolling motion of the unit subject to the wind just described is shown in Figure 11.

The rolling motions of the 8-column unit were also calculated for a random sea of 45-feet significant height and modal period of 16.5 seconds, and the combination of random sea with the unsteady wind previously described. Results for the random sea alone and the latter combined with unsteady wind are also displayed in Figure 11.

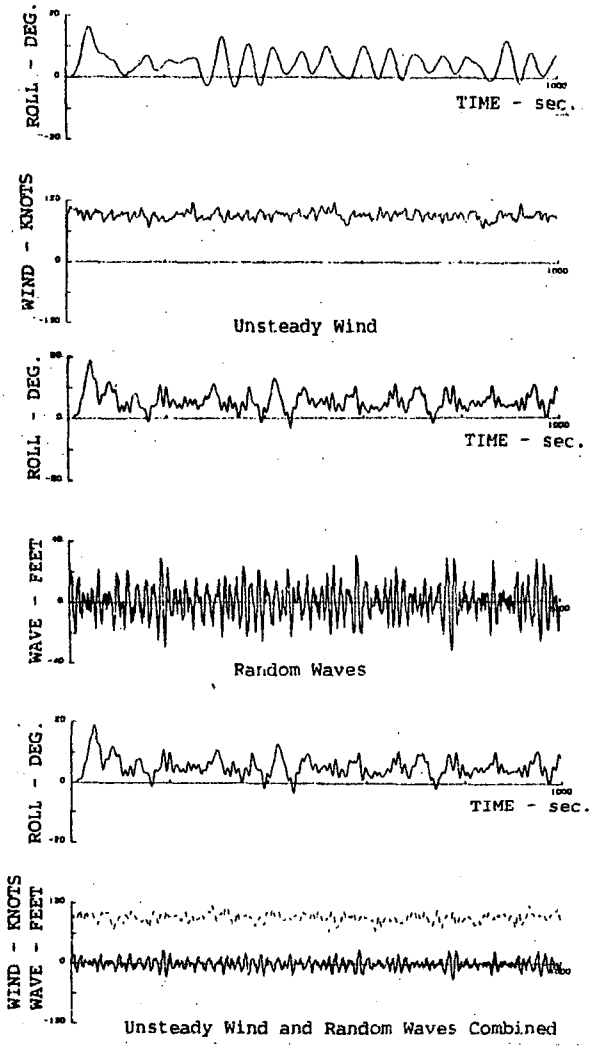

Fig. 11 Time Histories of Roll Motion for the 8-Column Unit Subjected to Three Different Environmental Conditions

It is apparent from Figure 11 that wind unsteadiness can have an appreciable influence on the motion response of a semisubmersible in heavy sea conditions. Under certain conditions, the unsteady roll caused by unsteady wind can equal that caused by the waves. Also, the unsteady wind-induced roll can equal the steady roll caused by the mean wind.

It is also to be noted that most of the available data on wind unsteadiness is based upon studies of wind over land [5]. The applications of such studies have been concerned principally with land structures such as tall masts and high rise buildings, all of which have relatively high

natural frequencies of response. Consequently, the emphasis has been on the high frequency end of the spectrum. Moored offshore platforms, on the other hand, respond to low frequencies in the range of 0.01 to 0.10 Hz and this part of the wind spectrum applicable to the study of ocean structure in a seaway has not been adequately studied.

4.3 Effects on DF-distance Due to Wind, Wave, and Current

A 70 knot wind, 50 foot, 14 seconds regular wave and 2 knot current were applied colinearly to the units to confirm the critical orientation determined from the static stability analysis. Various combinations of wind, waves and current were used in the analysis, while the heading angles were varied from head to beam seas. For each heading angle, motions and DF-distance at the critical downflooding point were calculated. The results were particularly interesting as they showed that the critical orientation angle determined from the static stability analysis is in good agreement with that from the motion simulation for cases of wind and waves alone and combined. However, for the case where current is applied in combination with wind and waves, the critical orientation may vary from that calculated in the static stability analysis.

From the analyses, it was found that the effect of current acting in the same direction as wind and waves, acts to stabilize the unit. The effect of current acting opposite to the wind and waves was not studied in depth. A few selected cases with opposing current were done and resulted in the expected trend opposite to that for current acting in the same direction as wind and wave. The effect of current from a direction other than the wind and waves, needs to be further investigated.

4.4 Mooring Effect

To ascertain the effect of the mooring system on the dynamic transient motion of the units subject to stepwise impulsive winds, several cases were investigated at the operating draft in combinations of a 70 knot wind, waves and a 2 knot current. Given these conditions the units were studied using no moorings and using moorings with the fairleads varied in the vertical position.

When the 8-column unit is moored in a 100 knot wind with an eight point mooring arrangement, the stability of the 8-column unit is slightly improved when compared to the freely floating case in the sense that the transient DF-distance at the critical downflooding point for the moored case is slightly larger than that of the freely floating case.

For the case of wind only, the effect of changing vertical fairlead location on the DF-distance at the critical downflooding point is small for the three units. For the cases of colinearly applied wind-wave and wind-wave-current, the effect of fairlead location on the DF-distance becomes significant for the three units.

5. CORRELATION OF STATIC STABILITY AND DYNAMIC MOTION

In order to explore the possible relationships between intact static stability and dynamic motion results, the condition under which the static stability was calculated, was simulated in the time domain simulation with a KG determined by the 1.0 area ratio in the static stability analysis and zero drag coefficient in the equation of motion, wherein the DF-distance was analyzed. A 100 knot stepwise wind was applied in the time domain simulation for the three units freely floating at the survival draft. Time histories under this condition are given in Figure 12, for the 8-column unit.

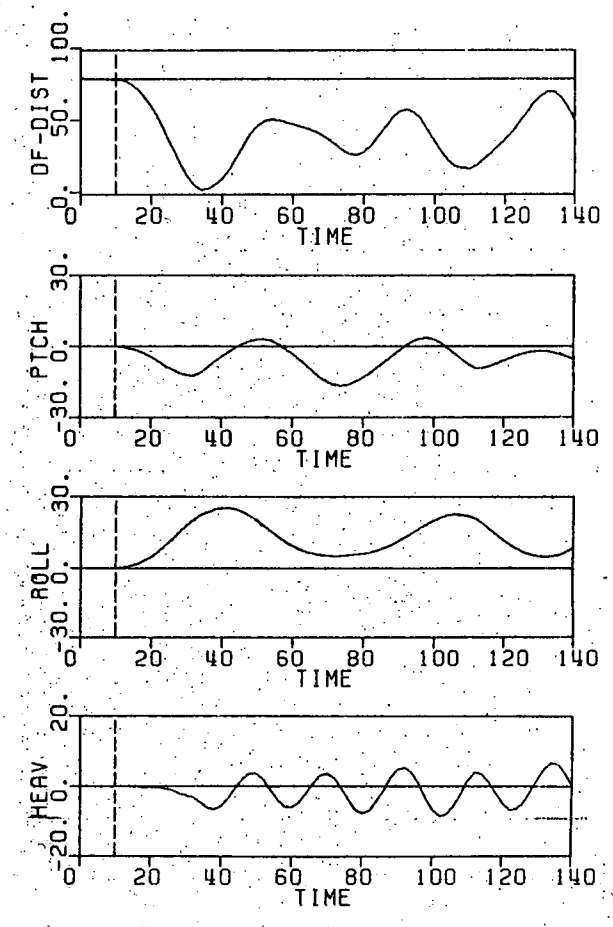

Fig. 12 Motion and DF-Distance of 8-Column Rig at Survival Draft; (100 kn, Ts = 10 s.), Freely-floating, zero damping, θ = 51°, 1.0AR, KG = 64.1', GM = 4.03'

The 8-column unit has a positive GM in the above described condition and a positive initial slope of the righting moment curve (Figure 4), indicating initial stability. For this condition, the DF-distance nearly reaches zero under the stepwise wind, as can be seen from Figure 12, implying that the time domain simulation corroborates classical static stability theory. It is therefore conceivable that the additional 0.3 area ratio for the unit operating at a KG determined by the required 1.3 area ratio represents a 30 percent safety margin to account for disturbances other than wind. It should also be noticed that in addition to the safety margin required by the stability criteria, there is some residual stability embodied in the stability calculation since, in reality, there exists dissipation of energy associated with the motion of the dynamic system, and the wind force used in the stability calculation is not felt instantaneously.

Similar correlation studies were also performed for the 4- and 6-column units, which have an initial negative GM value operated at KG values determined by the 1.0 area ratio. For these units, correlation between the time domain results and the static stability analysis are also obtained as in the case of the 8-column unit.

When the KG of the 4- and 6-column units are modified to have a zero GM, the area ratios become 3.075, and 1.376 respectively, at the survival condition. Even though these units meet the ABS stability requirement, and the time domain simulation shows no occurrence of downflooding in a 100 knot wind condition, the meaning of these area ratios in terms of safety margin becomes unclear and not readily quantifiable. This is due to the fact that the dynamic responses of different units in a seaway are not the same, as discussed in previous sections.

6. CONCLUDING REMARKS

Major findings of the pilot study, which were discussed in the preceding sections and are fully reported in Reference [6], are reiterated here:

- It has been shown through the correlation with model tests that the dynamic motion analysis procedure provides a reasonably accurate prediction of semisubmersible motion in waves.
- Characteristics of the static curve, particularly the extent and location of the change of slope, provide input to the understanding of a semisubmersible's static and dynamic behavior. The important parameters of the unit affecting the shape of the righting arm curve are GM, draft, column height, pontoon length, and pontoon separation, which directly affect the likelihood of pontoon emergence as the unit inclines.
- Large nonlinear motion and subharmonic motion in waves were observed in the time domain simulation of units having GM values approaching zero and relatively shallow drafts, when the variation in the time dependent restoring coefficient becomes significant in waves.
- Wind unsteadiness can have an appreciable influence on the motion response of a semisubmersible platform in storm conditions.
- Applying current colinearly with wind and waves tends to stabilize the unit.
- Mooring effects on the transient maximum motion and DF-distance of MODU's subjected to stepwise wind and/or waves are insignificant. However, mooring effects on steady and slow varying motions can be significant.

7. FUTURE WORK

Correlation between stability and the effects of steady forces of the environment such as current and steady wind is, and has been, established. In addressing the effects of fluctuating forces of waves and wind gusts separate from, yet accounting for, the effects of steady forces, it may be possible that semisubmersible stability characteristics can be identified and quantified with an acceptable degree of confidence permitting evaluation of existing stability criteria. This being accomplished, a rational stability criteria can also be formulated which will provide uniform margins of safety.

In order to reach this goal, a more comprehensive study to reassess and to confirm the existing criteria is necessary. This study should include at least some definition and evaluation of pertinent parameters of the environment, predictions of stability and motions for a parametric series of a generic semisubmersible, and correlation of calculated dynamic motions with model test results, in particular, to calibrate analytic predictions of large nonlinear motions. The future study should also include the analysis of semisubmersible stability in a damaged condition, because this condition can be more critical than the intact condition in determining the unit's needed overall stability.

ACKNOWLEDGEMENT

The authors would like to express their appreciation for the encouragement received from Dr. D. Liu, Vice President of the Research and Development Division, American Bureau of Shipping. Special appreciation is extended to Messrs. R. Ng, T. Grove and R. Tao for their technical assistance, editing and production efforts on this paper.

REFERENCES

1. American Bureau of Shipping, "Rules for Building and Classing Mobile Offshore Drilling Units", 1985.

2. Sarohin, T.H. and Goldberg, L.L., "Stability and Buoyancy Criteria for U.S. Naval Surface Ships", SNAME Trans. pp. 418-458, 1962.

3. Springett, C.N. and Praught, M.W., "Semisubmersible Design Considerations - Some New Developments", Twenty-eighth Annual Joint Meeting of California SNAME Sections, Monterey, CA, April 25, 1985.

4. Paulling, J.R. and Shin, Y.S., "On the Simulation of Large Amplitude Motions of Floating Ocean Structures", International Symposium on Ocean Space Utilization, Tokyo, 1985.

5. Maoha, J.M. and Reid, O.F., "Semisubmersible Wind Loads and Wind Effects", SNAME Trans. pp. 1-37, 1984.

6. Liu, D. et al., "Stability Study for Mobile Offshore Drilling Units (Phase I)", ABS Technical Report RD-85014, Sept., 1985.

Third International Conference on Stability of Ships and Ocean Vehicles, Gdańsk, Sept 1986

STAB'86

STUDY ON DYNAMIC RESPONSE OF SEMISUBMERSIBLE PLATFORM UNDER FLUCTUATING WIND

K. Ikegami; Y. Watanabe; M. Matsuura

ABSTRACT

Experimental investigations into the static and dynamic wind loads on a semisubmersible platform of 1/55 scale model were made by use of a large wind tunnel with measuring section 10 m x 3 m and fluctuating wind generator. Based on the test results, dynamic responses in waves and fluctuating wind were predicted by use of a time domain simulation technique. It is shown that the fluctuating wind induces low frequency motion which should be carefully considered for the safety operation of a semisubmersible platform.

1. INTRODUCTION

Safety operation of a semisubmersible platform under severe environment has been one of the most important concerns in the course of the design, since disasters of some semisubmersible platforms occurred consecutively in this decade. Wind load is one of the most influential factors to be considered for its safety and reliable operation in rough sea[1].

In the rules and regulations of the classification societies and governments, the wind load is an only environmental force for assessment of stability of semisubmersible platform and represented as the steady external force[2]. However, wind load is composed of not only steady component but also fluctuating one. This fluctuating component has significant effect on dynamic response of semisubmersible platform, when the natural frequency of its motion is close to the frequency of fluctuating wind [3]. Therefore, accurate prediction of fluctuating component of wind load is considered to be of primary importance for evaluation of dynamic response, and consequently assessment of safety operation of semisubmersible platform.

With these points as background, an attempt was made to clarify the characteristics of static and dynamic wind loads acting on a semisubmersible platform by wind tunnel test. And based on the test results, some computational studies were performed to predict dynamic response of a semisubmersible platform in waves and fluctuating wind by use of a time domain simulation technique.

2. STATIC WIND LOADS

In order to investigate into the characteristics of static wind loads on semisubmersible platform, wind tunnel test was carried out in the multi-purpose wind tunnel in the Nagasaki Technical Institute of Mitsubishi Heavy Industries. This facility is of blow-down type with a test section measuring 10 m x 3 m and capable of producing wind of up to 28 m/s in speed.

2.1 Wind Tunnel Test

The wind tunnel test was conducted with a large scaled model, 1/55 in scale, of a 2-lower hull/8-column type semisubmersible platform. Its principal particulars and side view are shown in Table 1 and Fig. 1, respectively.

The scheme of measuring arrangement in the wind tunnel is shown in Fig. 2. The model is mounted on the model attitude mechanism controlled by stepping motor for heel, trim and yaw angle in the water tank. By use of this apparatus, changes of test conditions can be rapidly accomplished.

The shear flow profile of wind is simulated by shear flow generator composed of a series of pipes installed across the wind tunnel nozzle. The wind

Table 1 Principal particulars of model of semisubmersible platform

Items	Model	Prototype
Length Overall	2.091 m	115.0 m
Length of Main Deck	1.364 m	75.0 m
Breadth Overall	1.364 m	75.0 m
Height to Main Deck	0.691 m	38.0 m
Draft	0.364 m	20.0 m
Displacement	194 kg	33120 ton
Reference Area	0.495 m²	1497 m²
Metacentric Height	0.052 m	2.87 m
Gyradius : Roll (K_{xx}/L)	0.457	0.457
Natural Period : Sway	13.2 sec	98 sec
: Roll	7.3 sec	54 sec

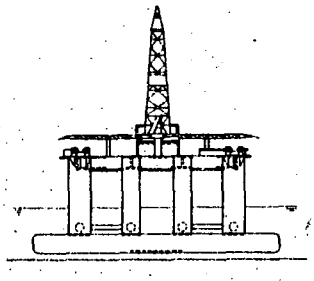

Fig.1 Model of semisubmersible platform

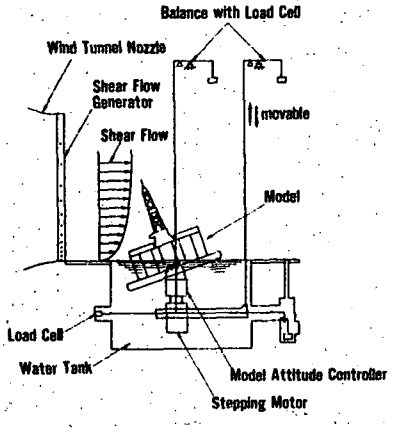

Fig.2 Test arrangement of static wind load test

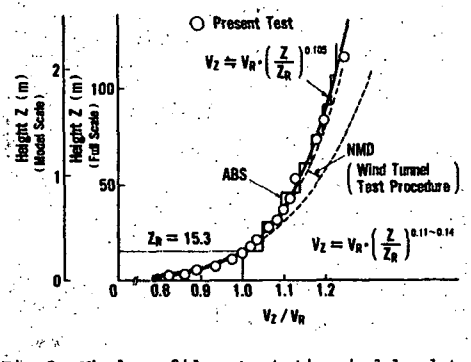

Fig.3 Wind profile at static wind load test

profile is shown in Fig. 3, and closely coincides with the profile specified by the regulations of the classification societies [4,5].

2.2 Test Results

In this paper, we restrict ourselves to the presentation of drag force, lift force and overturning moment about horizontal axis at the waterline.

In order to examine the effect of Reynolds number on the wind loads, the tests were conducted varying the wind velocity in the range from 4 m/s to 24 m/s (Reynolds number based on the corner column diameter = $0.5 \times 10^5 \sim 2.9 \times 10^5$). The test result is shown in Fig. 4 for the case of longitudinal wind direction. It is observed that C_D, C_L and C_{MP} remain nearly constant, and the effect of Reynolds number on the wind loads is small as already noted in reference [6].

The polar plots in Fig. 5 indicate the effect of wind direction on wind loads. In the longitudinal and transverse direction of the platform, it is said that the C_D becomes smaller due to the shielding effect of columns and braces. In the diagonal direction, the projected area of main deck, derrick and so on become larger so that the C_D becomes greater. The C_L tends to be larger in the wind direction range from 180 degrees to 360 degrees. The change of the C_{MP} to wind direction is comparatively small, where a fixed value of frontal projected area A is used.

The change of wind loads due to the inclination angle of platform is shown in Fig. 6. The C_L tends to increase remarkably as the inclination angle becomes larger, since the lift force is generated from the difference of pressure between upper side and lower side of main deck.

Although the C_D and C_L increase as the inclination angle becomes larger, the C_{MP} increases with increasing angle of inclination up to about 10 degrees, and decreases thereafter. The fact occurs, probably because the center of wind pressure on the deck shifts downwind according to the positive inclination.

At present, estimation of wind loads on semisubmersible platform is generally made by use of the

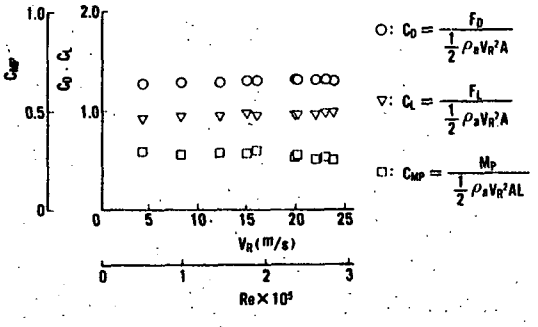

Fig.4 Effect of Reynolds number on wind loads

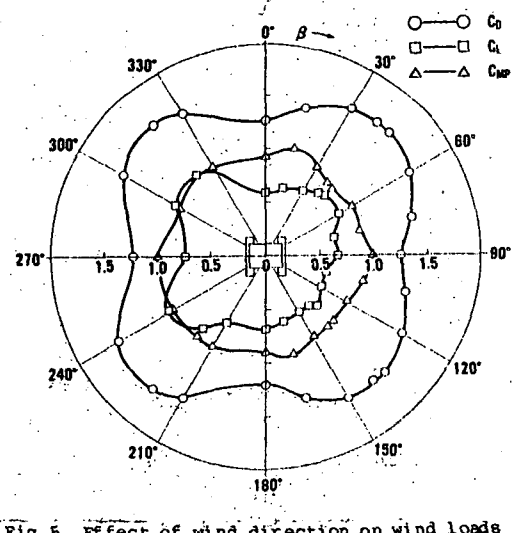

Fig.5 Effect of wind direction on wind loads

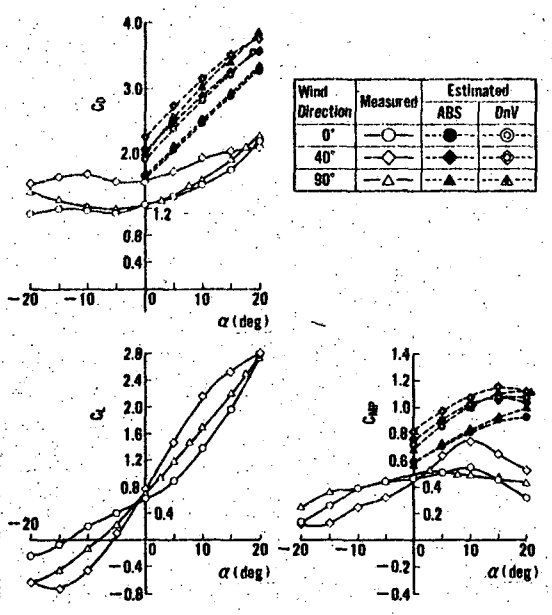

Fig.6 Effect of inclination angle on wind loads

procedure proposed by the American Bureau of Shipping (ABS) and the Det norske Veritas (DnV) [4,7]. Thus, as shown in Fig. 6, comparisons are made between the results of wind tunnel test and the results estimated by regulations of ABS and DnV. It is observed that the ABS and DnV procedures yield greater C_D and C_{MP} values than those from the present wind tunnel test. Discrepancy between them increases with increase of inclination angle. The difference of C_{MP} with increase of inclination angle may be due to the difference of pressure distribution on the main deck [8]. Therefore, it is necessary to clarify the characteristics of pressure distribution on main deck for accurate estimation of wind load.

3. DYNAMIC WIND LOADS

3.1 Wind Tunnel Test

In order to investigate into the characteristics of dynamic wind loads, the wind tunnel test was carried out under sinusoidal and random fluctuating winds. The scheme of measuring arrangement is shown in Fig. 7. A new type of gust generator with damper was installed at the both side of wind tunnel nozzle for generation of fluctuating wind velocity. The damper is composed of the many plates automatically controlled to change the sectional area of wind tunnel nozzle. Various kinds of fluctuating wind, sinusoidal and random, can be generated by use of computer control system.

Examples of fluctuating wind velocity measured at some points are shown in Fig. 8 having uniform property in space. The phase angles obtained from the measured results of sinusoidal fluctuating wind at three points in main flow are plotted as a function of reduced frequency fr/V in Fig. 9, where r is

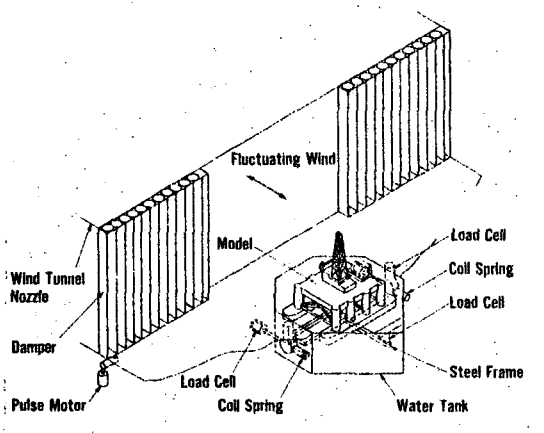

Fig.7 Test arrangement of dynamic wind load test

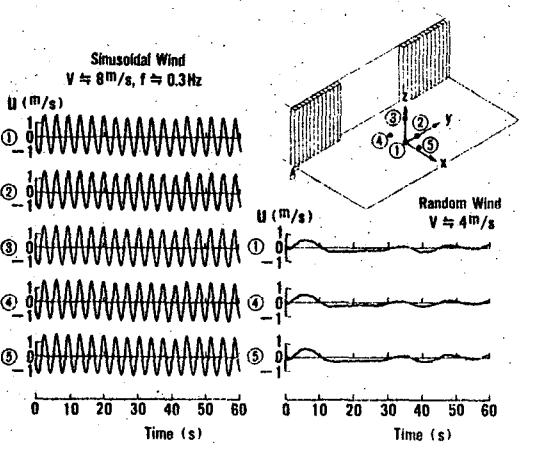

Fig.8 Samples of records of fluctuating wind

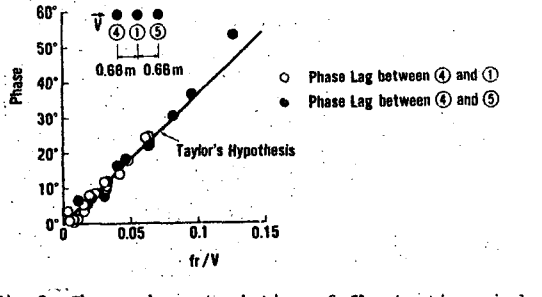

Fig.9 Phase characteristics of fluctuating wind

the distance between two points. A straight line indicates the phase based on the Taylor's hypothesis for natural wind. It can be confirmed that the fluctuating wind generated in the wind tunnel has almost the same phase property as that of natural wind.

3.2 Test Results

When a body is in wind having steady component V and fluctuating one u(t), wind load can be described as follows, based on an assumption that u(t) is much smaller than V.

$$F = 1/2\ \rho_a V^2 CA + \rho_a u(t) V C^* A \qquad (1)$$

where the first term is the steady wind load, and the second term is dynamic wind load due to fluc-

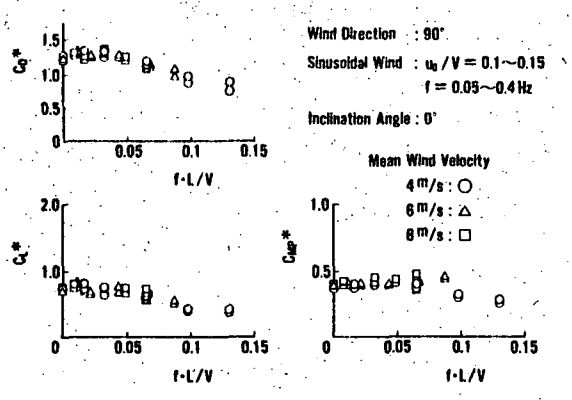

Fig.10 Coefficients of dynamic wind loads (Sinusoidal wind)

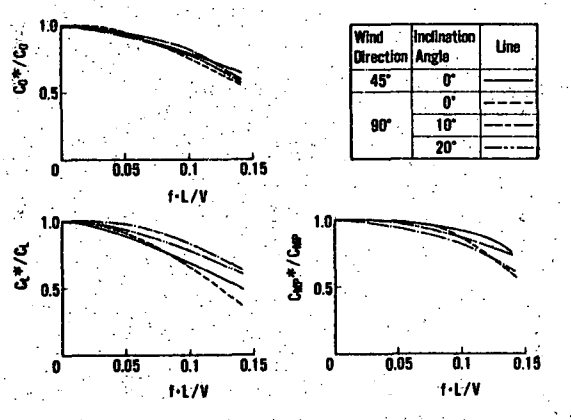

Fig.11 Aerodynamic transfer functions (Sinusoidal wind)

tuating wind component.

Dynamic wind load coefficients obtained in sinusoidal fluctuating wind test by use of the formula (1) are shown in Fig. 10 as a function of reduced frequency. The aerodynamic transfer function obtained as mean line from these results is shown in Fig. 11 for various test conditions. It is shown that the dynamic wind loads decrease with increasing reduced frequency, and this tendency is independent of the inclination angle and wind direction. The cause for the tendency is considered as follows.

(1) Phase lag of aerodynamic force on each point :

There exists the phase lag of the aerodynamic force on each point on the platform, which is due to the phase lag of fluctuating wind, and is in proportion to reduced frequency fL/V.

(2) Damping of amplitude of fluctuating wind and reduction of coherency :

Once the fluctuating wind acts on the front of the model, the amplitude of fluctuating wind is damped, and coherency is reduced because of breaking of wave profile.

The power spectra of random fluctuating winds used in these tests are shown in Fig. 12 in comparison with the Kármán type spectrum of natural wind. Wind B coincides with the Kármán type fairly well. The power spectrum of dynamic wind load and the

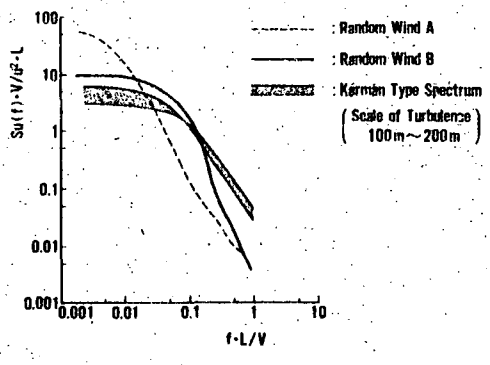

Fig.12 Nondimensional power spectrum of random wind

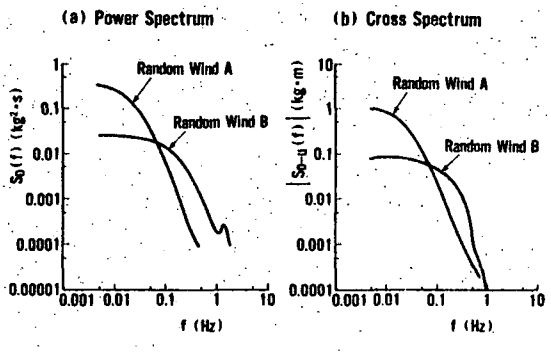

Fig.13 Power spectrum of dynamic drag and cross spectrum between dynamic drag and fluctuating wind

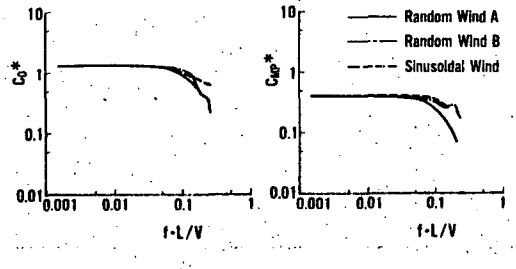

Fig.14 Coefficients of dynamic wind loads (Random wind)

cross spectrum of dynamic wind load and fluctuating wind are shown in Fig.13.

The dynamic wind load coefficients obtained from the power spectrum of fluctuating wind and the cross spectrum of dynamic wind load and fluctuating wind are shown in Fig.14. These figures also show that the dynamic wind load decreases with increasing reduced frequency.

4. SIMULATION OF DYNAMIC RESPONSE

Based on the results of wind tunnel test above, some computational studies were performed on dynamic response of a semisubmersible platform under fluctuating wind by use of a time domain simulation technique.

4.1 Time Domain Simulation Method

The equations of motions of a floating body moored in waves and wind are given as follows:

$$\sum_{j=i}^{6}[(M_{ij} + m_{ij})\ddot{D}_j + N_{ij}\dot{D}_j + Ne_{ij}(\dot{D}_j - \bar{U}_j)|\dot{D}_j - \bar{U}_j| + C_i(D_1, D_2, \ldots D_6) + G_i(D_1, D_2, \ldots D_6)] = F_{wi}(t) + F_{ai}(t) \quad (2)$$

$$(i = 1,2,\ldots,6)$$

i,j : Suffix, representing mode of motion, $i,j = 1,2,\ldots,6$. corresponding to surge, sway, heave, roll, pitch and yaw, respectively

D_j : Translatory and angular displacements of body

M_{ij} : Generalized mass of body

m_{ij} : Added mass

N_{ij} : Coefficient of wave damping

Ne_{ij} : Coefficient of viscous damping

C_i : Hydrostatic restoring force

G_i : Reacting force arising from mooring system due to displacement

$\bar{U}_j$: Mean value of orbital velocity of water particle in the direction of the mode of motion

$F_{wi}(t)$: External force due to wave

$F_{ai}(t)$: External force due to wind

The calculation method of external forces due to wind is as follows. The wind velocity V(t) can be represented by sum of the mean velocity V and the fluctuating velocity u(t): i.e.

$$V(t) = V + u(t) \quad (3)$$

and u(t) can be represented by use of power spectrum Su(f) of fluctuating wind as follows:

$$u(t) = \int_0^\infty \sqrt{4Su(f)df}\cos[2\pi ft + \varepsilon(f)] \quad (4)$$

where

$\varepsilon(f)$: Random phase angle between 0 and 2π

External forces due to wind are written as follows:

$$F_{ai}(t) = 1/2\,\rho_a v^2 C_{Di} A + \rho_a u(t) V C_{Di} \frac{C_{Di}^*}{C_{Di}} A \quad (5)$$

$$(i = 1 \sim 3)$$

$$F_{ai}(t) = 1/2\,\rho_a v^2 C_{Di} AL + \rho_a u(t) V C_{Di} \frac{C_{Di}^*}{C_{Di}} AL \quad (6)$$

$$(i = 4 \sim 6)$$

where C_{Di}^*/C_{Di} is aerodynamic transfer function in the direction of i-th mode of motion. The dynamic response of body can be obtained by solving the non-linear differential equations (2) in time domain. The integration scheme of the equations of motions adopted in the present analysis is the midpoint trapezoidal method [9].

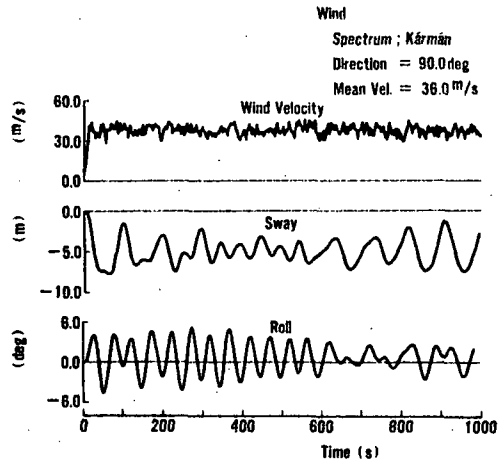

Fig.15 Time series of motions of semisubmersible Platform under fluctuating wind

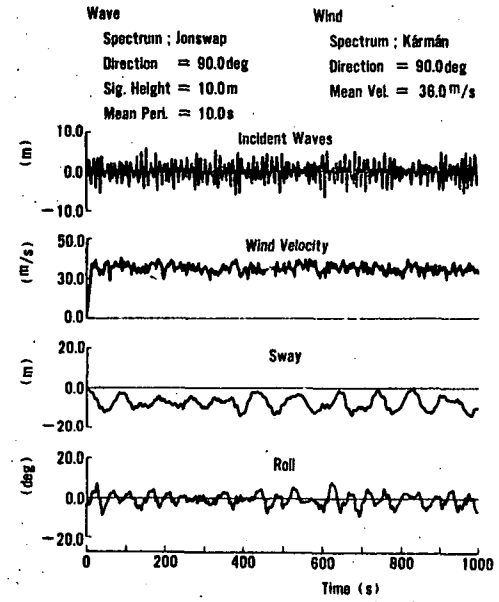

Fig.16 Time series of motions of semisubmersible platform in waves and wind

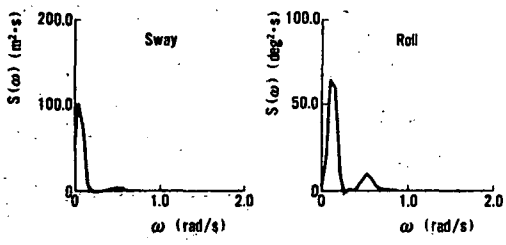

Fig.17 Spectra of motions of semisubmersible platform in waves and wind

Hydrodynamic forces acting on section of cylindrical members are calculated by use of the relative motion concept based on the Morison's equation.

4.2 Calculation Results

The platform is assumed to be moored by 4 sets of linear spring, and the principal particulars affecting the dynamic response are shown in Table 1.

The dynamic response of semisubmersible platform in random fluctuating wind is shown in Fig. 15. It can be found that the large shift in transverse direction and low frequency sway and roll motions with frequency components close to the natural frequencies of motions are induced for a semisubmersible platform by fluctuating wind.

The dynamic responses of semisubmersible platform in composed external forces due to waves and wind are shown in Fig. 16, and the results of spectrum analysis are shown in Fig. 17. Two peaks of energy densities of motions are found in sway and roll motions. This indicates that the motion of a semisubmersible platform in waves and wind is a combined motion in high frequency range and low frequency range. Amount of peak in low frequency range is much larger than that in high frequency range. The peak of the low frequency range is due to not only the slowly varying wave drifting force but also the fluctuating wind. It is pointed out that, therefore, consideration should be given to the low frequency motion induced by fluctuating wind for safety operation of semisubmersible platform.

5. CONCLUDING REMARKS

The characteristics of static and dynamic wind loads on a semisubmersible platform and its dynamic response were investigated by wind tunnel test and a numerical simulation. It is concluded that:

(1) The characteristics of static wind loads on a semisubmersible platform were studied experimentally. That is, the effects of the Reynolds number, wind direction and inclination angle of semisubmersible platform on static wind loads were obtained.

(2) Static wind loads measured in the present wind tunnel tests yield smaller values than those predicted by the ABS and DnV procedures. Discrepancies between them become greater with increasing inclination angle.

(3) The dynamic wind load coefficients on semisubmersible platform decrease with increasing reduced frequency.

(4) The low frequency motion is induced for a semisubmersible platform by fluctuating wind, and consideration should be given to this motion for safety operation of semisubmersible platform.

ACKNOWLEDGEMENTS

The authors wish to express their gratitude to Dr. H. Fujii, Chief Research Engineer of the Nagasaki Technical Institute of Mitsubishi Heavy Industries and all members concerned with this study for their valuable assistance.

NOMENCLATURE

A	= Frontal projected area above water (fixed value in the present test)
C_D	= Drag coefficient
C_L	= Lift coefficient
C_{MP}	= Overturning moment coefficient
C_D^*	= Dynamic drag force coefficient
C_L^*	= Dynamic lift force coefficient
C_{MP}^*	= Dynamic overturning moment coefficent
D_C	= Diameter of corner column
f	= Frequency of fluctuating wind
L	= Reference length (length of main deck)
R_e	= Reynolds number ($=V_R \cdot D_C/\nu$)
$u(t)$	= Fluctuating component of wind velocity
V	= Mean wind velocity
V_R	= Flow velocity at the reference height
α	= Inclination angle
β	= Wind direction
ν	= Air kinematic viscosity
ρ_a	= Air density
ω	= Circular frequency

REFERENCES

(1) J. M. Macha and D. F. Reid : Semisubmersible Wind Loads and Wind Effects, Trans. SNAME, Vol. 92, 1984.

(2) E. Numata, W. H. Michel and A. C. McClure : Assessment of Stability Requirements for Semisubmersible Units, Trans. SNAME, Vol. 84, 1976.

(3) A. Kareem : Dynamic Effects of Wind on Offshore Structures, OTC 3764, Offshore Technology Conference, 1980.

(4) American Bureau of Shipping : Rules for Building and Classing Mobile Offshore Drilling Units, 1980.

(5) Norwegian Maritime Directorate Wind Tunnel Test Procedure, 1973.

(6) P. Jacobsson and G. Dyne : Reynolds Number Effects in Model Tests with a Four Column Semisubmersible, Second International Symposium on Ocean Engineering and Ship Handling, 1983.

(7) Det norske Veritas : Rules for the Design Construction and Inspection of Offshore Structures Appendix A,B, 1977.

(8) H. Maeda, K. Nishimoto and S. Eguchi : A Study of Components of Wind and Current Loads on Semisubmersibles, Journal of the Society of Naval Architects of Japan, Vol. 156, 1984.

(9) M. Matsuura and K. Ikegami : Time Domain Simulation of Dynamic Response of Semisubmersible Platform in Severe Sea Condition, Fifth International Symposium on Offshore Mechanics and Arctic Engineering, Tokyo, 1986.

Third International Conference on Stability of Ships and Ocean Vehicles, Gdańsk, Sept. 1986 STAB'86

THE SEABRAKE
A DEVICE FOR ASSISTING IN THE PREVENTION OF BROACHING - TO

M.R. Renilson

1. ABSTRACT

This paper describes how a broach in severe following seas can occur and shows that the ship being surged by the waves to approximately wave speed is a prerequisite for this to happen.

In an attempt to prevent this surging, a two stage drag device which is towed behind the ship has been developed. This device is described in detail and the results of towing tank experiments and a simulation study are given.

2. INTRODUCTION

When travelling in following seas there is a possibility of "broaching-to" with its resultant loss of control and danger of capsize (Ref. 1,2). The steep waves which occur over a bar etc. Will increase the risk of broaching at exactly the moment at which precise directional control may be vital to the safety of the vessel.

The research carried out on this phenomenon by the author and by others (Ref. 3, 4, 5, 6, 7) has shown that the dangerous situation occurs when the ship is accelerated to wave speed by a wave of ship length or greater.

As concluded in (Ref.5) "Broaching-to" in following seas is caused by the ship being surged by the waves in such a way that it spends enough time in the longitudinal position in the wave where there is a larger wave induced yaw moment than there is restoring moment available from the rudder." Thus, the ability to maintain a low speed and to prevent the large surging velocities which are responsible for a potential broaching situation is important.

One means of increasing drag in an attempt to prevent this surging is to stream a sea anchor. Unfortunately this does not seem to help in practice and there is a school of thought which believes that this aggravates the situation. A possible reason for this is the sea anchor's lack of directional stability causing it to yaw violently when towed at speed. This initiates yawing of the vessel which may lead to a broach. Hence the search for a device capable of reducing the surging of the vessel without inducing yawing.

3. DESCRIPTION OF THE SEABRAKE

The seabrake has been developed over a period of about 10 years by Captain J. Abernethy, a charter boat operator in the Bass Strait. The early history of the project shows that Captain Abernethy developed a solid body cone, having spent considerable time to determine the angle and shape required to provide sufficient drag. This cone shaped device proved unsuitable and further prototypes were developed until finally the cone with a hollow body shape with four panels cut out at the base of the cone with lead ports was found to operate reasonably satisfactorily. Further modifications were made which provided for the doors to be opened inwards to a predetermined opening actuated by a central shaft which was in turn pulled up by a central towing lug at the apex of the cone attached to a towing warp fixed to a vessel.

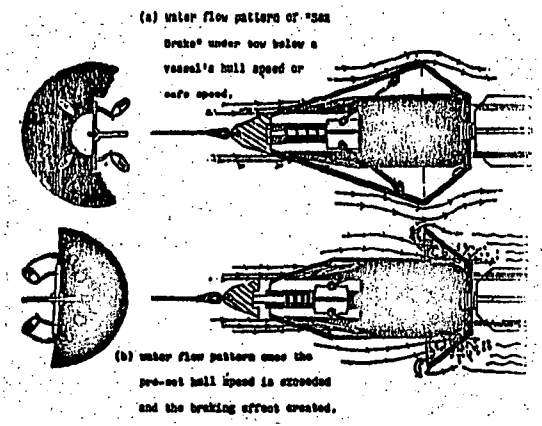

Figure 1. The Seabrake

This resulted in a two stage drag device which tracked well and which it was felt greatly improved a vessels down sea safety. (See appendix) The speed at which the doors opened is pre-set by a tension spring in the nose cone.

4. TOWING TANK TESTS

In order to quantify the force involved it was decided to carry out tests in the ship model towing tank at the Australian Maritime College (60m x 3.5m x 1.6m deep - Ref. 8) on an 18" diameter Seabrake and an 18" diameter conventional sea anchor (Ref. 9).

The Seabrake was towed at half the tank depth by a vertical steel rod connected to a conventional ship model calm water dynamoeter (Figure 2) on a large self-propelled towing carriage.

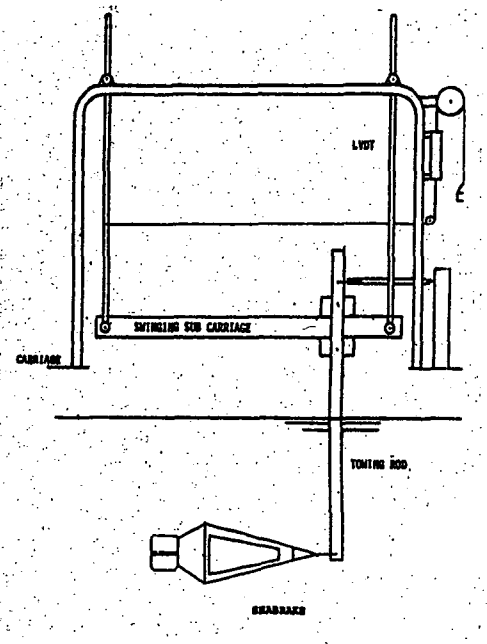

Figure 2. Towing Rig

The expected forces were much larger than those experienced with surface ship model experiments and so special springs had to be manufactured to take the loads. The dynamometer movement was measured by an LVDT and recorded using a pen recorder on the carriage. Three different springs were used with different spring constants and the results were cross-checked. Approximately 30 to 60 minutes were allowed between runs to allow the water to settle.

For the tests using the Seabrake a 50mm x 10mm mild steel rod was used. At the highest speed run attempted (5m/s) this bent in its own plane.

It was intended to use the same towing rod for the sea anchor, however, due to the sea anchor's violent lateral oscillations it bent sideways at a speed of 2.6 m/s. For this reason all the results for the Sea anchor were obtained using a heavier mild steel rod (75m x 12mm). This finally bent sideways at a speed of 3.8 m/s. A number of results with each towing rod alone were obtained and thus the resistance of the rod could be deducted from the total resistance to obtain the resistance of the Seabrake/sea anchor alone.

Great care was taken to ensure that the orientation of the Seabrake remained constant throughout. One of the stability ports was always at the top, and in this configuration it showed no tendency to rotate.

The tests showed that the drag on the Seabrake with its doors closed is the smallest and that opening the doors increases this by about 70%. The drag on the sea anchor is greater still, however, it is important to note that this was accompanied by considerable lateral osciallations whereas the Seabrake tracked very well. The sea anchor also had a tendency to rise to the surface while the Seabrake remained well submerged. From the

tests it was possible to conclude that the tracking ability of the Seabrake was far superior to the conventional sea anchor.

The comparison of the drag coefficients is given in Figure 3. This shows that the Seabrake in either configuration exhibits an almost constant drag coefficient (as to be expected from a streamlined body), however, the drag coefficient of the sea anchor is constantly decreasing with speed. The "two-stage" effect of the Seabrake can be clearly seen.

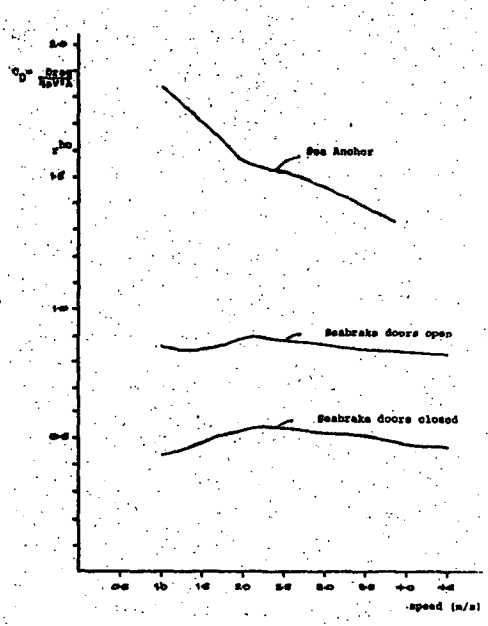

Figure 3. Drag Coefficient

5. SIMULATION

As discussed in the introduction the prime purpose of the Seabrake is to prevent the ship from being surged in such a way that it spends sufficient time on that part of the wave when the wave induced yawing moment is greater than restoring moment available from the rudder.

This is best illustrated by figures 4 and 5 which are taken from reference 3. In these figures positive X' indicates a forward force on the model for the wave and a positive δ_{equil} required indicates a potential broaching situation. Neglecting heel angle δ_{equil} is calculated from;

$$\delta_{equil} = \left(\frac{Y_v N_\alpha - N_v Y_\alpha}{N_v Y_\delta - N_\delta Y_v}\right)\alpha_0$$

where all the coefficients are taken to be functions of wave position and the values given are obtained from model experiments described in reference 3 ($\lambda/L = 1.07$ and $\lambda/h = 28$) from figure 5 it can be seen that a positive δ_{equil} exists for $\xi = 0.6$ though $\xi = 1.0$ to $\xi = 0/2$. (ξ is the non dimensional distance from the wave crest to the stern shown in figure 6). It is important to note that the area of the wave with the largest required ξ_{equil} (i.e. the area most likely to initiate a broach), $0.75 < \xi < 1.00$, corresponds to that with a positive forward force. Hence it would be expected that the ship could spend considerable time in this region allowing large values of heading angle to the waves (α) to be built up thereby initiating a broach. This was investigated using a hybrid simulation technique and was found to be the principle cause of broaching-to. (Ref. 4 & 5).

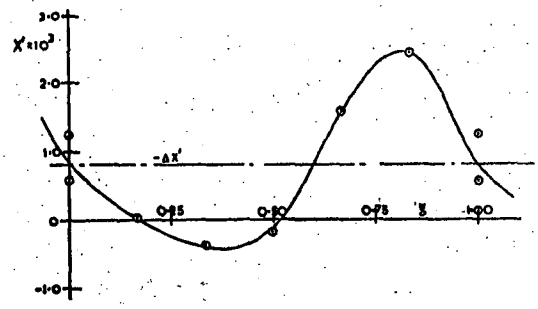

Figure 4. X' for Varying ξ

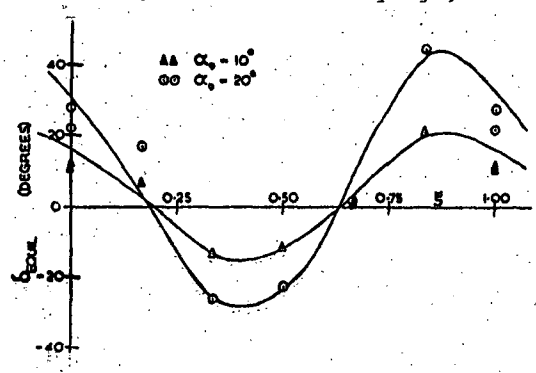

Figure 5. δ_{equil} for Varying ξ

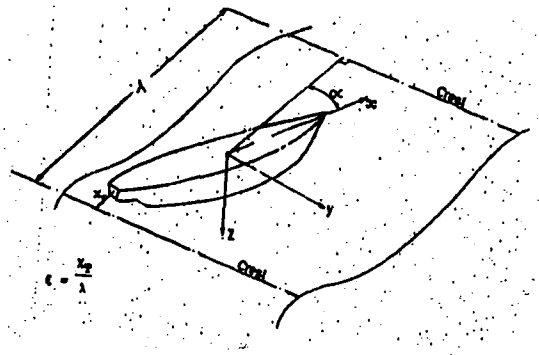

Figure 6. Schematic View Of The Hull in a Wave.

In order to investigate the effect of the seabrake on the surging motions it was decided to set up a digital simulation based on the following equations:-

$$0 = X_{u^2}U^2 + (X_{\dot{u}} - m)\dot{u} + X_{\xi} + X_{prop} + X_{seabrake}$$

$$\xi = \frac{1}{\lambda}\int_0^t [u - c]\, dt$$

The simulation employed the classic step by step process and was carried out for a 9m long vessel in a 9.63m long, 0.34m high regular following sea. Typical results showing the effect of the Seabrake in three different modes (doors closed, doors open, doors set to open at 3.0m/s) are given in figures 7 - 10.

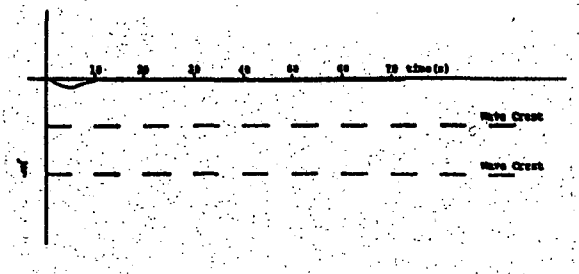

Figure 7. ξ against time for vessel without seabrake

(Initial speed 2.5m/s)

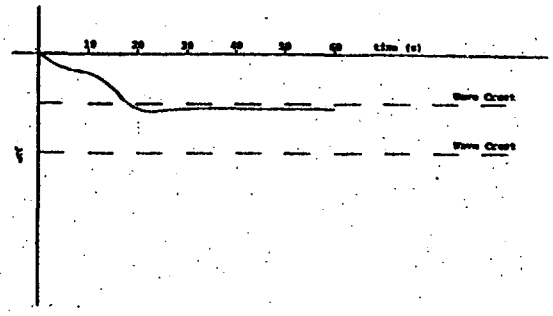

Figure 8. ξ against time for vessel with seabrake being streamed doors closed.

(Initial speed 2.5m/s)

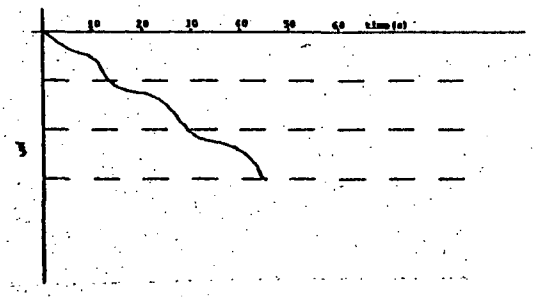

Figure 9. ξ against time for a vessel with seabrake being steamed - doors open.

(Initial speed 2.5m/s)

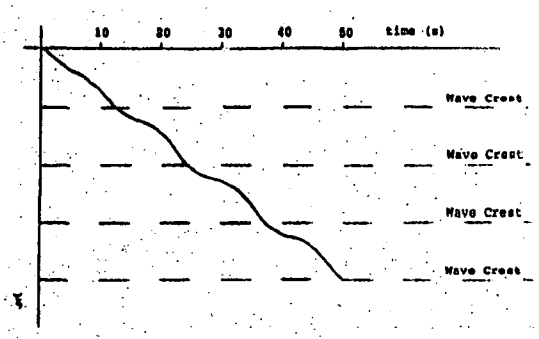

Figure 10. ξ against time for a vessel with seabrake being streamed-doors set to open at 3m/s.

(Initial speed 2.5m/s)

The time spent in the region $0.75 < \xi < 1.0$ plotted in figure 11 against initial ship speed for the four conditions tested; no seabrake, seabrake doors closed, seabrake doors open and seabrake doors set to open at 3.0 m/s. In each case the drag of the warp was neglected and the propeller thrust was assumed to remain constant at the self propulsion value. Initial

conditions for each simulation run were $\xi = 0$ (i.e. wave crest at stern) an U = self propulsion speed.

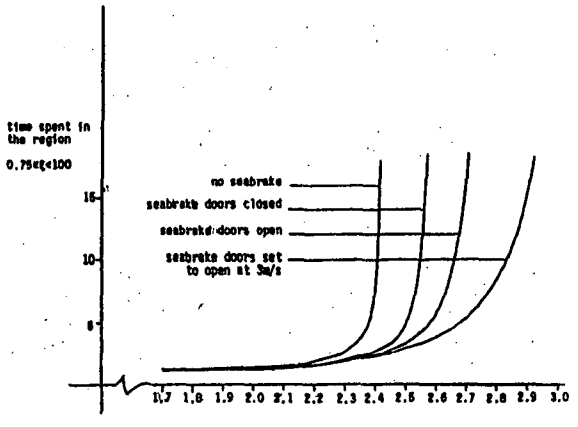

Figure 11. Length of time spent in dangerous position for the four different conditions simulated.

It can be seen from figure 11 that the length of time spent in the dangerous condition ($0.75 < \xi < 1.0$) decreases with decrease in ship self propulsion speed indicating a reduction in the possibility of broaching when speed is reduced. This is in accordance with the results of the full simulation carried out by one of the authors and described in reference 4 and 5. It can also be seen that the streaming of a seabrake increases the ship self propulsion speed required to spend a given time in the dangerous condition for speeds other than low speeds when it is anticipated broaching will not occur in any case. Thus, it would seem reasonable to conclude that the streaming of a Seabrake in an irregular following sea would reduce the tendency for the vessel to be surged by the waves into a situation when a broach could be initiated.

6. CONCLUSIONS

One of the prerequisites for a broach to occur in following seas is for the vessel to be surged by the waves in such a way that it spends enough time in a position on the wave where the wave induced yaw moment is greater than the restoring moment available from the rudder.

A device which increases the drag of the vessel without inducing yawing motion has been described and it has been shown by means of simulation that this has the effect of reducing the time spent in the dangerous position in the wave.

It is expected that this will reduce the tendency for a vessel to broach in an irregular following sea.

7. ACKNOWLEDGEMENTS

The author wishes to acknowledge the assistance of Seabrake International and of the original inventor of the Seabrake concept - Captain J. Abernethy.

8. REFERENCES

1. Du Cane, P., Goodrich, G.J.: "The Following Sea, Broaching and Surging." Trans RINA Vol. 104 April 1962.

2. Conolly, J.E.; "Stability and Control in Waves: A Survey of the Problem." Proceedings of Int. Symp. on Directional Stability and Control of Bodies Moving in Water 1972.

3. Renilson, M.R. and Driscoll, A.: "Broaching - An Investigation into the Loss of Directional Control in Severe Following Seas" RINA Spring Meetings 1981.

4. Renilson, M.R. : "An Investigation in the Factors Affecting the Likelihood of Broaching-to in Following Seas." 2nd International Conference on Stability of Ships and Ocean Vehicles, Tokyo, October 1981.

5. Renilson, M.R. : "Broaching - A Note on Some of Factors Involved." International Conference on Marine Safety, Glasgow, September 1983.

6. Fuwa, T., Sugai, K., Yoshire, T., and Yamamoto, T. : "An Experimental Study on Broaching of a Small High Speed Boat." Ship Research Institute Report No. 66 April 1982.

7. Motora, S., Fujino, M., Fuwa, T.,: "On the Mechanism of Broaching-Phenomena." 2nd International Conference on Stability of Ships and Ocean Vehicles, Tokyo, October 1982.

8. Renilson, M.R., : "The Ship Hydrodynamics Centre at the Australian Maritime College." Workshop on National Need, Capabilities and Resources for Offshore Engineering, Monash University, Melbourne, 1986.

9. Renilson, M.R., : "Measurements of the drag of a Seabrake - a two stage device designed to help prevent broaching-to." Australian Maritime College Report 84/1 1984.

9. APPENDIX

Trial 2 September 1985 (Chief Petty Officer G. Wilson)

Vessel: Aust. Navy Torpedo Recovery Vessel "Tuna".

Length 88'
Displacement 100 tons
Speed 12 knots (max.)

Trial was conducted aboard vessel TRV "Tuna" under command of Chief Petty Officer QMG Wilson - offshore from Sydney Heads.

(1) TRV Tuna was tasked with conducting trails on Seabrake on Monday 2 September 1985. Tuna proceeded to sea at 0850 and the following weather conditions prevailed:

Wind - Force 7-8 (30 knots - gusting to 40 knots)
Sea State - 5-6 (2.5 to 4 metres)
Swell - 2.5 to 3 metres from 160°

(2) Tuna was steering a course of 040° at speed 8 knots. The following observations were made:

(a) Rolling through centre approx. 20°+
(b) Yawing 20°+ to starboard of course
(c) Using 25°-30° of port helm to maintain course.

(3) Seabrake was streamed to approx. 130ft through centreline fairleads and the following observations were made:

(a) Rolling was damped dramatically to approx. 10°
(b) Yawing was damped dramatically to 7°-10°
(c) Using 5° port helm to maintain course.

10. NOTES

Prior to streaming Seabrake, the TRV showed the alarming characteristics of broaching, with a rough sea on a moderate swell on the starboard quarter. Excessive amounts of port helm were needed to counteract the broaching tendencies.

On streaming Seabrake, the vessel "stabilised" significantly, with the helm being reduced to 5° or less and the sea riding qualities of the vessel becoming more comfortable."

Third International Conference on Stability of Ships and Ocean Vehicles, Gdańsk, Sept. 1986 STAB'86

THE SAFESHIP PROJECT - A BASIS FOR BETTER DESIGN CRITERIA AND STABILITY REGULATIONS

H. BIRD Marine Directorate Department of Transport U.K.
A. MORRALL British Maritime Technology Limited U.K.

SUMMARY

Ship designers and approving authorities need to have guidance on what are acceptable safe minimum values of the stabililty properties for the many different types and sizes of ships.

As in other branches of engineering, safety rules have grown up from cumulative experience of failures and in the case of ship stability such an entirely empirical approach has lead to simple but rather crude statical stability criteria which are of questionable value in assessing safety.

The International Maritime Organization (IMO) known as the Inter-governmental Maritime Consultative Organization (IMCO) until 20 May 1982, has been working towards the development of "physical" criteria which would manifestly enable safety assessment relative to external forces and thus provide, for the first time, indications of safety margins. This is seen by IMO as a long-term development.

Considerable efforts have been made by Classification Societies over the years to develop scantling rules based on theoretical and measured structural responses to sea loads. Because knowledge to predict dangerous rolling and capsize has not hitherto been available, development of adequate stability rules has lagged behind.

Recent developments in ship hydrodynamics theory and experimental techniques also advances in computer technology have now made possible development of more realistic and effective stability criteria.

The SAFESHIP project was a comprehensive programme of research using these modern methods to accelerate progress in achieving such better safety criteria in the foreseeable future and thus benefit both the shipping industry and the Department of Transport which has responsibility for such matters.

1. INTRODUCTION

This paper introduces the SAFESHIP project and sets the scene for this Conference. In doing so, it is first necessary to present sufficient historical information to place the project in the context of the existing criteria and why research is needed to advance our knowledge sufficiently to develop more realistic stability criteria.

Until IMO Res. A167 and A168 were issued in 1968 and incorporated respectively into the Department's Load Line Rules in 1968, [1] and into the Fishing Vessels Safety Rules in 1975, [2] there was no official guidance to naval architects in this country on the minimum acceptable stability values for any type of ship. Naval architects therefore had to refer to text books or to what was available in the Institution's Transactions, e.g. [3] to [8]. Some countries had adopted Rahola's criterion which was published in 1939 [9].

The SAFESHIP project was conceived and formulated by the United Kingdom Intact Stability Working Group in the course of many and long discussions after the Group's formation in 1976.
Apart from Court of Inquiry Reports which are published, and the wide casualty experience recorded in the Department of Transport files, there is also an extensive background to this research project which is documented in the literature of IMO.

It is perhaps not surprising that when IMO commenced its work on ship stability in 1962 it should have followed Rahola's approach to establishing suitable minimum parameters of the statical righting lever curve from an analysis of casualty data. The method adopted is well described by Nadeinski/Jens [10], and Thompson/Tope [11], and will not be covered in detail here.

Essentially a comparison was made between a number of parameters of the statical righting lever curve, such as GZ_{30° at the time of loss and for the same parameters in the homogeneously loaded arrival condition.

These data were presented as pillar diagrams, Fig.1. In the case of GZ30° a dividing line was drawn, somewhat arbitrarily, at 20 cms, although some of the casualty sample had higher GZs. This may have been influenced by Rahola who also selected this value. Those with higher GZs were grouped under the heading of "excess stability or special circumstances" (e.g. cargo shift).

In Rahola's criterion there was also some overlap between three classes of data described, subjectively, as adequate, critical, and insufficient, Fig.2. Rahola, himself, had reservations about proposing these standards for general use on the grounds, inter alia, of the "unsuitability of the same standard stability arm curve both for large and small vessels". "A choice of a standard form for the statical stability curve, so that it would suit both all sizes and types of vessels, thus proves to be an unsurmountable difficulty".

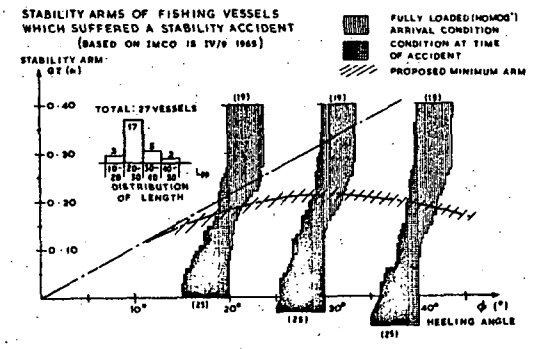

Fig.1 Histogram of Righting Levers of Fishing Vessels which suffered Stability Casualties (Based on IMO IV19 1965)

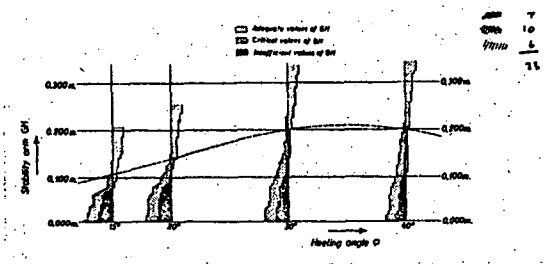

Fig.2 Histogram of Righting Levers of Vessels which suffered Stability Casualties (Based on Rahola 1939)

We might note the observation in the Jens/Kobylinski paper [12] that "there is no assurance that a ship satisfying the criteria referred to in this paper will, under all circumstances, be safe from capsizing. In the statistical analysis an average line between 'safe' and 'unsafe' ships was drawn showing that a number of ships having stability parameters lower than recommended had operated successfully over the years and some with higher parameters had capsized". Res. A167 warns Masters of their responsibilities for good seamanship.

That safety from capsize is partly a question of seamanship as well as of good design is well known but in no way obviates the need for safe design criteria or assists us in formulating such criteria. The Master is limited in the extent to which he can change the position of the ship's centre of gravity, by means of ballast or cargo, and he is furthermore dependent on guidance from the naval architect regarding safe upper limits.

The IMO Sub-Committee was well aware in 1968 that a considerable amount of research would be needed to provide a satisfactory basis for the improved criteria and information on systematic model experimental programmes was requested and has been continuously exchanged.

2. UNITED KINGDOM BACKGROUND

There have been quite a number of public inquiries into stability related losses during the last 25 years or so. A few of the most important ones being ARCTIC VIKING (1961), ARDGARRY (1962), SAREVA (1963), BOSTON PIONAIR (1965), ROSS CLEVELAND, ST. ROMANUS and KINGSTON PERIDOT (1968), LAIRDSFIELD (1970), BURTONIA (1972), GAUL and TRIDENT (1974), LOVAT (1975).

The most significant of these was the GAUL, a large stern trawler which disappeared with a crew of 36 on 8 February 1974. The Court of Inquiry [13] concluded that "she capsized and foundered due to taking a succession of very heavy seas on her trawl deck" - water trapped on deck, quartering seas and broaching in following seas were also considered as possibilities. Loss of stability due to flooding of the factory deck was also considered. The Court recommended the Department to carry out further investigations "with a view to promoting greater safety".

The Department consequently commissioned an extensive programme of model experiments which were carried out at the National Maritime Institute (now part of British Maritime Technology Ltd). These were carried out in various experiment tanks and in the open waters of the Solent during the period 1975 to 1977.] The project was fully reported in [14].

The stability characterisitcs of the GAUL complied with IMO Res. A168 with a substantial margin but nevertheless it required a considerable amount of

research to establish under what sea conditions such a ship could capsize. Compliance with Res. A168 provided no indication whatsoever of the degree of safety in adverse sea states.

2.1 Fishing Vessel Safety

As a consequence of the loss of several deep sea trawlers in 1968 a Committee of Inquiry [15] was set up to review all aspects of fishing vessel safety, thus covering both design and operation. The RINA paper "Fishing Vessel Safety" by J.H. Cox [16] describes how the recommendations of the Committee resulted in the introduction of Fishing Vessel (Safety Provisions) Rules 1975.

Two years later, in 1977, IMO held an International Conference on Safety of Fishing Vessels at Torremolinos.

Although these efforts did not result in a greater awareness of the need to develop realistic stability criteria, we are still in the situation described by the Norwegian "Safety Commission for the Fishing Fleet" in its report in January of this year: "the accident statistics for the fishing fleet continue to show an increasing number of founderings with loss of life". "Large vessel motion is a major cause in all types of injury to crews", and vessel "capsize" must be considered the most dangerous cause, since the majority (62.5%) of lives lost at sea are due to this cause".

3. INTERNATIONAL MARITIME ORGANIZATION

As a result of the Recommendations in Annex D to the 1960 Safety of Life at Sea Convention the IMO Sub-Committee on Subdivision and Stability was formed in 1962. Recommendation 7 in particular led to the studies subsequently carried out to achieve international standards for ship stability.

An excellent review of this Sub-Committee's activities was given in the Tokyo "Stability 82" conference paper by Jens/Kobylinski [12]. As stated there "-it was recognised that the development of international stability criteria needs to take account of external forces affecting ships in a seaway and also that this would be a very long-term project".

In order to make available usable criteria in the short term the Sub-Committee decided that "as a first step simple stability criteria applicable to ships under 100m in length should be formulated" [17]. These were to be based on an analysis of casualty data.

For longer-term development of improved criteria the Sub-Committee agreed [18] "to continue studies on ships' stability, paying particular attention to the effect of external forces and of variations on displacement on stability with a view to developing improved stability criteria". With this proviso the "Recommendation on Intact Stability for Passenger and Cargo Ships under 100 metres in Length" and "Recommendation on Intact Stability of Fishing Vessels" were referred to the Maritime Safety Committee for endorsement in 1967 and issued as IMO Resolution A167 and A168, respectively, the following year.

The "improved stability criteria" were to be based on comparison of the heeling moments due to external forces and the ship's righting moment [12]. As a first step in this direction the IMO Sub-Committee formed the "Joint Ad Hoc Group for the Study of External Forces Affecting Ships" (Chairman Prof G.J. Goodrich). This group had its first meeting in 1968 and functioned until 1973. Having completed its task as far as it could, the problems of preparing the "improved stability criteria" were passed over to a new Ad Hoc Working Group on Intact Stability which was formed in 1975 after a preliminary meeting in 1974.

4. IMO WORKING GROUP ON INTACT STABILITY

4.1 Brief history

The IMO Working Group has worked progressively towards both short-term and long-term improvements. The short-term efforts were directed to immediate problems such as presented by offshore supply vessels whose characteristics usually made compliance with Res. A167 impracticable, stability of ships in lightly laden and in ballast conditions, angle of vanishing stability (for good reasons not included in Res. A167 or Res. A168) and to the development of a weather criterion. There has also been much discussion about what to do about the dangers of following seas but without so far any conclusive results.

Until now the IMO work can, therefore, be seen as consisting, on the one hand, of progressive extensions to Res. A167, with all its uncertainties and on the other, towards development of "physical" criteria.

The IMO Working Group has proved to be an extremely useful form for discussing ship stability but, because of the complex nature of the subject, progress has unavoidably been rather slow.

4.2 Main tasks

In 1975 the IMO Working Group, Chairman H. Bird (presently Dr. Rakhmanin of USSR), was given both the long-term task of developing the improved criteria and the more immediate problems such as those associated with the developing offshore industry. The latter were usually solved by adaptations of Res A.167 [19].

It was agreed that the means to progress its work were by use of theoretical and model simulation and detailed study of particular casualties. Various delegations to IMO provided information on model experiments, usually related to casualties.

Since Res. A167 was developed for ships up to 100m in length and intended mainly for the load condition there was considerable debate as to how its application could be extended to larger ships in light or ballast conditions.

Other matters debated in addition to the stability of offshore supply vessels were the range of positive stability, stability in following seas and in breaking waves and the stability of pontoon barges.

Due to difficulties of progressing the long term more fundamental programme it was decided, as an interim solution, to develop a weather criterion. This took several sessions to complete and was based on a compromise between the USSR and Japanese regulations and has recently been issued as Res A562. (The bases for the Japanese and USSR regulations are given in Yamagata's 1959 RINA paper [20] and in USSR rules [21] respectively).

The weather criterion is an adaptation of what, in this country, is known as Moseley's theorem [22]. The present view in IMO is that this should supplement rather than replace Res A.167.

These two criteria taken together would not however, in many cases, provide sufficient stability to deal with the problems of following seas and consideration is currently being given to the addition of a third criterion in due course.

The Working Group has the long term aim of developing "physical" criteria which incorporate the dynamics of rolling in various sea conditions and directions.

It was decided that the effects of beam, quartering and following seas needed to be separately considered and the most dangerous conditions were identified as:-

(i) Beam wind and rolling and shipping water on deck.

(ii) Following seas involving pure loss of stability, parametric rolling and broaching.

The need for valid mathematical models for these various situations was acknowledged.

Considering the complex nature of the subject the Working Group has made substantial progress. Nevertheless it is evident that without the research being carried out in many countries, including the United kingdom, the transition from statical stability to effective "physical" criteria that are sufficiently realistic would be impossible.

5. UNITED KINGDOM INTACT STABILITY WORKING GROUP

This Working Group, Chairman H. Bird, had its first meeting on 12 May 1976 and consists of representatives of Shipowners, Shipbuilders and Fishing Vessel organisations, Lloyds Register, British Maritime Technology (previously National Maritime Institute and British Ship Research Association), Admiralty Research Establishment, Strathclyde and Southampton Universities.

Its purposes were to keep the United Kingdom industry informed about developments at IMO, to seek advice on policy, to agree priorities and discuss necessary research programmes. Also it seemed desirable to educate the shipping community about new developments as they progressed and to record the background to any future regulations.

During the past ten years the Group has had thirty meetings and discussed every aspect of how to advance existing knowledge on large amplitude rolling and capsize by means of mathematical modelling, model experiments, full scale observations and casualty analysis. Also the need to be aware of similar work abroad was recognised.

After many meetings and a Seminar at the National Maritime Institute in 1978 it was clear that the only way to make progress was by means of a co-ordinated research programme. Research has been carried out before that date independently at various places and had involved some duplication through lack of communication.

Model experiments had been carried out for some time in this country and elsewhere to seek an explanation for capsize losses [14], [23-28]. Apart from the fact that such experiments are expensive and time-consuming they yield incomplete

information e.g. because of the number of parameters involved and the inpracticability of isolating their separate effects. It was believed therefore that a theoretically oriented project would provide a more comprehensive basis for future stability regulations, observing the almost infinite combinations of hull and environmental parameters at various load conditions, speeds and wave directions. This tends, in our view, to rule out a purely experimental solution.

However, the importance of using both model experiments and full scale data to validate theoretical solutions was fully realised and these formed essential elements in the programme.

Other important aspects were seen to be reliable data on environmental forces and risk analysis methods which together would be needed to assess safety margins and establish practicable safety standards for the various ship types.

6. THE SAFESHIP PROJECT

6.1 Aims and Objectives

During the period 1978-1979 the group formulated a work programme which became known as the SAFESHIP Project. In the process of doing this account was taken of known previous research in the United Kingdom and abroad.

The aim of the SAFESHIP project was to advance existing knowledge of large amplitude rolling motions and capsize mechanisms and so to develop better design criteria and stability regulations.

The main objectives were as follows:

(i) To ascertain the present state of knowledge regarding ship motion stability in a world-wide context.

(ii) To sponsor extension of current theoretical and experimental research in the United Kingdom as necessary.

(iii) To establish by such research how the influence of the principal hull parameters should be reflected in future criteria.

(iv) Prepare the basis for future stability criteria which are related to acceptable survival probabilities and which recognise the influence of the parameters in paragraph (iii).

(v) To provide guidance to ship operators to assist them in avoiding dangerous situations when manoeuvring ships at sea.

6.2 Formulation of Research Programme

The intention was to establish a coherent programme that would address the relevant problem areas and which could be completed within about five years. The procedure adopted was as follows:

(i) A flow chart was prepared (Figure 3) indicating the types of forces, internal and external, acting on the ship; the ship properties affecting response behaviour; theoretical and experimental techniques for predicting motion behaviour under these forces and finally to devise a practical criterion based on casualty experience and using risk analysis techniques.

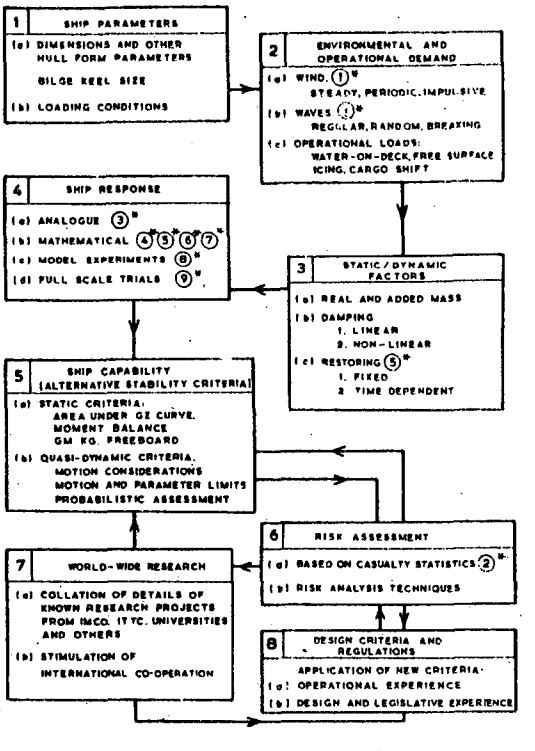

Fig.3 SAFESHIP Project Flow Chart
*Numbers in circles are SAFESHIP Project numbers.

(ii) To identify specific projects, e.g. Environmental Demand, Risk Analysis, Mathematical Models, Experimental programmes, Full Scale Measurements and Formulation of Criteria.

(iii) Having listed specific projects, to assess the approximate cost and time-scale of these individual projects and establish the likely overall cost.

(iv) From this a basic list of what were considered essential projects was made and specifications were drawn up. A document describing the SAFESHIP project and its aims was prepared and this together with the specifications were distributed to various Universities and research establishments.

(v) On receipt of tenders a short list was made of contractors who were interviewed by a Steering Committee and a final selection made.

Several different approaches to mathematical models were suggested and since all of these appeared to have merit we had four different projects of this type.

The projects comprising the SAFESHIP Project are listed Table 1.

Project No.	Research Project	Contractor
1	Environmental Demand	NMI
2	Risk Assessment	Newcastle University
3	Analogue Computer Simulation	BSRA
4	Mathematical Modelling	NMI
5	Mathematical Modelling	Strathclyde University
6	Mathematical Modelling	BSRA
7	Mathematical Modelling	Bishop & Price
8	Model Experiments	NMI
9	Full Scale Experiments	NMI

Table 1. SAFESHIP Projects and Contractors

A Steering Committee was formed in 1979 by the Ship and Marine Technology Requirements Board of the Department of Trade and Industry. Its purpose was to supervise the contractual procedure, to select suitable contractors and subsequently to monitor the technical and financial progress of the research. For various reasons these formalities delayed start of the project until April 1981.

When formulating this programme of research it was decided to break with traditional "statical" concepts of safety and explore dangerous rolling motion as well as capsize from a completely dynamic point of view.

It was an aim of the project that the contractors should co-operate with each other and wherever possible make use of the information generated as the project developed. International co-operation was also envisaged and to some extent this has been achieved. The greatest interest to date has been shown by scientists in Norway working on their SIS project [29] and those in the Fed. Rep. of Germany researching the stability of container vessels. These countries have contributed considerably to the fund of knowledge and we have been actively collaborating with them. More recently we have agreed to collaborate with France in research on small fishing vessel safety.

It was expected that the programme would take about 5 years to complete. The first phase of the work extended from 1981 to 1984, and the second phase started in 1985 and has just completed.

We had a seminar at RINA in 1982 [30], near the start of the work, which indicated a considerable divergence of opinion as to the best way forward. Whether we shall be any nearer now to agreement remains to be seen but at least we can now see the results of practical application of the theories to some sample ships.

Presentations will be made by the various researchers giving their findings and their recommendations as to the form of stability criteria they prefer. The real value of this Conference apart from informing naval architects what we have been doing, will be in trying to establish a degree of consensus within this Institution regarding how to exploit the findings of this research in the most effective way.

7. STABILITY STANDARDS

7.1 Calculation Procedures

Text books on naval architecture have traditionally tended to deal exclusively with the statical approach to stability. In the past, this has led to emphasis on the refinements of geometrical procedures and numerical integration techniques. Now that manual methods have been displaced by the computer we still have debates about accuracy notwithstanding the uncertain nature of the criteria themselves.

The computer has relieved naval architects of the drudgery of manual calculations and has conferred the following additional benefits:-

(i) Availability of accurate data earlier in the design process.

(ii) More reliable and extensive information, especially on damage stability.

(iii) Removal of artificial restrictions, e.g. constant trim on heeling, simplifying assumptions about free surface moments, etc.

(iv) Ready assessment of alternative dimensions,

proportions, sheer, superstructures etc.

(v) Facility to design closer to rule requirements [31].

(vi) Opportunities for on board computers to assist ships' officers.

Now that the computer has established these benefits we believe that the time is opportune to direct effort to answer the real question which is - what is sufficient stability? [32]. Only then can we be sure of designing ships which will be truly cost-effective in respect of stability.

7.2 Types of Stability Criteria

It will be useful to summarise here various types of criteria and to classify them into several distinct categories. This has no doubt been covered more extensively elsewhere, eg Bird/Odabasi [33]. However the purpose here is not to present an exhaustive list but rather to identify characteristics which would enable us to group them into types and then to comment on obvious advantages and disadvantages.

We could possibly group them as follows:-

(i) Statical stability (or still water) methods involving no explicit use of external forces or motion characteristics. Under this heading we have Rahola [9], IMO Res A.167, A.168 and A.469 [1], [2], [19], respectively. Also a proposal recently put forward to IMO by the Federal Republic of Germany [42].

(ii) Moment Balance methods which might include proposals by Steel [6], Wendel [8] also Abicht, Kastner and Wendel [34].

(iii Energy Balance methods such as proposed by Moseley [22], Pierrotte [4], Sarchin and Goldbery [7], IMO Res A14/562 (1986) and Strathclyde University [35].

(iv) Motion stability methods have been developed to cater for dynamic effects such as resonance with encounter frequency, jump phenomenon etc. Clearly static or quasi-dynamic methods cannot cope adequately with these. Amongst techniques developed are those using Mathieu equations by Abicht [36], Lyapunov functions by Odabasi [37], Caldeira-Saraiva [38] and roll/yaw coupling by Bishop & Price [39] non-linear roll response by Wellicome [40]).

7.3 Comments on Various Criteria

7.3.1

Simple statical righting lever curves will always serve a useful purpose. Because of their relation to the hull form geometry and obvious physical meaning they are helpful both to naval architects and to ships' officers. In future they could be more effectively derived indirectly from dynamic criteria instead of the statistical approach of Rahola or Res A.167.

Their disadvantages are that they cannot possibly give any indication of safety margins or of likely motion behaviour in any sea state except still water.

This could also be seen as an advantage to rule makers in that it does not commit them to making difficult decisions about wind and wave parameters and possibly of giving false guarantees of safety in any particular sea conditions.

7.3.2

Moment and energy balance methods bring us closer to reality in discriminating between safe and unsafe conditions. They are at best, however, fairly simple models of the real world and present only a quasi-dynamic picture, especially of the influence of wave motion.

The Strathclyde method is probably the ultimate form of development of such a criterion.

In spite of their limitations such criteria use conventional principles and procedures which are familiar to naval architects.

7.3.3

Because of the inadequacies in the two preceding approaches attempts have been made to account for motion effects by using Mathieu equations and Lyapunov functions.

Disadvantages of these are, firstly, that naval architects are not yet familiar with these concepts and secondly that such new forms of stability criteria may need considerable validation from practical experience, to be generally accepted.

7.3.4

Finally we need to consider the influences on safety of the randomness in the environment. A

truly probabilistic approach would need to account for random wind velocity/wave height/wave frequency combinations, speeds, wave directions, draught and weight component distributions over a ship's lifetime.

Such an approach is not only impractical from a computational or regulatory point of view but would not indicate the ability of a ship to withstand extreme conditions [41].

This type of approach is more appropriate to sea-keeping assessment of a ship's likely behaviour, but could also help to establish broad margins of safety, and hence safety levels which would be economically and socially acceptable.

7.3.5

Illustrations of past and current types of stability criteria are given in Appendix 1.

8. SAFETY APPROACHES BY OTHER ENGINEERING DISCIPLINES.

It had been our intention to study and comment on analogous problems in e.g. the structural safety of ships, bridges and aircraft and to compare their safety philosophies. Insufficient time has prevented this but we feel that some effort to harmonize safety rules or codes of practice is desirable and also because we could possibly learn from experience in other fields of engineering.

9. INTERNATIONAL CO-OPERATION

It has been the intention of IMO following 1960 S.O.L.A.S. to formulate criteria which could be agreed and applied internationally.

The United Kingdom has always advocated international collaboration e.g. for the purpose of establishing uniform standards, to share research effort and costs and to reduce the time-scale required to produce better criteria.

Such co-operation can be achieved via IMO meetings, international conferences such as this one, smaller seminars, by direct contact, and by joint IMO papers.

We have actively participated in all such activities and believe our efforts have thus made an important contribution.

10. CONCLUSIONS

The SAFESHIP project has confirmed how complex a subject is stability when attempt is made to account adequately for wind, waves and dynamic motions.

Alternative new forms of stability criteria have been developed from this research and considerable progress has thus been made in preparing the basis for future stability criteria.

It still remains to be decided what should be the form of future stability criteria. Should we depart from statical stability criteria or continue to use them in association with some form of physical criterion as has been proposed by IMO?

In the event of one of the SAFESHIP criteria being adopted which of these offers the best solution, taking all factors into consideration?

This conference is a good opportunity to debate the pros and cons and to establish a consensus view in this country. It is vital that in our relations with IMO that we are able to present a consistent policy and so to make an effective contribution towards agreeing criteria that will serve the industry for many years into the future.

11. ACKNOWLEDGEMENTS

The SAFESHIP project has been successively funded by the Departments of Trade and Transport and we are grateful for this support without which none of this research would have been possible.

We are grateful for the encouragement given by the Department of Transport and for their permission, together with that of the Directors of British Maritime Technology Limited, to publish this paper.

The active support of all the members of the UK Intact Stability Working Group and the SAFESHIP Steering Group throughout the development of the SAFESHIP project is also gratefully acknowledged.

Any opinions expressed are the authors' own and should not be attributed to the above mentioned organisations.

REFERENCES

1. Merchant Shipping Safety, The Merchant Shipping (Load Line) Rules 1968 S.I. 1968, No.1053.

2. Merchant Shipping Safety, The Fishing Vessels (Safety Provisions) Rules 1975 S.I. 1975 No.330.

3. DENNY, A: 'On the Practical Application of Stability Calculations' TINA 1887.

4. PIERROTTET, E: 'A Standard of Stability of Ships' TINA 1935.

5. SKINNER, H.E: 'The Safety of Small Ships' TINA 1935.

6. STEEL, H.E: 'The Practical Approach to Stability of Ships' TINA 1956.

7. SARCHIN, T.H. and GOLDBERG, L.L: 'Stability and Buoyancy Criteria for U.S. Naval Ships' Annual Meeting The Society of Naval Architects and Marine Engineers 15 November 1962.

8. WENDEL, K: 'Safety from Capsizing' Fishing Boats of the World 1960.

9. RAHOLA, J: 'The Judging of the Stability of Ships and the Determination of the Minimum Amount of Stability' Doctoral Thesis, Helsinki 1939.

10. NADEINSKI, V.P. and JENS, J.E.L: 'The Stability of Fishing Vessels' RINA Spring Meetings 1967.

11. THOMPSON, G. and TOPE, J.E: 'International Considerations of Intact Stability Standards' RINA Spring Meetings 1969.

12. JENS, J.L.E. and KOBYLINSKI L: 'IMO Activities in Respect of International Requirements for the Stability of Ships' Proc. Second International Conference on Stability of Ships and Ocean Vehicles, TOKYO 1982.

13. GAUL, M.V.: 'Formal Investigation Report of Court No. S493'.

14. MORRALL, A: 'The Gaul Disaster : An Investigation into the loss of a Large Stern Trawler' RINA 1980.

15. Trawler Safety Final Report of the Committee of Inquiry into Trawler Safety Chairman Admiral Sir Deric Hollan-Martin Cmnd:4144 HMSO.

16. COX, J.H: 'Fishing Vessel Safety' RINA Spring Meeting 1976.

17. IMCO Sub-Committee on Subdivision and Stability 5th Session Report, 1966.

18. IMCO Sub-Committee on Subdivision and Stability 7th Session Report, 1967.

19. Guidance for the Design and Construction of Offshore Supply Vessels IMO Res A.469 (X11).

20. YAMAGATA, M: 'Standard of Stability Adopted by Japan' RINA Spring Meetings, 1959.

21. USSR Register of Shipping, The Rules for the Classification and Construction of Sea-Going Ships, Part 4 Stability.

22. MOSELEY: 'On the Dynamical Stability and on the Oscillations of Floating Bodies' Royal Society London, 1850.

23. KURE, K and BANG C.J: 'The Ultimate Half Roll' Proceedings of The First International Conference on Stability of Ships and Ocean Vehicles 25-27 March 1975 University of Strathclyde, Glasgow.

24. DAHLE, E.A and KJAERLAND: 'The Capsizing of MS Helland Hansen' RINA 26 April 1979.

25. MORRALL, A: 'Capsizing of Small Trawlers' RINA 26 April 1979.

26. KASTNER, S. and RODEN, S: 'Kenterversuche mit einem Model in Naturlichen Seegang' Schiffstechnik, Vol.9, 1962.

27. AMY, J.R, JOHNSON, R.E, MILLER, E.R: 'Development of Intact Stability Criteria for Towing and Fishing Vessels' S.N.A.M.E. Annual General Meeting 1976, Paper No. 2.

28. TSUCHIYA, T., KAWASHIMA, R.1, TAKAISHI, Y.: 'Capsizing Experiments of Fishing Vessels in Heavy Seas' PRADS International Symposium, Tokyo, October 1977.

29. Seminar on the Norwegian "Ships in Rough Seas" SIS Project RINA February 1982.

30. SAFESHIP Seminar Proceedings of a Seminar held at the Weir Lecture Hall RINA London on 4 March 1982.

31. ASTON, J.G.L., MARSHALL, A.J., RYDILL, L.J: 'Assessing the Hydrostatic Stability of Marine Vehicle Designs' RINA Spring Meetings, 1986

32. HORMANN, H: 'Judgement of Stability-Questions to be solved - A Contribution from the Point of View of an Approving Authority' Proceedings of the Second International Conference on Stability of Ships and Ocean Vehicles, Tokyo 1982.

33. BIRD, H, and ODABASI, A.Y.: 'State of the Art: Past, Present and Future' Proceedings of the International Conference on Stability of Ships and Ocean vehicles, University of Strathclyde Glasgow, 25-25 March 1975.

34. ABICHT, W, KASTNER, S and WENDEL K: 'Stability of Ships Safety from Capsize and Remarks on Subdivision and Freeboard' Proceedings of the Second West European Conference on Marine Technology, London 1977.

35. VASSALOS, D, KUO, C, ALEXANDER, J.G. and BARRIE, D: 'Incorporating Theoretical Advances into Usable Ship Stability Criteria', RINA SAFESHIP Conference 1986.

36. ABICHT, W: 'On Capsizing of Ships in Regular and Irregular Seas', Proceedings of the International Conference on Stability of Ships and Ocean Vehicles, University of Strathclyde, Glasgow 25-27 March 1975.

37. KUO, C and ODABASI, A.Y.: 'Application of Dynamic Systems Approach to Ship and Ocean Vehicle Stability' Proceedings of the International Conference on Stability of Ships and Ocean Vehicles, University of Strathclyde Glasgow, 25-27 March 1975.

38. CALDEIRA-SARAIVA, F: 'A Ship Stability Criterion Based on Lyapunov's Direct Method' RINA SAFESHIP Conference 1986.

39. BISHOP, R.E.D., PRICE, G.P. and TEMAREL, P: 'On the Role of Encounter Frequency in the Capsizing of Ships' Second International Conference on Stability of Ships and Ocean Vehicles, TOKYO 1982.

40. WELLICOME, J: 'An Analytical Study of the Mechanism of Capsizing' Proceedings of the International Conference on Stability of Ships and Ocean Vehicles, University of Strathclyde Glasgow, 25-27 March 1975.

41. KRAPPINGER, Prof. O: 'On the Philosophy behind Assessing Ship Stability' Proceedings of the Second International Conference on Stability of Ships and Ocean Vehicles, Tokyo 1982.

42. Report on Stability and Safety against Capsizing of ships of Modern Design - IMO paper SLF/34, Sept 1984.

43. BIRD, H. and MORRALL, A: 'Ship Stability - A Research Strategy' Proceedings of the Second International Conference on Stability of Ships and Ocean Vehicles, Tokyo 1982.

44. ROBERTS, J.B., and STANDING, R.G.: 'A Probabilistic Model of Ship Roll Motions for Stability Assessment' RINA SAFESHIP Conference 1986.

45. SPOUGE, J.R.: 'The Prediction of Realistic Long-Term Ship Seakeeping Performance' Proceedings NECIES October 1985.

APPENDIX 1

CURRENT FORMS OF STABILITY CRITERIA

There are two basically different approaches which have been proposed for stability criteria. In the first or 'Rahola type' of criterion use is made of historical casualty data for a group of vessels. Measures of stability are chosen, such as the area under the righting arm curve, and the criterion is established by selecting a level of stability which exceeds that of most of the casualties. Since these parameter values are the same for all ships regardless of size, type, operating and weather conditions the margin of safety must vary and is unknown [43]. Furthermore, completely rational criteria for stability can not be achieved by this means alone for various reasons such as smallness of sample, variability of ship types, loading conditions and sea conditions at time of loss.

The Rahola stability criterion is illustrated in Fig.4 and the current stability criterion for fishing vessels Res. A168 is shown in Fig. 5.

The second approach might be called 'deterministic' in which the meassure and level of stability are defined to prevent a certain type of capsize under specific environmental conditions. In other words the criterion takes account of the external forces affecting behaviour of the vessel in an assumed environmental condition. The relationship between the stability and the occurrence of capsizing in this second approach is determined using theoretical, model or full-scale information.

The advantage of the deterministic approach is that specific criteria can be developed for different ship types and the particular hazardous situations.

Furthermore, design parameters which influence dangerous roll motion and the enviornmental conditions can be defined. This approach is also more suitable when some significant departures in design take place such as the introduction of a twin hulled semi-submerged ship (SWATH Ship).

One of the simplest forms of deterministic stability criterion is the dynamic wind-heel or 'weather criterion', such as the one introduced by Sarchin and Goldberg in 1962 [7] and this is illustrated in Fig.6. This type of criterion is intended to provide sufficient stability for a vessel to withstand the dynamics of being subjected to a sudden wind gust while rolling. Unfortunately this criterion does not relate to the real dynamics of a ship rolling in gusting winds. AMY et al [27] found that computer simulations of capsizing did not relate to the behaviour assumed in the classic weather criterion. The capsizings appeared to be more of a random event which depended upon phasing of the roll, wave slope and wind gust.

The recent IMO weather criterion introduced in 1985 is shown in Fig. 7 and the more elaborate moment balance criterion suggested by Wendel is shown in Fig. 8.

A simplified wind heel criterion developed by Amy et al [27] is illustrated in Fig. 9. In formulating this criterion it was assumed that the probability of occurrence of an extreme roll angle is in some way related to the rms roll angle and that capsizing will occur when the effective roll angle exceeds the range of stability. Based on model tests capsizing was also likely to occur if the rms roll angle exceeded about one quarter of the range of stability and this was considered a much better prediction of capsizing than some form of energy balance approach.

A stability criterion developed by Strathclyde University within the SAFESHIP project [35] which can be seen as a natural development of the Weather Criterion is illustrated in Fig.10. This criterion is appropriate to the capsize mode known as "pure loss of stability" and the assessment procedure explicitly allows for the effects of wind, waves and motions in a quasi-dynamic manner. This criterion has become known as the "butterfly diagram" where the outcome of an energy balance between excitation and restoring effects over an extreme half roll cycle is used to discriminate between "safe" and "unsafe" vessels.

Another stability criterion developed within the SAFESHIP project by British Maritime Technology [38]. The basic approach adopted is the utilisation of a demand-capability type analysis through the use of Lyapunov's Direct Method. Within the context of intact ship stability a ship's capability is defined by its region of stability in the phase plane. The basis of this method is then incorporated in a simplified stability criterion which is illustrated in Fig.11. In this approach Lyapunov theory is applied to the equations of motion which can be made to account for coupling effects, wave diffraction, parametric excitation, linear and non-linear damping and wind. The simplified stability criterion thus derived is based on the stability bounds for rolling motion which can be determined from the above method.

Roberts and Standing [44] have adopted the approach of estimating the mean time for such a capsize to occur. By comparing this time with the exposure of the vessel it should be possible to judge whether the vessel is safe or unsafe. Roberts also estimated the expected number of times the roll angle exceeds a specified critical level. Both of these approaches were used in a probabilistic model of ship motions using long-term statistics for periods of time, commensurate with the operating lifetime of the ship. A diagram illustrating the probabilistic approach is given in Fig.12.

A more conventional method for predicting the long-term distribution of ship motion is given by Spouge [45] which takes full account of roll non-linearities and voluntary changes of speed and heading due to the master's efforts to minimise critical responses in severe seas - see Fig. 13. From a practical point of view this approach could be useful in assessing the motions of vessel during its lifetime but it is not able to deal with parametric excitation and zero encounter frequency.

Intact stability criteria have evolved remarkably slowly over the last fifty years. Even the current IMO regulations Res. A167 and Res. A168 are of the same type as proposed by Rahola in 1939. With the exception of the IMO Weather Criterion Res. A14/562 (1986) no stability criteria have been introduced in recent times that explicitly allows for external forces and vessel motion. However, examples of these more advanced criteria have been developed within the SAFESHIP project as mentioned above which overcome the limitations of the existing Rahola approach.

Future intact stability criteria and the related safety of ships in extreme seas should ideally be rationally quantified in terms of risk of loss or of exceeding certain bounds of motion as a result

of environmental forces. In the short-term, criteria that are based on a 'deterministic' approach would be a step forward from the current situation. The margins of safety could then be assessed in relation to the severity of the environmental condition selected and the risk of loss assessed from the probability of this condition arising over the vessel's lifetime.

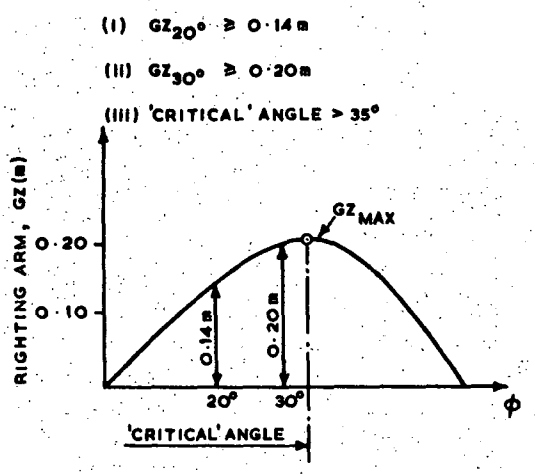

Fig.4 Rahola Stability Criteria

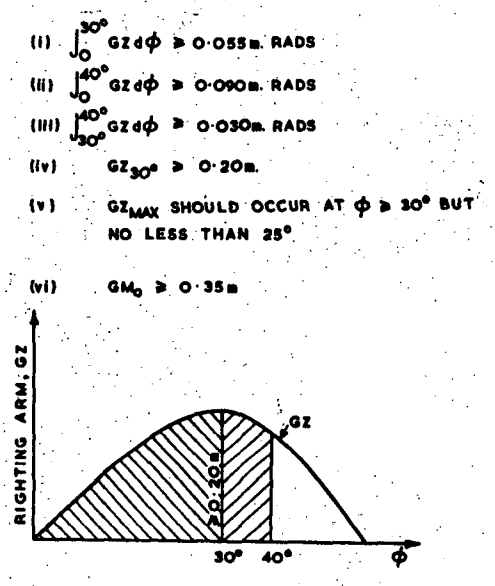

Fig.5 IMO Recommended Stability Criteria (For Fishing Vessels Res. A168)

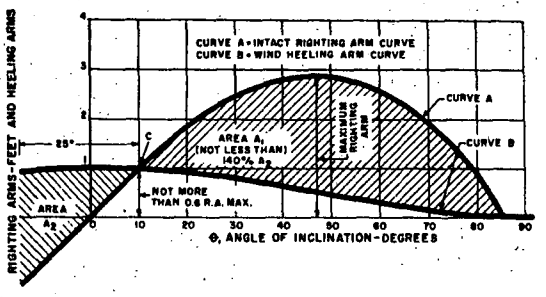

Fig.6 The Classical 'Weather Criterion' [7]

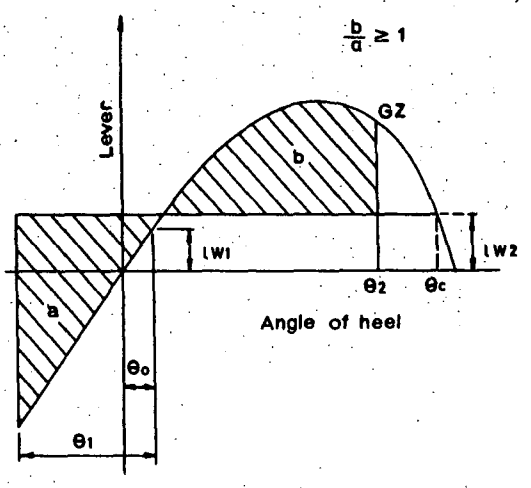

Fig.7 The IMO Weather Criterion

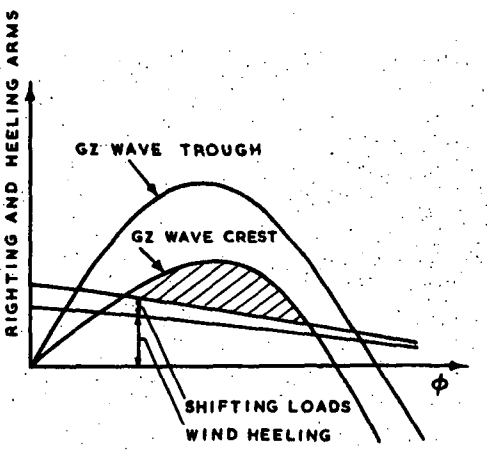

Fig.8 Balancing of Righting and Heeling curves proposed by Wendel [34]

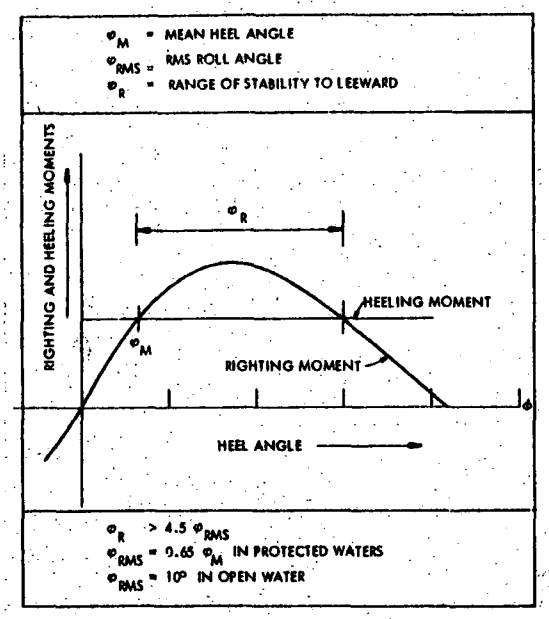

Fig.9 A Simplified Wind Heel Criterion developed by AMY [27]

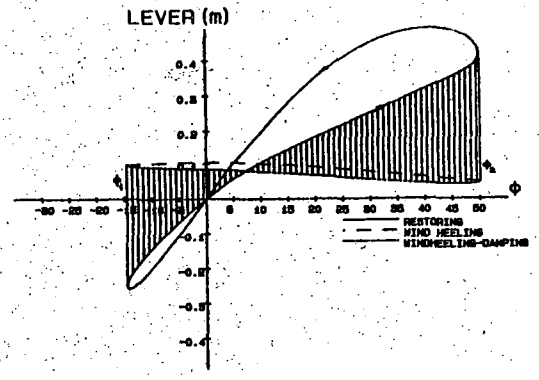

Fig.10 The Butterfly Diagram - Following Seas Proposed by Strathclyde University [35]

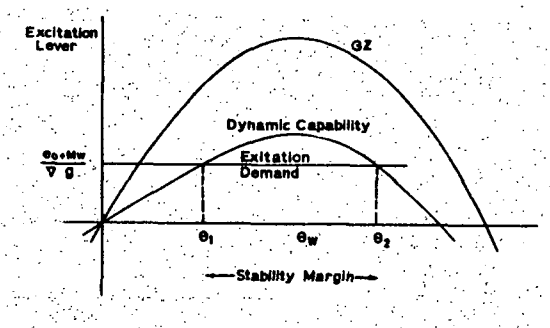

Fig.11 Stability Criterion Proposed by BMT Ltd [38]

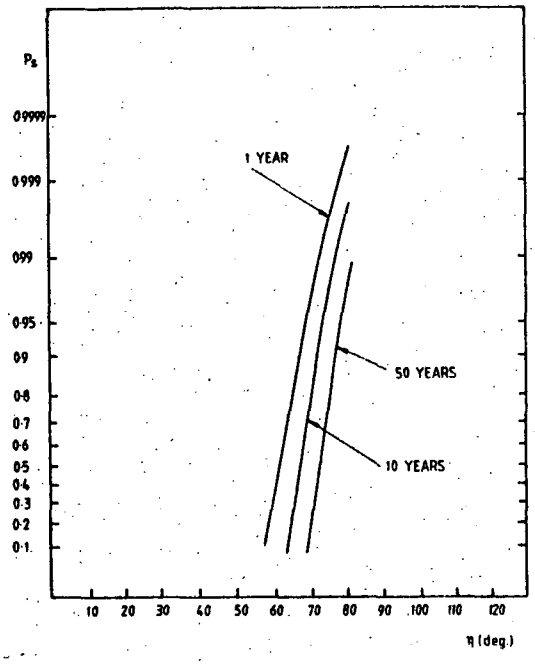

Fig.12 Variation of the probability of survival with critical amplitude level, for various long term periods [44]

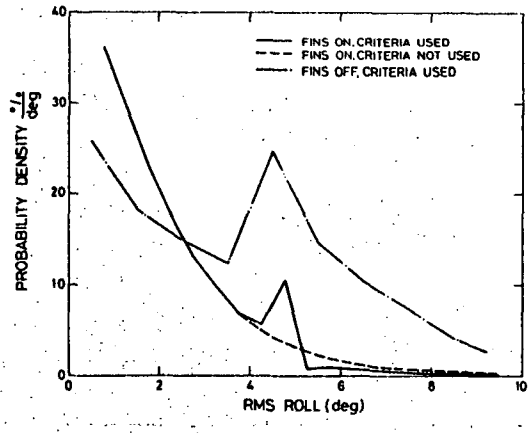

Fig.13 Prediction of long-term RMS roll response for FPV SULISKER [45]

Third International Conference on Stability of Ships and Ocean Vehicles, Gdańsk, Sept. 1986

STAB'86

LARGE AMPLITUDE ROLLING EXPERIMENT TECHNIQUES

by J.R. Spouge, N. Ireland and J.P. Collins

British Maritime Technology Limited

ABSTRACT

This paper describes the techniques used at British Maritime Technology Limited for large amplitude rolling experiments. Roll decrements, steady forced roll tests and transient forced roll tests are discussed, and sample results are given. The experiments at BMT make use of a gyroscopic roll moment generator, which produces a pure sinusoidal roll moment, even at large roll amplitudes. The theory and calibration of this equipment are presented. The associated instrumentation and analysis software are also described, which allow efficient research into the non-linearities of large amplitude rolling.

1. INTRODUCTION

Model experiments to study the rolling of ships have a long history but, until recently, they have either been unreliable or limited to fairly low amplitudes, and consequently the validity of their results as the ship approaches capsize is uncertain. The object of such tests has invariably been to measure the hydrodynamic damping of the roll motion, which has a major influence on a ship's roll response at sea, and has proved quite difficult to predict from theory. Potential flow calculations, which have proved successful at predicting motions such as pitch and heave, are unable to estimate the viscous component of roll damping, and so tend to over-estimate the roll motion. Theoretical methods have recently been developed to improve this, and these need experimental validation. Since the viscous forces are in general non-linear, the validation needs to be at large amplitudes (i.e. large enough for the non-linearities to be significant); typically in excess of 15^{o}.

An extensive programme of this type of model tests (Fig.1) has recently been completed at BMT Ltd, as part of a project to develop more accurate prediction methods for large amplitude rolling. The work was outlined in Ref.1, and sample results from the model tests were given. The present paper describes the model test techniques which were employed, concentrating on the gyroscopic roll moment generator, on which the test programme was based. The reasons for the choice of this type of test equipment are discussed below.

2. THE TYPES OF LARGE AMPLITUDE ROLLING EXPERIMENTS

2.1 Rolling in waves

Rolling experiments in waves are the most realistic form of modelling the full-scale problem, but are correspondingly complicated to analyse. The presence of non-linear wave loading, combined with non-linear damping and restoring, makes it difficult to separate the different forces, so that only the predicted overall roll response can be validated.

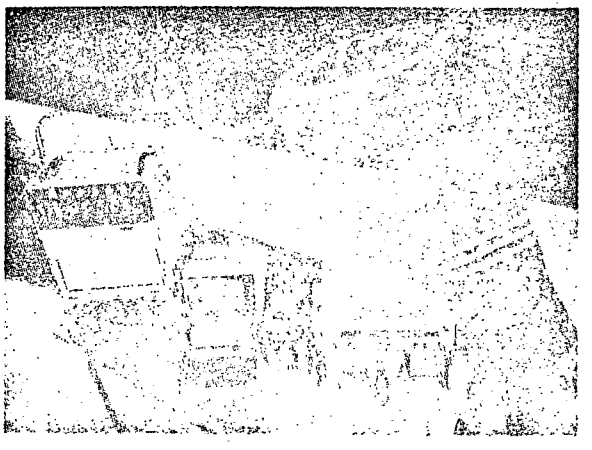

Fig. 1. Model rolling test at BMT Feltham

2.2 Forced motion mechanisms

Forced motion mechanisms compel the model to execute a known motion, usually sinusoidal, while the force of reaction is measured. They often consist of some form of scotch yoke, in which a rotational drive from an electric motor is converted to an oscillatory motion. The advantage of this system is its great simplicity, but it is severely restricted by the need to physically adjust the mechanism in order to vary the motion amplitude. The frequency of the motion is directly proportional to the motor speed.

The forced motion technique has the disadvantage that it does not represent the real problem of trying to measure the model's response to a known (wave) input, although it is theoretically equivalent to it. In practical terms, it requires the roll axis to be arbitrarily fixed, which makes the displacement volume vary with roll angle in large amplitude tests, and changes the GZ curve from its free-floating shape (usually making it more non-linear). Fixing the roll axis also suppresses coupled heave and sway motions, which simplifies the analysis, but tends to reduce the overall roll damping.

There is a further practical disadvantage in that it is more difficult to measure roll moments on the driving shaft of a forced motion mechanism than it is to measure roll angles on a model responding to a known moment. Roll moment measurements are more difficult to calibrate, more delicate to operate, and more liable to suffer from electrical noise and mechanical vibration.

2.3 Rotating weight mechanisms

Rotating weight mechanisms are commonly used for forced roll tests, in which a known moment is applied to the model and the resulting motion

measured. The simplest such arrangement is of two weights rotating in opposite directions in the horizontal plane so as to ensure that the yaw moments cancel out.

At small roll amplitudes, the roll moment is approximately sinusoidal. It has a static component whose amplitude can only be varied by changing the masses or the radius of rotation, which is a major inconvenience when testing. There is also a centrifugal component, whose amplitude is proportional to the square of the frequency, and which also depends on the height of the apparatus in the model. This may be eliminated by placing the equipment at the level of the model's centre of gravity, but this is usually too low to be practical.

The centrifugal forces from the transverse movement of the weights, which supply part of the roll moment, also comprise a sway force, which further complicates the motion. Although it is possible to eliminate this by using four weights, placed symmetrically on each side of the model and rotating in the vertical plane, this results in a bulky apparatus which is difficult to accommodate in the model.

With the conventional apparatus, at large roll amplitudes the static component is reduced if the weights are mounted low in the model, but may be increased if they are mounted very high. The roll moment becomes non-sinusoidal, and so quite difficult to analyse accurately.

2.4 Gyroscopic roll moment generators

Gyroscopic roll moment generators avoid the problems created by the moving weight systems. They use gyroscopic forces produced by the precession of spinning flywheels, whose centres of gravity may be kept constant.

An early arrangement is described in Ref.2, in which a single flywheel produced a sinusoidal roll moment, together with a yaw moment which had to be neglected. Subsequently, two flywheels have been used, precessing in opposite directions, so that the yaw moments cancel out and a pure roll moment remains; e.g. in Ref.3, where the precession consisted of an oscillation of the flywheels' spin axes.

It is clear that this type of apparatus has considerable potential for large amplitude rolling experiments, since the moment produced is almost entirely independent of the roll angle, and the gyroscopic principle was adopted as the basis for forced rolling experiments at BMT.

3. A DESCRIPTION OF THE BMT ROLL MOMENT GENERATOR

3.1 Principle of operation

The gyroscopic roll moment generator (RMG) is based on a fundamental principle of gyrodynamics: that a spinning body, whose axis of spin is changed, experiences a reaction torque equal to the rate of change of its angular momentum, measured in a fixed coordinate system. In practical terms, a flywheel spinning about one axis and forced to precess (or tumble) about a second orthogonal axis (Fig.2), generates a moment about the third orthogonal axis, whose magnitude is proportional to the spin and tumble rates and to the flywheel's inertia about the spin axis.

If a flywheel is mounted with a vertical spin axis in a ship model, and is forced to tumble at a steady rate in the model's centre-plane, a moment will be produced which changes between a

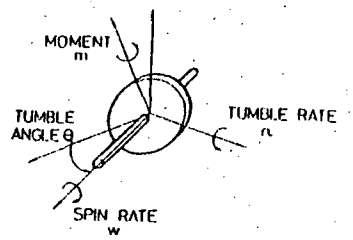

Fig. 2. Gyroscopic moment from a single flywheel

roll moment and a yaw moment as the spin axis tumbles. In the RMG, two flywheels are used, tumbling continuously in opposite directions (Fig.3), so that the yaw moments cancel out and a sinusoidal roll moment remains.

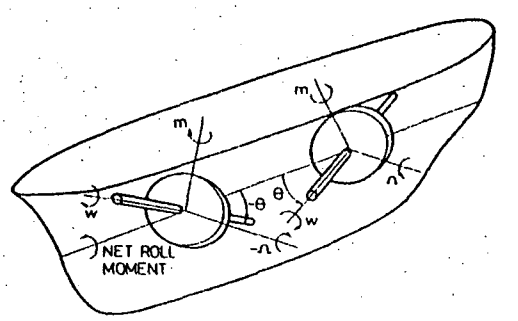

Fig. 3. Roll moment generator flywheel arrangement

Simple gyrodynamic theory gives the moment produced, if the flywheels have inertia I about the spin axes, with identical spin rates Ω (rad/s) and equal and opposite tumble rates ω (rad/s) as:

$$M = 2\ I\ \omega\ \Omega\ \sin\theta \qquad (1)$$

where θ is the instantaneous tumble angle:

$$\theta = \omega\ t \qquad (2)$$

which is zero when the flywheel spin axes are horizontal.

If the flywheels are tilted at an angle γ to the model's centre plane, the moment is reduced to:

$$M = 2\ I\ \omega\ \Omega\ \cos\gamma\ \sin\theta \qquad (3)$$

3.2 Construction

The BMT roll moment generator (Fig.4) embodies the gyrodynamic principle above in a compact and easily-controlled form which is suitable for model tests.

The flywheels are two balanced brass rotors of 50mm diameter, driven by motors spinning at 480 - 6700rpm. One motor is actively controlled while the other is slaved to follow it.

The spin motor and flywheel assemblies are mounted in gimbals which are driven by two motors at 6 - 120rpm via a single toothed-belt drive, which forces both flywheels to tumble at precisely equal rates. The use of two tumble motors, geared together and rotating in opposite

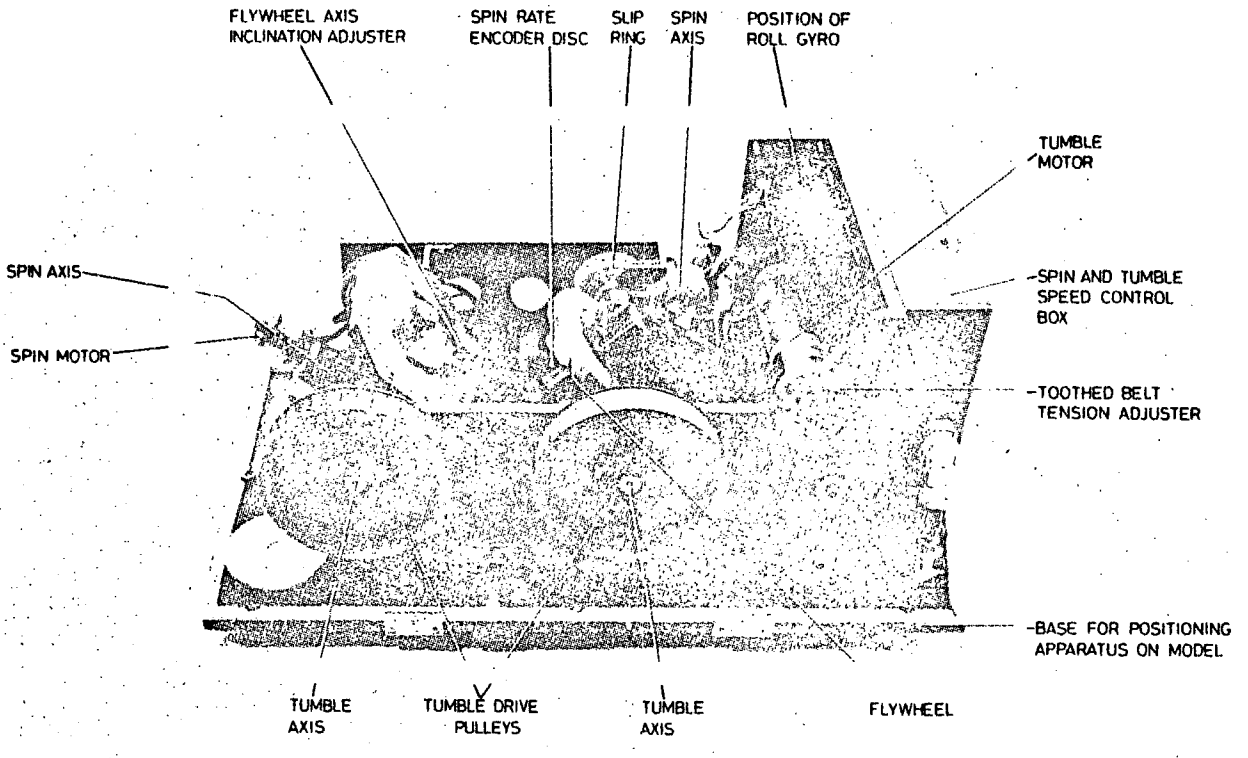

Fig. 4. The BMT Roll Moment Generator

directions, ensures that their reaction torques cancel out. The tumble drive is fitted with a rapid-acting solenoid-operated brake which allows sudden stops (while the spin continues) to commence a roll decrement.

The spin and tumble axes do not quite intersect, because the centres of gravity of the motor, flywheel and gimbal assemblies are designed to lie on the tumble axes, so that the overall centre of gravity remains fixed. The spin axes may be tilted from their basic orthogonal relationship with the tumble axes by up to 55^{o}, which allows a reduction in roll moment while retaining the ease of control of the higher spin rates.

The RMG uses shore-based control and power supply via light umbilical cables. The model's roll angle is measured by an internal roll gyro.

3.3 Control

The spin and tumble rates are set from the shore-based control panel, and the achieved rates are sensed by optical disc encoders in the RMG and displayed on LEDs, as well as being available in digital form for the analysis. The motors have frequency-locking feedback control, which keeps them to within 0.5% of the set speeds. The tumble angle is monitored by a cosine-potentiometer on one of the tumble axes, which produces a pure sinusoidal analogue signal as the flywheel assemblies rotate. This is the sin θ term in Eqn.1 and is proportional to the produced roll moment. It is used to determine the phase between the roll moment and the resulting roll angle.

The roll frequency is adjusted directly by the tumble rate control. There is no direct control of the roll moment amplitude, which is proportional to both spin and tumble rates, but it is readily calculated using Eqn.1.

3.4 Calibration

The simple gyroscopic theory used to derive Eqn.1 assumes that the RMG is correctly constructed (e.g. that the tumble assemblies have equal inertia) and that the equipment is static. In practice, imperfections in its manufacture and extra moments due to its motion in a rolling model might be expected. A dynamic calibration of the equipment was therefore carried out.

The calibration used the BMT rolling table to oscillate the RMG, while the roll moment was recorded by two strain-gauged torsion bars. The measured roll moments in general consisted of the moment generated by the RMG and also the dynamic moments due to the moving mass of the RMG and the components of the calibration frame supported by the torsion bars. The latter were predominantly an inertia moment (due to the acceleration of the RMG about the roll axis) and a quasi-static moment (due to the instantaneous displacement of the RMG centre of gravity from above the torsion bars), and were proportional to the roll angle for a sinusoidal roll motion.

Since the generated moment was large compared to the static and inertia moments, the measured moment was approximately sinusoidal, so that the generated moment amplitude could be found from:

$$M_G = M_m - (M_S + M_I) \cos \gamma \qquad (4)$$

where:

M_G = Generated moment amplitude
M_m = Measured moment amplitude
M_S = Static moment amplitude
M_I = Inertia moment amplitude
γ = Phase lag of tumble angle behind roll angle

The static moment (i.e. the RMG centre of gravity position) was found from the measured moments with the RMG and roll table stopped.

The inertia moment (i.e. the RMG roll inertia) was found from the measured moments with the RMG stopped and the table in motion. Then the generated moments with the RMG in motion could be found from the measured moments using Eqn.4.

The calibration revealed no significant measurable differences between the experimental moment amplitude from Eqn.4 and the theoretical moment amplitude from Eqn.1, over the complete working range of spin and tumble rates, for any phase angle between tumble and roll angles, and for any roll amplitude up to 15°. The calibration frame was not sufficiently strong to be operated at larger amplitudes. Experimental errors varied between 20% at the lowest moments and 0.8% at the highest moments, and so any deviation in the performance from Eqn.1 would have to be below this.

3.5 Theoretical analysis

A theoretical gyrodynamic analysis of the RMG in a moving model was carried out, in order to investigate any errors which might have been concealed by experimental inaccuracy in the dynamic calibration, and to determine the accuracy of Eqn.1 at larger amplitudes than the calibration could achieve.

The analysis firstly involved obtaining an expression for the angular momentum vector of each flywheel, measured in the flywheel axis system, taking account of the oscillatory roll and pitch motion and an assumed steady yaw drift of the model. The torque generated by the flywheel is equal to the rate of change of this vector, and the differentiation takes account of the fact that the axis system is moving in space. Then the gyroscopic torque is transformed into the model's axis system. Finally the torques from the two flywheels are combined to give the roll moment on the model.

If there is no model motion, Eqn.1 results. Otherwise, complicated expressions for an oscillatory roll moment and a yaw moment are obtained, which include both steady and oscillatory components. The theory predicts that all pitch moments are cancelled out. The equations may be simplified at roll resonance, where the phase between the roll angle and roll moment is 90°, and the phase between the pitch angle and roll moment is assumed to be 0°.

The roll moment in this case is equal to the ideal value from Eqn.1, reduced by an in-phase component, and a third harmonic of similar magnitude which acts to distort the roll moment without changing its amplitude. The fractional distortion amplitude is:

$$D = \frac{I_z \Phi \omega}{I \Omega} \qquad (5)$$

where:

D = Distortion amplitude as a fraction of M from Eqn. 1

I = Inertia of each flywheel about spin axis

I_z = Inertia of each flywheel assembly about an axis normal to to the spin and tumble axes

ω = Tumble rate

Ω = Spin rate

Φ = Roll amplitude (rad)

For a heavily damped model which is rolled to 15° at 0.5Hz by the maximum spin rate, the distortion amplitude is less than 1%. On a lightly damped model rolling at 40° amplitude, the distortion amplitude may reach 2%. However, the overall moment amplitude is unaffected, and only the total energy input is reduced by these percentages. This would cause a similar error in the damping measurements but since the general accuracy of damping estimates is low, these effects are negligible. For all practical purposes the roll moment may be assumed to be sinusoidal with amplitude given by Eqn.1.

3.6 Performance

The performance capabilities of the RMG are summarised in Table I. The maximum and minimum roll moment amplitudes are proportional to the selected roll frequency (i.e. tumble rate) as a consequence of Eqn.1. For a typical model with natural roll frequency 3 rad/s, the maximum available roll moment amplitude is 4.1 Nm.

TABLE I. BMT Roll Moment Generator principal particulars

Length	0.55m
Width	0.24m
Height (over case)	0.30m
Weight	19kg
Inertia of flywheel about spin axis	9.85×10^{-4} kgm^2
Spin rate range	50 - 700 rad/s
Tumble rate range	0.6 - 12.8 rad/s
Maximum spin acceleration (approx)	10 rad/s^2
Maximum spin deceleration (approx)	6 rad/s^2
Maximum tumble acceleration (approx)	10 rad/s^2
Tumble braking acceleration (approx)	20 rad/s^2

After three years' operational experience with the RMG, its performance may be summarised as generally excellent, though intermittently troublesome. The occasional poor performance, which is believed to be due to sub-standard electronic components, does not affect the quality of the experimental results, as no experiments are possible during such periods. Such problems, which are far outweighed by the excellent results which the equipment produces, are perhaps to be expected with sophisticated apparatus which is continually rolled though angles up to 40° at fairly high frequencies.

4. STEADY FORCED ROLL TESTS

4.1 Test techniques

Forced roll tests in their conventional form consist of applying a steady oscillatory roll moment and recording the model's steady state response. With the RMG, the applied roll moment is sinusoidal with known amplitude (given by Eqn.1) and frequency (equal to the RMG tumble rate). If the model's restoring characteristics are nearly linear, the response will be nearly sinusoidal, and only its amplitude and phase lag need be recorded. Otherwise, a Fourier analysis of the response is needed.

When the moment is first applied, the model's response includes a transient component, which may take a long time to die away if the damping is low. At forcing frequencies close to resonance, this appears as a slow increase in amplitude towards the steady state value or a slight overshoot in amplitude. Further away from resonance it appears as a beating effect, whose the amplitude slowly decreases. At very high or low frequencies the model's response may be dominated by motion at its natural frequency. This takes an extremely long time to die out, as the damping is low at the low amplitudes achieved away from resonance. It generally seems to be caused by small disturbances in the

tank, rather than sub-harmonic or super-harmonic resonance. If the tank is allowed to settle and the model is steadied by hand, a nearly sinusoidal response at the forcing frequency may be obtained. It may be monitored on a chart recorder until it is steady enough for data acquisition to begin. A typical forced roll sequence, followed by a roll decrement, is shown in Fig.5.

Data is usually acquired and averaged over 10-20 cycles. This is ample for obtaining a good averaged estimate of the roll amplitude and phase lag, and makes allowance for the error introduced by the practical sampling rate of 20 Hz available with the RMG microcomputer-based data acquisition system. Typical results of the on-line analysis of a forced roll test using the RMG are given in Table II.

Since the RMG spin rate is much higher than the tumble rate, it is usually set at a particular value and measurements are taken over a range of tumble rates before changing to a new spin rate.

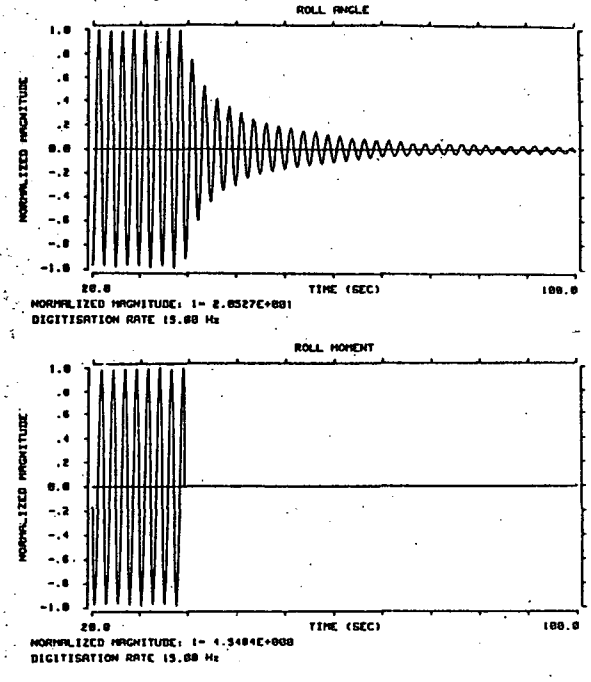

Fig. 5. Typical forced roll and decrement tests

This produces a set of amplitude and phase response curves such as Figs.6-7, in which the moment amplitude is proportional to the roll frequency. Plotting all the responses at given tumble rates gives a set of curves such as Fig.8, which clearly show the effects of non-linearities near resonance. Such curves are limited by the RMG performance envelope, and so a complete matrix of moment frequencies and amplitudes cannot be covered. Nevertheless, for any moment amplitudes which are covered at all frequencies of interest, the curves in Fig.8 may be used to construct conventional response curves at a constant roll moment amplitude. This method, despite the plotting involved, is a more convenient way of obtaining such curves than adjusting the spin rate to give a required moment amplitude for each selected roll frequency.

If the frequency-dependence of the damping coefficients is not of interest, a reduced test matrix is used, to produce a single curve such as Fig.6, which identifies the resonant

TABLE II. Typical forced roll analysis output

ROLL ANGLE
STATISTICS OF DATA

Zero crossing period	1.9857	sec
Zero crossing freq.	3.1642	rad/sec
Mean value	.4110	
Maximum value	17.1197	
Minimum value	-16.8457	
Standard deviation	11.7035	
Number of cycles	14	

	MEAN	STD.DEV.	VARIATION COEFF.
Zero crossing period	1.9871	.0070	.35%
Amplitude (positive side)	16.7227	.1660	.99%
Amplitude (negative side)	-16.3981	.1535	.94%
Mean amplitude	16.5604	.1152	.70%

ROLL MOMENT
STATISTICS OF DATA

Zero crossing period	1.9867	sec
Zero crossing freq.	3.1627	rad/sec
Mean value	.0700	
Maximum value	3.7985	
Minimum value	-3.7732	
Standard deviation	2.6251	
Number of cycles	15	

	MEAN	STD.DEV.	VARIATION COEFF.
Zero crossing period	1.9869	.0012	.06%
Amplitude (positive side)	3.7430	.0268	.71%
Amplitude (negative side)	-3.7017	.0257	.69%
Mean amplitude	3.7223	.0213	.57%
Phase lead to Ch.1 (deg)	87.4743	.7878	.90%

frequency, and then a single curve as on Fig.8 at that frequency (which does require varying the spin rate for each run). This identifies the non-linearity up to the largest obtainable roll amplitude. For models with significantly non-linear restoring characteristics, the resonant frequency will be amplitude-dependent. However, provided that sufficient measurements of roll frequency, amplitude and phase lag are taken at some frequency near to resonance, the analysis techniques (e.g. Ref 4) can account for this, and the tests need not be precisely at the resonant frequency for the current amplitude.

4.2 Assessment

The main advantage of forced roll tests is their excellent repeatability. With the RMG, large amplitudes may be repeated within 2%, with phase lags repeated within about 5%, which is a notable feature of the RMG and its associated data acquisition system. Consequently, every part of the response surface may be defined with confidence.

Typical analysis results, shown in Fig. 9, reflect this accuracy. The roll damping, determined by a linear analysis of each run, shows a clear trend with roll amplitude, which in this case is represented almost exactly by a linear + quadratic damping form, obtained from a non-linear analysis of all the runs at this frequency.

The principal disadvantage of steady forced roll tests is the laborious nature of defining the model's response, particularly if it is non-linear and sharply resonant, when tests at many moment amplitudes and frequencies are required.

5. ROLL DECREMENT TESTS

5.1 Test techniques

Roll decrement tests consist of a free decay in the model's roll motion, starting from some initial heel angle. A typical decrement is shown in Fig.5, and the peaks from a decrement are plotted in Fig.10, together with fits from linear and non-linear damping analyses.

The initial heel is commonly obtained by manually holding the model over at some suitable angle and releasing it; alternatively a steady

roll may be built up by repeatedly pushing on one deck edge of the model in time with the model's natural roll period. However, these methods suffer from the disadvantage that it is physically difficult to heel or roll a model to large amplitudes by hand without introducing heave or sway forces, which then result in extra motions which decay during the decrement and may affect the damping. Furthermore, only the first method achieves known starting conditions, and these conditions (starting from rest) are not realistic or continuous with the rest of the decrement.

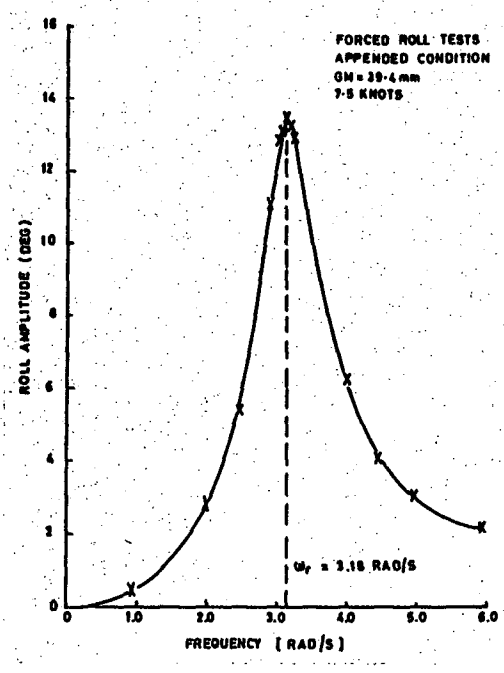

Fig. 6. Variation of roll amplitude with roll frequency

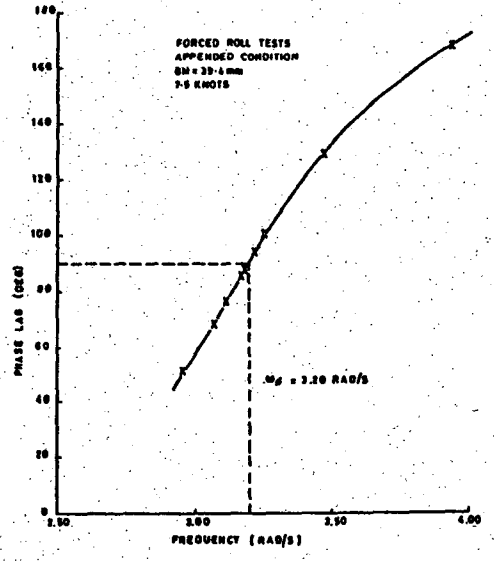

Fig. 7. Variation of phase lag with roll frequency

The RMG enables the forcing moment in a steady forced roll to be suddenly removed, allowing a roll decrement to commence from ideal steady oscillatory starting conditions. The moment may be stopped at any point in the cycle, although for a model being rolled at resonance it is normal to stop the moment as it crosses zero, which is the point of maximum roll due to the 90^{0} phase lag.

It is important to allow the decrement to continue for as long as possible, since longer decays give greater accuracy when determining the natural frequency, and also since the oscillations may often be productively analysed even after they appear to have stopped to an observer. However, there is a problem in deciding exactly when the decrement has ended, since reflected waves may eventually return and excite the model. This may be distinguished by monitoring a chart record, and stopping the decrement as soon as the amplitude increases on any cycle.

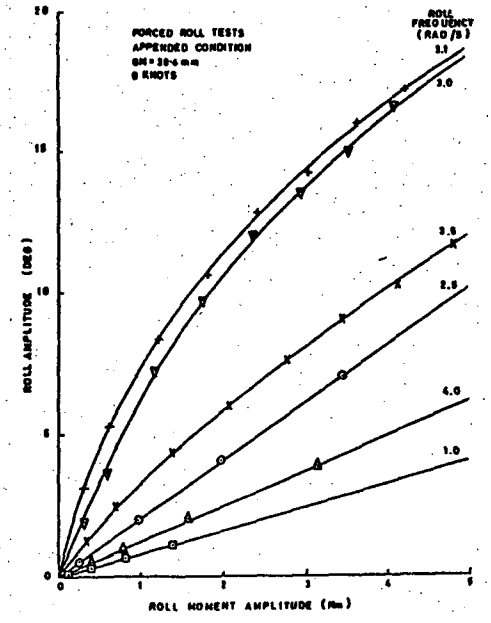

Fig. 8. Variation of roll amplitude with roll moment

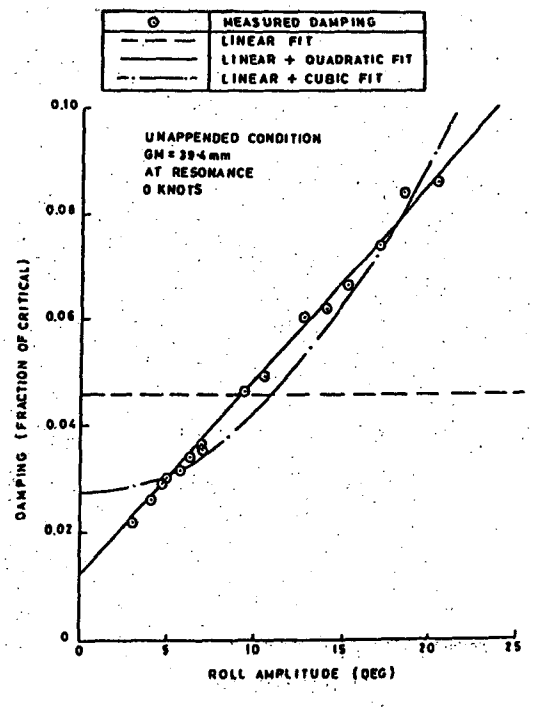

Fig. 9. Typical forced roll damping fit

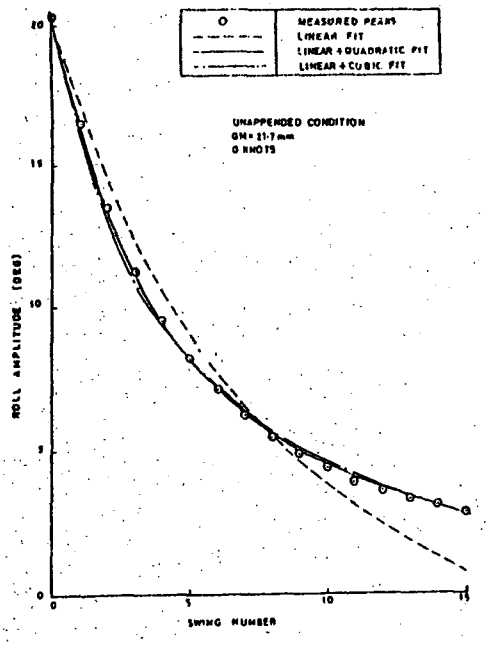

Fig. 10. Typical decrement fit

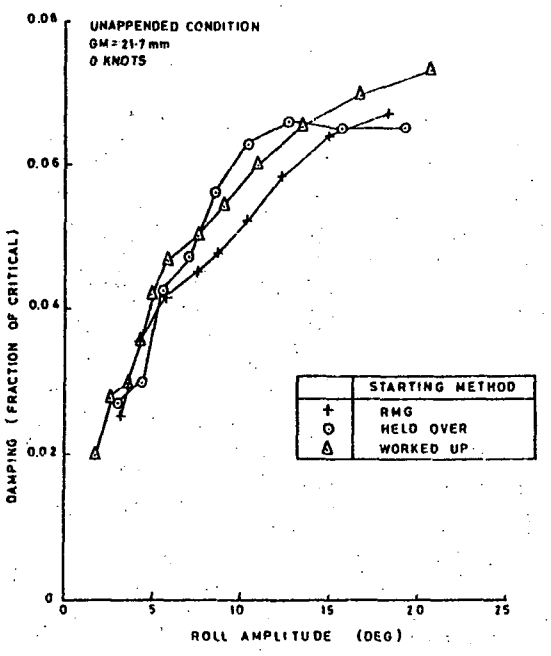

Fig. 11. Typical effects of starting methods in roll decrement tests

5.2 Assessment

The advantage of roll decrement tests is that they are extremely quick and simple to carry out. They may also be performed at full-scale.

Their principal disadvantage is their poor repeatability, even when the initial roll is created at a fixed amplitude by the RMG and the moment is stopped at virtually the same point in the cycle. Although this poor repeatability seems minor in the time-series of the decrement, a non-linear analysis amplifies the effect.

A comparison of the various methods of obtaining the initial heel is shown in Fig.11, in which the roll damping has been obtained from a linear analysis of each successive half-cycle. Using the RMG to create the initial roll produces damping with a trend similar to that from a decrement started from a roll worked up manually. However, both are distorted compared with the damping from forced roll tests on the same model shown in Fig.9. The decrement which begins with the model held over and released from rest is substantially more distorted. These results illustrate the "memory effect" from the discontinuity at the start of the decrement, which is believed to be the source of much of the unreliability in roll decrement experiments. A non-linear analysis of the decrements in Fig.11 produces higher linear coefficients and lower non-linear coefficients than corresponding forced roll tests.

A decrement provides very little data at large amplitudes since the decay is so rapid there, so the results are severely affected by even small errors. Omission of the first few peaks, in order to minimise the memory-effect problem, requires the decrements to be started at much larger amplitudes than equivalent forced roll tests, or else makes extrapolation of the results to larger amplitudes much less certain. At small amplitudes, where most peaks occur, the response is more easily disturbed by reflected waves. To mimimise this, the tests should be conducted at the centre of a long tank with beaches at each end.

Furthermore, roll decrements seem to be badly affected by roll gyro drift, which is perhaps provoked in part by the transient motion, since it is not usually appparent in steady forced roll data. This drift produces an apparent shift in the mean roll position of up to 1^{o}, which varies during the decrement. It may be removed by spline fairing techniques, but these are least accurate at the large amplitude end of the decrement.

Despite the above difficulties, by using advanced analysis techniques (e.g. Ref.4) and averaging of the results from at least 3 roll decrements, broadly similar results to forced roll tests at the natural frequency may be obtained. However, in the absence of forced roll tests, confidence in non-linear roll decrement results is always quite low.

Roll decrements are by definition restricted to the model's natural frequency but, provided that frequency-dependent analysis is not required, this is in fact an advantage, since it eliminates the difficulty in steady forced roll tests of finding the natural frequency.

6. TRANSIENT FORCED ROLL TESTS

Transient forced roll tests subject the model to an oscillatory roll moment, which is modulated in amplitude and/or frequency, and record the transient roll response. The tests are designed for use with parameter estimation analysis techniques, for which steady sinusoidal roll moments are not necessary, as long as the input moment variation and the output roll angle response are known exactly. This is extremely convenient with the RMG.

The tests may be carried out over a range of moment amplitudes and frequencies which best illustrate the model's response characteristics, and the test run continued for as long as necessary to complete the estimation with acceptable accuracy. A typical such test is illustrated in Fig.12, in which moment amplitude and frequency are reduced together, passing through resonance. Work is continuing on this technique and it would be premature to evaluate it here, except to note that it has the

potential to overcome both the problems of lack of repeatability with free transient roll decrement tests and of the laborious testing with steady forced roll tests.

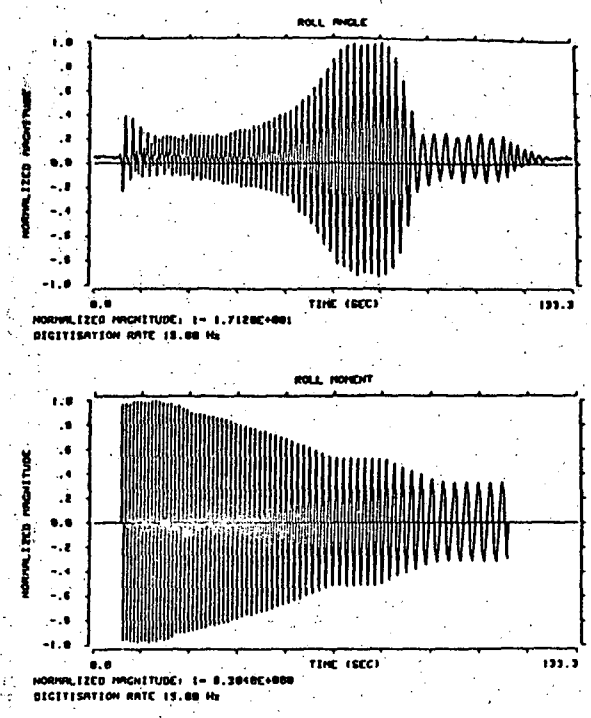

Fig. 12. Typical transient forced roll tests

7. CONCLUSIONS

In the search for reliable roll damping measurements, extensive experience in conducting large amplitude rolling tests in calm water has been gained at BMT, based on the gyroscopic roll moment generator (RMG). Although considerable difficulties were encountered in the development of this equipment (mainly due to false economies in its construction), it has amply repaid the investment in it with large amounts of high-quality forced rolling data.

Forced rolling tests with the RMG have been found to have excellent repeatability, and have been used to obtain roll damping measurements at up to 40^{o} amplitude. Although roll decrement tests can in principle obtain the same results at the resonant frequency, they have been found to be prone to error, mainly from memory-effects arising from the starting discontinuity. Use of the RMG to obtain the initial roll has been found to minimise these effects, but even this does not eliminate them. Nevertheless, roll decrements have the considerable advantage of simplicity, whereas the more accurate forced roll tests are comparatively laborious. Transient forced roll techniques are now being investigated, which have the potential to combine the advantages of both types of tests.

ACKNOWLEDGEMENTS

The authors would like to acknowledge the assistance of their colleagues at BMT in developing the techniques described in this paper, in particular, Mr.N.J.Allen (now of Vosper Thorneycroft Ltd) and Mr.A.J.B.Lees. The work was funded by the Department of Transport, Marine Directorate, as part of the SAFESHIP project. This paper is published by permission of British Maritime Technology Ltd.

REFERENCES

1. Spouge, J.R. & Ireland, N. : "An Experimental Investigation of Large Amplitude Rolling Motion", Int. Conf. on the Safeship Project, RINA, London, June 1986.

2. Blagoveshchensky, S.N. : "Theory of Ship Motions", Vol 2 Dover Publications, New York, 1954.

3. Sugai, K. & Yamanouchi, Y. : "A study on the Rolling Characteristics of Ship by a Forced Oscillation Model Experiment", Journal of Zosen Kiokai, Vol 114, 1963.

4. Mathisen, J.B. & Price, W.G. : "Estimation of Ship Roll Damping Coefficients", Trans RINA, Vol 127, 1985.

Third International Conference on Stability of Ships and Ocean Vehicles, Gdańsk, Sept. 1986

STAB'86

A PROBABILISTIC MODEL OF SHIP ROLL MOTIONS FOR STABILITY ASSESSMENT

J.B. Roberts; R.G. Standing

Summary

This paper describes the basic features of an approximate stochastic theory, based on a combination of averaging techniques and the theory of Markov processes, for predicting the rolling motion of a ship in irregular waves. The theory assumes a single degree of freedom equation for roll motion and leads to a prediction of the probability distribution of the roll amplitude, together with related statistics. Particular advantages of this approach are that non-linearities in both the damping and restoring moment can be taken into account and that the effect of the shape of the excitation spectrum on the response statistics can be assessed. It is shown that the theory gives good agreement with both digital simulation results and experimental results obtained from a model of the Fisheries Protection Vessel 'Sulisker', rolling in irregular beam seas in a wave tank, at zero speed.

It is demonstrated that the theory can also be used as a basis for computing long-term statistics of roll motion. This involves computing short-term statistics for single sea states of a few hours duration, and then integrating, in a suitable fashion, over all the states, where these states have a distribution representing the long-term climate. This integration process requires a knowledge of the joint distribution of wave height and wave period. To illustrate the method, the specific case of the FPV 'Sulisker', operating in a sector of the North Sea, is discussed and some numerical results are presented.

1. INTRODUCTION

Large roll motions are a serious threat to the safety of a ship and those on board. They may cause excessive loads on sea fastenings, shifting of cargo, shipping of water, loss of men and deck equipment overboard and possibly loss of control over the ship. These factors may contribute to capsize, or to structural failure. The ability to predict the probability of the roll amplitude reaching a specified critical level, for a ship in a specified sea state, is thus a matter of considerable practical importance. Since non-linearities exist in both the roll damping and restoring moments experienced by a ship, and both the wave input and roll response are stochastic in nature, it is evident that this prediction problem is both complex and difficult.

In tackling the problem of predicting the occurrence of an excessively large roll angle (possibly leading to capsize) one can follow one of two basic approaches. The first of these assumes that the wave excitation during a single "sea-state", lasting a few hours, can be treated as a stationary random process. With light roll damping the roll motion is then a narrow-band process such that successive peak amplitudes are highly correlated. High roll amplitudes occur, in this approach, as a result of slowly-varying, random fluctuations in peak amplitudes, over a period of time covering many consecutive rolls. The second approach is based on the assumption that excessive roll motion results from the sudden appearance of freak, unfavourable, wave conditions, which occur over a very short period of time. It involves the identification of "worst-case" wave motions, together with an estimation of their probability of occurrence. It would appear that both these basic approaches have their own particular advantages and that design procedures may well, eventually, require a synthesis of results drawn from each.

In the work summarised here, which was carried out as part of the SAFESHIP programme, the first of these two

approaches has been adopted. In principle, it is possible to obtain estimates of the probability of an actual capsize occurring in a given sea state, by treating the wave excitation as a stationary random process, with a specified spectrum. However, the formulation of the equation of motion becomes very uncertain at very high roll angles, which are close to capsize. Many highly non-linear phenomena, such as taking water on board, occur which are extremely difficult to represent in mathematical form. Fortunately, though, at more moderate roll angles, the uncertainties in the modelling diminish appreciably and one can formulate a reasonable equation of motion which retains significant non-linear terms (especially in the damping component). With this in mind, the work described here has, as a main objective, the development of a method of predicting the probability, $P_0(A)$, that the roll motion reached some specified critical amplitude level, A, which is somewhat lower than that at which capsize actually occurs. This level could represent, for example, the amplitude at which unacceptable shipping of water occurs. Comparison of $P_0(A)$ values for various ships, in a given sea state, offers a method of assessing, quantitatively, the relative degree of roll stability. Moreover, from an operational viewpoint, a knowledge of $P_0(A)$ enables weather routing decisions to be taken on a rational basis.

In this paper the basic features of an approximate theory for predicting rolling motion in a single sea state are outlined. The theory is based on a combination of averaging approximations and Markov process theory and leads to fairly simple analytical expressions for roll response statistical descriptions, such as $P_0(A)$. Validation tests for the theory are described, which involve comparisons with both digital simulation results and results from an experimental investigation of the rolling motion of a model ship in irregular waves. It is also pointed out that the theory may be used to predict statistics of the first-passage type, which are appropriate when the level of wave excitation is very high.

From a practical viewpoint one is often interested in the statistics of roll motion over very long periods of time, commensurate with the operating lifetime of the ship. During such long periods a variety of sea states will be encountered, the magnitudes of which are unpredictable from a deterministic viewpoint, but which can be described statistically in terms of a joint probability distribution for the wave parameters H (significant wave height) and T (the mean zero up-crossing wave period). In the final part of this paper it is shown how statistical information describing roll motion in a single sea state can be combined with long term wave statistics to produce long term roll statistics. Some numerical results are presented in graphical form for a simple, specific case.

The work summarised here is fully reported in Refs. 1 to 8.

2. BASIC ASSUMPTIONS

To arrive at a practical, useful method of predicting roll motion in random waves it is essential to make a number of simplifying assumptions and approximations. Those adopted in the present work are now briefly discussed. Some are plausible on physical grounds whereas others are motivated primarily by pragmatic considerations (i.e. the necessity of simplifying the mathematical description to the point at which an analysis becomes feasible).

2.1 Wave-Ship Interaction

The hydrodynamic forces experienced by a ship in waves depend not only on the wave motion but also on the motion of the ship. In general there will be some complex, non-linear interaction between these two motions, which leads to considerable difficulties in formulating appropriate equations of motion.

For the special case of small motions a linearised analysis is possible, which is very much simpler than the general case. According to linear theory the interaction effects mentioned above are absent, and the modelling procedure can be represented in block diagram form, as shown in Fig. 1. There are two distinct stages in the analysis:

a) computation of the wave forces on the ship, assuming that the ship is not moving (the wave diffraction problem);

b) formulation of the equations of motion of the ship, treating the wave forces from stage (a) as excitation terms (wave radiation and response problems).

Such a linear calculation can be carried out using a general purpose computer programme such as NMIWAVE (Ref. 9).

Here it is assumed, in the absence of further information, and to render the problem tractable, that the analysis can be carried out in the two distinct stages shown in Fig. 1, even when the roll motion is fairly large. A linear calculation procedure is used for the first stage, whereas non-linear effects are incorporated into the second stage. The validity of this approach can only be tested through a comparison with experimental observations of a ship rolling in waves; such validation work will be described in section 4.2.

2.2 Formulation of the Equations of Motion

It is assumed here, for simplicity, that, with a suitable choice of coordinates, it is possible to decouple the equation for roll motion from the other equations of motion. Numerical comparisons, based on linear theory, indicate that, at least in the case of beam waves, this is indeed a reasonable approximation (see Ref. 5).

Following most earlier authors, a general, uncoupled, roll equation of motion will be a second-order differential equation of the form

$$I\ddot{\phi} + \beta\, C(\dot{\phi}) + K(\phi) = M(t) \qquad .. (1)$$

where I is the roll inertia (including added inertia), ϕ is the roll angle, $C(\dot{\phi})$ is an arbitrary non-linear damping moment, M(t) is the roll excitation moment and β is a scaling parameter. As explained earlier, it is assumed that M(t) can be related to the wave motion through a linearised analysis. $K(\phi)$ is the hydrostatic restoring moment which can be computed theoretically or measured experimentally. $C(\dot{\phi})$, the damping moment, is assumed to be unaffected by incident wave motion and can thus be found, experimentally, from free-decay or forced-roll tests.

In the specific theoretical method used here, and described briefly later, it is necessary to assume that the damping is relatively light - i.e., that β is a small parameter. In this circumstance the bandwidth of the roll response process will be small compared with that of the roll moment process.

2.3 Wave Excitation Process

It is assumed here, initially, that the wave input can be represented as a stationary random process, with a known wave elevation spectrum, $S_w(\omega)$. This model is generally regarded as acceptable, for a single sea-state, covering a period of time of the order of a few hours. For such a sea state a standard form (such as JONSWAP) can be used for $S_w(\omega)$, with selected values for the significant wave height, H, and the mean zero crossing period, T. Later (in section 6) it will be shown how the analysis can be extended to deal with roll response behaviour over much longer periods of time, in which a large number of successive, differing sea states are encountered.

To keep matters simple, waves are assumed to be unidirectional. The elevation spectrum $S_w(\omega)$ is then a sufficient description, since the proposed method does not require a knowledge of the probability distribution of the wave heights.

2.4 Roll Response Process

The restoring moment, $K(\phi)$, will reduce to zero at some critical roll angle, ϕ^*, say. It follows that there is only a finite region of safe operation in the phase-plane, which is centred on the static, stable position ($\phi = \dot{\phi} = 0$). This is illustrated in Fig. 2 where trajectories for undamped, free motion are shown. With stationary random excitation the roll motion trajectories will eventually exit from the "safe" region, resulting in "capsize". For relatively weak levels of excitation the probability of a trajectory leaving the safe region is extremely small and one can, for practical purposes, assume that the roll motion is a stationary process (Ref. 1). However, for high levels

of excitation, and correspondingly severe roll motion, a capsize may occur in a reasonably short period of time; it is then inappropriate to discuss stationary response statistics, such as the standard deviation of roll, or the distribution of roll amplitude.

For severe roll motion a much more satisfactory approach is to consider the probability that the roll motion stays within definite amplitude limits, for a specified period of time. This probability is usually called "first-passage probability", and is closely related to the first-passage time, which is the time taken for a trajectory with given initial conditions to reach a prescribed level (Ref. 10).

Accordingly, it will be assumed that there are two basic classes of problem:

a) moderately severe roll motion. In this case non-linearities are important (especially in damping) but the probability of a capsize occurring (within a time interval of the same order as the time interval for which the sea state may be considered as stationary) is negligibly small;

b) very severe roll motion. Here the relevant statistics are of the first-passage type.

3. THEORETICAL TREATMENT

The theoretical approach used here is based on the adoption of equation (1) as an appropriate equation of motion. This can be simplified somewhat by dividing throughout by I. Thus

$$\ddot{\phi} + \beta\, F(\dot{\phi}) + G(\phi) = X(t) \qquad \ldots (2)$$

where $F = C/I$, $G = K/I$, $X = M/I$

The total energy envelope, V(t), associated with the roll response may be defined as

$$V = \frac{\dot{\phi}^2}{2} + U(\phi) \qquad \ldots (3)$$

where $\dot{\phi}^2/2$ is the kinetic energy and

$$U(\phi) = \int_0^{\phi} G(\xi)\,d\xi \qquad \ldots (4)$$

is the potential energy.

If the damping is sufficiently light then the energy dissipated through damping, in a typical roll cycle, will be a relatively small fraction of the total energy associated with that cycle. It follows that the energy process, V(t), will vary slowly with time. It is shown in Refs. 1 and 2 that, in these circumstances, V(t) can be approximated as a one-dimensional Markov process, governed by a first-order stochastic differential equation. In Itô form (see Ref. 11) this equation may be written as

$$dV = m(V)dt + D^{\frac{1}{2}}(V)dW \qquad \ldots (5)$$

where m(V) is the "drift coefficient", D(V) is the "diffusion coefficient" and W(t) is a unit Wiener (or Brownian) process. The derivative of W(t) is simply a white noise process. Both m(V) and D(V) can be expressed in terms of the spectrum, $S_X(\omega)$, of the excitation process, X(t) (Refs. 1, 2).

For moderate levels of excitation the probability of capsize is negligible (as pointed out earlier). One can then treat V(t) as a stationary process with a stationary density function, p(V). From the Fokker-Planck equation corresponding to equation (5) one obtains the expression

$$p(V) = \frac{C}{D(V)} \exp\left(2\int_0^V \frac{m(\xi)}{D(\xi)}\,d\xi\right) \qquad \ldots (6)$$

where C is a normalisation constant.

From p(V) one can deduce several important statistics; for example, consider the amplitude envelope process, A(t), defined by

$$V(t) = U[A(t)] \qquad \ldots (7)$$

Since $\phi(t)$ is a narrow-band process, A(t) will be the envelope of the peak amplitudes, and the probability distribution of A(t) can be used as a good approximation to the distribution of these amplitudes. One has

$$p(A) = p(V)\frac{dV}{dA} = G(A)\,p(V) \qquad \ldots (8)$$

where G(A) is the restoring function.

Many other statistical parameters (including the standard deviation of $\phi(t)$, denoted σ) can be deduced from the expression (see Ref. 12):

$$p(\phi, \dot{\phi}) = p(V)/T(V) \qquad \ldots (9)$$

where $p(\phi, \dot{\phi})$ is the joint density function for the roll amplitude, ϕ, and the roll velocity, $\dot{\phi}$, and $T(V)$ is the period of free, undamped oscillations at the energy level V.

3.1 Modified Theory

It can be shown that, according to the above theory, in the special case of a linear restoring moment, the shape of the input spectrum does not play a role in the determination of $m(V)$ and $D(V)$ - i.e. the only value that matters is that of $S_X(\omega)$ at $\omega = \omega_o$, where ω_o is the frequency of undamped, free oscillations. Thus, for linear restoring moments, the basic assumptions of the theory are equivalent to making a white noise approximation for $X(t)$, with constant spectral level $S_X(\omega_o)$.

For the linear case the error in approximating the input as a white noise is readily found by using linear system theory. In fact one can compute a value r, defined as the ratio of the square of the exact roll standard deviation to the square of the approximate, white noise result, σ_w - i.e.:

$$r = \sigma^2/\sigma_w^2 \qquad \ldots (10)$$

The ratio r can be used to correct, in an approximate fashion, the theory outlined earlier, for the general case of non-linear stiffness and damping. The technique is to replace $S_X(\omega)$, in the expressions for $m(V)$ and $D(V)$, by a modified spectrum

$$S_X'(\omega) = r\, S_X(\omega) \qquad \ldots (11)$$

In the linear case this will have the effect that σ^2 is now given exactly. In the non-linear case an equivalent linear system must be constructed, to compute r.

An appropriate equivalent linear system is

$$\ddot{\phi} + 2\zeta(V)\Omega(V)\dot{\phi} + \Omega^2(V)\phi = X \qquad \ldots (12)$$

where $\Omega(V) = 2\pi/T(V)$ is the natural frequency at energy level V, and $\zeta(V)$ is an amplitude dependent damping factor. The ratio r, computed on this basis, will of course depend on V.

A suitable definition of $\zeta(V)$ may be found by considering the free-decay of the non-linear oscillator. For $X(t) = 0$, equation (5) reduces to

$$\dot{V} = -L(V) \qquad \ldots (13)$$

where $L(V)$, the "loss function" is the average loss per cycle, due to damping; this can be readily calculated for any specific form of damping (Ref. 4). In the linear case

$$L(V) = 2\zeta V \qquad \ldots (14)$$

Thus, in the more general case

$$\zeta(V) = \frac{L(V)}{2V} \qquad \ldots (15)$$

can be regarded as an appropriate, amplitude dependent, effective ζ value, for use in equation (12).

4. VALIDATION OF THE THEORY

4.1 Comparison with Digital Simulation Results

A digital simulation study has been undertaken using a specific form of equation (2) (Ref. 3). After non-dimensionalisation this equation takes the form

$$\ddot{\Psi} + a\dot{\Psi} + b\,\Psi|\dot{\Psi}| + \Psi - \Psi^3 = x(t) \qquad \ldots (16)$$

The damping in here represented as a combination of linear and quadratic terms, with a as the linear damping factor and b the quadratic damping factor. Non-linearity in the restoring moment is represented by the cubic term in Ψ, where Ψ is a non-dimensional roll angle (Ref. 3).

In the simulation procedure, sample functions of the wave input process, $x(t)$, were generated digitally, using pseudo-random numbers at equi-spaced intervals of time. A numerical integration routine (a 4th order Runge-Kutta algorithm) was then used to solve the equation, thus generating sample functions of the roll

response process, $\Psi(t)$. Hence statistical estimates of $P(A)$, the cumulative probability distribution of the envelope process $A(t)$, and σ, the standard deviation of $\Psi(t)$, were obtained.

Since the objective of this study was to test the validity of the theoretical method, the sample function, $x(t)$, did not necessarily have to correspond to a specific, standard wave spectrum. It was sufficient that $x(t)$ should have a spectrum with roughly the correct overall character - i.e. a single peak and a bandwidth representative of real excitation processes. Accordingly, an input process, $x(t)$, was chosen which had roughly the right character, and for which sample functions could be generated in a very rapid and efficient manner, with a minimum of computational effort. This approach enabled long realisations of the output roll response to be generated, with the advantage that accurate estimates of the roll motion statistics could be found with a reasonable computational effort.

The input process chosen was generated from the relationship

$$x(t) = h[a(t) \cos \omega_p t - b(t) \sin \omega_p t] \quad \ldots (17)$$

where h is a height scale, and a(t) and b(t) are two independent, first-order processes, obtained by filtering white noises through first-order linear filters. The spectrum of x(t) for this process is

$$S_x(\omega) = \frac{h^2 \beta^2}{4\pi} \left(\frac{1}{\beta^2 + (\omega - \omega_p)^2} + \frac{1}{\beta^2 + (\omega + \omega_p)^2} \right) \quad \ldots (18)$$

where β is a bandwidth parameter (Ref. 3). For small values of β, $S_x(\omega)$ exhibits a single peak at $\omega \sim \omega_p$, with a bandwidth proportional to β.

In this simulation study the roll response depended on the damping parameters a and b, the non-dimensional frequency ratio $\Omega_p = \omega_p/\omega_o$, a non-dimensional bandwidth parameter, $\varepsilon = \beta/\omega_o$, and a non-dimensional input strength parameter, σ_x.

Fig. 3 shows typical results, for two sets of parameter values. It is found, in these and in other results (Ref. 3), that the modified theory generally gives an improved agreement with the simulation estimates. Over a realistic range of damping parameters, and for a realistic input bandwidth, the modified theory was found to give good agreement with the simulation estimates of the standard deviation, σ. (See Fig. 4, for a typical comparison of σ values). As the assumptions of the basic theory would lead one to expect, the agreement is best when the bandwidth ratio R, given by

$$R = \frac{\text{bandwidth of roll response}}{\text{bandwidth of excitation process}} \quad \ldots (19)$$

is small; this condition is achieved when the damping is light and also when the input bandwidth is large.

4.2 Comparison with Experimental Results

In view of the lack of previously documented experimental results, suitable for validating the theory, an experimental programme was undertaken at BMT, with the aim of providing reliable statistical estimates of the roll peak amplitude distribution for a ship at zero speed under controlled conditions. A 1:20 scale model of the Fisheries Protection Vessel 'Sulisker' was chosen for this study, and experiments were conducted with the model in the BMT No. 3 tank. The model was subjected to uni-directional, irregular beam waves, with spectra of various prescribed shapes. Beam waves were chosen to minimise coupling with the longitudinal motions of surge and pitch, and thus to simplify the analysis and interpretation of results.

4.2.1 Estimation of Damping

As a first stage in the experimental work, free-decay tests were performed on the unappended model (i.e. without bilge keels, fins, etc), in the absence of waves. By a suitable analysis (Ref. 4) of such free-decay data one can arrive at an estimate of the damping function $\zeta(V)$ (see equations (13) to (15)) and hence at estimates of the coefficients in an explicit, parametric mathematical representation of the damping term, $C(\dot{\phi})$, in equation (1).

Fig. 5 shows the result of analysing a number of free-decay curves obtained from the 'Sulisker', with various critical conditions (Ref. 4). Here $\zeta(V)$ is plotted against roll amplitude, ϕ. The pronounced variation of $\zeta(V)$ with roll amplitude, evident in Fig. 5, is due to the highly non-linear nature of the roll damping. The linear-plus-quadratic fit to the estimates of $\zeta(V)$, shown by the full line, was found to give a better representation than the linear-plus-cubic model, and was used in the subsequent theoretical model for forced roll motion.

4.2.2 Rolling in Irregular Waves

Tests were carried out on a naked hull model (i.e., no appendages such as bilge keels, propellers, etc). Irregular, uni-directional waves were generated by a wedge wave-maker at one end of the tank, and the model was positioned for beam wave encounter.

With the wave generator set of produce waves with a prescribed "target spectrum", simultaneous measurements were taken of the six components of ship motions and the wave elevation at either side of the model. Only the roll displacement and wave elevation records ware used in the present analysis.

Four different wave target spectra were chosen, as summarised in Table 1.

TABLE 1: Datasets and wave spectra

Dataset No.	Target Wave Spectrum	No. of Rolls Recorded
1	JONSWAP; H = 5.1m, T = 8.5s	1001
2	JONSWAP; H = 4.4m, T = 6.6s	1325
3	ITTC; H = 4.7m	1249
4	JONSWAP; H = 6.1m, T = 8.5s	580

4.2.3 Theoretical Modelling

With the aim of assessing the validity of the uncoupled roll equation (equation (1)) a comprehensive linear analysis was carried out using the NMIWAVE computer programme (Ref. 5). The calculations were carried out with the origin of the coordinate system located at the centre of mass of the ship. With this origin, there was found to be significant coupling between the ship's sway and roll motions, but other motions were much less strongly coupled with roll.

On the assumption that only the sway motion is significantly coupled with roll it was found possible to decouple the roll equation by moving the origin of the coordinate system to a new position, a "roll centre", vertically below the centre of mass (Ref. 5). The effect of this shift of origin was to change the roll inertia (slightly) and the roll moment transfer function (significantly). Calculations based on the resulting single-degree-of-freedom equation were found to give standard deviation values for roll displacement within ten per cent of the results from the fully coupled, six-degrees-of-freedom equations.

It was concluded that, at least for small motions, the roll can be modelled reasonably well by equation (1), provided that the origin is chosen to eliminate sway coupling. It was assumed hencefoxth that the roll centre was also the best origin to adopt in the case of larger, non-linear motions.

The following specific equation of motion was adopted for the purpose of comparison with experiment:

$$\ddot{\phi} + a\dot{\phi} + b\dot{\phi}|\dot{\phi}| + \omega_o^2\phi(1 + \varepsilon^2\phi^2) = X(t) \quad (20)$$

As shown earlier, the linear-plus-quadratic damping representation chosen here is in accord with the analysis of free-decay data for the unappended model; a and b are derived from this analysis (Ref. 4). The linear-plus-cubic form for the restoring moment, $G(\phi)$, in equation (20) is a good representation for the Sulisker model, for the roll amplitudes in the range $0-35^o$ (Ref. 5), if ε^2 is chosen appropriately. The spectrum of $X(t)$ was related to the wave elevation spectrum through a linear analysis, using NMIWAVE.

4.2.4 Comparison between Theory and Experiment

Figs. 6(a) to (d) show, for datasets 1 to 4 respectively, the variation of the cumulative probability, $P(A)$, with roll amplitude A, as obtained from the theory (original and modified) and from the experimental roll records. Also shown, for comparison purposes, is the Rayleigh

distribution in each case (calculated from the measured σ value). Rayleigh probability paper has been used in the presentation of these results; thus a Rayleigh distribution appears as a straight line.

In all four cases the modified theory gives a fairly good agreement with the experimental estimates, and the pronounced deviation from the Rayleigh distribution, at high roll amplitudes, is well-predicted by the theory. This deviation is principally due to the strong non-linearity in the damping, which is almost entirely quadratic. At high amplitudes the Rayleigh distribution seriously overestimates the probability of reaching larger amplitudes.

The theory was also found to give good agreement with the experimentally determined values of the roll standard deviation, σ. Table 2 shows a comparison between experimental and theoretical values of σ.

TABLE 2: Roll Standard Deviation - Theory and Experiment

Dataset No.	Experimental σ (degrees)	Theoretical σ (degrees)	
		Original	Modified
1	10.1	10.1	9.9
2	11.3	12.9	11.8
3	10.4	11.1	10.4
4	11.0	10.8	10.7

5. FIRST PASSAGE STATISTICS

The basic theory outlined earlier provides a foundation for estimating first passage probabilities. If the Fokker-Planck equation for V(t) is replaced by its adjoint form, one can obtain a differential equation for the probability, $W(V_o,t)$, that V(t) stays below a specified amplitude limit, h, in a time interval 0 - t, for trajectories starting at V_o.

For large values of h, and correspondingly long times to failure, it is shown in Ref. 6 that

$$W(V_o,t) \rightarrow e^{-\lambda_1 t} \qquad \ldots (21)$$

where λ_1 is an eigenvalue of the differential equation for W. Also

$$\bar{T} \rightarrow \frac{1}{\lambda_1} \qquad \ldots (22)$$

where $\bar{T}$ is the mean of the first-passage time. Thus a knowledge of $\bar{T}$ suffices to estimate $W(V_o, t)$, in the case of large $\bar{T}$. A simple, ordinary differential equation for $\bar{T}$ can be deduced, and solved numerically, by incorporating a suitable boundary condition (Ref. 6).

In Ref. 6 a number of comparisons are given between theoretical estimates of $\bar{T}$ and corresponding estimates from a digital simulation study. Generally it was found that the theory gave good results when the bandwidth ratio R was large. For smaller values of R the theory gave estimates of $\bar{T}$, and hence $W(V_o,t)$, which were conservative, and should, therefore, be of value for design purposes.

6. LONG TERM STATISTICS

We now consider the situation where a ship operates for a long period of time (N years) in a particular sea area, for a specified part of the year. During its operation it encounters a sequence of different single sea states, each of duration a few hours. Each single sea state can be regarded as approximately stationary, and may be specified in terms of the wave parameters H and T, referred to earlier. If, in addition, a specific form of wave spectrum is adopted (such as the JONSWAP form), and the waves are assumed to be unidirectional, the joint specification of H and T is a complete description. The long term wave climate may then be specified by the joint probability density function p(H,T) (Refs. 13 to 15). Such density functions are available in analytical form, with parameters derived by fitting the form to observed wave data (Ref. 14).

The theory outlined earlier enables roll statistics to be computed for a single sea state - i.e. for particular values of H and T. By computing such statistics for many values of H and T, and using the p(H,T) function for the long term wave climate, one can obtain estimates of long term roll statistics. Two approaches will be described briefly here, and illustrated by numerical results for the 'Sulisker'

operating in a sector of the North Sea in the winter months (see Ref. 7 for details).

For simplicity it is assumed that the ship operates at zero speed, and that only beam waves are encountered. It is possible, with extra computational effort, to include the effects of more general operating conditions (Refs. 7, 16 and 17).

6.1 Distribution of the Standard Deviation of Roll

The standard deviation of roll, σ, for a single sea state can be regarded as a function of H and T. Fig. 7 shows a contour plot of σ in the (H,T) plane, for the particular case referred to earlier. As one would expect there is a strong tendency for σ to be greater when the peak in the input spectrum coincides with the natural frequency of oscillation, $f_n = 1/T_o$. For the 'Sulisker', with the ballast condition used in the calculation, $T_o = 8.85$ sec and the peak in the spectrum (the mean JONSWAP) occurs at $f_o = 1/1.409T$. Hence the critical value of T, T_c, is given by $T_c = 8.85/1.409 = 6.28$ sec, as marked in Fig. 7.

The cumulative probability distribution, $P(\sigma)$, of σ can be found by computing the "probability mass" between closely spaced σ contours (Ref. 7). Fig. 8 shows the resulting variation of $P(\sigma)$ with σ, plotted on Rayleigh probability paper, for the present example. The computed points lie almost exactly on a straight line, indicating a distribution of the Rayleigh type; in fact the expression

$$P(\sigma) = 1 - \exp\left[- \left(\frac{\sigma}{6.33}\right)^2 \right] \qquad \ldots (23)$$

gives a very good fit.

From $P(\sigma)$, related long term statistics can be easily deduced. For example, one can compute the "return period", N_R, for a given critical level, η, of σ. This may be defined as the average period of time which occurs between states for which $\sigma > \eta$. In the present example, Fig. 9 shows the variation of σ with N_R, for different values of m, the number of hours in each single sea state. The main feature of this result is that σ varies only slowly with N_R and is fairly insensitive to changes in m.

6.. Level Crossing Rates

For a single sea state, with specified H and T values, one can compute the average number of up-crossings per "cycle", ν^+T_o, of the roll response process $\phi(t)$, for various amplitude levels, η (Ref. 7). Here ν^+ is the average numer of upcrossings, per unit time, of level η. If one fixes a certain critical crossing rate, $(\nu^+T_o)_{crit}$ say, as the limit of acceptability, from an operational viewpoint, then one can define, precisely, the region of unsafe operation in the (H,T) plane. In the present example, if $(\nu^+T_o)_{crit} = 0.001$ (i.e. one crossing every thousand cycles, on average), and $\eta = 40^o$, then the appropriate unsafe region is shown in Fig. 10(a). As η increases, the area of the unsafe region diminishes. Fig. 10(b) shows the effect of increasing η from 40^o to 50^o. The sizes of the unsafe regions are relatively insensitive to the choice of $(\nu^+T_o)_{crit}$ but are critically dependent on the choice of the η level.

The long term level crossing rate $(\nu^+T_o)_{LT}$ can be found by integrating over all sea states, as discussed in Ref. 7. For the present example, Fig. 11 shows the variation of $(\nu^+T_o)_{LT}$ with η^2, where the former is plotted logarithmically. A very good fit to the computed points is

$$(\nu^+T_o)_{LT} = k_1 \exp(-k_2\eta^2) \qquad \ldots (24)$$

where $k_1 = 9.14 \times 10^{-3}$ and $k_2 = 2.86 \times 10^{-3}$. From this result one can estimate the probability of "survival", P_S, as a function of the critical amplitude level, η. Here P_S represents the probability that the level η will not be exceeded, in the long term. Fig. 12 shows the variation of P_S with η, plotted on Rayleigh probability paper, for the periods N = 1, 10 and 50 years. This shows that P_S is very small if the critical response level η is chosen to be less than 55^o, but rises sharply with increasing values of η.

In assessing the significance of these results it must be remembered that the data has been derived from tests on an unappended model - i.e. with very low roll damping. The purpose of this calculation is to show how the method may be used, rather than to produce operational data for a specific vessel.

7. CONCLUSIONS

The main conclusions of this work are summarised as follows.

a) The Markov-averaging method gives good agreement with simulation estimates when the roll damping is light and when the wave excitation band-width is relatively large. A simple modification to the theory, to take further account of the input spectral shape, leads to improved accuracy when the input bandwidth is reduced.

b) A linear analysis of the small motion response, for the particular ship used for validation purposes (the FPV 'Sulisker') revealed that the roll motion was coupled principally with sway motion. A "roll centre" could be found as a coordinate origin, such that the linearised roll equation was approximately uncoupled from the sway motion equation. This result lends support to the basic assumption of a single degree of freedom equation for roll.

c) A simple non-linear equation could be constructed for the roll motion by incorporating a linear-plus-quadratic model (deduced from free-decay test data on a naked hull, without appendages) for the damping term and a linear-plus-cubic form for the non-linear restoring moment. In the present study the predominant non-linearity was in the damping term, which was mainly quadratic. To obtain the forcing term in the equation of motion, a linear relationship between wave elevation and wave excitation moment was assumed.

d) Good agreement was obtained between the theoretical and experimental probability distributions of roll angle amplitude, and the standard deviation of the roll angle, for the unappended hull in four different beam seas cases. In particular the theory correctly predicts the deviation from the Rayleigh distribution, for the roll amplitudes, which was observed in the experimental distributions. This deviation is principally due to the non-linearity in the damping, which is almost entirely quadratic in nature.

e) The theory can be used to predict first passage probabilities. Comparisons between theoretical estimates of $\hat{T}$ (the mean first passage time) and corresponding simulation estimates have shown that the theory gives conservative results, which can be useful for design and operational purposes.

f) By combining results from the theory with information on the long-term weather climate it has been possible to predict the long-term statistics of roll motion. A numerical example has demonstrated the feasibility of the proposed calculation method.

Acknowledgement

This work was supported by the Marine Directorate, Department of Transport, as part of the SAFESHIP project. This source of funding is gratefully acknowledged.

It is also a pleasure to acknowledge the contribution of Drs. Hogben and Dacunha to the work reported here on the long-term statistics of roll motion.

References

1. ROBERTS, J B. 'A Stochastic Theory for Non-linear Ship Rolling in Irregular Seas'. Journal of Ship Research, Vol. 26, No. 4, pp. 229-245, December 1982.

2. ROBERTS, J B. 'A Markov Energy Method for Non-linear Ship Rolling in Random Waves'. NMI (now British Maritime Technology) Report No. R173, March 1983.

3. ROBERTS, J B. 'Comparison between Simulation Results and Theoretical Predictions for a Ship Rolling in Random Beam Waves'. International Shipbuilding Progress, Vol. 31, pp. 168-180, July 1984.

4. ROBERTS, J B. 'Estimation of Non-Linear Ship Roll Damping from Free-Decay Data'. Journal of Ship Research, Vol. 29, No. 2, pp.127-138, June 1985.

5. ROBERTS, J B and DACUNHA, N M C. 'Roll Motion of a Ship in Random Beam Waves: Comparison between Theory and Experiment'. Journal of Ship Research, Vol. 29, No. 2, pp.112-126, June 1985.

6. ROBERTS, J B. 'First Passage Times for a Ship Rolling in Random Beam Waves'. NMI Report No. R172, 1983.

7. ROBERTS J B, DACUNHA N M C and HOGBEN N. 'The Estimation of Long Term Roll Response of a Ship at Sea'. NMI Report No. R169, 1983.

8. ROBERTS J B and STANDING R G. 'Final Summary Report on a Probabilistic Model of Ship Motions'. NMI Report No. R174, November 1983.

9. STANDING R G. 'Use of Wave Diffraction Theory with Morison's Equation to Compute Wave Loads and Motions of Offshore Structures', NMI Report No. R74, September 1979.

10. ROBERTS J B. 'First-Passage Probabilities for Randomly Excited Systems: Diffusion Methods', to be published in Probabilistic Engineering Mechanics, 1986.

11. ARNOLD L. 'Stochastic Differential Equations - Theory and Applications', J Wiley, New York, 1983.

12. ROBERTS J B. 'Response of an Oscillator with Non-Linear Damping and a Softening Spring to Non-White Random Excitation', Probabilistic Engineering Mechanics, Vol. 1, No. 1, pp.40-48, 1986.

13. OCHI M K. 'Wave Statistics for the Design of Ships and Ocean Structures', Trans. SNAME, Vol. 86, pp.47-76, 1978.

14. FANG Z S and HOGBEN N. 'Analysis of Long Term Joint Probability Distributions of Wave Heights and Periods', NMI Report No. R146, October 1982.

15. ANDREWS K S, DACUNHA N M C and HOGBEN, N. 'Wave Climate Synthesis', NMI Report No. R149, January 1983.

16. NORDENSTROM N, 'A Method to Predict Long-Term Distributions of Waves and Wave-Induced Motions and Loads on Ships and other Floating Structures', Det Norske Veritas, Report No. 81, April 1973.

17. SPOUGE J R, 'The Prediction of Realistic Long-Term Ship Seakeeping Performance', Trans. NECILS, Vol. 102, No. 1, pp.11-32, 1985.

FIGURE 1: Block diagram of mathematical model.

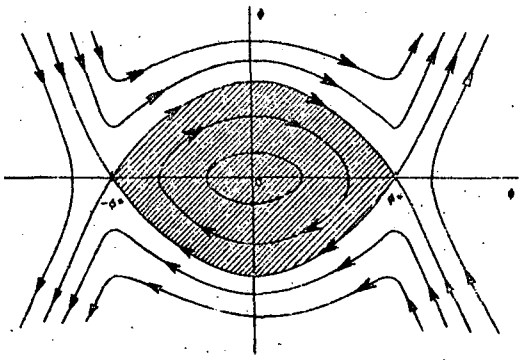

FIGURE 2: Phase-plane diagram.

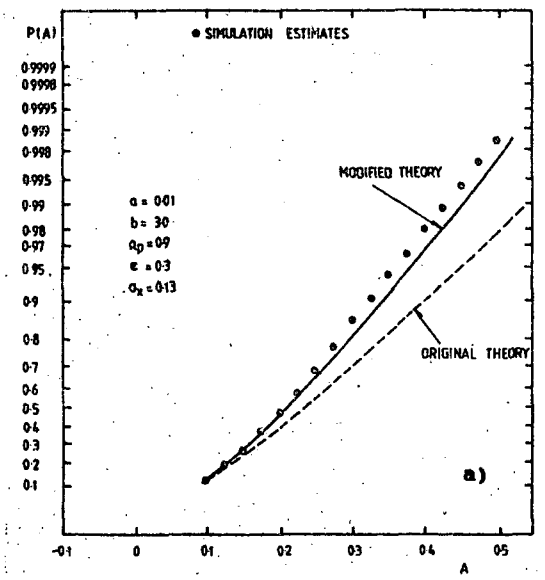

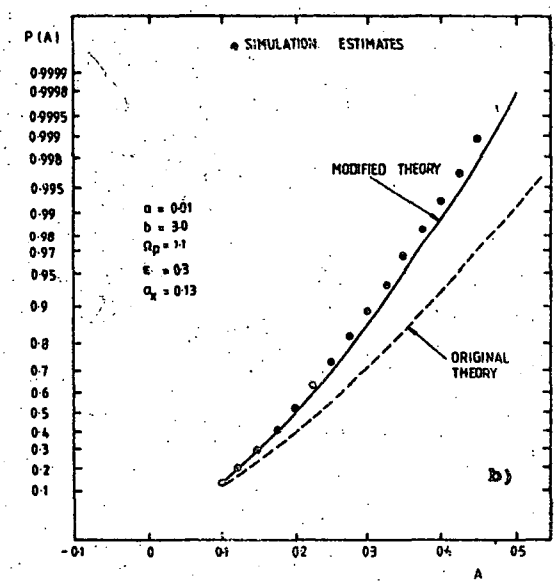

FIGURE 3: The cumulative probability distribution for A(t). Two comparisons between theory and simulation estimates.

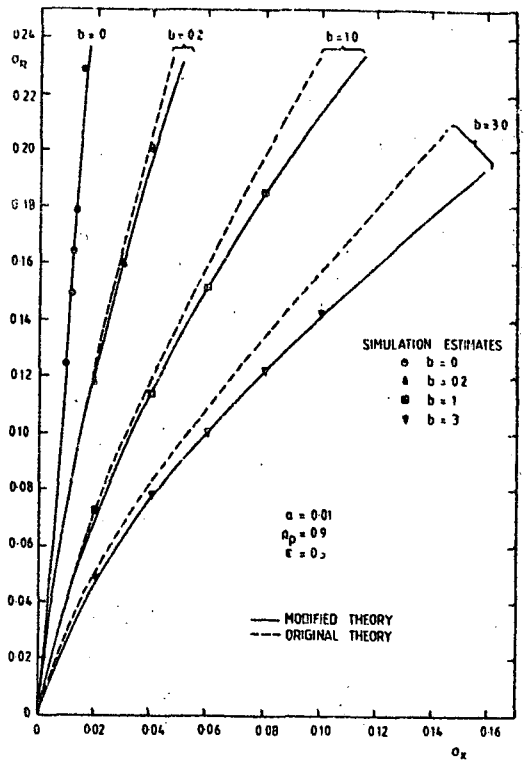

FIGURE 4: Variation of the roll standard deviation with the wave input standard deviation. Comparison between theory and simulation estimates.

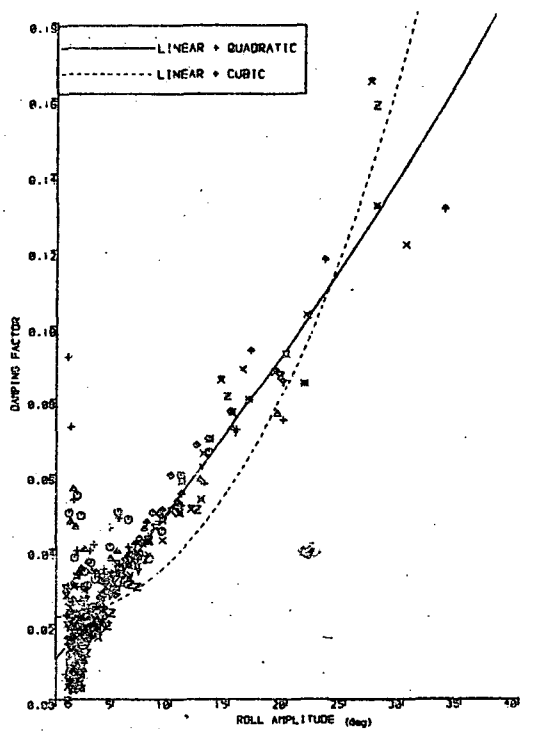

FIGURE 5: Variation of the damping function, $\zeta(V)$, with roll amplitude. Measured and fitted data.

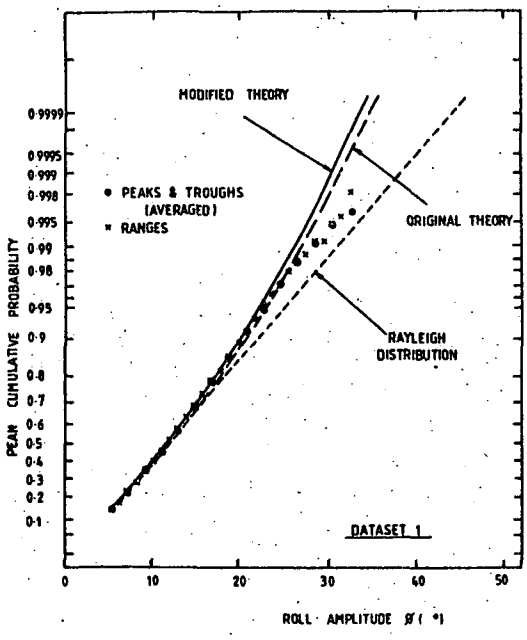

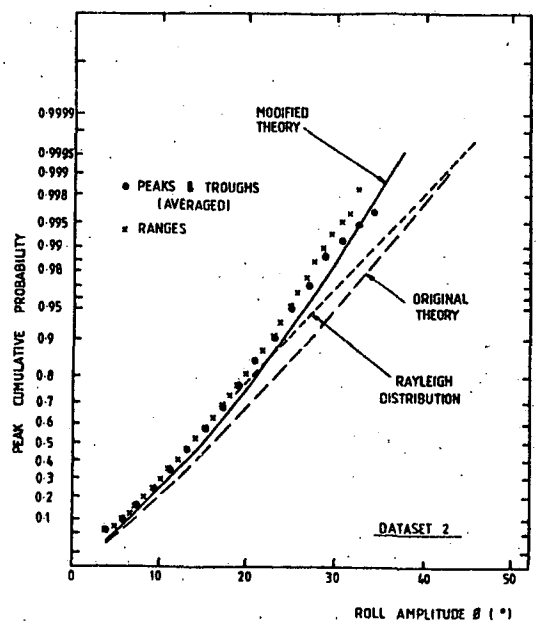

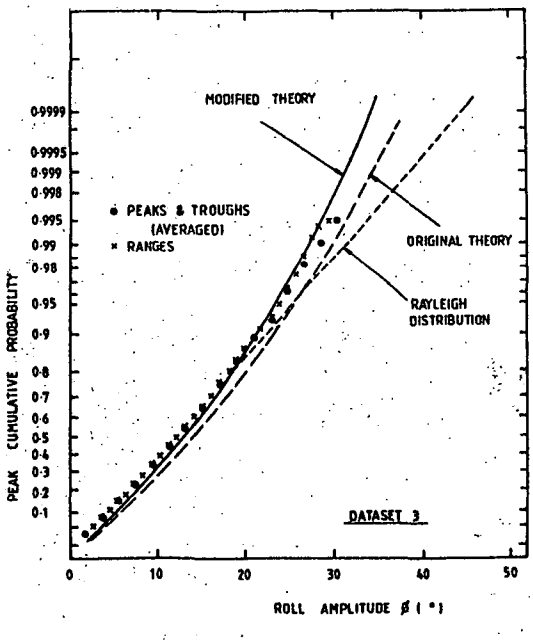

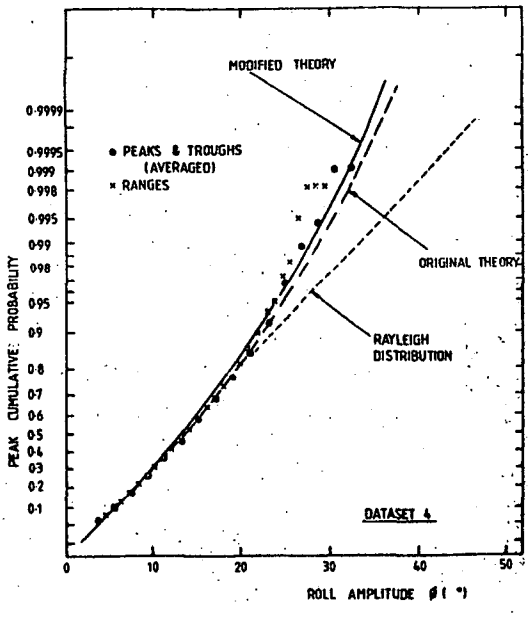

FIGURE 6: Roll peak cumulative probability. Comparison between theory and experiment for datasets 1 - 4.

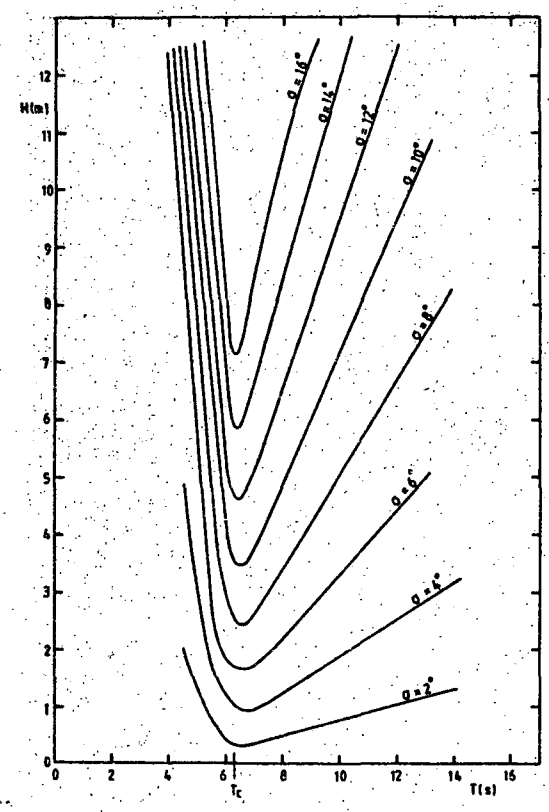

FIGURE 7: Contour plot of roll standard deviation σ in the (H,T) plane.

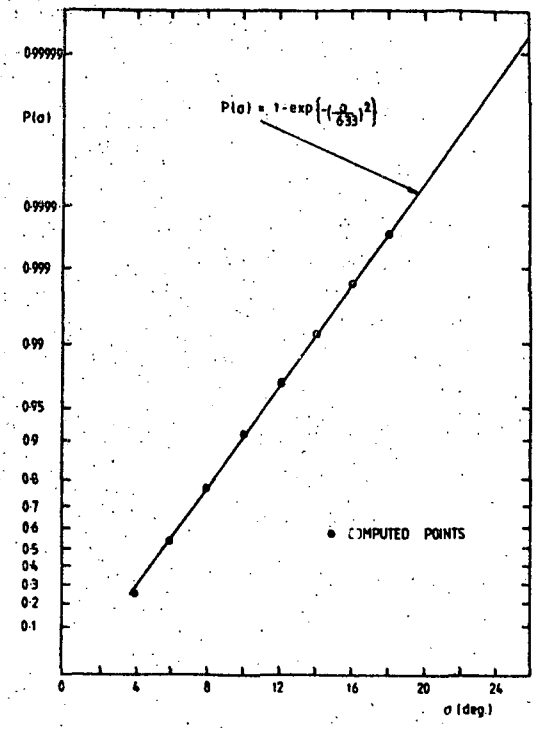

FIGURE 8: Long term probability distribution for σ.

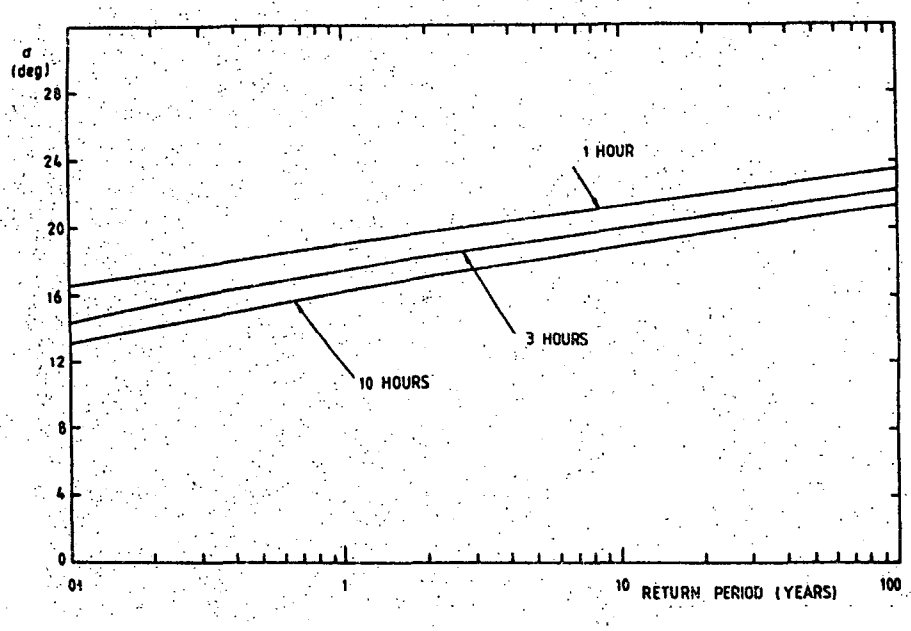

FIGURE 9: Variation of σ with return period, in years, for various single sea states.

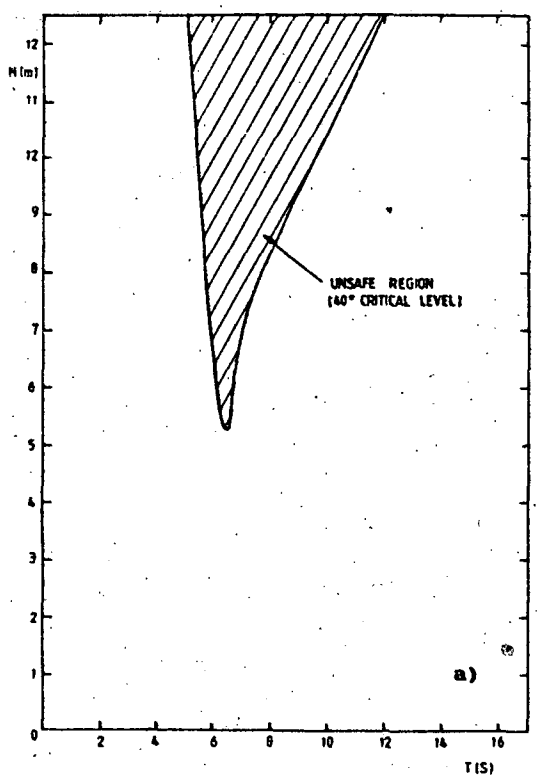

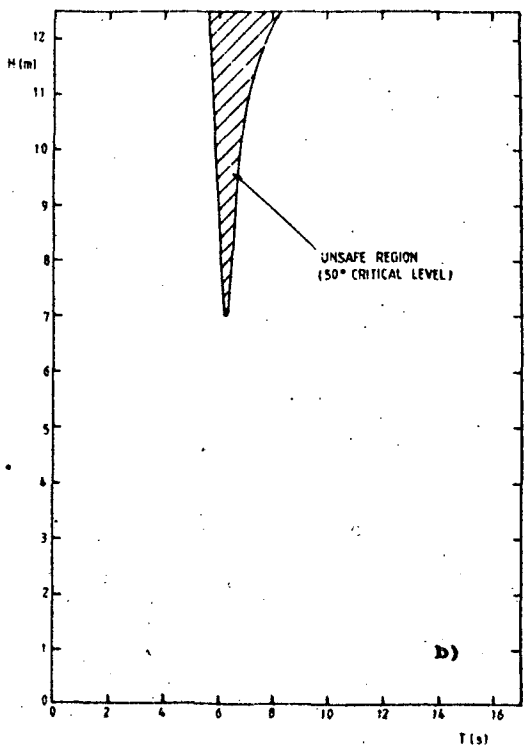

FIGURE 10: Unsafe regions in the (H,T) plane:

a) 40° critical level,
b) 50° critical level.

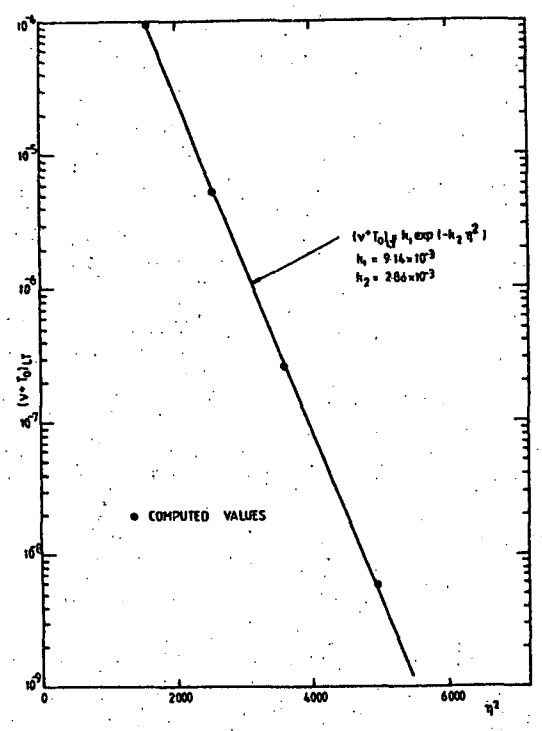

FIGURE 11: The variation of $(\nu^4 T_o)_{L/T}$ with η^2.

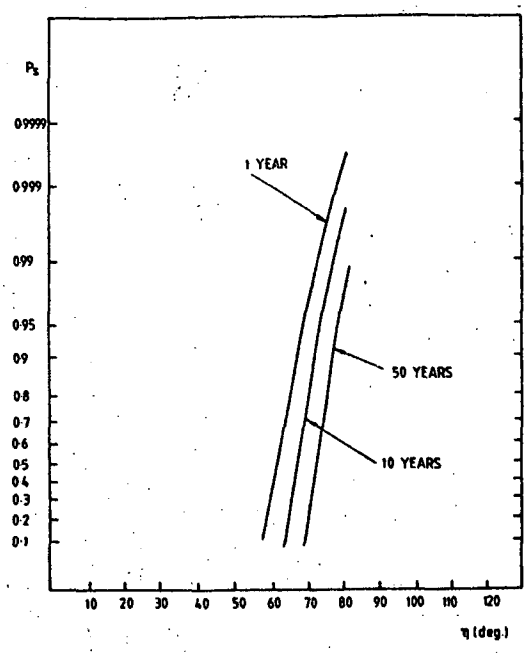

FIGURE 12: Variation of the probability of survival with critical amplitude level, for various long term periods.

Third International Conference on Stability of Ships and Ocean Vehicles, Gdańsk, Sept. 1986

STAB'86

PRINCIPAL AXES FOR DAMAGE STABILITY CALCULATIONS WITH UNSYMMETRICAL FLOODING

N. A. Hamlin

Abstract

Damage stability calculations sometimes ignore the angular rotation of the principal axes of the damaged waterplane which develops in the case of unsymmetrical flooding. The rotation of the axes and associated moments of inertia of the intact area after damage are given for several cases of unsymmetrical flooding on single hull and divided hull vessels. It is shown how ignoring the effect leads to large discrepancies on divided hull ships, and on single hull ships with low L/B and drastic unsymmetrical flooding, but little error on a typical single hull vessel with a lesser degree of unsymmetrical flooding.

Introduction

Damage stability calculations for single hull vessels customarily are made on the assumption that heel and trim after damage take place about axes parallel to the original longitudinal and transverse axes but shifted to pass through the center of flotation after damage. When the damage is symmetrical, the axes so shifted remain principal axes. Waterplane area moments of inertia are a maximum and minimum about these axes as are the corresponding metacentric radii $\overline{BM}_L$ and $\overline{BM}_T$; the corresponding metacentric heights $\overline{GM}_L$ and $\overline{GM}_T$ will also be maximum and minimum, respectively.

However, in the case of unsymmetrical flooding, the axes for maximum and minimum $\overline{BM}$ will no longer remain parallel to the original axes but will orient themselves at some angle β with respect to the direction of the original axes. Therefore, when calculations are made for heel and trim after unsymmetrical flooding, the corresponding moments of inertia of waterplane area, and inclinations, should be taken about the reoriented axes, which are the principal axes after damage. This paper addresses the degree to which neglect of the angular orientation of the damaged waterplane principal axes introduces error in damage stability calculations with unsymmetrical flooding.

Discussion

Hydrostatic ship characteristics are customarily computed using waterplane half breadths measured off and normal to the centerline of the vessel and a rule of integration, such as Simpson's first rule. Table I shows the additional columns and steps in such a calculation in order to find the product of inertia I_{xy} of the intact waterplane after damage about parallel axes through the center of flotation after damage. The calculation is shown for a passenger ship which has experienced drastic unsymmetrical flooding, that is, from the bow to amidships but only on the port side of a longitudinal centerline bulkhead, and assuming 100 percent permeability μ. The resulting angular rotation β of the principal axes is evaluated using the well known formula from mechanics

$$\tan 2\beta = 2 I_{xy}/(I_y - I_x)$$

where:

I_y is the longitudinal moment of inertia of the intact waterplane area after damage about a transverse axis normal to the centerline through the center of flotation after damage.

I_x is the transverse moment of inertia of the intact waterplane area after damage about a longitudinal axis parallel to the centerline through the center of flotation after damage. It is assumed $I_y > I_x$.

Figure 1 shows the orientation of the principal axes after damage for several vessels. The axes are turned through the angle β such that the longitudinal axis (x axis) moves away from the damage area and the transverse axis (y axis) moves closer to it. Call the new axes x_1 and y_1.

The minimum or maximum moments of inertia of the damaged waterplane area I_{x_1} and I_{y_1} may be evaluated by the following expressions:

$$I_{x_1} = I_x \cos^2 \beta + I_y \sin^2 \beta - I_{xy} \sin (2\beta)$$

$$I_{y_1} = I_x \sin^2 \beta + I_y \cos^2 \beta + I_{xy} \sin (2\beta)$$

As noted in texts on strength of materials, the variation of I_x and I_y with β can be represented by a Mohr's circle plot, as in Figure 2.

In order to demonstrate the effect of neglect of the change in orientation of the principal axes, several cases of drastic unsymmetrical flooding have been examined. In four of these cases, one quarter, or nearly so, of the originally undamaged waterplane area is assumed to have flooded (μ = 100 percent). The flooded area is all confined to one side of the centerline and one end of the vessel. The vessels assumed are summarized in Tables II and III and Figure 1. It should be noted, with regard to the first case for Vessel A, the nature of flooding would be unusual for a passenger vessel inasmuch as watertight longitudinal centerline bulkheads are seldom fitted, in order to avoid the heeling moment which results from flooding on one side only. Therefore, the first Vessel A case is one of extreme unfavorable flooding. The I_{xy} calculation for the first Vessel A case is that shown in Table I.

Table III summarizes the results of the calculations. Included are values of calculated moments of inertia of waterplane after damage using the two approaches, the angle β, and the ratio of moments of inertia.

Figure 3 plots the angle β and the ratio of minimum moments of inertia against overall length/breadth ratio. Also included in Table III and Figure 3 are values for Vessel A in which the flooding extends only from the bow to the forward quarter point, indicating rather small error for this case.

Table I

Calculation of Product of Inertia of Intact Area About Parallel Axes Through Damaged Center of Flotation for Vessel A

	Sta	y(m)	y^2	Lever	S.M.	Prod.
Bow	0	0	0	5	0.5	0
	0.5	1.25	1.55	4.5	2	13.95
	1	3.14	9.86	4	1	39.44
	1.5	5.36	28.72	3.5	2	201.03
	2	7.60	57.71	3	1.5	259.71
	3	10.96	120.03	2	4	960.27
	4	12.01	144.17	1	1.5	216.26
	4.5	12.04	144.94	0.5	1	72.47
Amids	5	12.04	144.94	0	0.5	0
						Σ = 1763.13

Damage I_{xy} about x, y axes through ℄ and Sta. 5

= (1/3) x (1/2) x S(-S) x Σ = (-1/6) x $(15.5)^2$ x 1763.13 = -70,600 m^4

Centroid of damage area = 29.8 m forward Sta. 5; 5.0 m to port of ℄

Centroid of intact area after damage = 13.0 m abaft Sta. 5; 1.30 m to stbd. of ℄

LCF of undamaged ship = 4.1 m abaft Sta. 5

Damage area = 556 m^2 Area of undamaged waterplane = 2,684 m^2

Then I_{xy} of intact area after damage about parallel axes through centroid of intact area after damage

$$= 2{,}684(-13.0 + 4.1)(1.30) - [-70{,}600 - 556.1(29.8)(-5.0) + 556.1(-29.8 - 13.0)(5.0 + 1.3)] = 106{,}640 \ m^4$$

Table II

Characteristics of Vessels

Vessel	A	B	C	D
Type	Passenger	Barge	Catamaran	Semi-submersible
Length, m	155	60	80	79.2
Breadth, m	24.08	20	28	48.8
Waterplane	Symmetrical	Rectangle	Asymmetrical	Four circles

Table III

Moments of Inertia of Waterplane After Damage

Vessel		A	A	B	C	D	D
Waterplane area before damage	m^2	2,684	2,684	1,200	652	1,051	1,051
Area of damage	m^2	556	171	300	169	263	526
Angular rotation of principal axes	β	2.7°	0.6°	7.6°	18.4°	16.8°	26.6°
I_y about parallel axis through c.f.	m^4	2.286	2.643	0.248	0.146	0.6671	0.4990
I_{y_1}	m^4	2.291	2.644	0.251	0.159	0.7163	0.6209
I_{y_1}/I_y		1.005	1.0001	1.016	1.088	1.074	1.244
I_x about parallel axis through c.f.	m^4	0.0656	0.1006	0.0275	0.0507	0.1791	0.1330
I_{x_1}	m^4	0.0619	0.1003	0.0235	0.0378	0.1299	0.0055
I_{x_1}/I_x		0.944	0.997	0.857	0.747	0.725	0.041

(Multiply I_x, I_y, I_{x_1} and I_{y_1} by 10^6)

As an extreme example of error which can be made by failing to account for the angular rotation of the principal axes, Figure 4 shows the same four column drilling platform as Vessel D. Column 3 has been flooded to offset the large inclining moment which would result from damage to column 1. Table III includes the moments of inertia about the principal axes after damage together with those disregarding the angular shift for this case. The great error which would result from the latter assumption is clearly evident.

Conclusions and Recommendations

As a result of the foregoing, the following recommendations appear justified:

Damage stability criteria for divided hull vessels, or vessels with unusually low L/B, should require that $\overline{GM}$ after damage be based upon moments of inertia computed about the principal axes of the damaged waterplane, rather than about axes parallel and normal to the vessel's centerline, when extensive unsymmetrical flooding occurs.

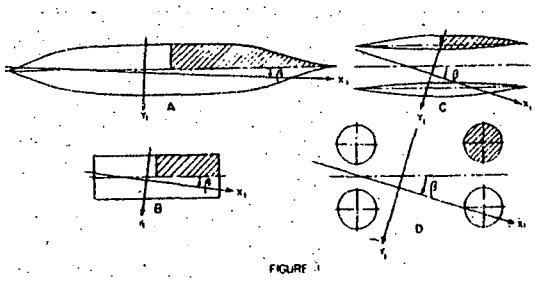

FIGURE 1

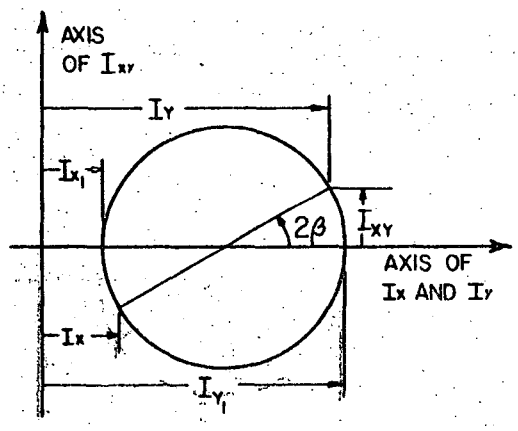

FIGURE 2

Damage stability criteria for divided hull vessels, or vessels with unusually low L/B, which specify a particular minimum freeboard and/or angle of heel after damage, should require, in the case of extensive unsymmetrical flooding, that these quantities be computed as a result of inclinations about the principal axes of the damaged waterplane.

N. A. Hamlin
Professor of Naval Architecture
Webb Institute of Naval Architecture
Crescent Beach Road
Glen Cove, New York 11542
USA

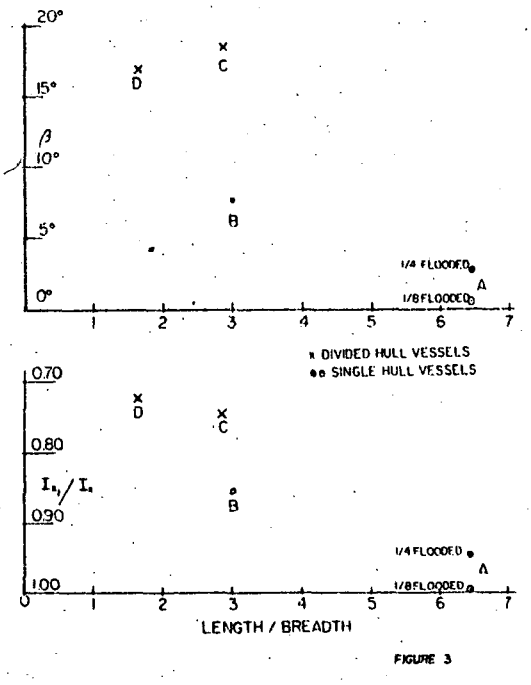

FIGURE 3

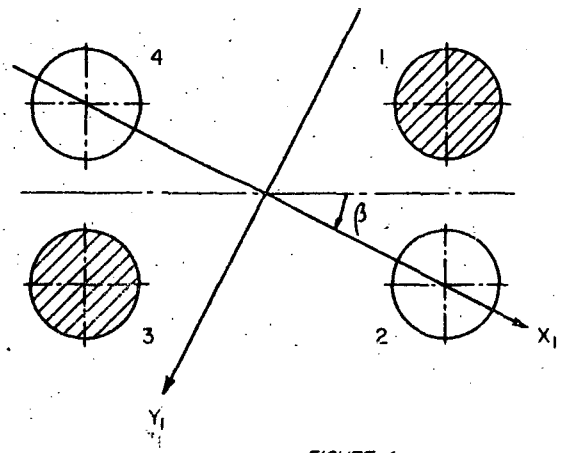

FIGURE 4

Third International Conference on Stability of Ships and Ocean Vehicles, Gdańsk, Sept. 1986

STAB'86

SOME ASPECTS OF SEAKEEPING FOR SMALL SHIPS

Kholodilin A.N., Trounin V.K., Oushakov B.N.

Abstract

In evaluating the safety of ship navigation it is adopted as a critical situation that a ship with zero speed expects rolling with her side turned to the incident wave system. However under the wind and wave action a ship is subjected to a drift which causes a variation in ship-wave frequency of encounter. In such a case the roll "transfer function" calculations demand the use of a frequency of encounter which is less than the true spectrum frequency. This phenomenon leads to displacing the maximum lever of the "transfer function" in the direction of high frequencies and results in an increase of the amplitudes of rolling in calmer seas. The paper presents roll calculations and dynamic stability estimates for small vessels in shallow water which illustrate the above-mentioned fact.

Evaluating the safety and seaworthness of a ship in a seaway it is adopted from a point of view of stability that the most dangerous situation expects a ship with zero forward speed rolling in beam seas. To calculate statistical and spectral characteristics of rolling a definite information is required about wave pattern and some properties of the ship as a dynamic system. The spectral method of analysis is based on the use of linear model of rolling, though it is well known that when ship oscillations are intense the damping moment and the restoring moment become nonlinear functions of velocity and angle of rolling. This phenomenon had necessitated the development of methods considering nonlinearities such as statistical linearization /1/ or Markov process technique /2/. The use of these methods requires the knowledge of the diagram of static stability of the ship and her hydrodynamic characteristics: the added inertia moment and the damping coefficient. While the stability diagramm can be calculated efficiently by well known method of statics, the question of reliable evalution of hydrodynamic characteristics of rolling sofar stands open.

The damping of rolling being on the whole of viscous nature, the common way of obtaining reliable results is the model experiment. Mostly it is carried out by means of the free-decay method as a simple one and convenient for performance and treating the experimental data. Such a method can be rather effective not only in model tests, but also when applied in full-scale with the aim of avoiding the scale effect. It is known that variations of damping change considerably the "transfer function" only near the resonance peak where amplitudes of rolling are large and the degree of damping is in a good agreement with quadratic law /4/. There is a lot of formulars evaluating quadratic damping coefficient from a free-decay data. They express it by means of the amplitude radio $t_i = \theta_{i+1}/\theta_i$ measured over half period of rolling. According to /3/ Fig.1 illustrates calculations performed by different authers' expressions. The actual function is formed from the solution of the equation

$$1-2W\theta_i t_i = (1+2W\theta_i)e^{-2W\theta_i(1+t_i)} \qquad (1)$$

Fig.1 shows that with the increase of damping when $t_i < 0{,}6$ the choice of investigation will alter significantly the corresponding results. Such a case may occure for ships with bildge keels, technical means and offshore structures. The minimum error gives the use of the expression obtained in /4/

$$W\theta_i = \frac{3}{2}\,\frac{1-t_i}{1+t_i}\,\frac{1}{\sqrt{t_i}} \qquad (2)$$

The influence of the sea depth is important in evaluating of rolling of small ships. The shallow water effects both the hydrodynamic characteristics of oscillations and the characteristics of incident waves. The results of model experiments carried out in the basin of Leningrad Shipbuilding Institute show that the increase of damping way be expressed appoximatly as follows /5/

$$\frac{W(H)}{W(\infty)} = 1+0{,}1\left(\frac{T}{H}\right)+0{,}4\left(\frac{T}{H}\right)^2 \qquad (3)$$

where T represents the mean draught; H - the depth of the sea. Transformation of the wave spectral characteristics in shallow water may be obtained with the help of the function recommended by J.M. Krylov in the form /5/

$$\begin{cases} S_\zeta(\omega) = K_n^2 S_{\zeta_0}(\omega) \\ S_\alpha(\omega) = \frac{K_n^2 \omega^4}{C^{*2} g^2} S_{\zeta_0}(\omega) \end{cases} \quad (4)$$

where

$$K_n^2 = \frac{\cos\varphi}{\sqrt{1 - C^{*2}\sin\varphi}} \left[C^* + \frac{2H\omega^2}{g} \frac{1}{\sinh\left(\frac{2H\omega^2}{C^* g}\right)} \right] \quad (5)$$

Here g represents the acceleration of gravity; ω - the spectral frequency; S_{ζ_0} - the spectral density of wave elevation in the case of infinite depth; S_ζ, S_α - spectral densities of wave elevation and wave slope in shallow water; φ - the mean angle between the direction of wave propagation and the line of constant depth; C^* - wave length ratio, obtained from the equation

$$C^* = \tanh\left(\frac{H\omega^2}{g} \frac{1}{C^*}\right) \quad (6)$$

The expressions (4)-(6) can be used for the depths H greater than the depth H_{BR} where incident waves are breaking. An approximate method for evaluating H_{BR} has been developed in /6/. Being applied to the standard spectrum /1/ together with the assumption that the mean wave frequency $\bar{\omega}$ is related to the wave height of 3% probability $h_{3\%}$ as

$$\bar{\omega} \simeq \frac{2}{\sqrt{h_{3\%}}} \quad (7)$$

for the case $\varphi = 0$ it gives

$$H_{BR} \simeq 0{,}86 h_{3\%} \quad (8)$$

This material had been the base for the algorithm and computer program of calculation of ship rolling and dynamic stability in shallow water /5/, /7/. Fig.2 illustrates an example of estimated data for a 5100 tonn ship, which shows that the influence of the sea bottom is significant when $H/T < 4$.

In treating ship safety a special attention should be paid to the choice of the critical situation. The initial information for the spectral analysis of rolling in random seas is the wave height $h_{3\%}$ and the mean wave frequency $\bar{\omega}$. A ship with zero speed expects rolling with here side turned to the general direction of wave propagation. From all types of wave motions one considers in shipbuilding only wind waves and swell waves. The periods of other waves being much greater than the natural periods of rolling the ships practically don't respond to them /8/. In random seas of definite force wave heigh and frequency vary with the degree of wave development. Approximation of oceanographic data (see /1/, /5/, /9/) gives the folliwing interval for the mean wave frequencies

$$\frac{1{,}6}{\sqrt{h_{3\%}}} < \bar{\omega} < \frac{2{,}5}{\sqrt{h_{3\%}}} \quad (9)$$

where the smaller values correspond to developing seas and the larger ones - for fading seas. In this connection the choice of the mean frequency the one according to (7) doesn't answer to the most dangerous conditions of seakeeping in definite sea force.

Moreover under the influence of wind and waves the ship expects transverse drift. The calculation of the "transfer function" of rolling in such a case needs the substitution of the spectral frequency by the frequency of encounter. Treating the drift of ships in beam seas the latter is less than the true spectral frequency:

$$\omega_e = \omega - \frac{v}{g}\omega^2 \quad (10)$$

where v represents the drift velocity. This phenomenon leads to displacing the maximum lever of the "transfer function" in the direction of high frequencies and results in an increase of the amplitudes of rolling in calmer seas.

Therefore in our view when choosing the mean wave characteristics it seems sensible to adopt as a guiding principle the closeness between the natural frequency of rolling n_θ and the frequency of encounter corresponding to the frequency of the maximum of the spectral density ω_{me}, that is

$$\omega_{me} = \begin{cases} \omega_{me}^{min}, & \text{when } n_\theta < \omega_{me}^{min} \\ n_\theta, & \text{when } \omega_{me}^{min} < n_\theta < \omega_{me}^{max} \\ \omega_{me}^{max}, & \text{when } n_\theta > \omega_{me}^{max} \end{cases} \quad (11)$$

For the spectrum adopted in the USSR /1/, /5/ the mean wave frequency is connected with the frequency of maximum spectral density as

$$\omega_m = 0{,}777\bar{\omega} \quad (12)$$

Thus the recommended way of determination of wave characteristics may be formulated as follows.

1. For the relevant wave force one chooses the maximum wave height with 3% probability (see i.g. /1/, /5/, /9/).

2. The minimum and maximum mean wave frequencies are calculated according to (9).

3. The corresponding frequencies of maximum spectral density are calculated from (12).

4. The frequencies ω_{me}^{min} and ω_{me}^{max} are calculated according to (10).

5. Comparing these values with the natural frequency n_θ according to (11) one accepts the frequency of encounter ω_{me}.

6. The frequency of maximum spectral density is calculated with the help of the following expression

$$\omega_m = \frac{g}{2v}\left(1 - \sqrt{1 - \frac{4v}{g}\omega_{me}}\right) \quad (13)$$

7. Finally the mean wave frequency is calculated from (12).

Fig.3 illustrates the results of calculations made for a small 45,8-tonn seiner. The amplitude of rolling of the ship drifting with velocity v devided by the amplitude of rolling without drift is plotted against the Froude number $F_{r_B} = v/\sqrt{gB}$, where B represents the ship's breadth.

The most difficult moment in the proposed method is a rational estimation of the drift velocity. While there are some recommendations concerning wind drift (see i.g. /5/), the question of drift among waves still stands open. The existing data /10/ are applied to the forces which cause the drift but their application to calculations of drift velocities is impeded with the character of damping of a rather complicated motion including transverse drift with constant speed and swaying of the ship. For approximate estimation a method may be recommended based on experimental evaluation of the drift velocity, performed with a free rolling model. The mean drift velcity is measured near the roll resonance where drift forces and velocities have maximum value (Fig.4). The rolling of a ship in random seas occuring with a frequency which is close to the natural one, it is possible to use the Tailor expansion and limit oneselt with its' first term.

For the last 20 years Leningrad Shipbuilding Institute carries out investigations on small ship stability. The first publication was made in the Proceedings of the 12th ITTC in 1969 /11/, when in the model basin of the Institute the first experiments of rolling in erupting waves had been performed. Lately attention was paid to the influence of drift on ships' stability. The scheme proposed in the present paper, in the authors' view, will enable engineers to evaluate the stability of ships in a seaway more accuratly.

RAFERENCES

1. KHOLODILIN A.N., SHMYREV A.N. "Seakeeping and stabilization of ships in waves". Leningrad, "Sudostroenie", 1976 (in Russian).
2. NEKRASOV V.A. "Probability tasks of seakeeping". Leningrad, "Sudostroenie", 1978 (in Russian).
3. ZINKOVSKY-GORBATENKO V.G. "Accurate estimation of inertia moment and damping parameters for two-term damping law". Hydrodynamics, v.28, Kiev, "Naukova Dumka", 1974 (in Russian).
4. LOUGOVSKY V.V., VOITKOUNSKAYA A.Y., TROUNIN V.K. "Nomograms for hydrodynamic characteristics of rolling". "Sudostroenie", N 11, 1983 (in Russian).
5. BIAGOVESHENSKY S.N., KHOLODILIN A.N. "Rolling of a ship in waves". Leningrad Shipbuilding Inst., 1983 (in Russian).
6. GORAVNEVA T.S., MIROKHIN B.V. "Estimation of the depth of wave-breaking under the influence of shellow water". Leningrad Shipbuilding Inst. Trans., v.114, 1976 (in Russian).
7. MIROKHIN B.V., TROUNIN V.K. "Computer calculations of ship rolling in shellow water", Reports of the Conference "Krylovskie chtenia". Leningrad, "Sudostroenie", 1977 (in Russian).
8. LOUGOVSKY V.V. "Sea dynamics". Leningrad, "Sudostroenie", 1976 (in Russian).
9. Ship Theory Handbook. Ed.by. Y.I.VOITKOUNSKY. Leningrad, "Sudostroenie", 1985 (in Russian).
10. TROUNIN B.K. "Estimation of the exciting forces and the drift forces". Trans. of the Krylov Science Society v.378. Leningrad, "Sudostroenie", 1983 (in Russian).
11. KHOLODILIN A.N, TOVSTIKH E.V. "The Model experiment for the stability of small ships on ernpting waves". 12ITTC, Proc., Rome, 1969.

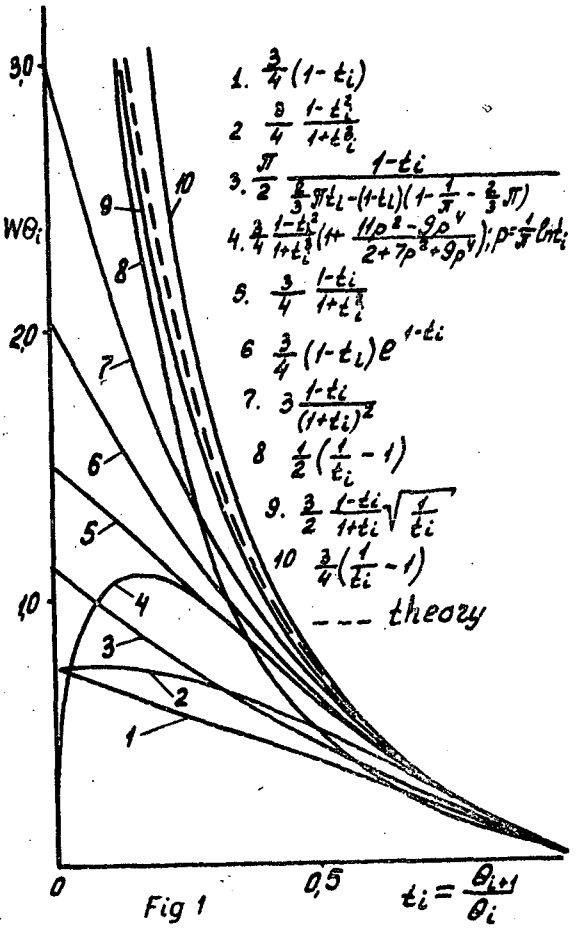

Fig 1

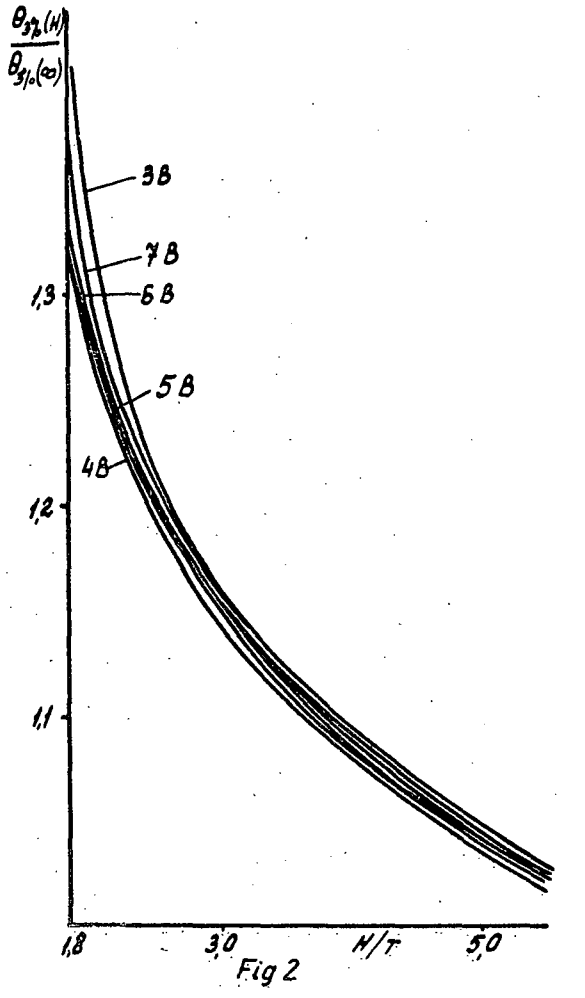

Fig 2

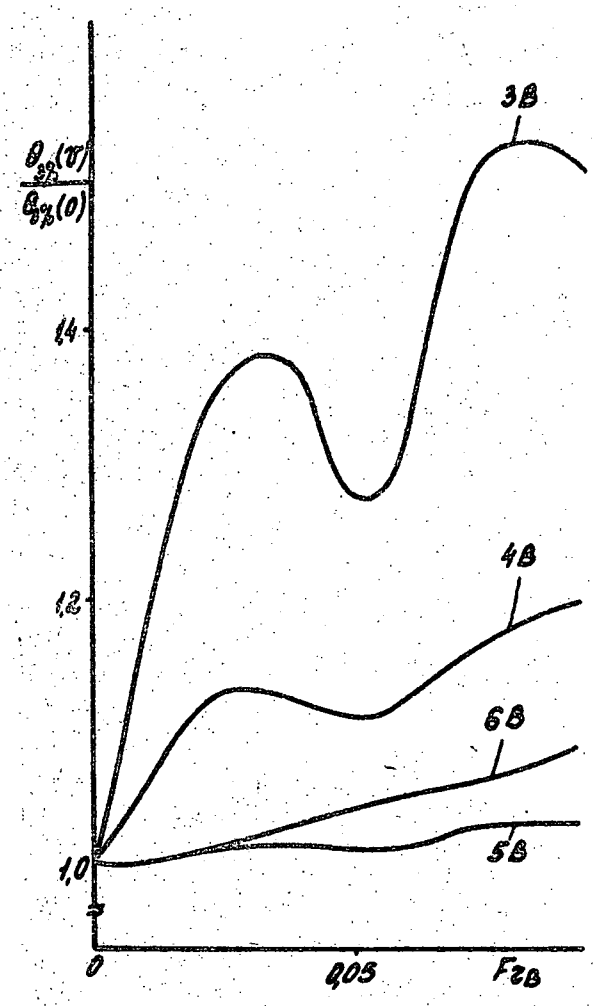
3B
4B
6B
5B
1,4
1,2
1,0
0
0,05
Fz_B

Fig 3

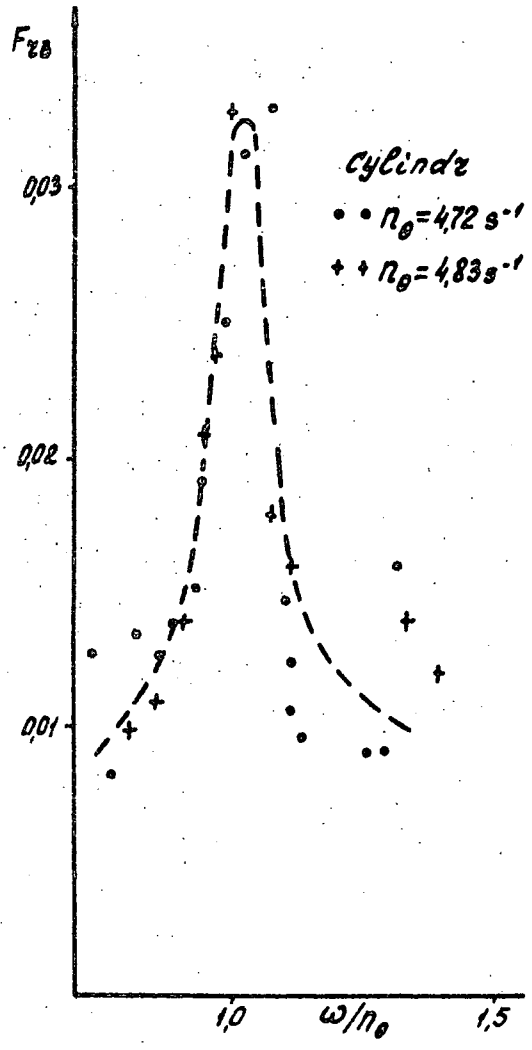
Fz_B
0,03
0,02
0,01
cylindr
n_0 = 4,72 s^-1
n_0 = 4,83 s^-1
1,0
ω/n_0
1,5

Fig 4

Third International Conference on Stability of Ships and Ocean Vehicles, Gdańsk, Sept. 1986

STAB'86

THE HUMAN FACTOR EFFECT ON THE SAFETY OF SHIP STABILITY AT SEA

M. Gerigk

ABSTRACT

This paper presents general information on the human factor effect on the safety of navigation.

The safety of ship's stability is described by means of statistical data.
The paper also presents conclusions which follows from the analysis of the cybernetical system Man-Ship-Environment.
For this purpose the elements of theory of systems have been used. A man is described here as an open system of steering. The rules for modelling of the system man-ship have been presented, which are important for the safety of ship stability. Finally the conclusions relative to this safety have been presented applying theory of games and theory of statistical decisions.

1. INTRODUCTION

All technical systems which are operated by man are the man-systems. An example of such a system is the man-ship system.

An activity of the man-ship system is accurately connected with the navigation as a part of the organized reality /see fig. 1./. Navigation is connected with the following categories of problems: political, economical, operational, technological and human. In consideration of the safety of navigation the human problem is one of the most important.
In navigation the human factor effect is connected with [10] :

1. man power /recruiting, teaching, training/.
2. career /qualifications, motivations, experience/.
3. life at sea /adaptation, assimilation/.

The scientific survey confirms that for the safety of navigation the human factor effect and the technical factor are equally important. Statistic data confirm the above as well.
The basis for the study of the influence of the human factor upon the safety of navigation is the theory of systems viewed as an interdisciplinary branch of science. In order to analyse the already existing systems such as man-ship system the most useful are: theory of operation, theory of probability, theory of games, methods of number simulation and theory of making decisions.
Danger threatening the man-ship system can take the shape of [3] :

1. self-destruction of the system,
2. destruction of the coexisting systems,
3. destruction of the environment of the ship.

It is often connected with health damage or loss of life. Navigation safety can be improved by means of application of special technological appliances /an accelerometer or other measuring apparatus/, the auxiliary appliances /auto pilot, radar/, antycollision systems whose work is inseparably connected with man's activity, man being a decisive factor of the ship safety.

2. STATISTICAL DATA

The total number of ships exceeding 100 DWT in the world fleet according to Lloyd Register of Shipping was 76 106 units for the year 1983 [11] .
In the years 1970÷1983 the world's fleet was suffering the loss of 300÷400 ships every year. The consequences of some of the casualties were frightening. We can mention here the cases of the Polish sis-

ter ships the "Kudowa Zdrój" and "Busko Zdrój".

The most important reasons of the majority of the casualties according to L.R.in 1983 are as follows:

1. weather conditions	13,69%
2. fires	34,94%
3. collisions	2,85%
4. overloads	0,49%
5. squats	24,02%
6. missings	1,22%
7. damages of construction	22,79%

In all those reasons we can trace the human factor, although there are certain difficulties in evaluating and defining its range. The results of the researches done by the US Coast Guard [12] have shown that a man is the most important and decisive factor for the safety of ship stability. The human effect upon the ship stability was manifested by the ignorance of information referring to the ship stability, the lack of general marine knowledge, wrong manoeuvring during the unfavourable weather.

The greatest number of casualties has been registered in case of small vessels /300 ÷ 400/ DWT - about 10% of the total number of stability casualties.

Similar survey led by the Ship Hydrodynamics Laboratory in Helsinki and by Lloyd Register [8] showed that stability casualties resulted primarily from the wrong operation by man. The majority of those casualties took place at night between midnight and 8 o'clock in the morning and in the evening, between 4 o'clock and midnight. This followed not only from the difficulties of identifying the situation but also from the predisposition of the crew /stress, tiredness, drowsiness/. It also appeared that the worst were the beginning and the end of the week, as it happens with the road traffic.

Despite the extensive statistical information published in various periodicals their reliability is doubtfull. It results from the fact that the reports are usually made on the basis of the so called casualty information charts. Taking the human nature into consideration the information about the human factor participating in the casualty is usually doubtfull, where as the information about the casualty with no witness alive are only hypothetical.

3. MODELS OF THE SYSTEM MAN-SHIP

A. CYBERNETICAL MODEL.

From the analysis of the reality it results the fact that man-ship system is a cybernetical system of operating /see fig. 1./.

System $\underline{def}$ set of elements of organized reality remaining in the interrelations [2] .

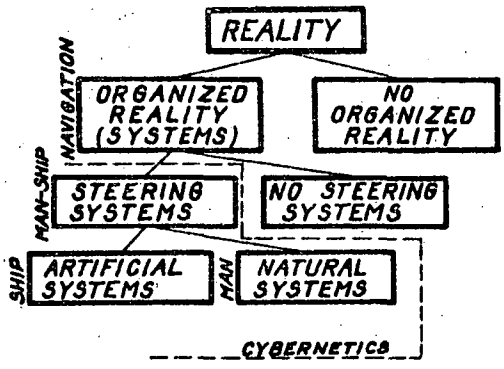

Fig. 1. Division of reality.

The cybernetical man-ship system is characteristic for its exchange of information between its elements, which should result in coordination of those elements.

The basic factors of the steering process are information and feedback, which assure the control of the elements within the man-ship system.

B. MATHEMATICAL MODEL.

Generally, the system can be described with the set of simultaneous differential equations [2] :

$$\begin{cases} \frac{dA_1}{dt} = f_1(A_1, A_2, \ldots, A_n) \\ \frac{dA_n}{dt} = f_n(A_1, A_2, \ldots, A_n) \end{cases} \quad (1)$$

where: A_i - element measures of the system

f_i - interrelations of the system.

The set of equations (1) works well with the analysis of the general properties of the system without the information referring to A_i and f_i . After rearrangement and development of the set of equations we obtain the following solution:

$$\frac{A_1 = C_{11}e^{\lambda_1 t} + C_{12}e^{\lambda_2 t} + \ldots + C_{111}e^{2\lambda_1 t} + \ldots}{A_n = C_{n1}e^{\lambda_1 t} + C_{n2}e^{\lambda_2 t} + \ldots + C_{n11}e^{2\lambda_1 t} + \ldots} \quad (2)$$

where: C_i - constant,

λ_i - roots of the characteristic equation:

$$\begin{vmatrix} a_{11}-\lambda & a_{12} & \cdots & a_{1n} \\ a_{n1} & \cdots & \cdots & a_{nn}-\lambda \end{vmatrix} = 0 \quad (3)$$

Stability of the system can be easily defined depending on the value of λ . The analysis of the set of equations (1) enables introducing of the following terms:

1. integrity of the system - alteration of an arbitrary element of the system yields the alterations of the remaining elements,
2. additivity of the system - alteration of the whole system is a sum of alterations of particular elements,
3. progressive segregation of the system - interaction between the elements of the system decreases within the time passing,
4. progressive mechanization of the system - loss of control abilities of the system results from its mechanization and automation,
5. progressive centralization of the system - minor alteration of one of the elements brings about the significant alteration within the whole system.

Man-ship system is of an nonadditive character in general. Its functioning is connected with the growth of complexity resulting from the progressive segregation and progressive mechanization. It can result in the loss of control abilities by the man-ship system in difficult situations.

4. MODEL OF MAN

From the classification of the systems into open and closed ones we can draw the conclusion that a man is an open system.

An open system $\underline{\text{def}}$ the system which continually exchanges the material with its environment [2] .

Man is characterised by his ability to perform a work depending on achieving stability in definite conditions. What is more, the characteristic features of a man are:

time of reaction, shooting above the crossbar and false starts /see fig. 2./.

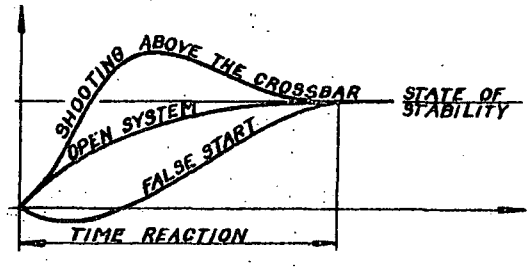

Fig. 2. Characteristic features of a man.

The basic feature of the human body is dynamical internal interaction consisting of the growth of internal order and decrease of entropy [2] . Man's control abilities depend on conditions dominating the whole system. Gradual mechanization of a man within the passing time brings about the situation in which man's control abilities are of the feedback character typical of the closed system. In feedback the quantity of information does not grow in number but it often changes into noise.

The correctness of decissions undertaken by man being the open system depends on form, kind and content of information which he acquires. The model of a man viewed as a closed system has many drawbacks in comparison with the model of a man viewed as an open system. The model of a man viewed as an open system is more correct as it takes into account the psychophysiological aspect of an organism, man's creativity and personality.

5. METHODS OF MODELLING AND INVESTIGATIONS

The most commonly applied methods of evaluating the influence of the human factor upon the navigation safety are [4] :

1. computer simulation tests,
2. investigations in full scale.

On modern ships a man takes the role of a controller-observer.

Fullfilling the variety of functions by

man on a ship is connected with receiving, transforming, sending and utilizing information. Man's behaviour during accomplishing the task is dependent, among others, on his ability, knowledge, experience and laws of physics governing, conditions of a ship movement and the forms of presentation of the information concerning the movement of the ship. The best method for determining the influence of the human factor upon the navigation safety is the real-time simulation on board with the help of a bridge simulator with two peripheral devices. Such a simulator enables improving the navigation safety due to simultaneous observation of the actual situation on the sea, training and projection of the original information in a form of an image, numerical data, decision etc. Knowing the mathematical model of a man it is possible to make the analysis of the safety of man-ship system by means of computer simulation according to the scheme shown in fig. 3. [7] .

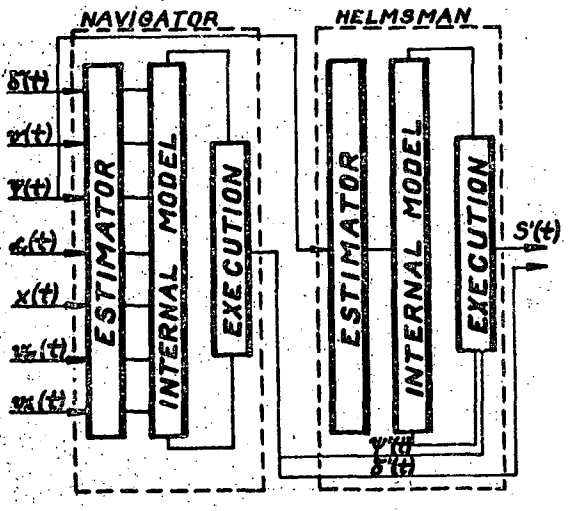

Fig. 3. Model of the navigator and helmsman.

6. RESULTS OF COMPUTATION

In the study [5] the analysis of the effectiveness and calculation of reliability of the navigation safety system has been made. There have been considered two different models of bridge navigation safety systems /see fig. 4./.
The calculations take into account the random character of faults made by man and the random character of faults made by the technical subsystems of a ship.

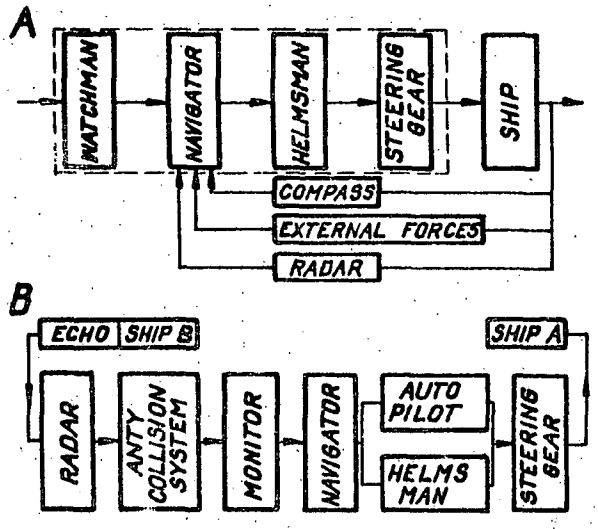

Fig. 4. Models of the ship safety system.

Conclusions resulting from the calculations are as follows:

1. reliability of both systems /A and B/ decreases with the time passing,
2. necessity of constant and progressive observations of a ship environment,
3. system A does not meet the requirements of safe operating man-ship system due to its minor reliability /after two hours of work the reliability goes down below 0,5/,
4. there exists the necessity of reducing the human factor effect in the ship operation process,
5. ship safety can be increased by automation of the navigation process where man's role would be that of the control element.

7. HUMAN FACTOR EFFECT ON STABILITY OF SHIP

Taking into consideration the information received from the outside the man-ship system is the match play system [13] . Man's influence upon the ship stability can be studied with the application of the theory of games. Roughly speaking, the game is governed by the rule that two players A and B perform the activities simultaneously. In case partner B is not in-

terested in the results of the game the role of a partner for the second player A is taken over by circumstances /in our case it is the state of the sea/.
In the above case the matrix of profits is:

B(circumstances)

A(man)	calm sea	rough sea
completing the task	a_{11}	a_{12}
not completing the task	$-a_{21}$	$-a_{22}$

(4)

where: a_{11}, a_{12}, $-a_{21}$, $-a_{22}$ - profits.

When a man performs a task and sea is calm the probability of the stability accident is a_{11}. The greatest possibility of this accident /$-a_{22}$/ occurs in case man does not complete the task and sea is rough. Man often undertakes the risk in the situation when he has not completed the task, aiming at the same time at reducing the expected value /the least probability of the stability accident/.
A pesimist will always perform the task while an optimist will rather wait for more favourable situation. Although, the later would probably decide quickly to complete the task if he knew the probability of the stability accident at that moment was e.g. 0,9.

Game between a man and circumstances can result in zero sum or non zero sum [6]. The basic criterion in games with zero sum result is the MINIMAX criterion [1] [9]. We can call it here the criterion of the smallest risk of the stability accident. MINIMAX respects to the saddle point on the surface $Z=f(x,y)$ which is the distribution of scores between the players A and B.
The profit of player A, accoording to the matrix (4) equals:

$$Z=x[ya_{11}+(1-y)a_{12}]+(1-x)[y(-a_{21})+(1-y)(-a_{22})] \quad (5)$$

where: $(x,1-x)$ - strategy of man A,
$(y,1-y)$ - strategy of circumstances B.

It is assumed that the strategy of circumstances for a given water regions are known.
Since the circumstances B are not interested in the result of the game the expected value equals zero $[E(Z)=0]$. Man's influence upon the value Z depends on his strategy $(x,1-x)$. When man employs strategy $(1,0)$ he decides to undertake the task and employs strategy $(0,1)$ he decides not to undertake the task.
Both strategies $(1,0)$ and $(0,1)$ are called clear.
If man A is not selfconfident he may change his strategy to prevent from the influence of the environment. The best strategy man A can employ in the game against the circumstances B is $(\frac{1}{2}, \frac{1}{2})$ for which $E(Z)=0$. Games with non zero sum are associated with the prisoner's dilemma. The prisoner's dilemma lies in reduction of risk of the stability accident by man. And if he knows that man B has not accomplished the task the matrix of profits is [9]:

	B_1	B_2
A_1	a_1, a_1	a_2, a_3
A_2	a_3, a_2	a_4, a_4

where: $2a_1>a_2+a_3>2a_4$, $a_3>a_1$, $a_3>a_2$, $a_4>a_2$.

The dilemma of both players lies in the question whether to accomplish the task what would influence directly the effects. The analysis of the prisoner's dilemma within the problems referring to the stability accident enables the formulation of the following conclusions:

1. cooperation of men is the most constructive in case the stability accident is certain,
2. man is indifferent to the safety of a ship when according to his opinion the probability of the stability accident is small,
3. the most desired strategy on the part of a man is the clear strategy (1,0),
4. the cause of man's lack of selfconfidence in the conflict situations is the lack of knowledge about the matrix of profits.

8. CONCLUSIONS

Despite growing process of automation in ship navigation man still remains a decisive factor for the ship safety at sea. Present research has shown that a man is the most important element of the ship safety system. The loss of control over a ship in a critical situation is the main

cause of casualties.

The aim of further research on the human factor effect upon the ship safety is working out a method of identification of the dynamics of man-ship system .

REFERENCES

[1] J.O. Berger - Statical Decision Theory. New York, 1980;

[2] L.V. Bertalanffy - General System Theory. Warsaw, 1984;

[3] A. Brandowski - Effectiveness and Reliability of the Ship Systems. Merchant Navy Academy. Gdynia, 1984;

[4] B. Chilo, B. Della Loggia /CETENA/, C.Deutsch, M. Routin /OPEFORM/ - Ship manoeuvrability aspects and human factors. Geneva, 1984;

[5] M. Gerigk - Reports of Ship Research Institute of the Technical University. Gdańsk, 1985-86;

[6] A.M. Glicksman - Linear Programming and the Theory of Games. Brooklyn, 1962;

[7] R.H.M. Huijsmans, W. Spaans - Computer simulation techniques in a ship control simulator. Conference: Automation for Safety in Shipping and Offshore Petroleum Operations. Trondheim, Norway, 1980;

[8] V. Kostilainen, M. Hyvärinen - Ship casualties in the Baltic,Gulf of Finland and Gulf of Bothnia in 1971-72. The Journal of Navigation, Vol. 27, No 2, 1974;

[9] T.B. Sheridan, W.R. Ferrell - Man-Machine Systems. Cambridge, Massachusetts, London. England, 1980;

[10] Ship Systems. Conference. London, 1979;

[11] Statics of damages. Morskoy Flot, No 6, 1985;

[12] R.L. Stroch. Small Boat Safety. Marine Technology. July, 1980;

[13] S. Ziemba, W. Jarominek, R. Staniszewski. Problems of the Theory of Systems. Ossolineum, 1980;

ABOUT THE AUTHOR

MIROSŁAW GERIGK is employed in the Ship Hydrodynamics Department of Ship Research Institute - Technical University of Gdańsk. He graduated in shipbuilding from the Ship Research Institute at Gdańsk Technical University in 1984.

Third International Conference on Stability of Ships and Ocean Vehicles, Gdańsk, Sept. 1986

STAB'86

FLOATATION INSTEAD OF STATICAL STABILITY PROPOSAL FOR CHANGES IN BASIC DEFINITIONS

J. Wiśniewski

SUMMARY

The aim of proposal is to separate the ship stability concepts from its statical origin, and enable on this way the proper dynamical deduction of it, also as a part of modern dynamic systems approach, positively developed in other branches of engineering.

Presented aim is not only of educational effect, which may be as well important. The scope of hydrostatics calculations for contemporary ships has been enlarged, and raised to the role of one of the main problems in methodology of ship design. On the other hand ship stability is very often approached now with the new tools of dynamics systems theory, what needs a common base with former practical solutions so effective till present time. For both of these practical aims proposed changes may be profitable.

The main change lies in proposal of the new definition of ship floatation. This is based on known conditions of equilibrium of floating body. There are given conditions of so defined floatation proved by the criterion of extrema of the potential energy.

Further, the scope and methods of checking these conditions are reviewed generally, outlining the practical problems of separated notion.

At the end the new situation of ship stability definition is discussed.

1. INTRODUCTION

Two critical conclusions may be formulated after retracing first chapters in naval architecture textbooks concerning the problems of ship hydrostatics. They constitute detailed arguments for actual general opinion that this part of naval architecture, being remain of history, should be modernised.

First conclusion states that almost all ideas of ship stability adapted and developed in practice, rised by IMO to the level of international rules, originate from statics, and some of them, missnamed, are still incrusted there. It makes difficult the effective application of modern dynamic systems approach to stability in naval architecture, in spite of positive results in other branches of engineering.

Second conclusion evaluates critically methods of formulation and solution of hydrostatics problems. Many different algorithms and simplifications for separately treated problems, elaborated during the long years of desk calculations, do not suit now the requirements and possibilities of computer techniques and modern methods developed in ship design methodology.

This paper aims to present the simple proposal of modernisation without detriment to the past. New definition of the ship floatation has been formulated at the beginning and a general review of practical problems and methods of solution has been presented in limits of the new definition, with all traditional notations of naval architecture. As the result of this presentation the possibility of detachment of ship stability ideas from their hydrostatics origin seems to be evident.

The author hopes, that his simple proposal is not only of formal value. The opinion of experts may answer, whether it may be

constructive also for practice.

2. NEW DEFINITION OF SHIP FLOATATION

Ursic proposed [x/] in his text-book [1] three conditions of ship floatation, which may be summarized in the following new definition: the floatation of a ship is her property to float in the position of stable equilibrium under the action of gravity and buoyancy forces. The novelty lies in the junction of the two previously separately treated conditions of equilibrium in one notion, adding the demand of firmity to them. The new definition casts the problem back to the times of classical formulation, when the early studies of equilibrium of the floating body are iniciated.

Thus examined equilibrium Bouguer [2] defining the metacentric radius in the middle of eighteenth century.

Like that in nineteenth century Dupin [3] and Davidov [4] continued the study of the problem. The needs of contemporary practice neglected their general attempt, disjoining in separate treatment the buoyancy, trimm and transverse stability problems. Today, generalisation is more actual. Let the body form be given in body axes system $Oxyz$ /fig. 1./.

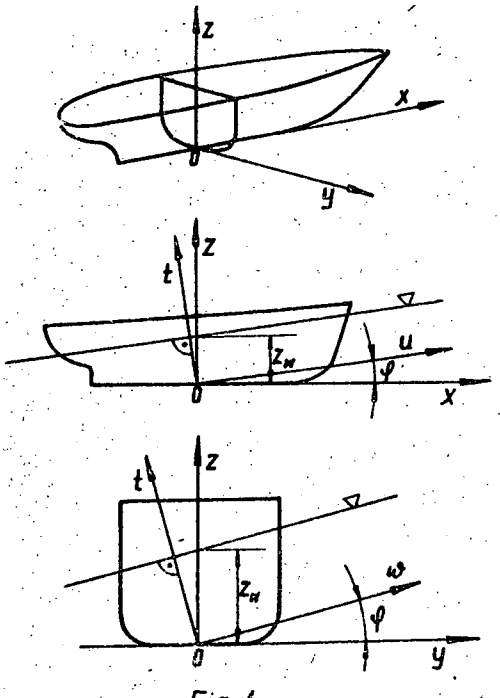

Fig. 1

In this system there are defined:

$\bar{P}(z_W, \psi, \varphi)$ - gravity force

$\bar{D}(z_W, \psi, \varphi)$ - buoyancy force

$\bar{K}_G(z_W, \psi, \varphi)$ - radius vector of the centre of gravity

$\bar{K}_V(z_W, \psi, \varphi)$ - radius vector of the centre of buoyancy

all of them being the functions of coordinates of the water plane z_W, ψ, φ. The solution of equilibrium problem in this general case of three-dimensional system is rather laborous and transcending the common description in naval architecture. Hence, observing the common treatment of the problem like in ship hydrostatics, let the ship position towards the water level plane be changed separately with one degree of freedom through parallel displacement along the axis Ot, and two rotations round the axes perpendicular to planes Otw and Otu of fixed axes system $Ouwt$ /fig. 1./. Axis Ot is always perpendicular to the floatation plane, and the origin of the system $Ouwt$ lies in the same point with the origin of the system $Oxyz$. For the ship in upright position the corresponding axes of both systems are in coincidence. The analitical geometry of the centre of buoyancy in both systems of reference is assumed to be known, at least for two-dimensional cases.

3. CONDITIONS OF FLOATATION

The criterion of equilibrium of the floating body is the extremum of its potential energy relatively to the water level, for stable position the extremum ought to be minimum.

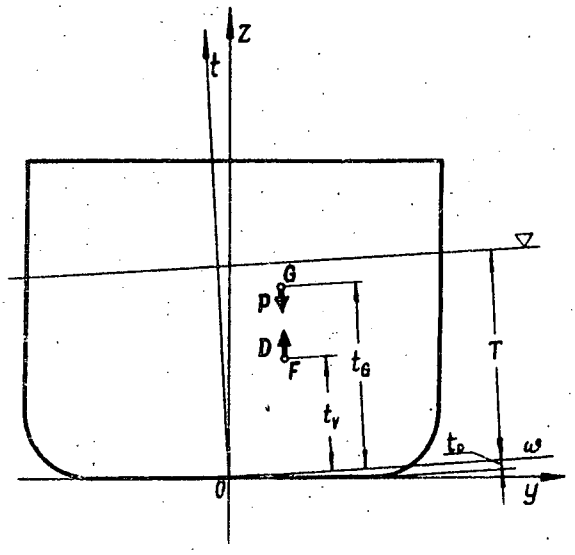

Fig. 2

x/ In spite of proposed conditions, the text of Ursic book is treating the problems of floatation, trimm and stability separately and in traditional composition.

Potential energy of the ship is /fig. 2./:

$$E_p = (t_G - T)P - (t_V - T)D \qquad (1)$$

Substituting for t_V and D:

$$t_V = \frac{\int_{t_o}^{T} S(t)t\,dt}{\int_{t_o}^{T} S(t)\,dt}; \quad D = \gamma \int_{t_o}^{T} S(t)\,dt$$

Where S is the area of waterplane, and putting $\gamma = 1$ for simplification, the energy may be written as:

$$E_p = (t_G - T)P - \int_{t_o}^{T} S(t)t\,dt + T\int_{t_o}^{T} S(t)\,dt \qquad (2)$$

The first derivative of energy with respect to T is:

$$E_p' = -P - S(T)T + \int_{t_o}^{T} S(t)\,dt + S(T)T = -P + D \qquad (3)$$

Hence, the condition of equilibrium for vertical displacement is the equality of gravity and buoyancy forces.

The condition of firmity needs:

$$E_p'' = S(T) > 0 \qquad (4)$$

This is always fulfilled for surface vessels.

When $S(T) = 0$, the equilibrium under the water level is theoretically neutral /assuming $\gamma(t) = const$/ since all further derivatives of energy equals zero, what is the condition of unproper extremum, and therefore - the neutral equilibrium.

In case of ideal compressive fluid the ship with $S(T) = 0$ is vertically in stable position.

For the ship inclined with balanced constant displacement, the potential energy is:

$$E_p = D(t_G - t_V) \qquad (5)$$

Substituting /for heeling/:

$$t_G = z_G \cos\varphi - y_G \sin\varphi; \quad t_V = z_V \cos\varphi - y_V \sin\varphi$$

$$\frac{dz_V}{d\varphi} = r\sin\varphi; \quad \frac{dy_V}{d\varphi} = r\cos\varphi$$

where $r = \frac{J_B}{V}$ is the metacentric radius, the first derivative with respect to φ will be /fig. 3./:

$$E_p' = D(w_V - w_G) = D \cdot \overline{GH} \qquad (6)$$

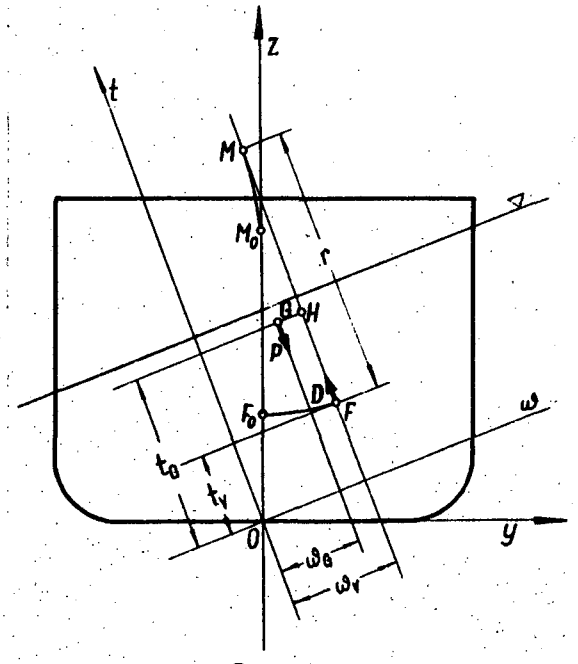

Fig. 3

Hence, the condition of equilibrium for balanced inclination needs the colineation of gravity and buoyancy forces.

The condition of firmity needs:

$$E_p'' = D(r + t_V - t_G) = D \cdot \overline{GM} > 0 \qquad (7)$$

Hence, in the position of equilibrium the distance between the centre of gravity and the centre of buoyancy ought to be smaller than the metacentric radius. Equivalently, the metacentric height must be positive.

The discussion of the case $\overline{GM} = 0$ must be longer [5]. It is the condition of neutral equilibrium for body of revolution forms only. For submerged ships the condition of firmity needs $t_V > t_G$.

On the same way may be derived the conditions for trimming, for which the checking of firmity has no importance practically.

4. CHECKING THE CONDITIONS OF FLOATATION

Two forces and coordinates of their centres, coordinates of the waterplane of equilibrium and two metacentric radii are the set of thirteen variables in floatation problems. The conditions of the stable equilibrium form the four relations of the variables.

Limitation to the two-dimensional problems reduces the number of variables to nine, and relations to three.

The force of gravity and the coordinates of its centre are calculated separately in tables of weights, if thye are not the unknowns in the problem under consideration. Complementary relations for the rest of variables $D, \varphi, z_V, y_V, t, r$ /or D, ψ, z_V, x_V, t, R / helping in the solutions of some problems, are given in form of geometrical characteristics, known under the names of cross curves of stability, trimm curves, hydrostatic curves, etc. Many problems have to be solved directly with the help of body lines for direct calculations of complementary variables.

The first condition of floatation is being fulfilled through the parallel displacement of the waterline along the axis $0t$. Using geometrical characteristics, the solution may be obtained but for upright and trimmed position only. The answer can not be obtained from the characteristics for transversely inclined ship, as well as for inclined three-dimensionally. Cross curves of stability do not represent the relation between the buoyancy and the height of corresponding waterline. In these cases the body lines must be directly used.

For small changes of the buoyancy the problem may be linearised to the relations:

$$\begin{aligned} \Delta V &= S \cdot \Delta t \\ u_{\Delta V} &= u_S \\ w_{\Delta V} &= w_S \\ t_{\Delta V} &= t_S + \frac{\Delta t}{2} \end{aligned} \qquad (8)$$

where S is the area, and ω_S, u_S, t_S - the coordinates of the centre of actual waterline. Linearised formulae are prefered even if the possibility of the use of geometrical characteristics exists.

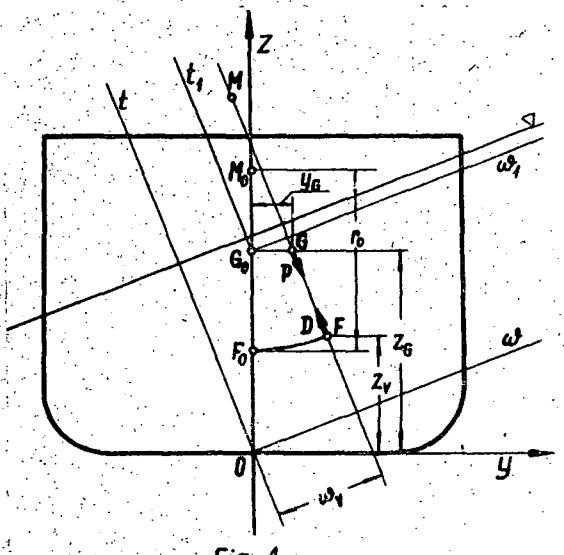

Fig. 4

The second and third conditions of floatation may be chacked grafically in respect to φ using the cross curves of stability /or trimm curves in respect to ψ / from /fig. 4./:

$$P y_G \cos\varphi = D(w_V - z_G \sin\varphi) \qquad (9)$$

where $w_V(\varphi)$ for D = const. must be interpolated form the diagrams of cross curves. The stable angle of equilibrium is the solution, and this is to recognise from the slope of resultant curve at the point of intersection with 0φ axis. There is no other simple possibility to control the sign of metacentric height at tose angles of heel as no other possibility of the determination of metacentric height for inclined ship exists, expect as from the body lines.

Approximating the locus of the centres of buoyancy with the arc described by the metacentric radius, the condition (9) may be formulated analytically for upright position as:

$$P y_G \cos\varphi = D \cdot \overline{GM_0} \sin\varphi \qquad (10)$$

Hence, the angle of equilibrium will be:

$$tg\,\varphi = \frac{y_G}{\overline{GM_0}} \qquad (11)$$

Although the metacentric approximation may be used close to the centre of buoyancy of the ship with any trimm and heel, practically geometrical characteristics in form of hydrostatic curves allow to do it only for upright position. Sometimes trimm curves include the information about the metacentric radii of trimmed ship.

All the problems with combined trimm and heel, if not simplified by superposition, have to be solved directly on the body lines. In particular methods special geometrical characteristics are calculated in the process of solution. Detailed discussion of methods used in three-dimensional cases excess the limits and needs of this paper. For the brevity of main text, already the review of actual practice for calculation the more complicated two-dimensional problems of floatation with liquid cargo, in damaged condition and with support is to be continued in appendix. To it will be also refered in further argumentation.

5. SHIP FLOATATION TOWARDS STABILITY

The review of newly separated floatation problems /including appendix/ using the notation of classical naval architecture only, proves that it is possible to build a new chapter in it, using traditional elements. It contains solutions of the whole ship hydrostatic problems without any need of reference to stability notion. The ship stability, free of handicaping with static, is open to new approach. The ship as a dynamic system defined in differential equations of her motion should be the object of stability investigation.

The stability of a system is to be able to remain in accepted boundaries of defined state under the action of predetermined magnitude and character of forcing. The state may be a stable equilibrium position under the action of gravity force, and the forcing-due statical changes of its location or/and magnitude.

This case, called "statical stability" is included now in whole into floatation problems. Practically there are no other statical excitation forces acting on the ship. Hence, stability may be started as a problem of dynamics. Starting with the solutions of linear equations of the motion, discussing some nonlinear solutions, then introducing modern dynamic system approach based on the Lyapunov ideas, the chapter on ship stability may be newly formulated and developed. References [7], [8], [9] closer explain this opinion.

There is also the space in this chapter for what is called actually "the dynamical stability" of a ship - the base of contemporary international criteria of safety in stability regulations. Moseley derived the idea of "dynamical stability" discussing rolling motions of the ship. His followers linked it to the statics. How to derive "dynamical stability" through integration of simplified equation of motion see e.g. [6].

Evidently, all equations of motion include statically defined restoring terms, and some of stability regulations - additional statically defined conditions. But all details for this use may be quoted from floatation chapter. Those remain the only needed link between stability and hydrostatics.

BIBLIOGRAPHY

[1] Josip Ursic — Plovnost Broda. Sveučilište u Zagrebu 1966;

[2] P. Bouguer — Traite du Navire, de la construction et de les mouvements. Paris 1746;

[3] C. Dupin — De la stabilite des corps flottants. Paris 1814;

[4] A. Davidov — Tieoria Ravnoviesia Tiel Pogružennych w Zydkosti. Moskva 1848;

[5] J.Wisniewski — O równowadze objętej statku. Acta Technica Gedanensia Nr 4,Gdańsk 1967;

[6] J.Wisniewski — Mechanical Criteria of Ship Stability. Schiffstechnik 1961, Heft 41;

[7] H. Bird, A.Y.Odabasi — State of Art: Past, Present and Future. International Conference on Stability of Ships and Ocean Vehicles, Glasgow 1975;

[8] W. Bogusz — Stateczność techniczna PWN, Warszawa 1972;

[9] C. Kuo, A.Y.Odabasi — Application of dynamic Systems Approach to Ship and Ocean Vehicle Stability. International Conference on Stability of Ships and Ocean Vehicles,Glasgow 1975.

Appendix

Checking the conditions of floatation in special cases.

1. Liquid cargo problems.

All the basic problems may be complicated through changes of the coordinates of the centre of gravity with the position of the ship. That's the case when liquid cargo fills only a part of watertight compartment. In this case the second condition of floatation (9) may be found from /fig. 5./:

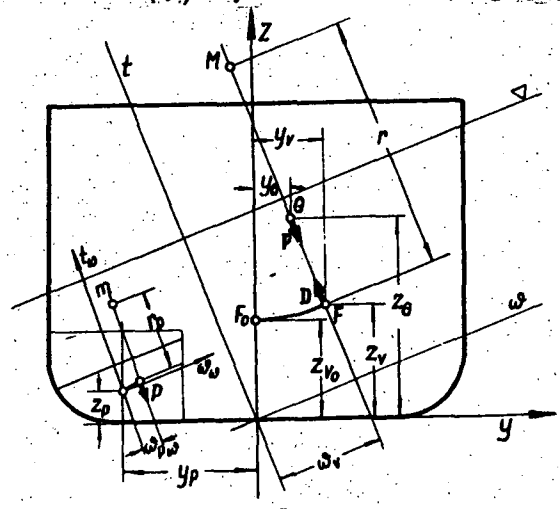

Fig. 5

$$p(y_G\cos\varphi + \frac{p}{D} w_{pw}) = D(w_V - z_G\sin\varphi) \qquad (12)$$

where: p - weight of the liquid cargo,
w_{pw} - coordinate of the centre of gravity of the liquid cargo in fixed system of reference with the origin in point (x_p, y_p, z_p) - the centre of gravity of liquid cargo being the component in calculations of the centre of gravity of the ship upright position.

The solution may be easy obtained, when the characteristics in form of cross curves for the compartments are previously computed, analogically to the cross curves of stability for the body lines. It is rare the case, and mostly metacentric formulae, or cross curves of simple box forms, approximating the shape of real tanks, are used.

Substituting accordingly into (12) :

$$z_V - z_o = \int_0^\varphi r\sin\varphi\, d\varphi; \quad y_V = \int_0^\varphi r\cos\varphi\, d\varphi: \qquad (13)$$

$$z_{pw} = \int_0^\varphi r_p\sin\varphi\, d\varphi; \quad y_{pw} = \int_0^\varphi r_p\cos\varphi\, d\varphi \qquad (14)$$

where: $r_p = \frac{i_p}{\nabla_p}$ - metacentric radius of liquid cargo, then rearranging and returning to the fixed system of reference, the second condition of floatation changes to the form:

$$py_G\cos\varphi = D(w_{1V} - z_G\sin\varphi) \qquad (15)$$

where:

$$w_{1V} = z_{1V}\sin\varphi + y_{1V}\cos\varphi$$

$$z_{1V} = \int_0^\varphi \frac{J_B - i_p\frac{\gamma}{\gamma_w}}{V}\sin\varphi\, d\varphi + z_o \qquad (16)$$

$$y_{1V} = \int_0^\varphi \frac{J_B - i_p\frac{\gamma}{\gamma_w}}{V}\cos\varphi\, d\varphi$$

The simple formal operation replaces the real shifting the centre of gravity by apparent change of coordinates of the centre of buoyancy, with no difference of the result. There is no spare of calculation when formula (15) is used. Substituting (16) into (6) in place of w_V ,then differentiating, the apparent metacentric hight in the condition of firmity (7) will be:

$$\overline{GM}_{app} = \frac{J_B - i_p\frac{\gamma}{\gamma_w}}{V} + t_w - t_G = \overline{GM} - \frac{i_p\frac{\gamma}{\gamma_w}}{V} \qquad (17)$$

In this form metacentric hight is commonly used for calculations with metacentric approximation. The other possibility /not practicised/ is to calculate the position of the centre of gravity of the whole ship, with the centre of gravity of liquid cargo rised to the point of its metacentrum.

2. The influence of flooding, or floatation when damaged.

The separate group of problems in naval architecture are the equilibrium conditions for a ship with freely flooded watertight compartment. The second condition of equilibrium in this case may be written as:

$$P_1 y_{G_1}\cos\varphi = D_1(w_{V1} - z_{G1}\sin\varphi) \qquad (18)$$

where:

$$y_{G1} = \frac{Py_G + py_p}{P_1}$$
$$z_{G1} = \frac{Pz_G + pz_p}{P_1}$$

coordinates of the centre of gravity of the ship with added liquid cargo p .

$$w_{V1} = \frac{Dw_V + dw_d}{D_1}$$

coordinate of the centre of buoyancy of the ship, where added buoyancy $d=p$ and w_d is the coordinate of its centre (fig. 6.).

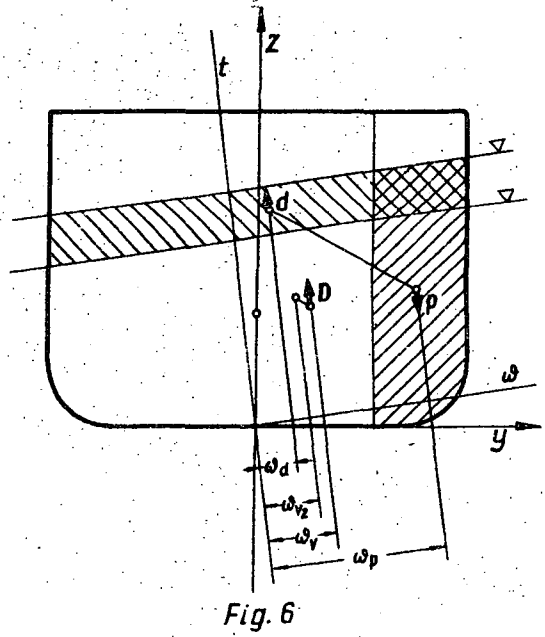

Fig. 6

In this case the water in compartment is treated as the added weight. Calculations of the position of equilibrium using (18) are laborous. The added weight is a function of φ, and even if the characteristics $w_p(p,\varphi)$ are in disposition, an iterative process must be used.

Substituting formulae for z_{G_1}, y_{G_1} and w_{V_1} in (18) and rearranging it will be obtained:

$$\rho y_G \cos\varphi = D(w_{2V} - z_G \sin\varphi) \quad (19)$$

where:

$$w_{2V} = \frac{D w_V - \rho w_p + d \cdot w_d}{D}$$

It is seen on the fig. 6., that w_{2V} is the coordinate of the centre of buoyancy of the ship without the volumen of the flooded compartment. The loss of the buoyancy of watertight compartment is equalised through the immersion to the waterline WL_1.

The new cross curves of stability $w_{2V}(V,\varphi)$ for recessed lines may be calculated and the problem (19) is reduced to (8).

This method of "lost buoyancy" is more simple as the method of "added weight" of (18). Grafical results of both solution are identical. But there is no identity when in place of moments only the levers are calculated, what is the common practiced case in naval architecture. Dividing (18) by D_1 and (19) by D and rearranging gives accordingly:

$$\frac{\rho}{D_1} y_G \cos\varphi = \frac{D}{D_1}\left[w_V + \frac{\rho}{D}(w_d - w_p) - z_G \sin\varphi\right] \quad (18A)$$

$$y_G \cos\varphi = w_V + \frac{\rho}{D}(w_d - w_p) - z_G \sin\varphi \quad (19A)$$

It is evident that both curves differ in values proportionally.

Also the metacentric hights will differ at every point.

Substitution y_{G_1}, z_{G_1} and w_1 from (18) to (6) and differentiation give the result:

$$\overline{GM}_{app} = \frac{D}{D_1}\left[t_{2V} + \frac{J_{B_1} - i_p}{D} - t_G\right] \quad (20)$$

and the same operations with w_{2V} from (19) have the result:

$$\overline{GM}_{app} = t_{2V} + \frac{J_{B_1} - i_p}{D} - t_G \quad (21)$$

It makes no difference for evaluating the state of equilibrium, as the sign of both metacentric hights will be always the same. But for calculations with metacentric approximation, or for checking the requirements of the Safety of Life at See Conference, proper value must be used.

3. Floatation with support

Docking, launching, grounding, or in some circumstances rising the sunken ship are the problems in which equilibrium is investigated under conditions that the weight of the ship is equal the sum of buoyancy force and supporting reaction of the bed:

$$P = D + R \quad (22)$$

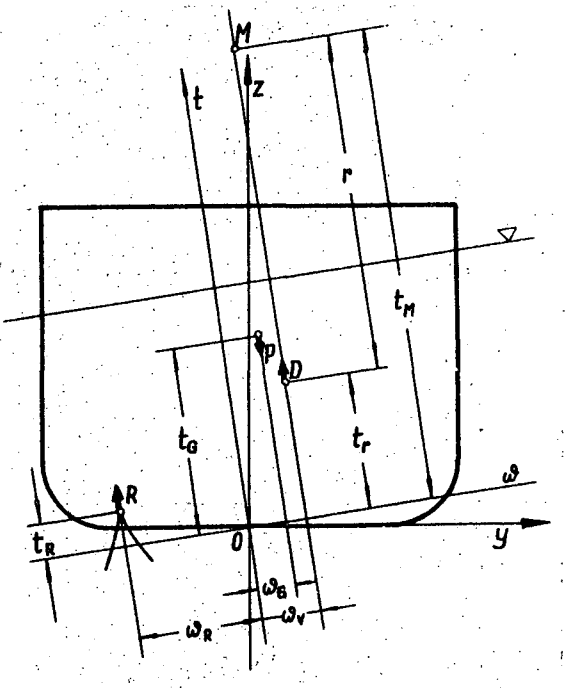

Fig. 7

Potential energy of the system will be fig. 7./:

$$E_p = P t_G - D t_V - R t_R \quad (23)$$

Hence, for inclined equilibrium position it should be satisfied:

$$D w_V + R w_R - P w_G = 0 \quad (24)$$

As the $\frac{D}{R}$ ratio is a function of φ, the condition (24) must be solved by trial and error method.

In the position of equilibrium the second derivative of energy gives the condi-

tions of firmity in the form:

$$p\left[r+t_V-t_G-\frac{R}{p}(r+t_V-t_R)\right]>0$$

what gives the condition for apparent metacentric hight in the position of equilibrium:

$$\overline{GM}-\frac{R}{p}(t_M-t_R)>0 \qquad (25)$$

Hence, the critical state will be when:

$$\overline{GM}<\frac{R}{p}(t_M-t_R) \qquad (26)$$

In particular case, when the ship is supported in plane of symetry, and $\varphi=0$, the apparent metacentric hight will be :

$$\overline{GM}_{app}=GM-\frac{R}{p}z_M \qquad (27)$$

ABOUT THE AUTHOR

JERZY WIŚNIEWSKI dr. ing., docent, graduated in 1949 in naval architecture from the Faculty of Shipbuilding, Technical University of Gdańsk. Since 1945 he is the member of teaching staff of the University, starting as a junior assistant. Presently held the position of the Head of Ship Design Department of Ship Research Institute, Technical University - Gdańsk. His main subjects are ship dosign methodology and CAD.

Third International Conference on Stability of Ships and Ocean Vehicles, Gdańsk, Sept. 1986

STAB'86

PROBABILITY OF NON-CAPSIZING OF A SHIP AS A MEASURE OF HER SAFETY

W. Błocki

ABSTRACT

There are views that the probability of non-capsizing of a ship is a good measure of her stability safety. The paper describes shortly how to calculate this probability. The method used is based on the Goda's concept of the wave groups. The roll of the ship is simulated on a computer and differential equation of ship motion is solved for random initial conditions. The solution makes it possible to calculate the probability of capsizing caused by one group of waves. Next, the probability of capsizing is calculated with respect to the action of any group of waves according to the formula for the entire probability. The probability of non-capsizing in a difinite period of time is obtained and this probability is recommended as a measure of stability safety.

The results of calculations of non-capsizing probability for small trawler at Baltic Sea are presented. The method of the choice of a suitable probability level up to which the ship may be regarded as safe is shown.

1. INTRODUCTION

In the history of naval architecture different quantities were taken as measures of the ship's stability safety.
In the 18th and 19th centuries metacentric height, righting arms of the statical or dynamical stability were used as those measures. Safety, similar like the reliability, is a probabilitic quantity. At present the opinion exists that the probability of ship's non-capsizing is a good measure of ship stability safety. It is a convenient measure, because the probability of ship's non-capsizing increases nonotonously with an increas of ship's stability safety. This is the number from the interval $[0,1]$.
For the most dangerous ship, with no stability, the probability of her non-capsizing is zero, and for the absolutly safe ship this probability is one.

2. METHOD OF COMPUTING THE PROBABILITY OF SHIP'S NON-CAPSIZING

The randomness of ship's capsizing is caused mainly by the fact that sea waving is a random process. The groups of high waves, which happen in stochastic process, may cause capsizing of a ship. The stochastic model of the wave group was proposed by Y. Goda (1970) . This model defines the probability distribution of the length and frequency of groups of high waves [1] [2] . In this model of the wave group a single wave is considered as independent random event. The wave group of length j is defined as a series of single waves which consecutively exceed the level ζ in $(j-1)$ - trials and fail to exceed in the j-th trial.
This length and distance between two wave groups are shown in fig. 1.
It is assumed that the amplitude of waving is distributed according to the Rayleigh's density function.
Therefore, the probability of exceeding of the level ζ by a single wave is given by:

$$p = P(\zeta_A \geq \zeta) = \exp\left(-\frac{\zeta^2}{2\sigma^2}\right) \qquad (2.1)$$

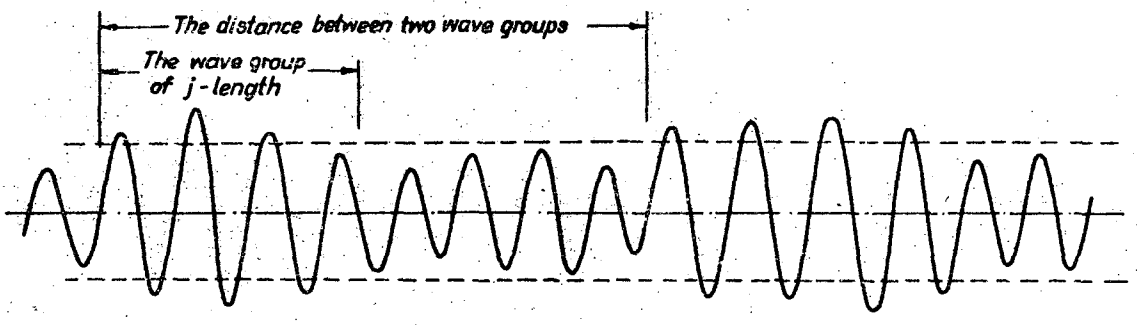

Fig. 1. The length and the distance between groups of high waves.

The probability of the occurence of the wave group of length j is expressed as [1]:

$$P_1(j) = p^{j-1}(1-p) \qquad (2.2)$$

The mean value of this distribution is:

$$E(j_1) = \frac{1}{1-p} \qquad (2.3)$$

On the other hand, the probability of the distance between two subsequent wave groups is expressed by [1] :

$$P_2(j) = \frac{p(1-p)}{2p-1}\left[p^{j-1} - (1-p)^{j-1}\right] \qquad (2.4)$$

with the following mean value:

$$E(j_2) = \frac{1}{p} + \frac{1}{1-p} \qquad (2.5)$$

Computation of the probability of ship's capsizing is based on the solution of the differential equations of ship motions for random initial conditions. Strictly speaking this consists in determining of the critical initial conditions which cause capsizing of a ship. It is assumed that the ship undergoes random oscillations until she meets the wave group and then she undergoes determinate oscillations. At the moment of occurrence of the group of waves the angular velocity $\dot{\phi}$ of roll is random.

It is assumed that the group of high waves can be approximated by means of a regular wave [3] . This is schematically shown in fig. 2.

The random event of ship capsizing is denoted by symbol B. The probability of ship capsizing as a result of wave group of length j, may be expressed by:

$$P(B|j) = \int_G p(\dot{\phi})\, d\dot{\phi} \qquad (2.6)$$

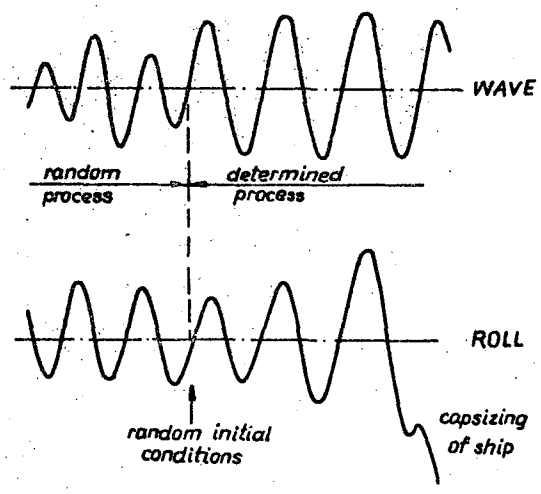

Fig. 2. Scheme of capsizing of a ship as a result of the wave group.

where G denotes the space of initial angular velocity of roll for which capsizing of the ship occures.

Whereas the probability of ship capsizing as a result of any single group of high waves may be calculated for the entire probability by the following formula:

$$P(B) = \sum_j P_1(j)\, P(B|j) \qquad (2.7)$$

The random event of ship non-capsizing is denoted by symbol A. Of course, the probability of non-capsizing of a ship as a result of any single group of high waves can be simply calculated as follows:

$$P(A) = 1 - P(B) \qquad (2.8)$$

Any group of waves is the trial which may cause either non-capsizing of a ship /success/ or capsizing of a ship /failure/.

The success occurs with the probability $P(A)$ and failure with the probability $P(B)$. The probability of ship non-capsizing for n trials /that is for n groups of waves or in other words n successes in n trials/ is given by:

$$P_n(A) = [P(A)]^n \qquad (2.9)$$

This probability is related to the safety of ship stability [4]. The relationship between four quantities: the number n of groups of waves, the mean period T_1 of a wave, the mean distance $E(j_2)$ between the groups of waves and the period of time t of stay of a ship in definite conditions is given by the formula:

$$t = n\, T_1\, E(j_2) \qquad (2.10)$$

Thus, the probability $P_t(A)$ of ship non-capsizing during the poriod of time t may be expressed by:

$$P_t(A) = [1 - P(B)]^{\frac{t}{T_1 E(j_2)}} \qquad (2.11)$$

The mean $E(j_2)$ of the probability distri - bution of the distance of wave groups given by formula (2.5), reaches the least value for p = 0,5. This value is $E(j_2) = 4$. This is the most dangerous case.
Taking into the overmentioned statements we can transform (2.11) into:

$$P_t(A) = [1 - P(B)]^{\frac{t}{4T_1}} \qquad (2.12)$$

This is a useful proposal to take the probability $P_t(A)$ of non-capsizing of the ship as a measure of ship stability safety.

3. EXAMPLE OF COMPUTATION OF PROBABILITY OF SHIP NON-CAPSIZING IN BEAM SEA

An illustrative computation was carried out for a small Polish trawler of type KB-21. Parameters of this fishing vessel are as follows:

length between perpendi-oculars	Lpp	= 18,4 m
breadth	B	= 6,0 m
draught	T	= 2,13 m
volume of displacement	V	= 116,5m^3
height of the centre of gravity	KG	= 2,60 m
metacentric height	GM	= 0,65 m

The approximations of the curve of statical stability and of the coefficient of roll damping are shown on fig. 3. and fig. 4.

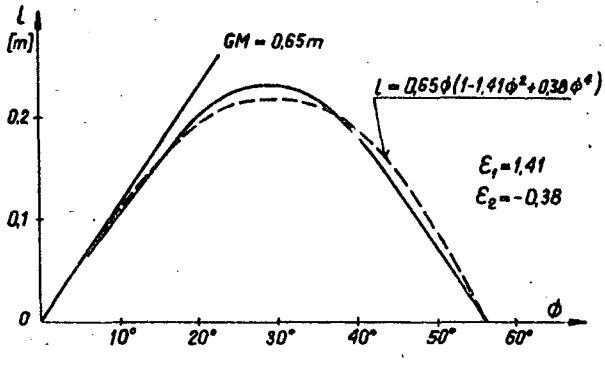

Fig. 3. The approximation of the curve of statical reghting arms for trawler KB-21.

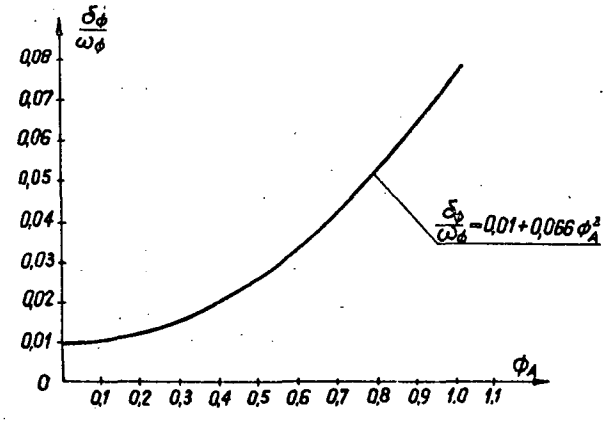

Fig. 4. Non-linear coefficient of roll damping for trawler KB-21.

It was assumed, that the following dif--ferential equation describes the roll motion of this vessel:

$$\ddot{\phi} + 2\delta_\phi\left(1 + \frac{\varepsilon_1}{\omega_\phi^2}\dot{\phi}^2\right)\dot{\phi} + \omega\phi^2\left(1 - \varepsilon_1\phi^2 - \varepsilon_2\phi^4\right)\phi = m_f \cos\omega t \qquad (3.1)$$

Four states of the Baltic Sea were considered with two parameters determined by significant wave height $\xi_{w1/3}$ and mean characteristic period of wave T_1. The wave spectrum $S(\omega)$ corresponded a suitable state of the Baltic Sea.
The variance of the random process of the roll angular velocity was calculated by the formula:

$$\sigma_{\dot{\phi}}^2 = \frac{1}{g^2}\int_0^\infty \omega^6 H^2(\omega)\, S(\omega)\, d\omega \qquad (3.2)$$

The amplitude transfer function of roll $H(\omega)$ was calculated for the ship treated as a nonlinear object. Computed standard deviations of roll angular velocity of trawler KB-21 for some states of the Baltic Sea are compiled in table 1.

Table 1.
Parameters of waving $\xi_{3\%}$ and T_1 for the Baltic Sea and standard of roll angular velocity for trawler KB-21

$^\circ_B$	$\xi_{3\%}$ [m]	T_1 [s]	$\sigma_{\dot\phi}$ [s^{-1}]
5°	0,85	3,8	0,047
7°	1,60	4,8	0,095
9°	2,50	5,8	0,139
11°	3,80	6,3	0,187

Equation (3.1) has been solved numerically for different initial angular velocities of roll.
The critical initial velocity of roll was found.
The capsizing of the vessel occured for velocities higher than critical. One level of excess was used, because it was assumed that the probability of the ship capsizing is independent of it. Separate computations confirmed this assumption. Exemplary runs of simulation of roll with capsizing of the trawler are shown in fig. 5.
The critical initial velocities of roll for different lengths j of wave groups are compiled in table 2.

Table 2.
Critical angular velocity of roll $\dot\phi_k$ for trawler KB-21

j	$\dot\phi_k$ [s^{-1}]
1	0,66
2	0,35
3	0,18
4	0,09
5	0

The probability distribution of the initial angular velocity of roll coincides with the Rayleigh's distribution. Therefore formula (2.6) for the probability of ship capsizing as a result of the wave group has the following form:

$$P(B|j) = \exp\left(-\frac{\dot\phi_k^2}{2\sigma_{\dot\phi}^2}\right) \qquad (3.3)$$

Probabilities $P(B|j)$ computed from (3.3) are compiled in table 3. Probabilities $P(j)$ of the occurence of the wave group of length j computed by formula (2.2) for $\xi = \xi_{4\%} = 4{,}2$ m are compiled in table 4.

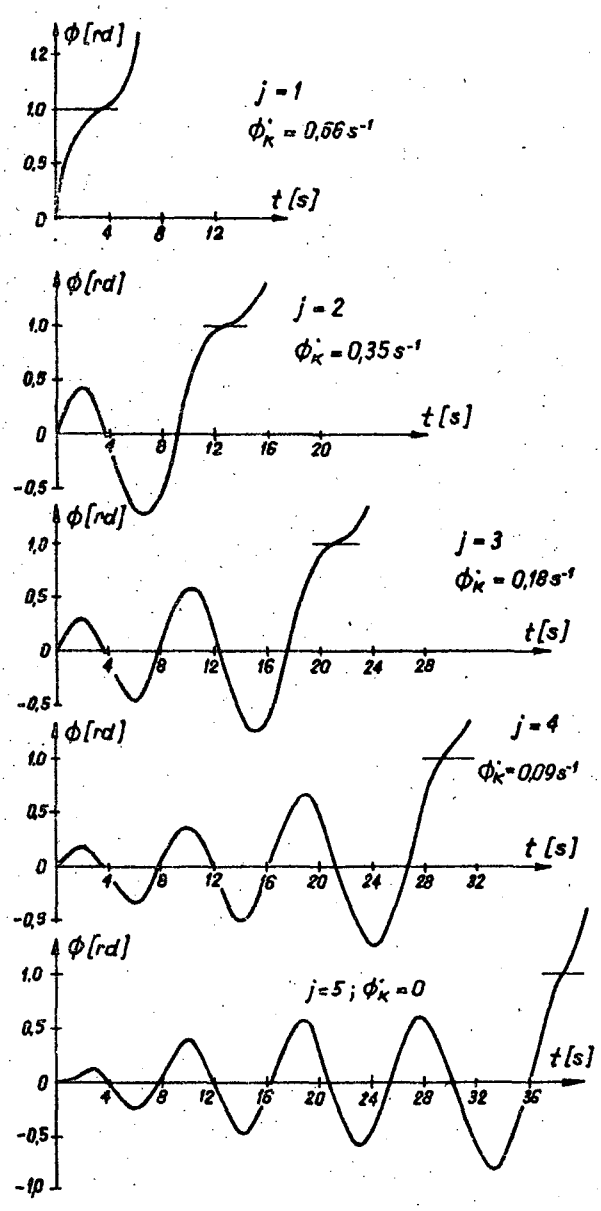

Fig. 5. Runs of simulation of roll with capsizing for trawler KB-21.

Next, probability P(B) of capsizing of the trawler as a result of any single group of high waves was computed according to formula (2.7) and the results are shown in table 5 and fig. 6.

Finally, probability $P_t(A)$ of non-capsizing of the trawler during the period of time t = 1 hour, 10 hours, 24 hours in the Baltic Sea was computed and are shown in table 6 and fig. 7.

Table 3.

Probability $P(B|j)$ of capsizing of trawler KB-21 as a result of wave groups of length j (for ζ_A = 1,2 m).

$^\circ B$	j = 1	j = 2	j = 3	j = 4	j=5
5°	$9,13\cdot10^{-43}$	$1,50\cdot10^{-12}$	0,0007	0,1653	1
7°	$4,22\cdot10^{-11}$	0,0012	0,1692	0,6413	1
9°	$1,39\cdot10^{-15}$	0,0431	0,4352	0,8122	1
11°	0,0020	0,1733	0,6294	0,8906	1

Table 5.

Probability $P(B)$ of capsizing of trawler KB-21 as a result of any single wave group.

$^\circ B$	P (B)
5°	$1,00\cdot10^{-17}$
7°	$3,42\cdot10^{-5}$
9°	0,0181
11°	0,1992

Table 4.

Probability distribution $P(j)$ of wave group (for ζ_A = 1,2 m)

$^\circ B$	j = 1	j = 2	j = 3	j = 4	j = 5
5°	1,0000	$1,15\cdot10^{-7}$	$1,32\cdot10^{-14}$	$1,51\cdot10^{-21}$	$1,74\cdot10^{-28}$
7°	0,9890	$1,09\cdot10^{-2}$	$1,20\cdot10^{-4}$	$1,32\cdot10^{-6}$	$1,45\cdot10^{-8}$
9°	0,8423	0,1328	0,0209	0,0033	$5,21\ 10^{-4}$
11°	0,5505	0,2475	0,1112	0,0500	0,0225

Table 6.

Probability $P_t(A)$ of non-capsizing of trawler KB-21 for different periods of time t.

$^\circ B$	$P_t(A)$		
	1 hour	10 hours	24 hours
5°	1,0000	1,0000	1,0000
7°	0,9936	0,9378	0,2141
9°	0,0583	$4,55\cdot10^{-13}$	0
11°	$1,64\cdot10^{-14}$	0	0

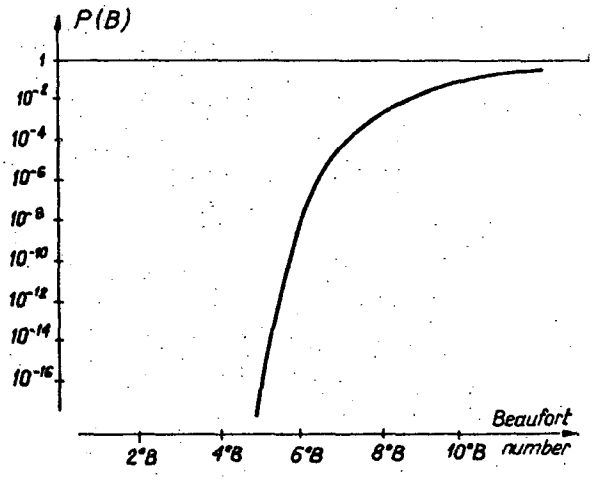

Fig. 6. Probability of capsizing of trawler KB-21 as a result of any single group of high waves.

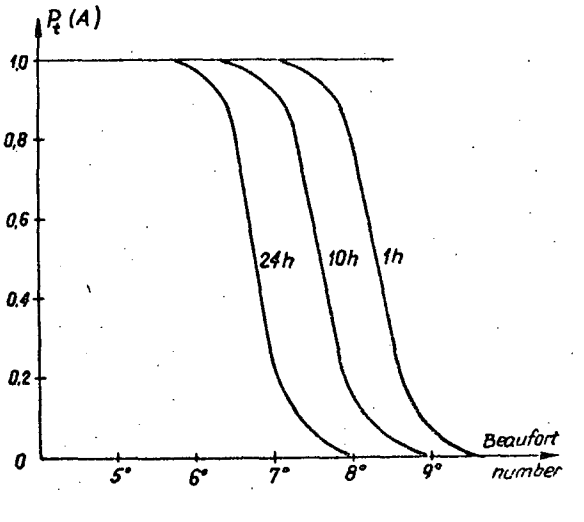

Fig. 7. Probability of non-capsizing of trawler KB-21 during the period of time t.

4. CONCLUSIONS

A graph of computed probability $P_t(A)$ of non-capsizing of the vessel has the expected shape; i.e. this probability decreases for higher sea states and for longer period of stay of the ship in given conditions. The same can be said about probability $P(B)$. This confirms correctness of the presented method. Fig. 5. shows that probability $P_t(A)$ of ship non-capsizing rapidly decreases after exceeding a certain specific sea state from value near to one to nearly zero. Thus, the capsizing of the ship for sea state higher than the specific one is practically certain. This agrees with common intuition.

Here arises a question what an admis-

sible value of probability $P_t(A)$ should be assumed to regard the ships as safe. The admissible sea state, up to which her operation is admitted, is know. How to find this admissible value of the probability is explained in fig. 8.

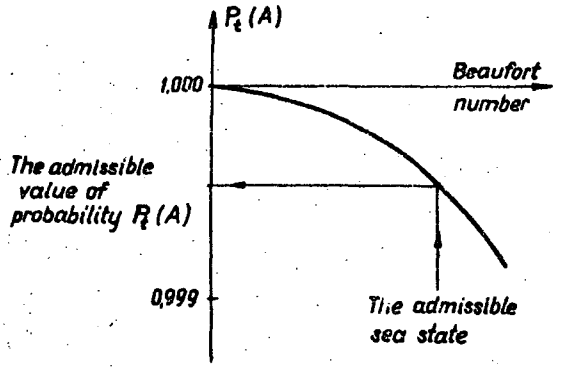

Fig. 8. Admissible value of the probability of ship capsizing.

Trawler KB-21 operates to 4-5 sea state which corresponds to 5^0-6^0 Beaufort number. For this condition the probability of non-capsizing of the trawler is about $P_t(A) = 0,99995$ /for 24 hours/.

The above discusion indicates that probability $P_t(A)$ of non-capsizing of the ship can serve as a good measure of the ship stability safety.

NOMENCLATURE

- A - random event of non-capsizing of a ship
- B - random event of capsizing of a ship
- ^oB - Beaufort number
- a_1 - non-dimensional coefficient of non-linear part of damping moment
- $E(j_1)$ - mean value of the length of a wave group
- $E(j_2)$ - mean value of distance between two wave groups
- g - acceleration of gravity
- $H(\omega)$ - non-linear amplitude transfer function of roll
- j - length of wave group
- m_f - amplitude of wave excitation moment of roll
- n - number of trials of ship's capsizing
- p - probability of exceeding level ζ
- $p(\dot{\phi})$ - probability distribution of initial angular velocity of roll
- $P(A)$ - probability of non-capsizing of a ship as a result of any single wave group
- $P(B)$ - probability of capsizing of a ship as a result of any single wave group
- $P(B|j)$ - probability of a ship's capsizing as a result of wave group of length j
- $P_1(j)$ - probability distribution of length of a wave group
- $P_2(j)$ - probability distribution of the distance between two wave groups
- $P_n(A)$ - probability of non-capsizing of a ship in n trial
- $P_t(A)$ - probability of non-capsizing of a ship in the time period t
- $S(\omega)$ - wave spectrum
- t - time, period of time
- T_1 - mean characteristic period of sea wave
- δ_ϕ - coefficient of roll damping
- $\varepsilon_1, \varepsilon_2$ - coefficient of non-linear restoring moment
- ζ_A - amplitude of a regular wave which approximates the wave group
- $\zeta_{1/3}$ - significant height of sea wave
- ζ - level of excess
- σ^2 - variance of random process of the sea wave
- $\sigma^2_{\dot{\phi}}$ - variance of random process of the roll angular velocity
- $\sigma_{\dot{\phi}}$ - standard deviation of the random process of the roll angular velocity
- $\phi, \dot{\phi}, \ddot{\phi}$ - roll angle, angular velocity of roll, angular acceleration of roll
- ϕ_A - amplitude of roll
- $\dot{\phi}_K$ - critical angular velocity of roll
- ω - frequency of wave
- ω_ϕ - natural frequency of roll.

REFERENCES

[1] Goda Y. "On wave groups", An International Conference on Behaviour of Off-Shore Structures, Norwegian Institute of Technology, Trondheim, Proceedings, Vol. one, Boss 1976;

[2] Ewing J. "Review of recent work of the length of groups of high wave heights", IMCO FF V/10 Annex VI, 1973;

[3] Błocki W. "Ship safety in connection with parametric resonance of the roll", International Shipbuilding Progress, Vol. 27, nr 306, Feb. 1980;

[4] Blocki W. "Probabilistyczna koncepcja oceny bezpieczeństwa statecznościowego statku", Budownictwo Okrętowe, rok XXVI nr 3, Gdańsk marzec 1981;

[5] Hattendorff H.G. "Regelmässige Wellen und unregelmässiger Seegang", Handbuch der Werften XII Band, Hamburg 1974;

ABOUT THE AUTHOR

Witold Blocki, graduated in marine engineering from the Technical University of Gdańsk in 1966.
Next he joined the Ship Research Institute of this University and have been working as a researcher at the Ship Hydromechanics Division. In 1977 he completed his Ph. D. thesis.

Third International Conference on Stability of Ships and Ocean Vehicles, Gdańsk, Sept. 1986 STAB'86

IMPROVEMENT OF GRAIN LOADING CAPACITY FOR DRY CARGO SHIP

F.L. Feeder

1. ABSTRACT

This paper deals with three possibilities to enlarge the actual capacity of grain cargoes for dry cargo ships and how to avoid costs for grain fittings and grain securing.

By applying a new method to calculate heeling moments vertical centres of cargo after shift can be calculated exactly whereas the older method called for a rough addition to the moment caused by transverse shifting. Since there is actually a cargo shift downwards in fully loaded holds and not upwards as in partly filled holds, the more accurate calculation achieves smaller nominal moments causing about 10% less heeling angles and 30% greater residual area between heeling and righting arm curves.

Computer programs were prepared to simulate the behavier of the cargo and to do the extensive calculations for fully and partly filled holds and to plot the required drawings of grain sections and diagrams.

By adjusting the steel structure design to the behaviour of grain, heeling moments can be reduced by as much as 60 %. About 250 different hold sections were calculated to investigate the influence of the most important design parameters.

By adequate cargo handling, e.g. using the advantages of SOLAS-74 for "separate loading" of upper and lower holds and by an intelligent employment of the above mentioned diagrams for partly loaded holds the actual grain capacity also can be improved.

2. INTRODUCTION : HISTORICAL REVIEW

Hazards caused by shifting of grain cargoes were known very early. So it was already in 1875, even before the first detailed freebord rules were issued, when measurements were called for against these hazards in the British Shipping Act.

"Common loading" of upper and lower holds at that time was arranged with openings in tween decks ,with grain feeders to fill up the lower portions, and by securing of the grain surface in the upper hold using centreline shifting boards and bagged grain.

Since 1948 rules for loading grain in bulk have been issued by the SOLAS-Convention.

In 1960 the requirement for shifting boards in tweendeck feeders was dropped for ships with a minimum initial stability $\overline{GM}=1(ft)$. Bulkcarriers were even allowed to have partly filled holds without shifting boards or securing with bagged grain if it could be proved by calculation that after a 2% settlement and 12 degree shift of the cargo the heeling was less then 5 degrees.

Now SOLAS 1974 [1] provides rules for the carriage of grain in bulk. These rules became effective world wide by 1980. Requirements for dry cargo ships now depend on heeling moments caused by an assumed shift of cargo too. This enables dry cargo ships to carry grain in bulk without temporary fittings in case of good stability data.

The rules are based on IMCO's extensive investigation on the behaviour of grain cargoes and it was TOPE [2], who presented his substantial report on that to the RINA in 1971.

The main points of this investigation were:

-There is actually not a 2% settlement of the cargo, but there are spaces below decks which cannot be completely filled by trimming. During the voyage gargo moves from above to these voids. The height of the void spaces was analysed as function of the

depth of girder hindering the loading and the distance to the boundary below deck.

-A quasi-static calculation which assumes a 30 degree rolling and 28 deg. angle of repose of the cargo results in an 8 to 10 degree wedge angle of cargo.

Taking into consideration dynamical model tests with 10 deg. initial heeling angle and a margin of safety, a 15 deg.surface shift in fully loaded and a 25 deg.surface shift in partly loaded holds was assumed.

-A movement of the cargo from the HIGH SIDE to the LOW SIDE can be assumed in common loaded holds as shown in Figure.3

This author's intention was to improve the methods of calculating heeling moments on the basis of the SOLAS-74 requirements, to investigate the properties of hull and structural design on heeling moments and to provide for a better understanding of the rules in Germany by expounding on TOPE's work.

The results of these investigations were published in 1982 as a thesis at the RWTH AACHEN [3] and in the form of a lecture to the STG-Fachausschuss in 1983 [4].

3.0. RULES AND ARRANGEMENTS

3.1. THE SOLAS-74 RULES FOR GRAIN CARRIAGE

This paper is based on Chapter VI of SOLAS-74. Supposing that all of this exellent audience are more or less familiar with these rules, let me give here a very short summary of the items relevant to my investigations.

3.11 ASSUMPTIONS OF VOID SPACES

The shifting of cargo in "filled compartments", which have been trimmed in accordance with the rules, is caused by void spaces below all boundary surfaces having an inclination to the horizontal less than 30 degrees.

The void depth, Vd, is calculated by the formula .. Vd = Vd1+0.75(d-600) =) 100(mm) where Vd1 = standard void depth given in a table as a function of b and d.

b = distance to boundery of compartment
= "understow distance"

d = actual girder depth (hindering the loading of the space behind the girder).

Figure 1 demonstrates that girder depth is of much more importance than the understow distance.

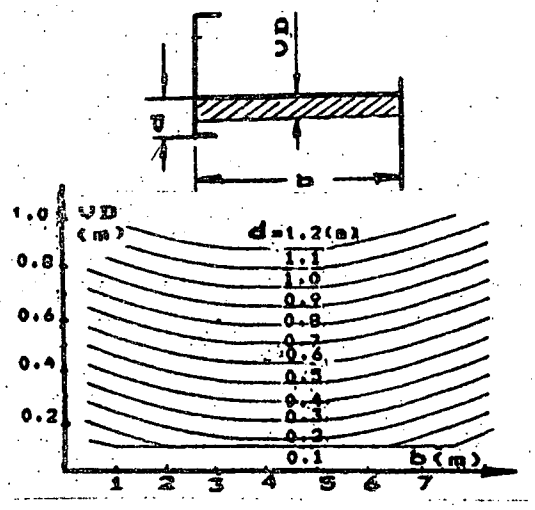

Fig.1 Vd = F(d, b)

3.12 SHIFTING OF CARGO

The wedge angle at the cargo surface caused by shifting is assumed to be 15 degrees in "filled" compartments and 25 deg.for partly filled holds.

In common loaded upper and lower holds voids shift not only transversely but also vertically from decks at the LOW SIDE to hatchway and decks at the UPPER SIDE.

Figure 3 gives TOPE's illustration of principles of the static pattern of grain surface behaviour to be assumed when calculating an estimation of the heeling moment.

3.13 ASSUMPTION OF HEELING MOMENTS

(1) The heeling moment is calculated by the moment caused by the transverse shift.

(2) Heeling moment caused by vertical shift of cargo is accounted for in two ways:

(2.1) In cases where VCG, the vertical centre of gravity of cargo, is assumed to be the centre of whole cargo space, no addition is made to the moment caused by transverse shift.

(2.2) If the calculation of the VCG of cargo for a filled compartment has included the effect of the horizontal underdeck voids, an addition of 6% is made to the transverse moment.

(3) In partly filled compartments an addition of 12% has to be made to the moment caused by the transverse shift.

(4) Other equally effective methods to compensate for the a.m. requirements may be adopted.

The author's method is based on statement No 4. Consideration of heeling moment caused by vertical shift is done by accurate calculation of VCG of cargo after shift.

3.14 CRITERIA FOR INTACT STABILITY

The stability characteristics shall meet at least the following criteria throughout the whole voyage, taking into consideration free surfaces of liquids in tanks and the heeling moments caused by shifted grain.

Initial metacentric height: GM) = 0.30(m)

Heeling angle . . . . . ϕ_1) = 12 (deg)

ARD = Residual area between heeling and righting arm curve to max residual lever or to 40 deg., or to flooding angle, whichever first occurs. Heeling arm curve to be linear up to 40 degrees.

Residual area . . . ARD) = 0.075(m rad).

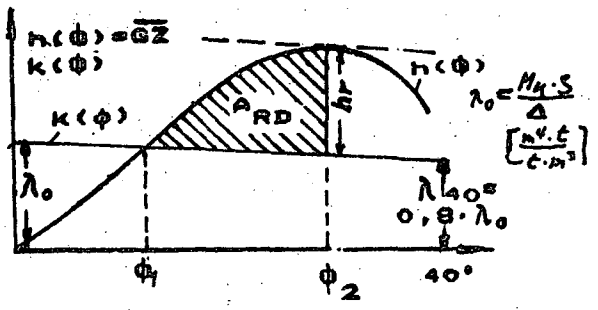

Fig.2 Stability Characteristics

Fulfilment of the a.m. requirements has to be proven for all loading conditions:

- by comparison with maximum safe heeling moment, which can be computed by a computer program as a function of draught and $\overline{KG}$.
- by conventional calculation of the stability characteristics using SIMPSON-integration with 7 stations for ARD.

3.15 ARRANGEMENTS TO LIMIT HEELING MOMENTS

When heeling moments caused by shifting of grain are too great to meet the requirements, they have to be reduced by temporary fittings or securings according to Part C of Chapter VI of SOLAS-74.

In filled holds this can be done by:

- divisions
(centreline shifting boards and feeders)
- saucers
- bundling of bulk
- securing hatch covers of filled compartm.

In partly filled holds it can be done by:

- bagged grain
- overstowing arrangements
- strapping or lathing

(saucers, bundling of bulk, strapping and lashing according to drawings of National Cargo Bureau, NY)

All these methods of temporary grain fittings cause costs to such an extent that dry cargo ships cannot compete with bulkcarriers in the carriage in grain in general.

As dry cargo ships are nevertheless employed e.g. in grain services to shallow water harbours of the third world, it was the author's objective to improve their qualities.

4.0. IMPROVING THE CALCULATION METHODS

4.1. HEELING MOMENTS OF FILLED HOLDS

4.11. THE OLD METHOD

The older method was to calculate the heeling moment caused by transverse shift by multiplying the shifted cargo mass by the transverse distance of shift. The latter was measured from the sectional drawing, which is also required by authorities.

This method has disadvantages :

- it makes unfavourable assumptions, e.g. the centre of additional area from 2nd deck to hatchway is not the centre of whole void area in hatchway.
- it causes a tremendous amount of work
- it is the reason for poor utilization of stability criteria because the centre of cargo is assumed to be too high.

4.12 THE IMPROVED METHOD

In 1976 the author proposed a method for calculation of heeling moments including an accurate calculation of the VCG of cargo after the assumed shift.

The behaviour of grain surface is simulated by an analytical calculation which delivers the shape and moments of voids after the assumed shift.

At the LOW SIDE the maximum retained area is calculated, at the HIGH SIDE the maximum increased area.

From the voids heeling moments and centre of the cargo can be deducted:

VCG(cargo) = vert.moment of filled hold
+ vert.mom.of voids within hatch cover
- vert.moment of total voids after shift

For a manual calculation paper blanks and supporting tables were prepared.

4.13 PREPARATION OF STAB-DOCUMENTS BY CAE

The above mentioned new method enables us to prepare calculations and drawings by means of computer aided engineering (CAE). This is worth the more as it is a tremendous amount of work to do.

In the discussion of TOPE's paper in 1971 it was mentioned that this job would take 8 to 16 weeks, depending on whether only horizontal moments were taken into

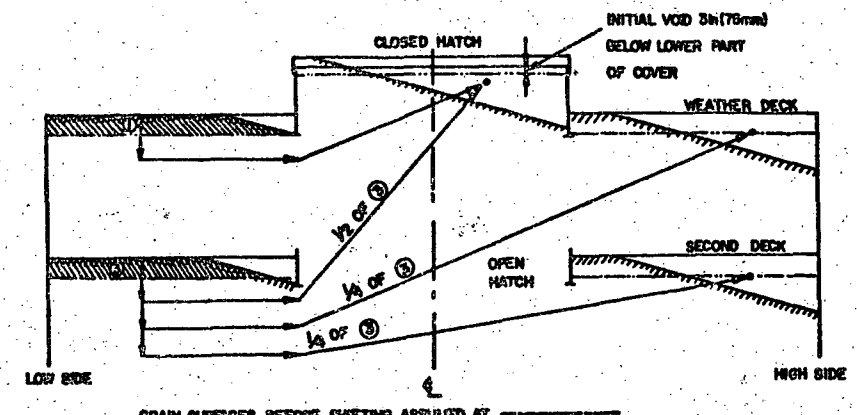

Fig.3 Principles of static pattern of grain surface behaviour, TOPE [2]

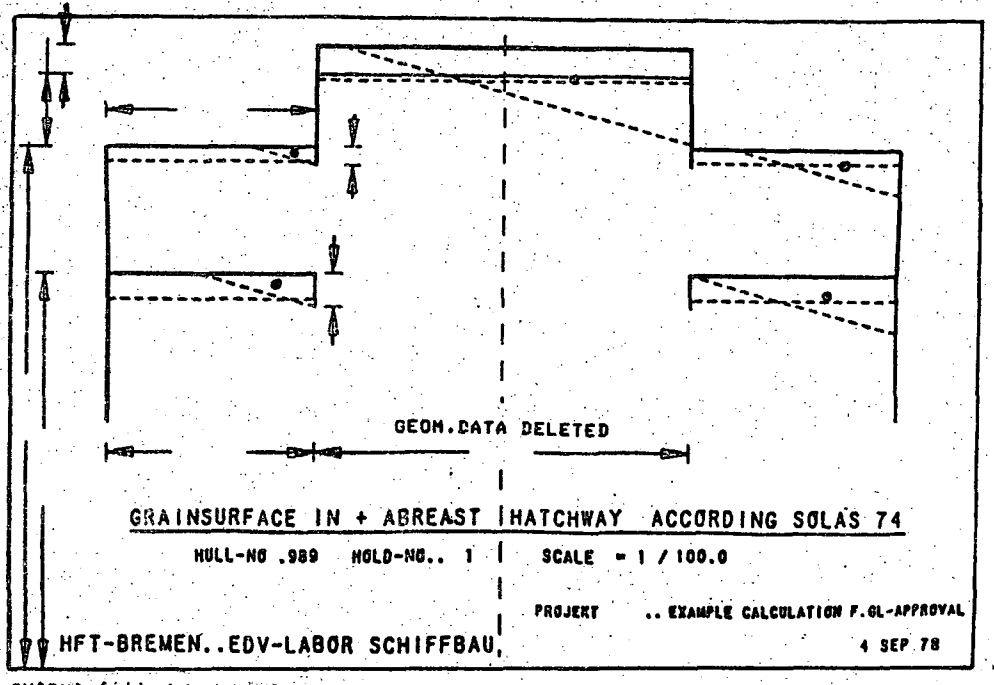

Fig.4 Plotter-output, filled hold

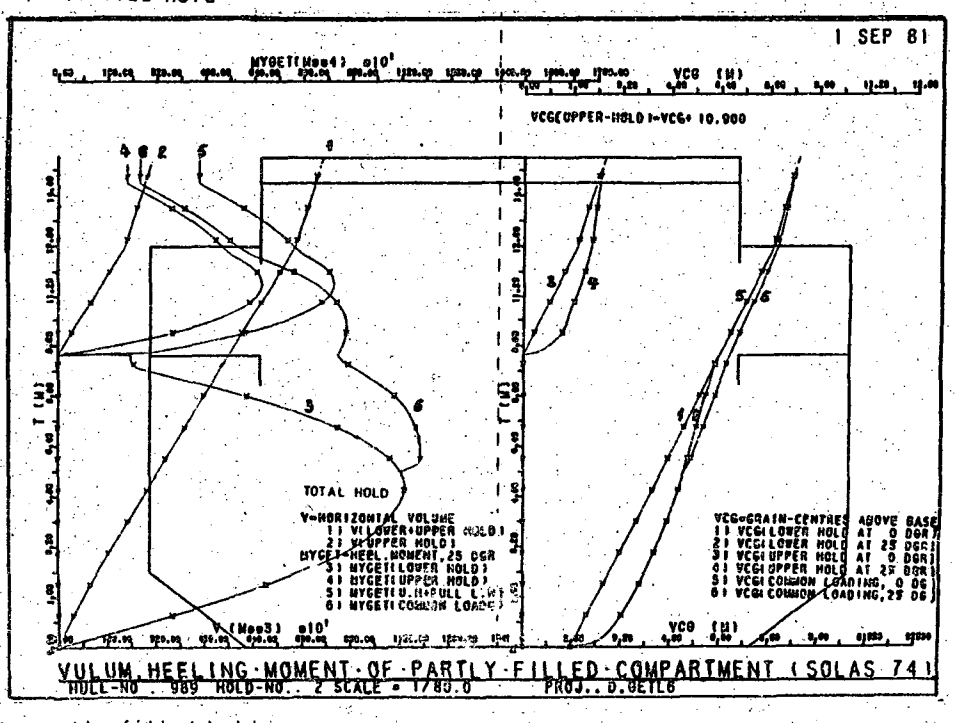

Fig.5 Plott for partly filled hold

consideration or the vertical moment of cargo before shifting was also considered. When calculating vertical moments after shift instead of this, it would take even more time.

The author prepared computer programs to do the calculations and drawings for common and separate loading, each with one section before, abaft and behind the hatchway.

These programs work for very many structural designs, including single and tween decker, with centreline division, girders, feeders, etc or without these elements.

Input data refer to steel section, longitudinal distances and to volume and centre of hold.

Feasible elements can be seen in Fig.10 and Fig.11, the illustration of input data.

The output of calculations for each section, each hold, and summerized for the whole ship is prepared in such a way that it can be checked in detail.

By means of the plotted grain section drawings (seeFig.4) the user can quickly ensure that input data are correct. They show centres for all single voids too, thus proving that the program also works for special steel design.

Before plotting these drawings on paper they can be checked at a graphical display, thus saving time and paper.

The calculation method as well as the computer programs were approved by GERMAN LLOYD in 1978.

4.14 HARD AND SOFTWARE REQUIREMENTS:

64 KB core, FORTRAN compiler,
PLOT-10-software(CALCOMP-plotter)
PREVIEW-routine by TEKTRONIX

4.15 ADVANTAGES OF NEW METHOD

SOLAS-74 gives two alternatives of assuming VCG of cargo after shift:

-If the VCG of total hold volume is used, no addition has to be made to the heeling moment for vertical shift of cargo.

-If VCG is assumed to be the centre of cargo before shift, which is much more labourous, an addition of 8% has to be made to the moment caused by transverse shift. This achieves better stability data.

When applying the accurate VCG of cargo after shift, as proposed, no addition is to be made to the heeling moment caused by transverse shift.

This method covers the actual condition best, though calling for even more calculations. It achieves smaller nominal stability loads especially for ships with structural designs which cause large voids below decks. For some ships a reduction in heeling angle of 10% and an inorease of residual area ARD of 30% was observed.(see Fig.6)

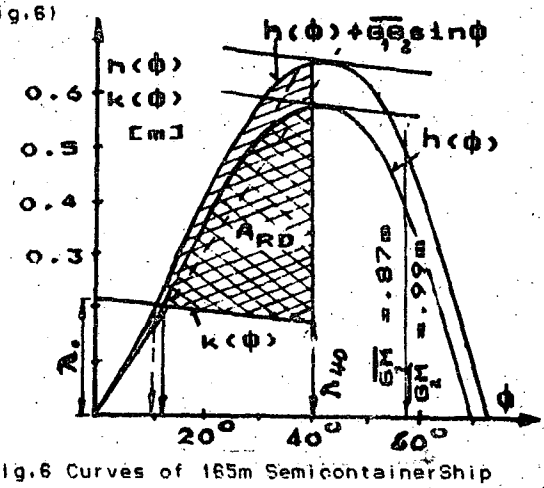

Fig.6 Curves of 165m SemicontainerShip

By doing the calculations by means of computer program the risk of failures can be reduced and time and costs can be saved.

4.16 CONSTRAINTS ON THE NEW METHOD

Better utilization of the stability criteria by applying the new method is only advisable when it is accompanied by a cautious choice of the input data for the program. Moreover, weight and centres of loading condition, as well as considering of free surfaces should be done for the worst condition to be expected during the voyage, which is in general when ballasting is begun after consumption of half of the fuel.

4.2 MOMENTS OF PARTLY FILLED HOLDS

4.21 GENERAL

According to SOLAS-74 a wedge angle of 25 degrees has to be assumed. Vertical shift is accounted for by adding 12% of the heeling moment due to the transverse shift. Diagrams or tables of volume, VSG and expected heeling moment for partly filled compartments need to be prepared. Data have to be provided for levels of grain surface every 10 cm in height.

These data could be determined by equalization the shifted areas as indicated in Fig.7.

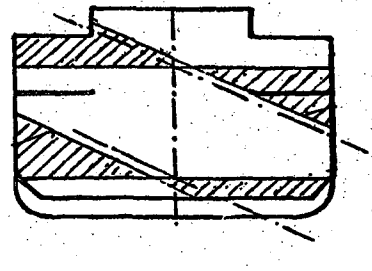

Fig.7

4.22 ANALYSIS OF VERTICAL SHIFT MOMENT IN CASE OF UNLIMITED VERTICAL SHIFTING

According to Fig.8 the grain level rises or falls at the boundary by h=(B/2)tan(25).

And hence the area of the triangle A is

A = (B**2 / 4) * tan(25)

** is the symbol for "power of"

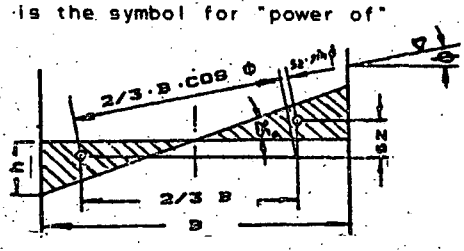

Fig.8 Vertical unlimited shift of cargo

When the surface shifts the centre of the triangular area changes vertically by (2/3)h=(B/3)tan(25) and transversely by (2/3)B.

Given a heeling angle ϕ for inclination of the whole compartment the area moments can be defined as follows:

MYA = Moment of Area due to shift to Y

MYA = (1/12)(B**3)*tan(25)*cos(ϕ)

MZA=Moment of Area due to shift to Z

MZA = (1/2')(B**3)*tan(25)*sin(ϕ)

hence: MZA/MYA = 0.5*tan(25)*tan(ϕ)

if ϕ = 0 (deg) then MZA/MYA=0

if ϕ = 12 (deg) then MZA/MYA=0.05

if ϕ = 40 (deg) then MZA/MYA=0.20

The Requirement of SOLAS to increase the transverse moment by 12% results in a greater heeling angle, but about the same ARD.

4.23 ANALYSIS OF VERTICAL SHIFT MOMENT IN CASE OF LIMITED VERTICAL SHIFTING

When considering that any compartment has a bottom and a deck we are aware of the limitation of the heeling moment in the upper and lower part of hold.(see Fig.9)

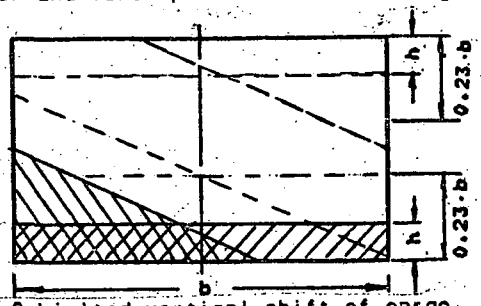

Fig.9 Limited vertical shift of cargo

As derived in [3]

$$ZA/MYA = \frac{0.322*(h/b)**0.5 - 0.5*(h/b)*\tan(\phi)}{0.5 - 0.69*(h/b)**0.5}$$

h / b	0.23	0.11	0.06
MZA/MYA	5%	4%	3%

Result: Unlimited shifting take place only when h is greater than 0.23xb or less than 0.77xb.

That means, that for half of the loading height the required addition for vertical shift MZA=0.12xMYA is too large so that an accurate evaluation of VCG of cargo is advantageous.

4.24 HEELING MOMENTS IN PARTLY FILLED HOLDS

The author wrote a program to analyse and document the behaviour of grain in partly filled ship compartments assuming a 25 degree shift.

Results for the conditions before and after shift were plotted for each section calculated and the total hold.(see Fig.5)

EXPLANATION OF Fig.5

Curves 1 and 2, on the left, show hold volume V in cubic meter after separate or common loading to the sounding height T.

Curves 3 through 6 ,on the left, show MYGET, the volumetric heeling Moment of Grain caused by transverse shift (Y-direction) for common and separate loading.

From curve No.6 it is apparent that grain will begin to flood into the tween deck when lower hold is filled to about half.

Curves 1 through 6, on the right, show the vertical centre, VCG, of cargo before and after shift.

These diagrams are also checked at a graphical display and plotted by CALCOMP plotter.

5.0 IMPROVING THE STRUCTURAL DESIGN

5.1. PROBLEM AND MEANS OF SOLUTION

5.11 GENERAL

The heeling moments caused by shifting of grain are neither considered during project phase nor during structural design in general.The reason for this is that calculation of these moments seems to be complicated and their results not so important. The preparation of safety documents for the carriage of grain is done at a later stage and brings difficulties very often.

There is a demand for a simple method to estimate heeling moments in project stage and for know-how to consider the shifting of grain during structural design.

It was the author's objective to improve

this situation. He analysed structural elements with regard to their influence on the heeling moments and gives advice below on how to reduce heeling moments by adjusting structural design to the behaviour of grain. Some of his points are also of use for ships already in service.

5.12 CRITERION OF COMPARISON. ESTIMATION OF HEELING MOMENT.

A specific value of the area moment caused by transverse shift of cargo area, MYA, was defined as the criterion to compare different structural designs :

CMYA = 100 * MYA / B**3

This specific moment was calculated for very many structural designs, for each deck and for whole sections.For a judgement of the quality of total hold, specific moments were calculated also on an average of total hold. (B=ships bredth)

By use of specific moments of similar design heeling moments of shifted grain can be estimated by the following formula..

MYGET=RHO*SUM [l(i)*CMYA(i)*B**3 /100](mt)

RHO = density of grain (t/m**3)

l(i)= legth with same section

5.13 SURVEY OF DESIGNS INVESTIGATED

Three different tweendeckers were investigated and the following average specific areamoments were calculated for commom loading.

S1. 165m-Semicontainership, 1976: CMYA=0.79
S2.. 80m-Coaster......, 1957: CMYA=0.61
S3. 126m-General-cargoship, 1970: CMYA=1.10
S3a 151mShip,S3,linear distortion CMYA=1.21

Results show that specific areamoments are of the same order for different ships. They depend on structural design and of ship size. Specific moments for separate loading are somewhat greater as outlined later.

Starting from the above three ships the structural design elements were varied. More than 250 different deck sections were calculated and their specific moments presented in [3].

In this paper only some general statements for the most important elements are given. In paragraph 5.5 a diagram shows the total reduction of moments to be achieved for ship S1.

5.14 SURVEY OF PARAMETERS INVESTIGATED

The design items investigated are shown in Fig.10 and 11, where input data for calculation programs for filled holds are demonstrated. Any item can be deleted by setting it to zero.

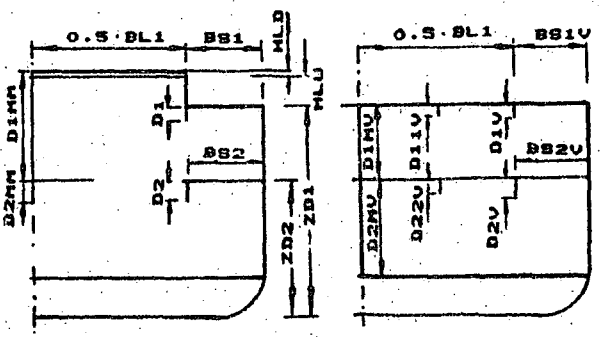

Fig.10 Program input data, sectional design

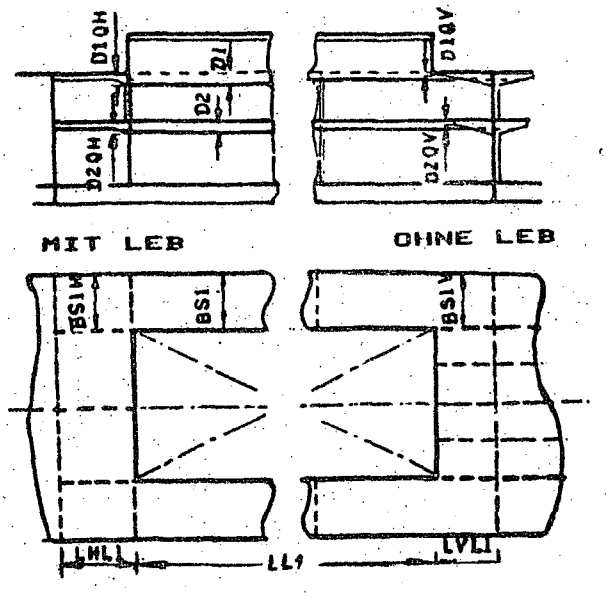

Fig.11 Additional program input data

5.2 REDUCTION OF MOMENTS IN HATCHWAY

Heeling moments of filled spaces in and abreast hatchways can be reduced by using the following measures.

5.21 SEALING OF HATCHCOVER

This measure is to avoid shifting of grain into the inner part of hatch cover. Efficiency of this measure depends on the relation of breadth of hatch to breadth of hold = BL1/B ,and relation of height of hatchcover to breadth of hatch = HLD/BL1.

For ships with wide hatches (BL1/B=0.68) and high hatch covers (HLD=BL1/20), as given with ship S1, the heeling moment could be reduced: by 50% for common loading; and for separate loading by 61%

for the upper and 67% for the lower hold.
For ship S3 with narrow holds (BL1/B=0.36) and normal height of hatch cover (HLD=BL1/25), this measure is much less efficient. Here the reduction was: 2% for common loading and for separate loading 7% for the upper and 19% for the lower holds.
Conclusion:
Since sealing of hatchcovers at lower edge increases their building costs by about 5% this measure should be considered especially for ships with wide hatchways, and for those lower holds only, which have to be loaded separately in the carriage of heavy grain, when some upper holds have to remain empty.

5.22 SMALLER HATCH SIDE GIRDERS

The reduction of hatch side girder depth is of interest for ships with narrow hatches, for instance S3. A 25% reduction of the depth of hatch side girders results in a 11% reduction in heeling moment. A 50% height reduction results a 27% reduction of moment.
A reduction of girder depth can be achieved by the following alternative designs: two web girder, consol brackes, double hatches.

5.23 CENTRELINE DIVISION

IN CASE OF COMMON LOADING

For wide hatches (BL1/B=0.68) a centreline division, which is extending down to the lower edge of hatch side girder of 1st deck, can reduce the moment by 49% respectively 62% if it extends down to the hatchside girder of 2nd deck.
For narrow hatchways (BL1/B=0.36) reduction of moment was 40% resp. 16%.

IN CASE OF SEPARATE LOADING:

For wide hatchways and divisions down to hatchside girders reduction of moment was 58% in the upper and 9% in the lower hold.
With divisions down to 0.6 m below hatch side girder reduction of moment was 64% and 60%, respectively.
In case hatch covers to be sealed, reduction of heeling moment was 45% less.

CONCLUSION

Centreline divisions in or below hatchways can reduce heeling moments intensely. They can be realized by double hatch design, and should extend down to 0.6 m below 2nd deck hatch side girder.
In case hatchway is too narrow for double hatch design, centreline division may be realized by special hatch covers, folded up into this plane.

5.24 GRAIN FEEDERS IN UPPER HOLD

Grain feeders can reduce heeling moments of the lower hold
- in narrow hatches (BL1/B=0.36) by 45%
- in wide hatches, (BL1/B=0.56) by 38%

The grain feeders can be arranged by special side-folding hatch covers.

5.3 REDUCING MOMENTS, FILLED SPACES BEFORE AND ABAFT HATCHWAYS.

5.31 PARAMETER OF VOID DEPTH

Void spaces have to be calculated with elements shown in Fig.10 and 11. In space between continuation of hatch side girders the depth of the hatchend beam D1QV and the longitudinal understow LVL1 have to be used for calculation of void depth.
For the two outside parts, the greater of longitudinal or tranverse understow (LVL1 or BS1V) and the greatest depth of hatchside girder, its continuation or of hatch end beam has to be considered for the void depth.
Reduction of heeling moments can be achieved by smaller void depth and/or greater longitudinal girder to prevent grain surface from shifting.
Heeling moments can be reduced by measures outlined as follows:

5.32 SMALLER HATCHEND BEAMS

The relevant girder height depends on type of hatch construction (see Fig.11) On the left side of this drawing we see a hatch-end-beam-design. (In Germany it is called SCHELLENBERGER-Luke). The load of the hatch is transfered to hatch end beams, which may be supported by centreline bulkheads or stanchion.
On the right side the load of the hatch is tranferred by continuations of hatch side girders to the bulkhead.
This more modern design was employed with ship S1. By reducing depth of hatchside coaming below deck, D1Q and D2Q, to 82% resp. 56% of depth of side girder D1 resp. D2 heeling moment could be reduced by 16% resp. 37%.
In case the hatchside coamings would be reduced to D1Q=0.46xD1 resp. D2Q=0.28xD2 and supported by consol brackets, which reduce shifting, reduction of moments would be 43% respectively 72%.
It must be mentioned that in case of such small hatchend coamings the tortional stress has to be checked.

5.33 LONG.GIRDER BETWEEN HATCHWAYS

Longitudinal girders just before and abaft hatchways reduce the shift of cargo in this region. Fig.12 obviously shows how shifting of void spaces is reduced by 5 different arrangements of 3 longitudinal girders inboard of the continuation of hatchside girders.

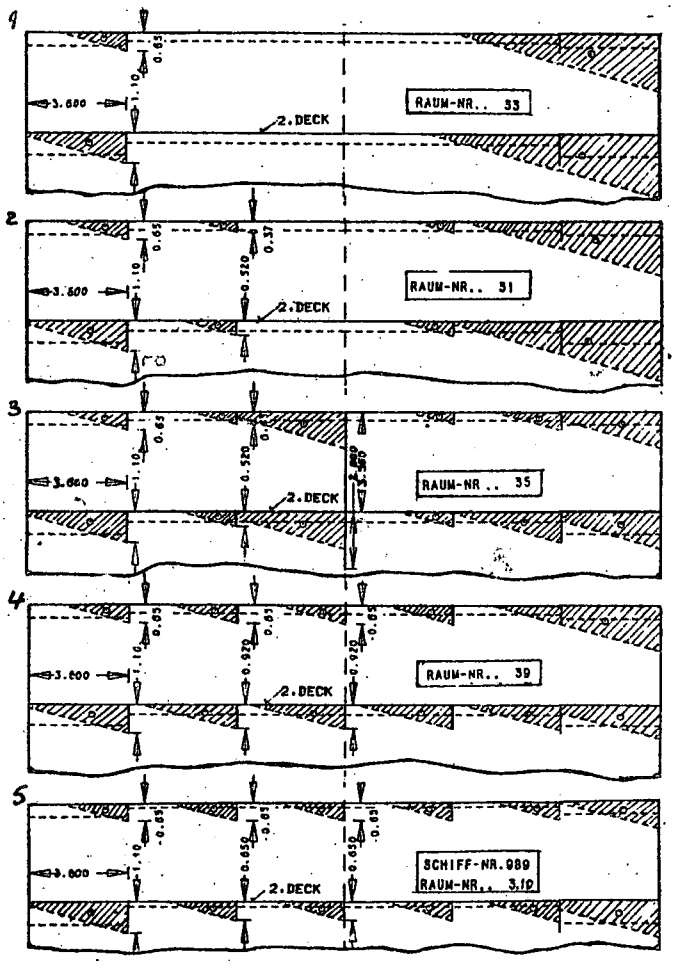

Fig.12 Longitudinal girder between hatches. Sketch 2 for No 31 hold shows 2 additional girders with about half of the depth of hatchside girder continuation. This was the design of the yard and achieves a 7% resp. 13% additional reduction in moment in 1st respectively 2nd deck.

Sketch 3 shows for No.35 hold the functioning of additional centreline bulkheads ,which increase reduction of moments in 1st resp. 2nd deck to 61% resp.69%.

Sketch 4 shows for No.39 hold the efficiency of 3 additional girders with depth of hatchside girders, reducing the moment by 36% resp. 76%.

Sketch 5 demonstrates how these three girders work when void depth is reduced by smaller hatchend coamings and thus moments are reduced by 72% respectively 77%.

Consideration of side girders as outlined above was accepted by several authorities with the exception of LR. This classification society accept longitudinal girders only if they extend down to .6 m below the voids.

5.34 CENTRELINE DIVISION

The hatchend beam design causes large voids and moments. These moments can be reduced by 60% resp. 56% by longitudinal division in lower resp. upper hold.

A centreline girder below 2nd resp. 1st deck with depth of hatchside girder can reduce moment by 12% resp. 25%.

5.4 SIGNIFICATION OF LONG.UNDERSTOW

The specific areamoments before and abaft the hatchway are 20% to 36% greater than those below hatchways.

In case of the semicontainership it was even 160% greater when hatchcovers were sealed.

In case of ship S3 it was 85% greater if a centreline division was arranged in the lower hold only and 21% less if bulkheads were arranged in upper and lower hold.

CONSEQUENCE: The longitudinal understow distance should be as small as possible.

5.5. TOTAL REDUCTION OF MOMENTS

Total reduction of heeling moments for sections and full holds of semicontainership S1 was represented in diagrams Fig.13 and 14.

From these diagrams the specific area moments in way of hatch and before and abaft of it can be seen as well as their longitudinal extension.

Reductions of the heeling moments by the different measures are presented graphically. The area of these diagrams represent the whole volumetric heeling moment.

Fig.13 represents a 58% reduction of moment by sealing of hatchcover, reduction of hatchend girders and arrangement of three longitudinal girders just before and abaft upper and lower hatchway.

Fig.14 represents a 62% reduction of moment by arrangement of longitudinal divisions only.Inside the hatchway it can be done by a double hold design.

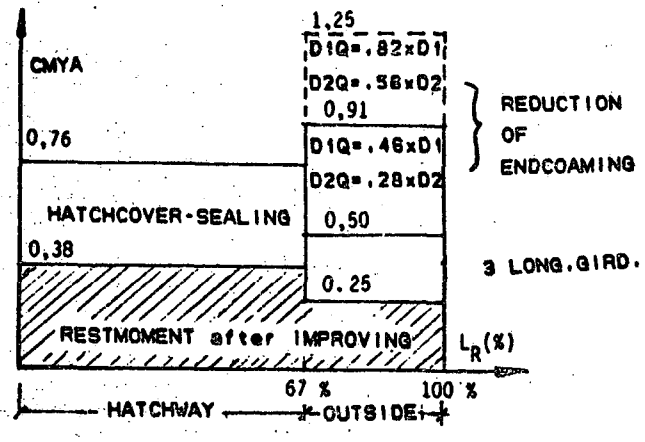

Fig.13 Improvements without long.divisions

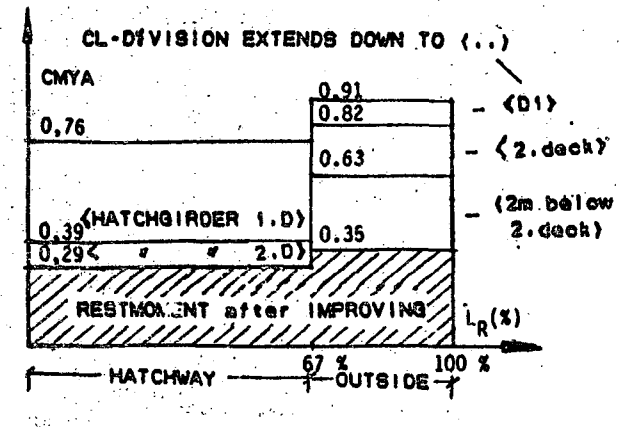

Fig.14 Improvements by long. divisions

6. IMPROVEMENT OF LOADING

By adjustment of the loading to the SOLAS-74 rules and by use of general know how regarding part loading, the securing of grain cargo can be reduced and consequently dry cargo ships improved in competition.

6.1 SEPARATE LOADING FULL HOLDS

SOLAS-74 enables dry cargo ships to carry grain in separate loaded upper and lower holds without securings.

Since in this case there is shifting of cargo in upper and lower holds the total heeling moment exceeds that of common loading, for instance with ship S1 by 44%. Moreover, separate loading causes additional costs in trimming the cargo.

So the shelterdecker measurement,with closed hatches in tweendecks, will hardly be good for the carriage of full grain loadings.

But leaving empty some upper holds is a very effective method to improve initial stability, GM, to such an extent that securing of cargo surfaces can be avoided.

In case of ship S1 cargo capacity could be increased by 48%.

6.2 IMPROVING PARTIAL LOADING

The actual grain cargo capacity can be improved by use of the following techniques for partly filled holds:

6.21 CLOSING OF TWEEN DECK HATCHES

In case a lower hold is filled more than half, tweendeck hatchcover should be closed. Curves 3 and 6 of Fig.9 demonstrate that up to 75% of the moment could be reduced by that.

6.22 LONGITUDINAL DIVISION

A centreline division on total length of hold can reduce the moment by 75%. That is indeed very effective but in most cases not possible.

To have centreline divisions only before and abaft the hatchway is of no effect for modern ships with relatively long hatches. SOLAS-74 calls for consideration of a reduced length of bulkhead because cargo shifts around such divisions.

6.23 USING No1 HOLD FOR PARTLOAD

Using No 1 hold for partly filling is advantageous because this hold is not so wide (the specific area moment is about 30% less) and it is not so long.

6.24 GRAIN FEEDERs IN UPPER HOLD

In case a feeder can be arranged in way of hatch in the upper hold, for instance by side folding hatchcovers having the breadth of the hatch BL1, the specific area moment can be reduced ..

by the factor (BL1 / B)**3

7. CONCLUSION AND ACKNOWLEDGEMENTS

Since the author did not get any support ,nor any discharge from his lecturing duties of 18 hours a week,this research took more than six years and actuality of the ships treated has suffered therefrom.

The author is deeply grateful for advice and continous encouragement of Prof.Dr.-Ing.Schneekluth of RWTH Aachen and Prof.Dr.-Ing.Nowacki of TU Berlin.

Financial support of the Foreign Ministry and of Deutsche Forschungs Gemeinschaft to attend the Third Stability Conference is gratefully acknowledged.

8. NOMENCLATURE

A	(m**2)	sectional area of void
ARO	(m rad)	residual stability area
b	(m)	distance to comp.boundary
B	(m)	ships breadth
LB1	(m)	breadth of hatch,1.deck
BS1/BS2	(m)	width of 1. resp.2.deck outside of hatchway
BS1V/BS1H		same before/aft hatchway
CMYA	(-)	specific area moment
d	(m)	depth of girder
D1/D2	(m)	depth of hatchside girder of 1. resp. 2.deck
D1V/D1H		same before/abaft hatch
D1Q	(m)	depth hatchend girder
GM	(m)	metacentric height
h(O)	(m)	righting arm
HLD	(m)	height of hatchcover
HLU	(m)	heiht of hatchcoaming
K(O)	(m)	heeling lever
L	(m)	length of ship
LL1	(m)	length of hatch,1.deck
LVL1/LHL1	(m)	length before/abaft hatch
MK	(m**4)	volumetric heeling moment
MYGET / MZGET	(m**4)	vol.grain heeling moment due to transv./vert.shift
MYA / MZA	(m**3)	areamoment " " "
RHO	(t/m**3)	density of grain
ALPA	(degree)	wedge angle of cargo
ϕ	(degree)	heeling angle

9. REFERENCES

[1] IMCO,London, SOLAS 74,Intern.Convention

[2] TOPE,Nav.Architecture1971,"Carriage of Bulk Grain without Temorary Fittings"

[3] FEEDER,Diss.RWTH Aachen,1982:
"Die Stabilitaetsbelastung von Trocken-Frachtern durch uebergehendes Getreide"

[4] FEEDER,HANSA 1984,"Verbesserung der Getreideladefaehigkeit von Trockenfrachtern"

10. ON THE AUTHOR

The author studied Naval Architecture in Hannover and Hamburg and received his diploma in 1960. He worked as a naval architect at Flenderwerke,Luebeck, Howaldtswerke,Kiel and HDW, Hamburg.

In 1972 he becames Professor of Ship Hydrostatics, Informatics, Computer Applications and Operations Research at the HOCHSCHULE BREMEN. Beside his lectures he manages the Laboratory for Electronic Data Processing.

In 1982 he received the degree Dr.-Ing. of the RWTH AACHEN.

Third International Conference on Stability of Ships and Ocean Vehicles, Gdańsk, Sept 1986 STAB'86

STABILITY PARAMETERS OF SHIPS INVESTIGATED BY MEANS OF DISCRIMINANT ANALYSIS

M. Jagiełka

SUMMARY

The paper includes:

1. A concise description of discriminant analysis in the range sufficient for achieving the established purpose.
2. A discussion of the results of this analysis, based on a sample of 166 casualties /the cases are included in original IMO list/. The analysis of stability parameters was carried out for the ships at time of loss and for the same ships at fully loaded arrival condition.
3. Proposals of stability criteria as discriminant functions, separately and jointly for cargo ships and fishing vessels.

INTRODUCTION

In 1966 delegations of the Federal Republic of Germany and Poland to IMCO presented the analysis of statistical data concerning stability accidents [1] .

In 1984 the Institute of Ship Research, Technical University of Gdańsk was offered to repeat this analysis including new statistical data complied by IMO. Paper [2] submitted to IMO in 1985 included the results of this analysis for the extended population /166 capsized ships/. In order to make a direct comparision possible, the analysis was prepared in exactly the same way as previously i.e. by comparison of respective histograms and intersecting distribuants.

Simultaneously, having such a large sample of casualty data at our disposal, some modern methods of analysis were employed for their treatment.

At the same time Krappinger [3] published a paper concerning the determination of the parameters of the righting straightening arm curve by means of the discriminant analysis. This paper may be considered as the first attempt to put into shipbuilding practice this powerful method.

The present paper gives some conclusions in consequence of applying the discriminant method to the statistical analysis of the above mentioned sample of casualty records, particularly taking into consideration the question of critical parameters of the righting arm curve.

1. METHOD OF INVESTIGATION

Two separate populations of ships are compared: The population of lost ships is considered to represent unsafe ships [1]. The second population represents ships in arrival condition [2]. Some parameters of these ships are chosen for investigated characteristics.

As an example an investigated characteristic is the righting lever arm for 20^0 heel ($x_j = GZ_{20}$). The height $x_{ij}^{(k)}$ of a single column of a histogram is the value of the j-th characteristic (GZ_{20}) for the i-th ship of population k ($k=1,2$).

R.A. Fisher /1936/ adopts discriminant α as a measure of discrimination of the two populations.

$$\alpha = \frac{\left(\bar{x}^{(2)} - \bar{x}^{(1)}\right)^2}{\frac{1}{2}\left(v_x^{(2)} + v_x^{(1)}\right)}$$

in which

$\bar{x}^{(k)} = \frac{1}{n_k}\sum_{i=1}^{n_k} x_i^{(k)}$ - is the mean value of characteristic x in the k-th population

$v_x^{(k)} = \frac{1}{n_k - 1}\sum_{i=1}^{n_k}\left(x_i^{(k)} - \bar{x}^{(k)}\right)^2$ variance of x

n_k - number of elements in the k-th population

The compared populations demonstrate the better discrimination the higher the

difference of their mean values is and the greater concentration of their values around their mean values is.

Thus discriminant α determines the measure of differentation of the two populations regarding the given parameter. In this way this adds a quantitative value to the discrimination and thereby makes it quantitative possible to compare the analysis.

In order to investigate simultaneously several (m) characteristics ($x_1, x_2, \ldots, x_m$) we assume so-called criterion function

$$z = c_0 + \sum_{j=1}^{m} c_j x_j$$

and maximize

$$\alpha_z = \frac{\left(\bar{z}^{(2)} - \bar{z}^{(1)}\right)^2}{\frac{1}{2}\left(v_z^{(2)} + v_z^{(1)}\right)}$$

where

$$\bar{z}^{(k)} = \frac{1}{n_k}\sum_{i=1}^{n_k} z_i^{(k)} = c_0 + \sum_{j=1}^{m} c_j \bar{x}_j^{(k)}$$

$$v_z^{(k)} = \frac{1}{n_k - 1}\sum_{i=1}^{n_k}\left(z_i^{(k)} - \bar{z}^{(k)}\right)^2 = \frac{1}{n_k - 1}\sum_{i=1}^{n_k}\left[\sum_{j=1}^{m} c_j\left(x_{ij}^{(k)} - \bar{x}_j^{(k)}\right)\right]^2$$

After comparing to zero, derivatives $\frac{\partial \alpha_z}{\partial c_j}$ and imposing condition $\bar{z}^{(2)} - \bar{z}^{(1)} = \frac{\alpha}{2}$ the following system equations is obtained:

$$\sum_{j=1}^{m} c_{j'}\theta_{jj'} = \bar{x}_j^{(2)} - \bar{x}_j^{(1)} \equiv \bar{x}_j$$

where:

$$\theta_{jj'} \equiv \frac{1}{2}\left(\theta_{jj'}^{(2)} + \theta_{jj'}^{(1)}\right); \quad \theta_{jj'}^{(k)} \equiv \frac{1}{n_k - 1}\sum_{i=1}^{n_k}\left(x_{ij}^{(k)} - \bar{x}_j^{(k)}\right)\left(x_{ij'}^{(k)} - \bar{x}_{j'}^{(k)}\right)$$

from which one can find coefficients c_j, determining what share of x_j characteristic should be in the criterion function z to maximize discriminant α for the two populations.

The imposed condition $\left(\bar{z}^{(1)} - \bar{z}^{(2)} = \frac{\alpha}{2}\right)$ normalizes the function z in such a way that the distance between the mean values $\bar{z}^{(1)}$ and $\bar{z}^{(2)}$ is equal to α_{max} and results in $z = 0$ situated exactly in the middle of these mean values.

From this it follows

$$c_0 = -\frac{1}{2}\sum_{j=1}^{m} c_j\left(\bar{x}_j^{(2)} + \bar{x}_j^{(1)}\right)$$

$z = 0$ may be taken as a criterion ($z > 0$ - safe ships). This criterion may be easily mitigated or sharpened just by changing only the free term c_0.

The value α may be obtained from formule:

$$\alpha = \bar{z}^{(2)} - \bar{z}^{(1)} = \sum_{j=1}^{m} c_j\left(\bar{x}_j^{(2)} - \bar{x}_j^{(1)}\right) \equiv \sum_{j=1}^{m} c_j \bar{x}_j$$

The analysis of the obtained discriminant functions is an extremely difficult task. Even the leaders of multidimensional variation analysis, whose idea is that of discriminant analysis, vary on the subject of the means of its precise interpretation. The paper [3] includes in principle sufficient description of the way of analysing the obtained results applicable to investigate the ships stability parameters.

The following observations are worth noticing (more of them are contained in the author's paper [4])

1/ α increases together with the number of characteristics taken into account, so

$$\alpha_{p+1} - \alpha_p = \frac{\begin{vmatrix} \theta_{11} & \theta_{12} & \ldots & \theta_{1p}\bar{x}_1 \\ \theta_{21} & \theta_{22} & \ldots & \theta_{2p}\bar{x}_2 \\ \ldots & \ldots & \ldots & \ldots \\ \theta_{p1} & \theta_{p+1,2} & \ldots & \theta_{p+1,p}\bar{x}_{p+1} \end{vmatrix}^2}{W_p \; W_{p+1}} = \frac{c_{p+1,p+1}^2}{W_p W_{p+1}} \geq 0$$

because each main determinant W in the equation system is also positive.

2/ Although the calculation of all 2^m discriminant functions doesn't cause any great difficulties in the age of computers, nevertheless it is advisable to limit the number of parameters taking part in discrimination and to seek the ones which are most significant.

The test of reliability with respect to the obtained information (if taking into consideration q of m out of all available parameters) may be a quantile for $(m-q)$ and $(n_1 + n_2 - m - 1)$ degrees of freedom

$$F = \frac{n_1 + n_2 - m - 1}{m - q} \cdot \frac{n_1 n_2 (\alpha_m - \alpha_q)}{(n_1 + n_2)(n_1 + n_2 - 2) + n_1 n_2 \alpha_q}$$

In a similar way many other hypotheses may be verified e.g. the ones concerning individual coefficients of discriminant functions.

3/ An increase of the number of characteristics by one, changes the coefficient in the following manner

$$c_{jp+1} = c_{jp} - \frac{\begin{vmatrix} \theta_{11} & \theta_{12} & \ldots & \theta_{1j-1} & \theta_{1p+1} & \theta_{1j+1} & \ldots & \theta_{1p} \\ \theta_{21} & \theta_{22} & \ldots & \theta_{2j-1} & \theta_{2p+1} & \theta_{2j+1} & & \theta_{2p} \\ \ldots & \ldots & & \ldots & \ldots & \ldots & & \ldots \\ \theta_{p1} & \theta_{p2} & \ldots & \theta_{pj-1} & \theta_{pp+1} & \theta_{pj+1} & \ldots & \theta_{pp} \end{vmatrix}}{W_p \; W_{p+1}} c_{p+1,p+1}$$

2. DATA FOR THE ANALYSIS

2.1. Intact stability casualty records at IMO sample of 166 ships.

A set of data concerning the stability parameters and circumstances of the casualty /place, time and weather conditions/ is included in [2] .

The parameters of the same ships at time of loss and in fully loaded homogeneous arrival conditions were compared and discriminated. In such an approach to the subject there is no problem in choosing the adequate comparable populations but there appears the problem of small differences - relatively small discrimination a priori, causing certain numerical difficulties.

The sample was divided into two categories: cargo ships and fishing vessels. The analysis was carried out for each population separately and for both of them taken together (C & F) . A general view of Fig. 1. confirms the significance of this decision.

Furthermore, a separate analysis made with regard to nondimensional parameters for the same populations of ships as above (the effect of which is best seen in Fig. 1. for sample 2.3) .

2.2. To draw some comparable conclusions I shall present some average data corresponding to populations used in the above mentioned paper [3] .

2.3. Also for the same purpose there was presented a sample from [5] diploma work treated in a similar way as in p.2.1.

3. ANALYSIS OF DATA

The most characteristic property of the above 3 samples is the difference of the ship dimensions in the discriminated populations. As it was noted in 2.1. sample the problem does not exist because the same ships are subject to comparison. In 2.2. sample the mean length of lost unsafe ships is 49,2 m and for safe ships 83 m.

Though it cannot be stated that the righting arm curve parameters are in proportion to the length of ships nevertheless it may be considered that such a great difference of dimensions of the ships under consideration is the reason of a great a priori discrimination.

There is quite a different relation between the dimensions of the compared ships in sample 2.3. where the unsafe ships were larger L=62m than the safe ones L=42m . As it is to be expected the values of GM as well as the values of the righting arm curve are larger for the lost ships than the safe ones. After dividing the GM values as well as the righting lever arm by the length of a ship values decrease and are below the similar values referring to safe ships. Thus to conclude the stability parameters would prove to be quite opposite if they were not non-dimensional. On the other hand using the non-dimensional parameters for a great range of ship dimensions is not safe. The analysis of 2.1. sample made separately for cargo ships L=52m and for fishing vessels L=26,3 m seems to be the most reliable. As a joint conclusion from the preliminary analysis for all 3 samples may be a remark that in case of cargo ships smaller metacentric height is safer whereas for all ships a greater range of the righting arm curve.

4. ANALYSIS OF THE RESULTS

The analysis of the obtained results is on the one hand a simpl task and on the other a complicated one.

One obtains, as a result of the application of the discriminant analysis for each combination of characteristic ships and the question may be considered as solved.

However, a more detailed analysis of the discriminants and the individual coefficients may be the source of considerable qualitative conclusions very often inexplicit. The analysis carried out with reference to sample 2.1. concerned 14 characteristics - 10 stability parameters, 3 parameters of sea states and the length of the ship. It seems that some parameters are merely of an interesting piece of information as it is difficult to determine their values in population[2]. We know how many and which ships were lost, e.g. in winter or wind force condition but nothing can be said regarding the opposite population (the ships being in service) .

The available data with respect to these characteristics for unsafe ships may be used indirectly to determine other characteristics, e.g. assuming an arbitrary con-

stant height of wave h in population [2] one obtains the following criterion functions for combination with individual values of GZ

$$z = c_o + 2,11\ GZ_{10} - 0,2h$$
$$z = c_o + 1,50\ GZ_{20} - 0,2h$$
$$z = c_o + 0,90\ GZ_{30} - 0,2h$$
$$z = c_o + 0,16\ GZ_{40} - 0,2h$$

From each of these functions we may draw a trivial conclusion that each GZ value should increase while the h value decrease. Though after a combined comparison of these functions one may note that the most responsive for the height of waves are the values of the righting arm curve for small angle of heel.

The presentation of all the obtained conclusions is impossible as well as of no use. I confine myself only to presentation of several selected discriminant functions. Each of these functions may serve as criterion of the ship stability.

CARGO SHIPS dimensional

$$z = -6,92 - 7,0\ GM_o + 73,5\ GZ_{20} - 34,2\ GZ_{40} + 0,243\ \theta_m - 0,00168\ \theta_v \quad (\alpha = 3,37)$$

$$z = -4,45 + 5,05\ GZ_{10} - 9,53\ GZ_{40} + 0,074\ \theta_m + 0,04\ \theta_v + 17,02\ e \quad (\alpha = 1,48)$$

$$z = -4,59 - 2,67\ GM_o + 21,9\ GZ_{10} - 9,0\ GZ_{30} + 4,0\ GZ_m + 0,0195\ \theta_m + 0,07\ \theta_v + 2,4\ e \quad (\alpha = 1,45)$$

CARGO SHIPS non-dimensional

$$z = -5,98 - 152,3\ GM_o + 1641,3\ GZ_{20} - 1097\ GZ_{40} + 0,176\ \theta_m + 0,026\ \theta_v \quad (\alpha = 2,3)$$

$$z = -4,13 + 23,3\ GM_o - 1126,6\ GZ_{40} + 0,16\ \theta_m + 1874\ e \quad (\alpha = 1,43)$$

$$z = -6,0 + 286\ GZ_{10} - 1087\ GZ_{40} + 0,143\ \theta_m + 0,039\ \theta_v + 1765\ e \quad (\alpha = 2,01)$$

$$z = -3,16 - 75,38\ GM_o + 695,1\ GZ_{10} + 196\ GZ_{30} - 319,1\ GZ_m + 0,05\ \theta_m + 0,035\ \theta_v - 27,6\ e \quad (\alpha = 1,28)$$

FISHING VESSELS dimensional

$$z = -0,34 + 3,2\ GM_o + 11,41\ GZ_{20} - 2,12\ GZ_{40} - 0,0085\ \theta_m - 0,053\ \theta_v \quad (\alpha = 0,60)$$

$$z = -2,64 + 31,4\ GZ_{10} - 2,08\ GZ_{40} - 0,025\ \theta_m - 0,048\ \theta_v + 11,8\ e \quad (\alpha = 0,67)$$

FISHING VESSELS non-dimensional

$$z = -0,847 + 104\ GM_o + 186\ GZ_{20} - 234\ GZ_{40} + 0,028\ \theta_m - 0,045\ \theta_v$$

$$z = -1,36 + 46,6\ GM_o - 318\ GZ_{10} - 35,6\ GZ_{30} - 25,5\ GZ_m + 0,02\ \theta_m + 0,0044\ \theta_v + 413,7\ e \quad (\alpha = 0,3)$$

$$z = 0,334 + 400\ GZ_{10} - 64,45\ GZ_{40} + 0,0013\ \theta_m - 0,044\ \theta_v + 219\ e \quad (\alpha = 0,46)$$

The following tendencies being the general conclusions of the partial analysis for stability parameters may be noted:

a/It is advisable to tend to the reduction of metacentric height (the highest admissible value of $GM_o \approx 0,6$ m or $GM_o/L \approx 10^{-2}$ for cargo ships)

b/ It is advisable to increase the range of the righting arm curve

c/ It is advisable to decrease the values of the righting arm curve for small angles of heel and to increase their values for large angles of heel.

In other words conclusions b/ and c/ may be summarized as a trend towards increasing the static moment of the area under the righting arm curve with respect to GZ axis.

LITERATURE LIST

1 Kobyliński,L. Dudziak,J.: Prace polskie nad statecznością statków morskich w ramach Międzynarodowej Organizacji Doradczej /IMCO/, M.W.I.O.P.G. nr 79, Gdańsk, 1968;

2 Kobyliński,L., Jagiełka,M., Dumara, K.: Intact stability analysis of intact stability casualty records. P.B. I.O. P.G. 2010/84, Gdańsk, 1984;

3 Krappinger, O. und Sharma, S.D.: Sicherheit in der Schiffstechnik. 69 Annual Meeting of the Schiffbautechnische Gesellschaft, 1974;

4 Jagiełka, M.: Koncepcja systemu bezpieczeństwa stateczności statków nieuszkodzonych. P.B. I.O. P.G. 2342/MR-1199/85, Gdańsk, 1985;

5 Liszka, B.: Analiza dyskryminacyjna w zastosowaniu do wypadkowości stateczności okrętu. M. Sc. Thesis, Gdańsk, 1986;

MIKOŁAJ JAGIEŁKA, graduated in marine engineering from the Technical University of Gdańsk.
Next he joined the Ship Research Institute of this University and have been working as a researcher at the Ship Hydromechanics Division.
In 1983 he completed his Ph. D. thesis.

SAMPLE 2.1

DIMENSIONAL

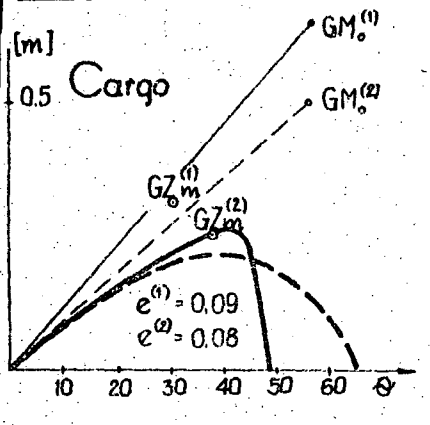

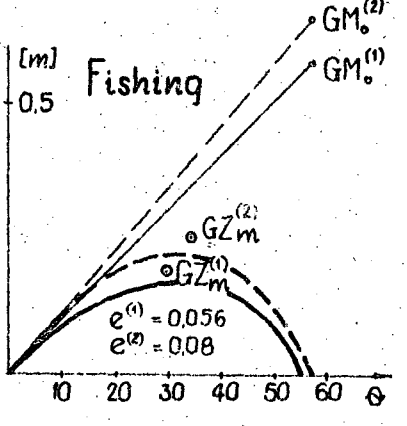

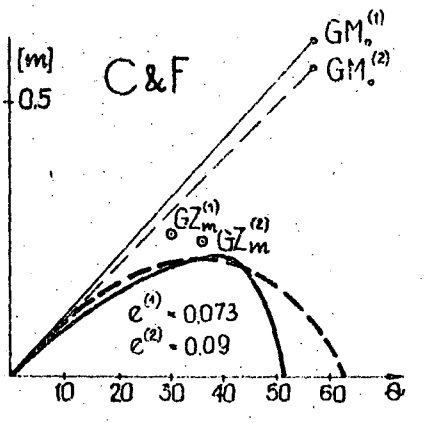

NONDIMENSIONAL

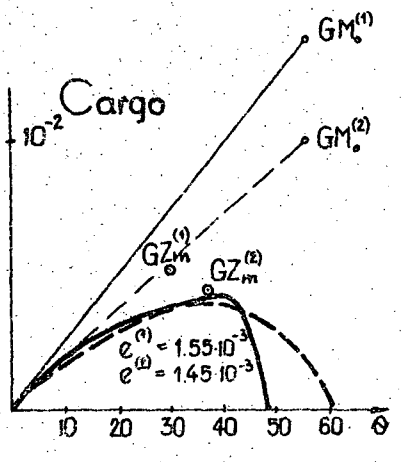

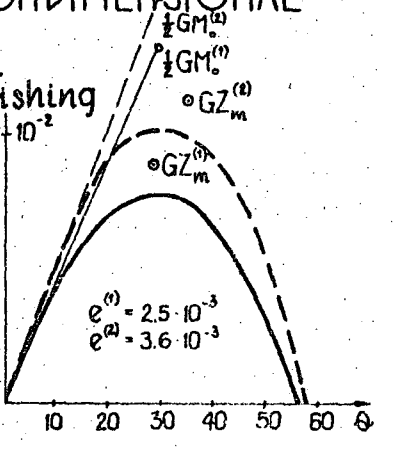

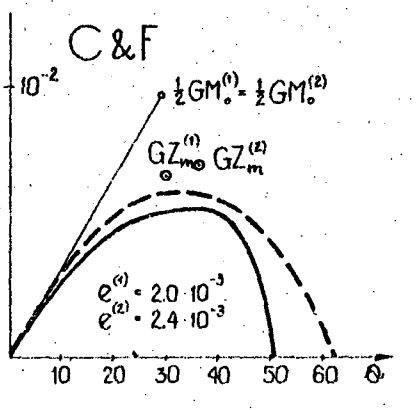

SAMPLE 2.2

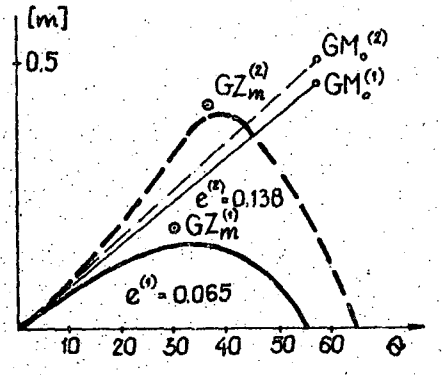

SAMPLE 2.3

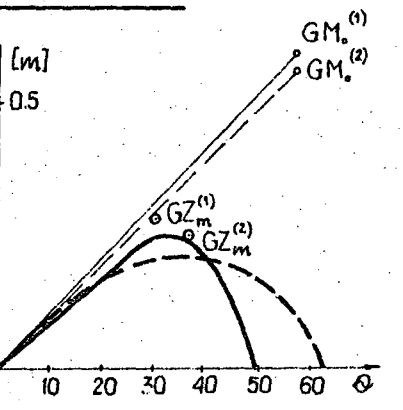

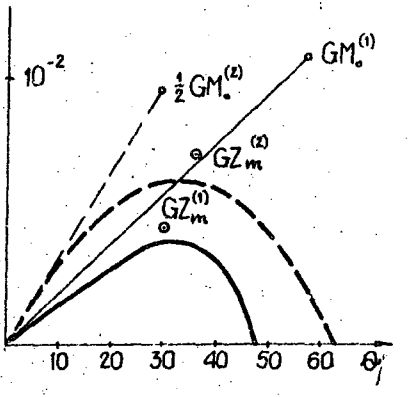

Fig. 1 Mean values of stability parameters for three samples

—— "unsafe" (1) ships

– – – "safe" (2) ships

Third International Conference on Stability of Ships and Ocean Vehicles, Gdańsk, Sept 1986 STAB'86

EXPERIMENTAL INVESTIGATION OF A VESSEL RESPONSE IN WAVES WITH WATER TRAPPED ON DECK

Bruce H. Adee, M.S. Pantazopoulos

1. ABSTRACT

Experiments were conducted in a wave channel to verify theoretical predictions of the roll respose of a model in waves with water trapped on deck. Results are included for the heave and roll motions of a high deadrise fishing vessel model in waves with water on deck. The model had high bulwarks and no freeing ports to maintain a constant amount of water on deck. Pseudo-static heel plays a very important roll in the total response of the vessel in waves and must be included in any theoretical approach. The measured pseudo-static angle is usually very close to the calculated static angle of heel although wave slope may have a small effect. The presence of water on deck increases the roll oscillation when the metacentric height is lower. Capsizing occurs only in the tests with water on deck and is associated with additional water overtopping the bulwark to enter the deck at large roll angles.

2. INTRODUCTION

At the Second International Conference on Stability of Ships and Ocean Vehicles, one of the authors presented a paper which described a method for calculating the sloshing of water trapped on the deck of a vessel [1]. The paper discussed a series of experiments in which a tank of water was oscillated to simulate the rolling of a ship while the movement of the water in the tank was monitored by measuring the shape of the free surface. These experiments showed that the calculations for the sloshing of water on deck were very accurate under almost all but resonant conditions.

The theory for predicting sloshing when coupled with a theory for predicting the rolling motion of a vessel in waves provide a method for calculating the solution of the complete problem of a vessel in waves with water on deck (at least in two-dimensions). A set of experiments was developed so that predicted motions could be compared with motions measured using a two-dimensional model placed in a wave channel.

The series of model tests used two models. Both models were close to the proportions of a fishing vessel. The first had a high deadrise hull, and the second had a flat bottom. Both models use the same tank on deck to represent water on deck. In order to provide the most useful data for verifying the theoretical calculations, water was restricted from entering or leaving the deck during the experiments. Consequently, the models were constructed with high bulwarks and no freeing ports so that a fixed amount of water would be retained on deck.

Preliminary experiments and a number of references [2,3] indicated that the phenomenon described as a pseudo-static angle of heel would play an important role in the response of the vessel. Most of the available research into the pseudo-static angle of heel was performed with the goal of establishing stability standards for vessels. Consequently, the models used in previous tests had realistic bulwark heights and freeing ports which allowed water to enter or leave the deck.

The goal of the experiments conducted for this paper was far more modest. It was to provide results which could be used for comparing and improving the theoretical predictions of vessel roll in a two-dimensional test with water on the deck.

3. THE MODEL AND EQUIPMENT

3.1 Wave Channel

The University of Washington has a small wave channel which is 48.8 m long, 1.22 m wide, and has 0.79 m water depth. The wave channel is equipped with a wavemaker capable of generating regular waves only over a range of periods from 1.2 to 0.5 seconds.

3.2 Motion Measurement Apparatus

The motion measurement apparatus was situated 24.4 m from the wavemaker. It uses potentiometers to measure the heave, roll, and sway response of

the model. The total travel of the carriage in the sway axis is 1.2 m, which limits the duration of some tests where the model moves down the tank rapidly.

3.3 Model Description

The model was constructed of plywood over a solid wooden frame with ballast provided by steel flat bar cut to the appropriate size. Overall, the model was constructed to have a scale ratio of approximately 40 to 1 when compared with standard sized fishing vessels of the Pacific Northwestern United States.

Because of limited space, only the results for the high deadrise model are included in this paper. A cross-sectional view of this model is shown in Figure 1. Important properties of the model are given in Appendix A.

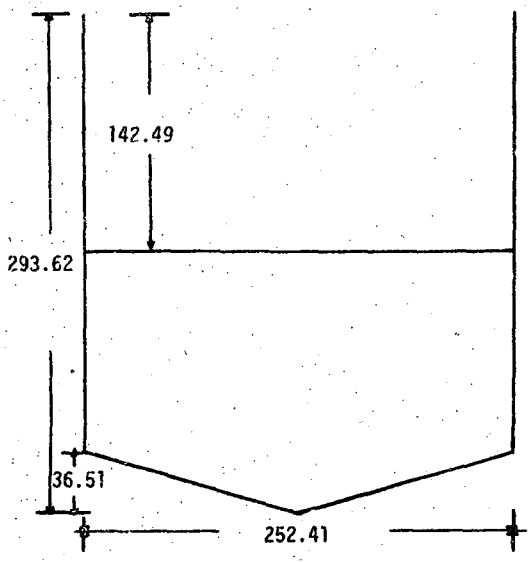

Figure 1. Cross-section of the high deadrise model

3.4 Model Testing

During the model tests, model response was measured for variations in wave frequency, wave slope, model displacement, metacentric height, and the amount of water on deck. For each value of displacement and metacentric height, five sets of model tests were conducted. These included:

a. Model with no water on deck
b. Model with 12.7 mm of water on deck
c. Model with a fixed weight equivalent to 12.7 mm of water on deck
d. Model with either 25.4 or 19.05 mm of water on deck (depending on whether the model will stay upright or not)
e. Model with fixed weight equivalent to either 25.4 or 19.05 mm of water on deck

4. MODEL TEST RESULTS

Before proceeding to describe the results of the model testing, it is important to define certain terms.

Wave slope = wave height/wave length

Static heel angle = θ_s = angle where the righting arm curve and the heeling arm curve due to water on deck intersect. An example of a plot of the θ_s curves is shown in Figure 2.

Pseudo-static heel angle = θ_{ps} = angle about which the model with water on deck oscillates during the experiments.

Maximum roll angle θ_{max} = when the waves first hit the model with water on deck, it rolls to a large angle and then returns to the pseudo-static angle. This angle is measured as the maximum roll angle. It is greater than the pseudo-static angle.

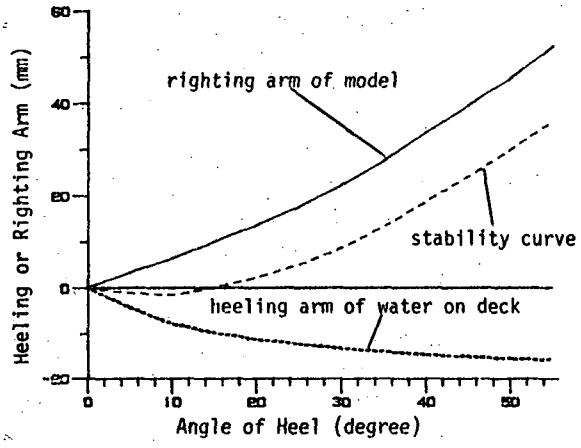

Figure 2. Righting arm and heeling arm due to water on deck (lower displacement, high GM, 12.7 mm of water on deck)

Amplitude of roll oscillation = θ_{osc}.

Model test results are presented in tabular form in Appendix B. These give the incident wave characteristics and the model response for variations in the model displacement, metacentric height, and the amount of water on deck.

4.1 Selected Model Response Time Histories

During a model test the following sequence of events was typical:

a. Model is set in upright position with water on deck.
b. Wavemaker is turned on.
c. Model rolls to the maximum angle as the first waves impinge upon it. The oscillations caused by the rapid heel quickly die out and the model assumes a large angle of heel (first waves are very small and it takes several cycles for the waves to increase to a steady state).
d. As waves reach a steady state, the roll and heave amplitude build to a steady state.

A typical time history of heave and roll as a function of time is shown in Figure 3.

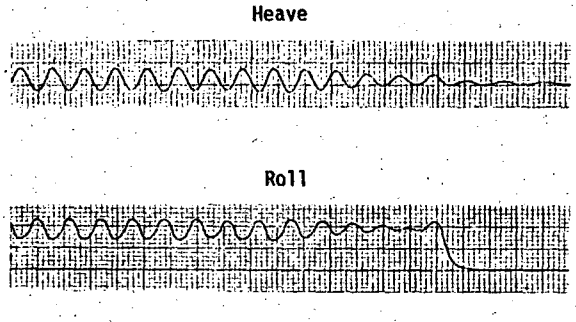

Figure 3. Typical heave and roll as a function of time (lower displacement, high GM, 25.4 mm of water on deck, wave period = 1.20 sec, wave amplitude = 19.09 mm)

Experiments were also performed with a fixed weight on deck equal to the amount of water on deck. Figure 4 shows the roll time history of a typical experiment with a fixed weight on deck.

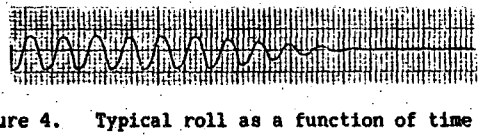

Figure 4. Typical roll as a function of time with a fixed weight replacing the water on deck (lower displacement, high GM, fixed weight equivalent to 25.4 mm water on deck, wave period = 11.20 sec, wave amplitude = 54.76 mm)

At certain frequencies, the roll response was quite irregular. In this case, the sloshing effect of the water on deck made a significant contribution to roll. Unfortunately, these experiments are often time limited because the model moves down the tank along the sway axis and reaches the maximum sway permitted by the motion measurement apparatus. An irregular roll response and the associated heave response are shown in Figure 5.

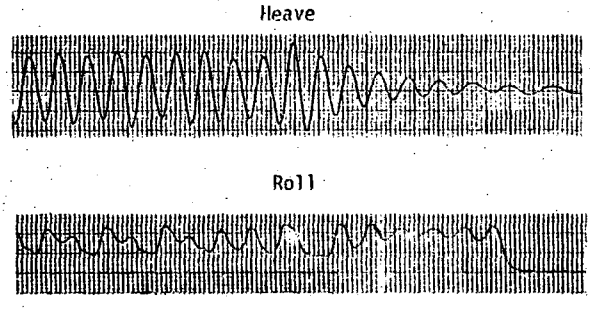

Figure 5. Irregular roll response and heave response, time histories (lower displacement, high GM, 25.4 mm of water on deck, wave period = 1.20 sec, wave amplitude = 54.76 mm)

In a small number of experiments, the model first heels to a pseudo-static angle into the incident waves and after some oscillations it heels to a pseudo-static angle in the opposite direction. This occurred only in cases where the metacentric height of the model was large (smaller pseudo-static angle) and the wave slope was also large (larger roll excitation). In every case, it first heeled into the waves and then reversed itself. A time history of one of these cases is shown in Figure 6.

In several cases, the model capsized. Capsizing may occur into the waves or in the same direction as the waves are propagating. When the

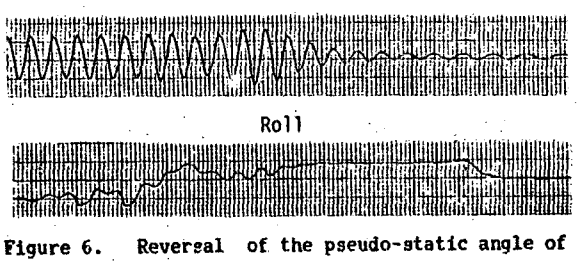

Figure 6. Reversal of the pseudo-static angle of heel (lower displacement, high GM, 12.7 mm of water on deck, wave period = 0.97 sec, wave amplitude = 36.63 mm)

model capsizes into the waves, it starts in the upright position, then rolls to the maximum angle and seems to settle at an angle of heel close to the static angle of heel. As the waves increase, the model oscillates about a pseudo-static angle of heel but water comes onto the deck over the top of the bulwark. The angle about which the model is rolling increases as the water on deck increases

until the model capsizes. Figure 7 shows a time history of a capsize into the waves.

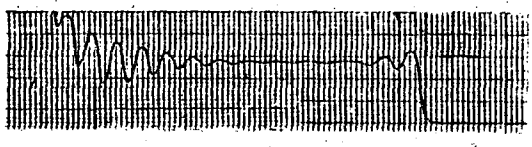

Figure 7. Capsizing into the waves (lower displacement, low GM,19.05 mm of water on deck, wave period = 0.97 sec, wave amplitude = 36.33 mm)

Capsizing also occurred in the same direction as the waves propagated. In this case, the water came over the bulwark at a slower rate and it took a longer time for the model to capsize. Figure 8 shows a capsizing in the same direction as the waves propagated.

5. OBSERVATIONS AND CONCLUSIONS

5.1 Pseudo-Static Angle

For most of the experiments, the measured pseudo-static angle and the calculated static angle are very close. The value of the pseudo-static angle is strongly affected by the vessel's static

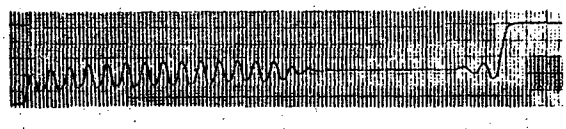

Figure 8. Capsizing in the same direction as wave propagation (lower displacement, low GM, 19.05 mm of water on deck, wave period = 0.90 sec, wave amplitude = 30.42 mm)

stability and the amount of water on deck. The less stable the vessel, the greater the pseudo-static angle becomes for a given amount of water on deck. When the amount of water on deck is increased, the pseudo-static angle increases.

Although this does not hold true for every specific experiment, in general, increasing the wave slope leads to a lower pseudo-static angle. This is clearly demonstrated by the higher displacement, intermediate GM, with 12.7 mm of water on deck case shown in Appendix B.

For the smaller wave slope cases, the correlation between the static angle of heel and the pseudo-static angle is best.

In previous model experiments [2], with three-dimensional models and normal bulwarks in beam seas it was reported that: "model capsizes or is getting large pseudostatic angle of heel to the "windward" side/towards the wave." In the present tests in a wave channel the lower displacement model showed no preferred direction when it rolled to the pseudo-static angle. It rolled to a pseudo-static angle into the waves almost as many times as it rolled in the same direction as wave propagation. The higher displacement model rolled into the waves over twice as many times as it rolled in the same direction as wave propagation. In specific tests which were repeated under the same conditions, the model would often heel in one direction during the first test and in the opposite direction during the second.

Under the format used for these experiments, it appears that the model which initially sits in an unstable equilibrium position rolls in the direction which corresponds to the direction of the initial moment excited by the waves. In the three-dimensional model tests in beam waves, one would expect water to come over the top of the bulwark on the incident wave side resulting in a preference for rolling into the incident waves.

5.2 Capsizing

During several experiments the model capsized. Each of these cases was related to a large static or pseudo-static angle of heel, which results from a combination of low metacentric height and/or large amounts of water on deck. All the capsizings occurred for the incident waves of larger slopes, and in all cases additional water came over the top of the bulwark onto the deck before the model capsized.

There were no capsizings in any of the tests without water on deck. That includes tests of the model by itself or the model with a fixed weight on deck equivalent to the weight of water.

Capsizing generally occurred in a band of wave frequencies near the natural frequency of the model with a fixed weight on deck equivalent to the weight of the water on deck. There was one exception to this which occurred for the lower displacement, low GM, 19.05 mm of water on deck case at a wave period of 0.70 seconds. During the first test at this condition, the model rolled to a pseudo-static angle in the direction of wave propagation and only oscillated a small amount around this angle. In the second test it rolled into the wave and a large amount of water came over

the top of the bulwark, which preceded and contributed to the capsizing.

5.3 Response With Water on Deck Compared to Response With a Fixed Weight on Deck

This comparison is very interesting because tanks with water sloshing have been used as stabilizers.

For high metacentric height and a small amount of water on deck the presence of the water reduces the roll oscillations (of course one should recognize that in all cases the amount of water on deck was sufficient to cause a significant pseudo-static angle of heel which is not included in this discussion). It is not clear from the tests whether the decrease in roll oscillation is a result of the dynamic effect of water sloshing or from the reduction of the effective metacentric height due to the free-surface effect.

For the high metacentric height case where the amount of water on deck is increased the results are no longer consistent at all frequencies. This indicates that the sloshing may be more important under this circumstance with a larger mass of water moving back and forth on the deck.

For the intermediate and low metacentric height cases, the presence of water on deck results in a larger roll oscillation than occurs when the water is replaced by a fixed weight. In conjunction with the roll to a pseudo-static angle, this rolling behavior indicated that the presence of water trapped on deck is a very dangerous situation.

Similar results are obtained when the model response with water on deck is compared with the case of no water on deck.

6. ACKNOWLEDGEMENT

The authors gratefully acknowledge the support provided to the Fishing Vessel Safety Center at the University of Washington by the Washington Sea Grant Program. This research was fully funded under National Oceanic and Atmospheric Administration Grant Number NA 84 AA-D-00011.

7. REFERENCES

1. Adee, B., Caglayan, I., "The Effects of Free Water on Deck on the Motions and Stability of Vessels," Proceedings of the Second Conference on Stability of Ships and Ocean Vehicles, Tokyo, Japan, Oct. 1982, pp. 413-426.

2. Szponar, K., "Some Suggestions into Fishing Vessel's Stability," IMO PFV XIII/6/1, 1 February 1973.

3. Soviet Delegation, "Freeboard of Fishing Vessels," IMO PFV VI/22, 2 October 1967.

4. Caglayan, I., "Effect of Water on Deck on the Motions and Stability of Small Ships," PhD Dissertation, University of Washington, 1983.

APPENDIX A: MODEL PROPERTIES

Table A-1. Model Properties and Depth of Water on Deck for Lower Displacement Model

	High GM	Intermediate GM	Low GM
Displacement (kg)	25.45	25.42	25.42
Radius of gyration*	91.0	104.0	103.6
Metacentric height-GM*	36.7	13.3	5.37
Depth of water-case 1*	12.7	12.7	12.7
Weight of water on deck as a % of displacement	12.2	12.2	12.2
Depth of water-case 2*	25.4	25.4	19.05
Weight of water on deck as a % of displacement	24.4	24.4	18.3

Table A-2. Model Properties and Depth of Water on Deck for Higher Displacement Model

	High GM	Intermediate GM	Low GM
Displacement (kg)	31.03	31.03	31.03
Radius of gyration*	94.8	93.7	92.1
Metacentric height-GM*	27.7	13.0	5.09
Depth of water-case 1*	12.7	12.7	12.7
Weight of water on deck as a % of displacement	10.0	10.0	10.0
Depth of water-case 2*	19.05	19.05	19.05
Weight of water on deck as a % of displacement	15.0	15.0	15.0

*in mm

Table A-3. Other Model Properties

Length of model	=	1054.1 mm
Length of tank on deck	=	1020.8 mm
Beam of tank on deck	=	234.6 mm

Table B1. RESULTS OF MODEL TESTS
Lower Displacement, High Metacentric Height, 12.7 mm Water on Deck
Metacentric Height = 36.7 mm (with no water on deck)

Wave period (sec)	0.70	0.86	0.90	0.94	0.97	1.10	1.20	1.20
Wave amplitude (mm)	7.64	11.61	30.42	14.20	36.63	47.83	19.09	54.76
Wave slope	0.0200	0.0201	0.0481	0.0206	0.0499	0.0507	0.0170	0.0487
θ_{max}	16.6	16.6	17.5	16.6	16.6	16.3	17.3	20.4 1st 15.9 2nd
θ_{ps}	14.8	14.6	14.9	14.9	15.94	10.2	14.9	14.1 1st 12.2 2nd
θ_s	14.5	14.5	14.5	14.5	14.5	14.5	14.5	14.5
θ_{osc} (water)	0.51	*	--	*	--	--	1.53	3.05 1st -- 2nd
θ_{osc} (weight)	*	0.86	7.35	1.71	12.57	15.39	4.28	14.71
θ_{osc} (no water)	0.68	3.39	11.19	5.85	11.28	11.19	2.04	10.01
Heave (water) Wave amplitude	0.43	0.82	0.93	1.06	0.92	1.01	0.93	0.96
Heave (weight) Wave amplitude	0.15	0.89	0.83	1.04	0.86	0.98	1.01	0.99
Heave (no water) Wave amplitude	0.31	0.84	0.87	0.96	0.97	1.02	0.98	0.97
Notes			1		1	2		3

Lower Displacement, High Metacentric Height, 25.4 mm Water on Deck
Metacentric Height = 36.7 mm (with no water on deck)

Wave period (sec)	0.70	0.86	0.90	0.94	0.97	1.10	1.20	1.20
Wave amplitude (mm)	7.64	11.61	30.42	14.20	36.63	47.83	19.09	54.76
Wave slope	0.0200	0.0201	0.0481	0.0206	0.0499	0.0507	0.0170	0.0487
θ_{max} (deg)	39.2	39.5	39.7	39.5	38.5	38.3	37.6	39.3
θ^{max}	32.8	32.8	28.1	32.3	27.0	26.0	31.5	27.2
θ^{ps}	33.0	33.0	33.0	33.0	33.0	33.0	33.0	33.0
θ^{s}								
θ_{osc} (water)	*	1.03	--	1.81	--	--	7.18	--
θ_{osc} (weight)	*	*	1.37	0.51	2.91	7.01	1.20	13.17
θ_{osc} (no water)	0.68	3.39	11.19	5.85	11.28	11.19	2.04	10.01
Heave (water) Wave amplitude	0.39	0.79	1.07	1.06	0.97	0.96	0.79	0.93
Heave (weight) Wave amplitude	0.19	0.82	1.01	1.18	1.00	0.93	1.02	0.98
Heave (no water) Wave amplitude	0.31	0.84	0.87	0.96	0.97	1.02	0.98	0.97
Notes			4		4	4		4

Lower Displacement, Intermediate Metacentric height, 12.7 mm Water on Deck
Metacentric Height = 13.3 mm (with no water on deck)

Wave period (sec)	0.70	0.86	0.90	0.94	0.97	1.10	1.20	1.20
Wave amplitude (mm)	7.64	11.61	30.42	14.20	36.63	47.83	19.09	54.76
Wave slope	0.0200	0.0201	0.0481	0.0206	0.0499	0.0507	0.0170	0.0487
θ_{max} (deg)	41.7	41.3	41.7	41.3	42.0	42.0	41.3	42.3
θ^{max}	34.4	33.4	29.3	32.4	31.6	26.0	33.7	31.4
θ^{ps}	31.5	31.5	31.5	31.5	31.5	31.5	31.5	31.5
θ^{s}								
θ_{osc} (water)	0.69	2.41	5.34	3.44	8.52	9.04	6.20	14.2
θ_{osc} (weight)	*	*	*	*	*	*	*	*
θ_{osc} (no water)	*	*	*	*	*	*	*	*
Heave (water) Wave amplitude	0.55	0.72	0.94	0.84	0.83	0.94	0.95	0.93
Heave (weight) Wave amplitude	0.15	0.85	0.98	1.01	0.93	1.00	0.96	0.96
Heave (no water) Wave amplitude	0.31	0.95	0.96	0.98	0.98	1.03	0.99	0.97

Lower Displacement, Intermediate Metacentric Height, 25.4 mm Water on Deck
Metacentric Height = 13.3 mm (with no water on deck)

Wave period (sec)	0.70	0.86	0.90	0.94	0.97	1.10	1.20	1.20
Wave amplitude (mm)	7.64	11.61	30.42	14.20	36.63	47.83	19.09	54.76
Wave slope	0.0200	0.0201	0.0481	0.0206	0.0499	0.0507	0.0170	0.0487
θ_{max} (deg)	54.3	54.3	54.2	54.0	54.3	54.2	54.2	53.8
θ^{max}	46.6	46.8	43.1	45.2	39.7	43.8	43.0	44.9
θ^{ps}	43.3	43.3	43.3	43.3	43.3	43.3	43.3	43.3
θ^{s}								
θ_{osc} (water)	0.69	3.28	capsize into wave	10.70	11.90	16.22	4.57	14.32
θ_{osc} (weight)	*	*	0.52	*	*	*	*	*
θ_{osc} (no water)	0.68	3.39	11.19	5.85	11.28	11.19	2.04	10.01
Heave (water) Wave amplitude	0.51	0.90	0.79	0.53	0.98	0.99	0.89	0.88
Heave (weight) Wave amplitude	0.27	0.81	0.99	1.10	1.06	1.05	1.01	0.97
Heave (no water) Wave amplitude	0.31	0.95	0.96	0.98	0.98	1.03	0.99	0.97
Notes			5					

Lower Displacement, Low Metacentric Height, 12.7 mm Water on Deck
Metacentric Height = 5.37 mm (with no water on deck)

Wave period (sec)	0.70	0.86	0.90	0.94	0.97	1.10	1.20	1.20
Wave amplitude (mm)	7.64	11.61	30.42	14.20	36.63	47.83	47.83	47.83
Wave slope	0.0200	0.0201	0.0481	0.0206	0.0499	0.0507	0.0170	0.0487
θ_{max} (deg)	47.5	49.6	48.9	49.6	48.9	49.9	48.2	47.9
θ^{ps}	39.7	39.9	39.3	39.7	39.0	38.3	39.3	38.3
θ^{s}	37.5	37.5	37.5	37.5	37.5	37.5	37.5	37.5
θ_{osc} (water)	0.68	4.19	8.38	7.87	13.00	15.05	3.93	16.08
θ_{osc} (weight)	*	*	*	*	*	1.20	*	*
θ_{osc} (no water)	*	*	*	*	1.03	0.86	*	0.86
Heave (water) / Wave amplitude	0.67	0.67	1.00	0.79	0.99	0.90	1.01	0.92
Heave (weight) / Wave amplitude	0.41	0.93	1.15	1.10	1.07	1.07	1.01	1.01
Heave (no water) / Wave amplitude	0.35	0.96	0.99	1.08	0.99	1.00	0.99	0.95

Lower Displacement, Low Metacentric Height, 19.05 mm Water on Deck
Metacentric Height = 5.37 mm (with no water on deck)

Wave period (sec)	0.70	0.86	0.90	0.94	0.97	1.10	1.20	1.20
Wave amplitude (mm)	7.64	11.61	30.42	14.20	36.63	47.83	47.83	47.83
Wave slope	0.0200	0.0201	0.0481	0.0206	0.0499	0.0507	0.0170	0.0487
θ_{max} (deg)	59.0 1st 60.8 2nd	55.8	57.8	57.1	55.6	55.3	57.3	55.9
θ_{ps}	48.4 1st 52.2 2nd	46.7	50.6	47.7	46.3	39.1	45.5	46.0
θ_{s}	43.3	43.3	43.3	43.3	43.3	43.3	43.3	43.3
θ_{osc} (water)	0.43 1st capsize 2nd	4.29	capsize	7.38	capsize	13.21	2.92	11.50
θ_{osc} (weight)	*	*	1.03	*	*	*	*	*
θ_{osc} (no water)	*	*	*	*	1.03	0.86	*	0.86
Heave (water) / Wave amplitude	0.55 1st unsteady 2nd	0.97	1.27	1.21	unsteady	1.03	0.99	0.91
Heave (weight) / Wave amplitude	0.53	0.96	1.02	1.15	1.09	1.06	1.03	1.01
Heave (no water) / Wave amplitude	0.35	0.96	0.99	1.08	0.99	1.00	0.99	0.95
Notes	6		7					

Higher Displacement, High Metacentric Height, 12.7 mm Water on Deck
Metacentric Height = 27.7 mm (with no water on deck)

Wave period (sec)	0.70	0.86	0.90	0.94	0.97	1.10	1.20	1.20
Wave amplitude (mm)	7.64	11.61	30.42	14.20	36.63	47.84	19.09	54.76
Wave slope	0.0200	0.0201	0.0481	0.0206	0.0499	0.0507	0.0170	0.0487
θ_{max} (deg)	17.19	17.19	17.19	16.34	17.54	18.91	18.57	16.34
θ^{ps}	16.3	16.2	17.2	14.8	15.1	16.2	16.2	14.1
θ^{s}	14.4	14.4	14.4	14.4	14.4	14.4	14.4	14.4
θ_{osc} (water)	0.69	*	1.72	*	1.20	--	*	--
θ_{osc} (weight)	*	*	2.15	*	5.85	14.10	2.41	16.16
θ_{osc} (no water)	*	*	6.36	0.344	12.47	15.13	0.86	13.76
Heave (water) / Wave amplitude	0.37	0.92	0.99	1.41	1.04	1.06	1.09	1.00
Heave (weight) / Wave amplitude	0.12	1.00	1.00	1.25	1.05	0.97	1.03	1.02
Heave (no water) / Wave amplitude	0.21	0.87	0.98	1.20	1.00	1.03	0.96	1.00
Notes			1		1	1,4		1,4

Higher Displacement, High Metacentric Height, 19.05 mm Water on Deck
Metacentric height = 27.7 mm (with no water on deck)

Wave period (sec)	0.70	0.86	0.90	0.94	0.97	1.10	1.20	1.20
Wave amplitude (mm)	7.64	11.61	30.42	14.20	36.63	47.83	19.09	54.76
Wave slope	0.0200	0.0201	0.0481	0.0206	0.0499	0.0507	0.0170	0.0487
θ_{max} (deg)	24.76	25.10	25.79	25.10	30.09	25.79	25.10	28.89
θ^{ps}	21.0	20.6	19.8	21.0	23.7	23.7	20.6	13.8
θ^{s}	20.9	20.9	20.9	20.9	20.9	20.9	20.9	20.9
θ_{osc} (water)	0.43	0.52	1.55	0.77	1.12	*	*	--
θ_{osc} (weight)	*	*	1.20	0.17	3.44	11.52	*	16.16
θ_{osc} (no water)	*	*	6.36	0.344	12.47	15.13	0.86	13.76
Heave (water) / Wave amplitude	*	0.45	0.92	1.07	1.03	1.04	1.17	1.03
Heave (weight) / Wave amplitude	0.08	0.64	1.08	1.36	1.14	0.98	1.08	1.01
Heave (no water) / Wave amplitude	0.21	0.87	0.98	1.20	1.00	1.03	0.96	1.00
Notes					1	1		2,4

Higher Displacement, Intermediate Metacentric Height, 12.7 mm Water on Deck
Metacentric Height = 13.0 mm (with no water on deck)

Wave period (sec)	0.70	0.86	0.90	0.94	0.97	1.10	1.20	1.20
Wave amplitude (mm)	7.64	11.61	30.42	14.20	36.63	47.83	19.09	54.76
Wave slope	0.0200	0.0201	0.0481	0.0206	0.0499	0.0507	0.0170	0.0487
θ_{max} (deg)	33.72	35.10	30.97	34.41	30.46	35.79	35.10	34.41
θ^{ps}	29.3	29.4	21.3	28.4	22.4	21.5	28.6	23.4
θ^{s}	27.7	27.7	27.7	27.7	27.7	27.7	27.7	27.7
θ^{osc}_{osc} (water)	0.69	1.55	*	2.58	*	--	6.19	--
θ^{osc}_{osc} (weight)	*	*	*	*	*	*	*	0.69
θ^{osc}_{osc} (no water)	*	*	*	0.17	*	*	*	*
Heave (water) / Wave amplitude	0.60	0.81	0.86	1.06	0.99	0.97	0.75	0.89
Heave (weight) / Wave amplitude	0.14	0.72	1.08	1.19	1.16	1.09	0.94	1.00
Heave (no water) / Wave amplitude	0.17	0.84	1.09	1.22	1.09	1.11	1.03	1.03
Notes						2,4		2,4

Higher Displacement, Intermediate Metacentric Height, 19.05 mm Water on Deck
Metacentric Height = 13.0 mm (with no water on deck)

Wave period (sec)	0.70	0.86	0.90	0.94	0.97	1.10	1.20	1.20
Wave amplitude (mm)	7.64	11.61	30.42	14.20	36.63	47.83	19.09	54.76
Wave slope	0.0200	0.0201	0.0481	0.0206	0.0499	0.0507	0.0170	0.0487
θ_{max} (deg)	43.70	44.39	44.39	44.05	44.39	44.39	44.05	45.08
θ^{ps}	38.0	32.7	32.7	34.1	29.9	29.9	36.5	31.0
θ^{s}	34.2	34.2	34.2	34.2	34.2	34.2	34.2	34.2
θ^{osc}_{osc} (water)	0.86	2.58	7.05	6.19	--	13.25	9.12	13.77
θ^{osc}_{osc} (weight)	*	*	*	*	*	*	*	0.86
θ^{osc}_{osc} (no water)	*	*	*	0.17	*	*	*	*
Heave (water) / Wave amplitude	0.49	0.74	1.10	0.92	0.95	0.94	0.79	0.92
Heave (weight) / Wave amplitude	0.21	0.55	1.04	1.28	1.20	1.14	1.01	1.05
Heave (no water) / Wave amplitude	0.17	0.84	1.09	1.22	1.09	1.11	1.03	1.03
Notes					4			

Higher Displacement, Low Metacentric Height, 12.7 mm Water on Deck
Metacentric Height = 5.09 mm (with no water on deck)

Wave period (sec)	0.70	0.86	0.90	0.94	0.97	1.10	1.20	1.20
Wave amplitude (mm)	7.64	11.61	30.42	14.20	36.63	47.83	19.09	54.76
Wave slope	0.0200	0.0201	0.0481	0.0206	0.0499	0.0507	0.0170	0.0487
θ_{max} (deg)	37.85	43.36	39.92	37.17	37.17	38.89	39.40	38.71
θ^{ps}	34.1	35.3	32.5	31.8	25.0	26.8	32.7	26.8
θ^{s}	35.1	35.1	35.1	35.1	35.1	35.1	35.1	35.1
θ^{osc}_{osc} (water)	*	*	0.86	4.13	7.92	10.67	1.55	12.04
θ^{osc}_{osc} (weight)	*	*	0.69	*	0.35	*	*	*
θ^{osc}_{osc} (no water)	*	*	*	*	*	*	*	*
Heave (water) / Wave amplitude	0.17	0.71	0.91	1.00	1.01	0.98	0.71	0.88
Heave (weight) / Wave amplitude	0.03	0.68	1.01	1.20	1.11	1.08	1.01	0.97
Heave (no water) / Wave amplitude	0.24	0.87	1.07	1.26	1.14	1.10	1.02	1.04

Higher Displacement, Low Metacentric Height, 19.05 mm Water on Desk
Metacentric Height = 5.09 mm (with no water on deck)

Wave period (sec)	0.70	0.86	0.90	0.94	0.97	1.10	1.20	1.20
Wave amplitude (mm)	7.64	11.61	30.42	14.20	36.63	47.83	19.09	54.76
Wave slope	0.0200	0.0201	0.0481	0.0206	0.0499	0.0507	0.0170	0.0487
θ_{max} (deg)	41.99	45.93	41.99	45.93	42.50	41.48	41.13	42.50
θ^{ps}	38.4	38.4	33.6	37.7	34.3	32.2	36.00	36.00
θ^{s}	40.1	40.1	40.1	40.1	40.1	40.1	40.1	40.1
θ^{osc}_{osc} (water)	1.03	4.97	capsize	8.23	5.14	15.77	1.72	11.65
θ^{osc}_{osc} (weight)	*	0.17	1.21	0.52	1.03	*	*	*
θ^{osc}_{osc} (no water)	*	*	*	*	*	*	*	*
Heave (water) / Wave amplitude	0.40	0.53	0.75	0.66	0.99	0.83	0.97	1.00
Heave (weight) / Wave amplitude	0.07	0.59	0.87	1.04	1.04	1.05	0.99	1.01
Heave (no water) / Wave amplitude	0.24	0.82	1.07	1.26	1.14	1.10	1.02	1.04

*very small oscillation

NOTES:
1. Model first rolls into the waves and then rolls to the opposite side (in the same direction as the incident waves).
2. Model first rolls into the waves and then tends to roll to the opposite side but does not roll all the way before experiment is terminated.
3. Model test conducted twice. In first test it rolls in the same direction as the waves. In second test it rolls in the opposite direction (into the incident waves), but is tending to roll back toward the same direction as the waves as the test is terminated.
4. Model roll oscillations are quite irregular.
5. Water enters over top of bulwark.
6. Experiments performed twice. In the first model, rolls in same direction as wave propagation. In second model, capsizes after rolling into the wave.
7. Model rolls in same direction as wave propagation. It oscillates as water enters deck over bulwark and then capsizes.

ldk:5,75

Third International Conference on Stability of Ships and Ocean Vehicles, Gdańsk, Sept. 1986

STAB'86

DESIGN-REGULATIONS

BY W. A. CLEARY, JR

WITH LCDR R. M. LETOURNEAU USCG

ABSTRACT

The relationship of existing stability criteria of either the initial stability (GM) or the righting curve type is examined against the types of known stability accidents which may occur. It is noted that there can be more than two dozen types of stability accidents and several damage stability accident types. Additionally there are variations of each one of these accidents which might require refinement of stability criteria. Finally, the major types of design which have been developed over the past 20 years and those which appear to be developments of the next decade will be reviewed against known types of stability accident for research desired.

1. BACKGROUND

1.1 Agreed worldwide stability standards are conspicuous by their absence. Many national standards exist but little agreement exists at the international level although we have made a major step toward a general intact stability standard during the four years between the second and third International Stability Conferences. One advantage of having no comprehensive agreed intact stability standard is that very little restriction has been placed on designers thus far, by administrations. Designers have had considerable freedom to respond to the economic requests of ocean commerce, limited only by their own professional judgement or by the requirements of the flag state.

Until the past two decades, ship designs have evolved quite deliberately over many centuries so that the effect of any modification on stability usually was able to be judged over a period of years. As late as 1960, ships could be placed into three main groups - passenger ships, tankers, and dry cargo ships. Their form and size were matters of general similarity world wide.

However, during the past 26 years, the types of ocean vehicles have proliferated. Therefore an increasing danger exists that among the many new types of commercial ships. There may be some which are not as safe as is assumed from experience.

1.2 The role of the Intergovernmental Maritime Organization in creating standards is misunderstood by some. The SubCommittee which is responsible for stability (both intact and damaged) is also responsible for four (4) international conventions and the stability aspects of a dozen codes. All items must be reviewed in a few hours, once a year. The Subcommittee cannot discuss research in detail while in session. The SubCommittee needs to review the results of stability research in making a decision for a new worldwide standard and the SubCommittee has in the past recommended research and should recommend priorities in order to assist its program.

1.3 Therefore, there must be another forum to provide full discussions of stability research. The several International Conferences on Stability of Ships and Ocean Vehicles (now the Third Conference - Gydansk 86) should be that forum. Such an organization should have an intersessional correspondence program and should adopt the objective of an international meeting of all stability research persons approximately every 4 years. If such an organization is possible, the following design problems should receive priority in research between now and STAB #4-1990.

2. EXISTING STABILITY STANDARDS METHODOLOGY

2.1 To date most stability standards use the geometrical and mathematical relationship of the monohull ship form in heeling (both static and dynamic heel) rather than pitch, heave or other ship motions. This procedure has been acceptable and safe because the usual monohull has been more vulnerable to capsize in the transverse heel attitude than in pitch or other motions.

As late as 1940, stability standards were merely suggestions in the literature which remained quite simple, based on a recommended metacentric height (GM) of about 2 feet (0.6 meter), with no specific relations to ship shape or type of hull or size.

However, the commercial vessels available

for comparison at that time were of a very few distinct types and only a very few were out of the normal size range for the ocean going vessels.

2.2 The GM type of standard has been popular because it allowed a simple formula to be used by a designer in evaluating ship safety. One of the simplest evaluation standards is the provision of a minimum GM based on a steady wind.

In addition to the initial metacentric height (GM) evaluation, the righting arm curve standard has been used in many variations by different organizations, and national administrations. This curve can not only show the initial metacentric height but also can measure total energy needed to heel and to return upright. The righting moment curve has been less often used, usually with the explanation that it is the same shape as the righting arm curve so it means the same thing. It is, of course, the same shape but it does not have the exact same physical meaning for ships of great differences in size form or loading arrangement.

2.3 However, these two methods of stability evaluation do not actually cover all the stability accidents that may occur. They do provide a relative measure of stability for ships of similar type and service. Indeed, our ignorance of the seaway and its affect on ships of all sizes has caused us to create many arguments for statical arm curves of one type or shape when in fact we do not know the full effect of seaway, and its variation with size, period and relative steepness.

FIG 1

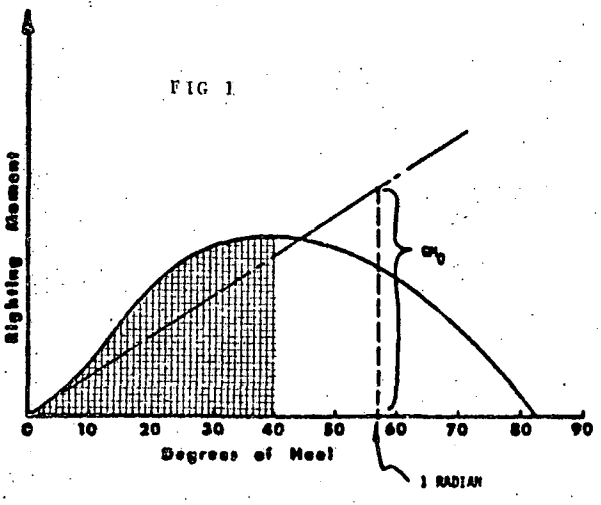

Also, whether enough reserve stability is contained in these formulae to account for all the stability accidents that may occur, remains a relatively unknown quantity in 1986.

2.4 Table 1 provides a list of 34 causes of capsize for an otherwise undamaged ship.

Table 1 Capsize causes for undamaged ship

Cause	Example of Hazard
1. Single broadside wave	beam single wave rollover
2. Resonant rolling	beam steady period, exact frequency waves
3. Steep wave system	wave slope, following sea
4. Bow/stern steep waves	heaving, loss of waterplane
5. Following sea	loss of waterplane
6. Wave grouping	uneven rolling
7. Mass distribution (large radius of gyration)	cargo or structure outboard of hull or vertically above and below hull
8. Wind	steady heeling moment
9. Wind gusts	impulse heeling moment
10. Cargo and ballast distribution	
11. Deck loads	high center of gravity
12. Icing	high center of gravity
13. Ballast shift	solid ballast shift, or liquid drains to off-center tank
14. Ballast, lack of	tanks being used, fuel oil, ballast
15. Free surface (interior)	water on interior decks
16. Free surface (emulsion)	baric ballast, deteriorating chemicals
17. Water on deck	
18. Bulk cargo, shift	bulk cargo slides or shakes down
19. Cargo shift	
20. Lifting weights with ship's gear	heavy-lift ships
21. Movement of people on board	passenger ships
22. Anchor lines	trim by bow—loss of waterplane
23. Moorings (general)	pipelaying, MODU's
24. Towing hawser—self-tripping	tugs—short hawser
25. Towing hawser—tow tripping	tow yaws and overwhelms tug
26. Nets or trawls—surface	vessel heaves on wave
27. Nets or trawls—submerged	vessel heaves on wave
28. Nets or trawls—bottom	net hangs up on wreck
29. Hauling blocks	power block causes excessive heeling lever
30. Voyaging at very light or deep drafts	loss of waterplane at small angle
31. Partial groundings	change trim, waterplane, and lifts
32. Lateral currents	inland tug crossing river outflow
33. Maneuvering at high speed	rudder action heeler
34. Wave impact at high speed	impulse heel or heave on surface-effect ships

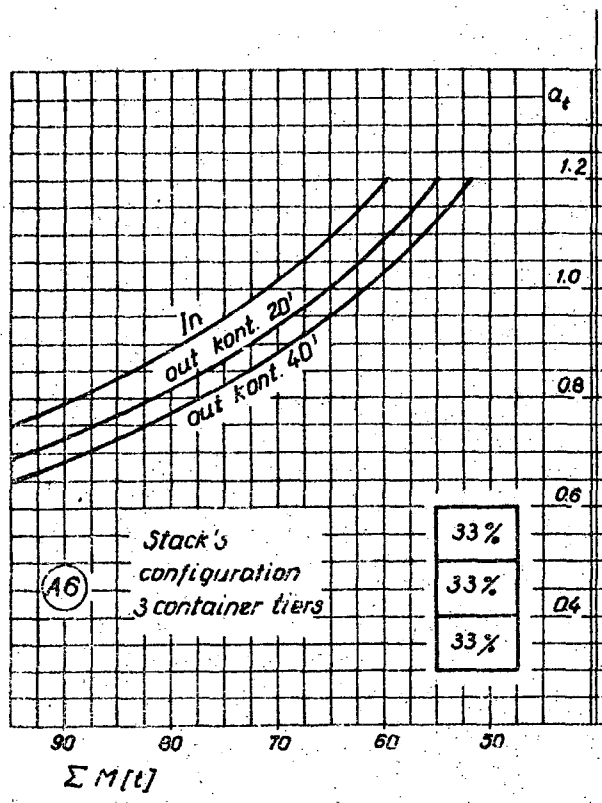

FIG. 3. ADMISSIBLE ACCELERATIONS.

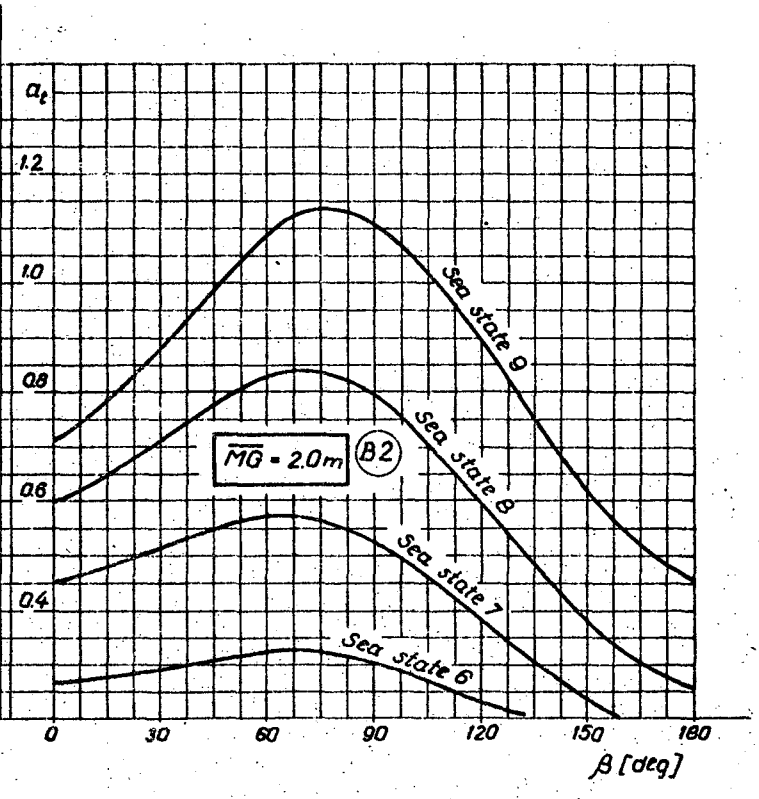

FIG. 4. SHORT-TERM PREDICTION OF ACCELERATION.

ted formulation of the problem this part of regulations /equations to calculate some standard values of accelerations/ becomes out of date.

The uselessness of equations for calculating the long-term prediction for the ship's accelerations under waving conditions within the framework of container lashing regulations does not mean to eliminate them from the code at all and to diminish it's significance on behalf of the lashing problem in particular. It is simply maintained that such equations however, in some more rational form [x], should constitute the integral part of the code of classification society and be intended for the so-called preliminary design stages. Their significance would consist in making it possible for the designing of ship to be of the best seakeeping quality in general. In consequence, in an indirect way with respect to the designed lashing system there would be satisfied the condition of the external forces to be consciously minimized on account of temporary control of the ship in operation, while the stability of the load mass would be fulfilled at possibly the lowest level of these forces.

2.4. Usefulness of the Document under the Title "Lashing System of Containers on Weather Deck" in Ship's Operation

The stability of the load mass is decided in the following three basic spheres of activities:

- at stowage time,
- at lashing time and
- while shipping the cargo.

In other words the containers under consideration will be stable if they have been sufficiently well stowed, properly lashed and the ship is "guided" in the right way. Proper lashing is only connected with performing some routine procedures explained e.g. in Fig. 2. and, first of all, checking the reliability of carrying out that operation [x], Thus there remains only to take into consideration the stowage and navigational operations, the more so, that it is them that the analyzed conception of

[x] in form of the so-called nonstructural models i.e. relatively simple expressions with requirements which on one hand are the ship's designing parameters, and on the other governing parameters for the described phenomenon /[2] /..

[x] crews of classical container ships are rather only obliged to check the lashing which is carried out by the port service.

Thus functions (3) make it possible to determine the admissible acceleration a_t with a defined mass M, or the admissible mass M with an assumed acceleration a_t.
A complete information requires preparation of a set of diagrams as illustrated in Fig. 3. for a designed ship including various possible configurations of stack lashing.

2.3.3. To prepare an information on dependence of the ship's acceleration a_t upon the sea state and, the load condition /Fig. 4./ seems to be the most time - consuming procedure and simultaneously the most difficult one. For the determination of function a_t = /sea state, load condition, ship's velocity/ it is necessary to carry out some calculations by application of advanced programs and computers.
Moreover such substantial problems like the description of the sea state and mainly the selection of an appropriate measure of accelerations call here for a careful examination. The point is that the information should be, if possible univocal [x] and as far as the value of a_t is concerned comparable with some equivalents resulting from the lashing technique /Fig. 3./.
At present it is suggested that the sea states were described by two-parameters /e. g. $\bar{H}_{1/3}$ and $\bar{T}_V$ or $\bar{H}_{1/3}$ and $\bar{L}_w$/, while accelerations a_t should be the external most probable values a_{NP} / [1] /. In this question, however, it is indispensable to carry on further investigations of some general character than it would arise from the needs of preparing some concrete objective information.
The load condition and the ship's velocity for these requirements are best described by the values of metacentric height $\overline{MG}$ and the relative heading angle respectively.
For the reason that the transverse accelerations a_t still depend on many other factors, they are definitely the most significant ones [xx], and should be noted that the objective information cannot be too complicated. The information specified at this point is required to be prepared for a given ship for several states of the sea and several states of the ship. The selection of these parameters is dependent, of course, upon the specifity of the shipping line both with respect to the characteristic of its waving and potentially possible variants of ship's loadings.

2.3.4. The set of information described at points 2.3.1. ÷ 2.3.3. constitutes a document entitled "Container lashing system on weather deck", which should be subject to approved by a classification society. In particular the object of classification should include:

- lashing technique in the sense of lashing gear certification both loose /rods, turnbuckles, connectors, etc./ and permanent fittings /catches and all kinds of foundations/;
- information on the permissible external loadings /admissible masses or accelerations/ in the sense of conformity of calculations with the recommended by regulations algorithm. In case if the objective calculations are carried out according to one's own /the shipyard's/ algorithm, the algorithm itself should also be a subject to approval;
- information related to the relation of the ship's accelerations to operating and waving parameters understood as conformity of calculations in compliance with the recommended programme or acceptance of the programme applied by the designer.

The above classification procedures are determined by requirements for the sake of requirements themselves, which in their part related to stowage and container lashing should include:

- determination of standards and methods of testing the lashing gear;
- algorithm of lashing strength calculations;
- recommendation to apply a specified computing programme of the short-term prediction of ship's acceleration with identification of form presenting the obtained results.

The latter requirement is a substantial novelty as far as objective regulations are concerned, which in their current form determined the way of calculating the accelerations meant as long-term prognosis, as criterion values, univocally dimensioning the admissible load masses. In the presen-

---

[x] a complete univocal meaning is impossible on account of a random character of sea waves and ship's motion.

[xx] experiments prove that in general the transverse accelerations a_t determine mainly the container lashing and their dependence upon the ship's velocity with sufficient accuracy in relation to practice can be identified with the dependence upon the relative heading angle only.

ner's experience.
The information regarding the lashing technique should be explained in graphic form, as it is shown in Fig. 2.

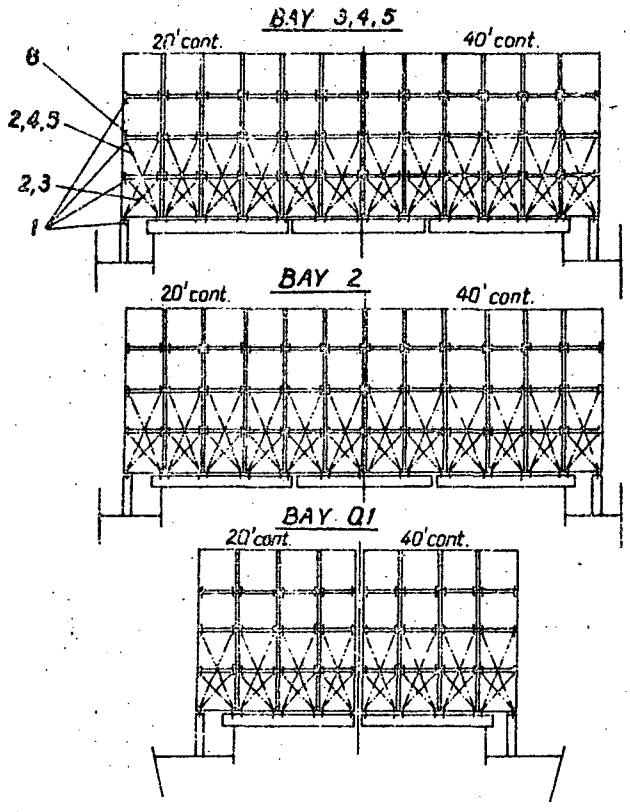

6	GE 19 Penguin hook	
5	BR 02 (50) Lashing rods	
4	BR 01 (50) Lashing rods	
3	BR 05 (50) Lashing rods	
2	TE 150.2 Turnbuckles	
1	CI - 5 - 1L Twist locks	

FIG. 2. TECHNIQUE OF LASHING.

2.3.2. However, the preparation of diagrams, as in item b/, requires calculations of the type:

$$M a_t \leq A - B F_w \qquad (1)$$

where:

- M - total mass of the containers stack,
- a_t - transverse acceleration,
- A,B - coefficients dependent upon the strength parameters of lashing and stack's configuration,
- F_w - additional force for external /OUT/ stacks. For internal /IN/ stacks $F_w = 0$.

It should be noted that the form of equation (1), and also the values of coefficients A and B also depend on the adopted mathematical model of lashing construction. The idea of these calculations is always such that they lead to the determination of the external admissible inertial force $F = M \cdot a_t$, for which the stack stability is still maintained. The up-to-now testing calculations, which have been mentioned earlier are based on the determination of:

$$M \leq \frac{A - B F_w}{a_t} \qquad (2)$$

where on the contrary to equation (1), acceleration a_t was imposed by the classification society regulations.
In this way attention was concentrated on finding only the admissible stack mass M, but not admissible force F. Thus the calculations according to equation (2) were of a long-term prediction character determinated.
This followed from the way of determining acceleration a_t.
The determination according to equation (1) of the admissible force $F = M \cdot a_t$ gives a more universal information, and thereby really useful for the benefit of the ship's operation and whole shipping line. The universality of such an approach is based on the fact that for determined admissible force F constant with regard to the defined lashing technique and configuration of the container stack it is possible to apply in an interchangeable way relations:

$$a_t = \frac{F}{M} \quad \text{or} \quad M = \frac{F}{a_t} \qquad (3)$$

ipment and the method of its application/,

b/ information regarding the maximum permissible values of accelerations resulting from lashing technique and the current integrally being lashed mass of cargo,

c/ information about dependences of accelerations upon the sea state, ship's velocity and loading condition.

The lashing system block scheme is presented in Fig. 1.

The lashing system understood in this way should be a document prepared by the shipyard, approved by classification societies and applied on ship's like stability information to the master.

a document are:

scheme of the lashing technique and diagrams related to information b/ and c/. As an example here can be Fig. 2,3 and 4.

2.3.1. The designing of the lashing technique is based on making a selection which lashing method should be chosen /e.g.stack lashing by use of two pairs of lashing rods with turnbuckles, and the like/, choice of an appropriate loose lashing gear within the range of the offered variety of the specialized suppliers, and a project of applicable lashing catch on deck.

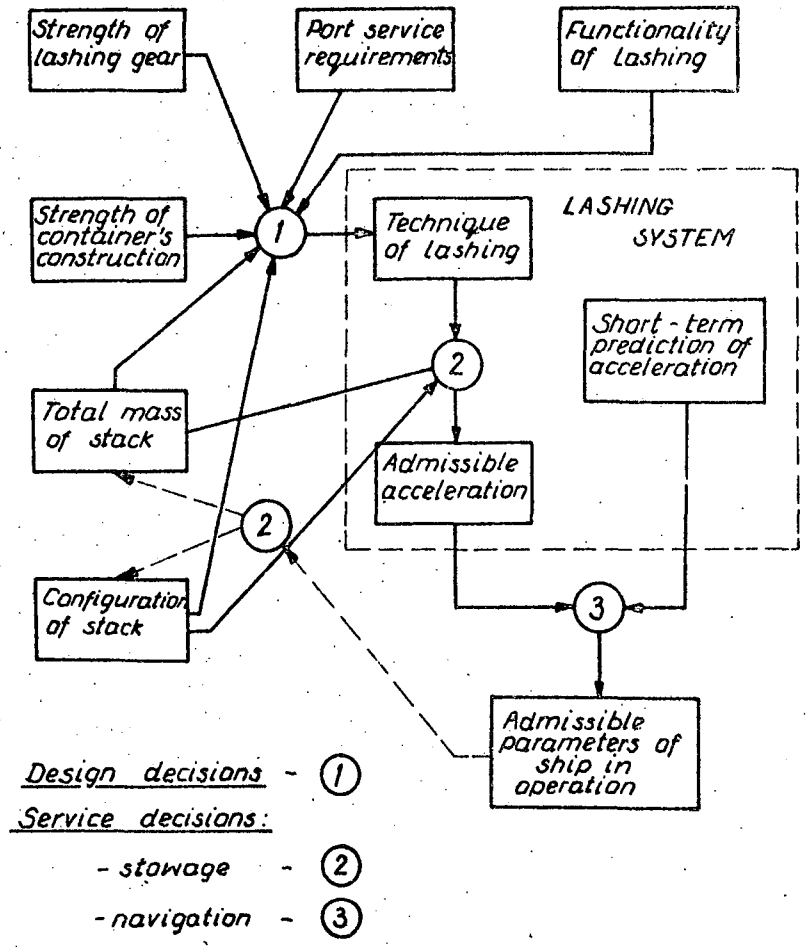

FIG. 1. THE LASHING SYSTEM BLOCK SCHEME.

2.3. Designing and Approval of Lashing System

The objective tasks of disigning have been defined in previous point and can be reduced to elaboration of an appropriate document containing some information as in points a/, b/, and c/. It is assumed that the most advisable form of such

The above design activities are characterized, primarily, by the fact that strength calculations intended to check the lashing gear for the referred to as standard acceleration values are not necessarily carried out. The loose lashing gear is simply chosen in compliance with the ship owner's requirements and the desig-

2. STOWAGE AND LASHING SYSTEM OF CONTAINERS SHIPPED ON WEATHER DECKS OF LO-LO AND RO-RO VESSELS

2.1. Significance of the Problem

The stability of cargo is a significant ship's stability determinant in general. Numerical data indicate that at least 25% of accidents connected with capsizing are caused by shifting of cargo. However, it is likely to assume the real share to be greater for the reason that many incidents remain unexplained or have been roughly qualified as "due to pure loss of stability". Even if the breaking away of cargo does not lead to the loss of the ship it causes a serious threat to safety and undoubtedly it is a definite economical loss.

The stability of cargo depends not only on the lashing itself but also on external load magnitudes which are directly connected with the ship's movements upon wave - mainly due to roll motion. And in this matter there is a close relation between cargo stability and the ship's safety against capsizing. In one case and the other there exists the same effective measure of risk expressed in characteristics of roll motion.

Conventional general cargo was stowed and lashed in holds and on deck individually depending on the kind of cargo, specifity of shipping line, but primarily on the experience of the cargo officers. Up-to-date lo-lo and ro-ro technologies constituting already an important and constantly developing part of sea transport call for lashing the cargo and at least the technique of lashing to be determined as early as in the design phase of the ship. Thus there has appeared a new technical subsystem of the ship the solutions of which worked out during the design stage and applied in course of ship's operation affect both the economics of contemporary sea transport and its safety. In view of the above there are sufficient reasons for which the objective technical subsystem of the ship should become a system[x/] whose design ought to be:

- rationalized by making use of all the capabilities of science both in the sphere of naval hydromechanics, and structural mechanics,
- defined, supervised, and approved by classification societies having at their disposal appropriate regulations.

At present the practice is far from such solution. However the classification societies determine rules of designing the containers lashing techniques, but solely the technique and only in form of instructions.

Moreover, the designer is not obliged by anything to elaborate an instructive document /e.g. similar to the information on stability/ to be utilized by the ship's crew at work. The stimulated by current regulations designing of lashing procedures exoludes any effect of the ship's crew upon the cargo stability - its role is reduced to the control of technical state of lashing. The project univocally determines the maximum configuration /number of layers and distribution of mass in layers/of container stack and, what is most important, it does not give any information for a rational performance of operational navigation which affects the values of the external load of the cargo. Hence, it is a typical long-term solution, "insensitive" to constantly changing operational conditions relating both to weather and economy.

The proposed idea of so-called lashing system is to be a solution which deprived of the above mentioned drawbacks gives a chance of an optimal and effective fulfilment of the safety requirements and economics of the shipping trade.

2.2. Definition of the Lashing System

The lashing system is a complex set of information, both about the lashing technique and the unitary dependences of external forces /accelerations/ affecting the cargo as a function of ship's velocity[x/] for a determined state of loading and weather conditions.

From a formal point of view the lashing system consists of:

a/ description of the lashing techniques /description of the lashing equ-

x/ the system is the property of an appropriate technical structure; it is a structure of transformational relations and coupling relations related to the operation of technical structure.

x/ the ship's velocity is understood here as a vector described both by the speed /length of the vector/ and the relative heading angle /angle between the ship's velocity and the main directional propagation of waves/.

Third International Conference on Stability of Ships and Ocean Vehicles, Gdańsk, Sept. 1986 STAB'86

LASHING OF SHIP CARGO AS AN ESSENTIAL FACTOR DETERMINING STABILITY SAFETY AND ECONOMICS OF VESSELS

J. Stasiak

SUMMARY

The paper presents a concept of a rational system for lashing of cargo carried in sea transport and shows particulary a solution of the system for containers carried on open decks. The proposed system is understood here as a complete set of information both the applied technics of lashing and about the external forces acting on the ship and cargo for a given sea state.

The rationalism of the proposed system is based on a more complete utilization of the up-to-date achievements of ship hydrodynamics and on taking, in a better way as yet, into account so called human factor.

The presented system of cargo lashing is thought, in general, as an example of solution to one of the basic problems related to stability safety of the shipping. It follows from the fact that statistically about 25% ships which capsized in rough seas did so because of loss of cargo mass stability. This dangerous situation happens more frequently due to lack of sufficient information about the all phenomena determining stability of cargo on board a ship rather than due to plain crew remissness.

1. INTRODUCTION

Safety and economics of ships often present in their solutions some controversial problems and at the same time they are two basic factors determining the usefulness of shipping. It is necessary for the shipping industry to be economical and safe, but not economical or safe. The problem of optimum reconciliation between these reasons is always accompanying both the designers and the users. The difficulty of solving the problem is magnified by the fact that the ship as a material structure univocally defined at the design stage, which operates under various conditions and in many cases the external loads exceed the accepted permissible designed values. The reality, however, reveals that there is a possibility to adapt the ship effectively to every in principle situation. It results from the fact that the ship presents a closed controlled system where the feedback element determines its homeostatic capability[x]. It indicates that every ship's reaction may be and is controlled and regulated within some permissible limits. The subject of these operations is broadly understood as ship's management [xx], which consequently makes it necessary for all the problems of the ship's operation, including the reconciliation of safety with economics to be cybernetic [xxx] problems.

As in every cybernetic problem phenomenon the effectiveness of solutions is also here conditioned by quality and quantity of information. This paper presents this fact by discussing the idea of rational system of container lashing on the weather decks of lo-lo and ro-ro types of vessels. The proposed idea is here not only an example of significance of the information for the accomplishment of a defined cybernetic task, but also a utilitarian solution of a specific cargo stability problem which to a great extent determines the ship's safety in general.

---

[x] physiological term denoting the capability of living creatures to retain a permanent internal state in spite of some external variations

[xx] crew and harbour service

[xxx] cybernetics - a word of Greek origin meaning "control of a ship"

Polish/. Report of Ship Research Institute, Gdańsk, 1986.

ABOUT THE AUTHORS

MIŁOSZ FRĄCKOWIAK, graduated in naval architecture from Technical University of Gdańsk in 1956 and since then started his work at the Ship Hydromechanic Division and have been working there till now. Ph. D. in 1966, since 1970 assistant professor. In the period 1970-73 professor at Marine Engineering Department, Basra/Irak/ and in 1981-1983 Marine Engineering Department, Port Harcourt /Nigeria/.

MACIEJ PAWŁOWSKI, graduated in naval architecture from the Technical University of Gdańsk in 1970. Next he joined the Ship Research Institute of this University and have been working as an academic teacher at the Ship Hydromechanic Division.
In 1978 he completed his Ph.D.thesis and in 1986 his D.Sc. thesis, both connected with the ship safety in damaged condition based on the probabilistic concept.

5. It is a trend now to increase the dimensions of boat. This is connected with the installation on some beaches mechanical hoists which replace the man power in pushing the boat into the sea.
The boat for open sea should have the length not less than 7.5 m and the freeboard not less than 0.25 m. The freeboard at F.P. should be not less than 0.55 m. These values have been obtained from shippment of water calculations for sea state No 4 corresponding to $h_{1/3} = 0.6$ m and $T_1 = 3.4$ sec.
The length of the boat cannot exceed 12 m because for larger boats the tax in Poland is much higher.
6. On the Polish sea side the shape of the body created by tradition was not changed during many years. The average ratio $\frac{L}{B}$ is below 3, block coefficient $C_B = 0.39 - 0.56$, waterplane coefficient $C_W = 0.68 - 0.78$.
The range of length is mainly between $L = 5.5 \div 9$ m and power of the engine mainly up to 30 HP.
7. It is advisable for boats other than woodon, to employ some buoyancy elements to improve the behaviour when the boat ispartially flooded.
8. It is recommended that any hydrostatic calculations should be limited only to design condition. For this draught the displacement and the area of the waterplane must be estimated whereas the metacentric ordinate may be calculated by the formula as follows:

$$KM = \frac{d}{1 + \frac{C_B}{C_W}} + \frac{C_W^2}{11.7 C_B} \cdot \frac{B^2}{d}$$

This result in many cases is more accurate than by a computer program.
9. The ordinate of centre of gravity for design displacement can be determined from inclining experiment or by means of an assessment.
10. A good stability criterion for all open deck fishing boats appears the following requirement

$$\frac{GM}{B_{max}} \cdot \frac{F_{min}}{B_{max}} \geq 0.033$$

determined only for design condition, but $\frac{F_{min}}{B_{max}}$ in that formula should not be greater than 0.15.
11. It is recommended that the dimensions for the registration cards of Maritime Administration as well as in future rules of the Polish Register of Shipping should be given in an uniform way. The following dimensions are necessary.

- L_{OA} - length overall but without rubrail and permanent fittings stioking out from the hull construction,
- L - length of the design waterplane, as above,
- B_{max} - breadth overall without rubrail,
- B - maximum breadth of design waterplane including shell plating,
- D - depth measured from the base plane /the keel is not included/ to the lowest point of gunwale,
- d - design draught measured from the base plane.

12. It seems that the only known rules of Det Norske Veritas with many details are not too excellent. There are very strong requirements due to floating capabilities and stability when flooded. The Polish boats formally do not fulfill these requirements.
13. Nowadays it is appropriate to provide the rules of Polish Register of Shipping for fishing boats construction. The rules should not be very wide, with many details but should be rather simple. The rules should not intervence much into the traditional construction. The rules should be only limited to the survey of general condition of the boat to check the correctness of design, to fulfill the requirement of the freeboard and to introduce a simple index number to ensure the boat a proper stability.

The application of buoyancy elements inside the boat could be recommended but not compulsory.

BIBLIOGRAPHY

[1] Rules for Construction and Certification of Boats; Det Norske Veritas 1981;
[2] Frąckowiak M., Netcer J., Phan Van Pho; The Record of Polish Open Deck Fishing Boats /in Polish/. Report of Ship Research Institute, Gdańsk 1986;
[3] Frąckowiak M., Pawłowski M.; The Safety of Small Open Deck Fishing Boats /in

Table 5.

		Boat A			Boat B			Boat C			Boat D		
V	m^3	2.475	2.750	3.025	3.607	4.008	4.409	12.55	13.94	15.33	16.78	18.65	20.52
KM	m	1.228	1.208	1.189	1.413	1.387	1.368	1.727	1.684	1.667	2.138	2.065	2.014
GM	m	0.773	0.753	0.734	0.830	0.804	0.785	0.957	0.914	0.897	1.368	1.295	1.244
KZ	m	0.346	0.308	0.273	0.529	0.491	0.456	0.470	0.397	0.325	0.518	0.432	0.348
ϕ	deg	17.04	15.12	13.47	22.87	21.23	19.75	15.83	13.50	11.18	14.12	12.00	9.90
GZ	m	0.213	0.189	0.167	0.302	0.280	0.259	0.260	0.217	0.176	0.330	0.272	0.216
GM sinϕ	m	0.227	0.196	0.171	0.323	0.291	0.265	0.261	0.213	0.174	0.334	0.269	0.214
GM $2F/B_{max}$	m	0.218	0.190	0.166	0.320	0.287	0.260	0.260	0.211	0.175	0.328	0.266	0.213

		Boat E		
V	m^3	14.49	16.10	17.71
KM	m	2.22	2.20	2.16
GM	m	1.26	1.24	1.20
KZ	m	0.954	0.867	0.794
ϕ	deg	26.7	24.80	23.0
GZ	m	.523	0.464	0.419
GM sin ϕ	m	.566	0.520	0.469
GM $2F/B_{max}$	m	.563	0.512	0.455

Thus the basic stability criterion is as follows:

$$\frac{GM}{B_{max}} \cdot \frac{F}{B_{max}} \geqslant \frac{1}{4}\left(\frac{p}{\Delta}\right)_{crit} \qquad (5)$$

and it is sufficient to apply it only at the design condition;

- F/B_{max} at formula (5) should not be taken greater than 0.15;
- the metacentric height GM should be evaluate for the design condition according to the plans. In case of lack of detailed data KG may be taken as 0.6 D.

At Table 6 there are given the valuas of p/Δ in % for the 5 fishing boats.

Table 6.

Boat	A	B	C	D	E
100 p/Δ	17.1	18.7	12.2	13.6	19.5

It is suggested to take as a minimum allowable value of

$$\left(\frac{p}{\Delta}\right)_{crit} = 13\%$$

If we assume that the smallest value of p should not be less than about 200 kg in case of a motor-boat then the above condition yields that for such a boat the smallest volume displacement should not be less that about 1.6 m^3. In this way we get that the length L of the smallest fishing boats is about 5 m.

The values of p/Δ given at Table 6 are a good measure of the boat stability which agrees with common intuition. On the basis of body plans itself, without any calculations or experiments, boats C and D seem to be clearly worse than the others as far as their stability safety is concerned.

From stability criterion (5) it follows that two quotients B/D and B/d are of the basic importance for the stability of the boat.

4. CONCLUSIONS

From the investigations of the Polish small open deck sea fishing boats the following conclusions can be drawn out:

1. To all appearance although the boats operate frequently in severe conditions they are safe. From many years since the sail was replace by the engine the annuals were not registered any accidents of loss a boat and fisherman.
2. The equipment of the fishing boats has great influence on their safety. Each boat should be outfitted at least with; life-jacket for each fisherman, life-saving ring, signaling pistol, compass and walkie-talkie.
3. Because the boat construction has been moved to the workshops where they are built by more people according to the technical drawings it is growing up an awareness to cover this activity by rules of classification society together with a supervision of their performance.
4. If it is decided to take such boats under the supervision of the Polish Register of Shipping the rules should cover only the motor boats. The rowboats should be beyond this consideration because they serve as auxiliary boats and operate very near the shore.

would be given by the following formula:

$$BM = \frac{C_W}{2(1+C_W)(1+2C_W)} \cdot \frac{C_W^2}{C_B} \cdot \frac{B^2}{d} \qquad (2)$$

This formula can be simplified further as the first term in it yields the numerical values nearly constant for the interesting range of waterplane block coefficient C_W from 0.60 up to 0.85. The numerical values of this term are as follows:

Table 3.

C_W	0.60	0.65	0.70	0.75	0.80	0.85
	11.73	11.68	11.66	11.67	11.70	11.75

Assuming that $2(1+C_W)(1+2C_W)/C_W = 11.70$ we get that:

$$BM = \frac{1}{11.7} \cdot \frac{C_W^2}{C_B} \cdot \frac{B^2}{d} \qquad (3)$$

The actual values of KB and BM for the fishing boats can differ from the values given by the above formulae. To get actual values these formulae must be therefore multiplied by correction coefficients a_B and a_M. The values of these coefficients for the 5 boats are given at Table 4.

Table 4.

Boat	A	B	C	D	E
a_B	1.021	1.031	1.018	1.010	0.987
a_M	1.002	0.994	1.010	1.022	1.017

As can be seen the ordinate of the centre of buoyancy differs from -1 to 3% from the values given by formula (1) whereas the metacentric radius - from -1 to 2% from the values given by formula (3) .Thus these differences are not greater than the accuracy of numerical calculations. Due to this reason it is advisable to assume that $a_B = a_M = 1$.

3. STABILITY ASSESSMENT

The small fishing boats are of open type, i.e. with no deck therefore their stability is limited to initial stability, i.e. up to the angle of deck immersion. Due to this reason it is convenient to take as a measure of boat stability the righting arm at the angle of deck immersion. At Table 5 there are compiled these arms for the individual boats and for three volume displacements equal to 0.9, 1 and 1.1 of the design displacement. The value of KG is assumed the same for all these three load conditions.

As we can see the righting arm at the angle of deck immersion can be approximated with a good accuracy by means of a product of the initial metacentric height and a double freeboard related to the maximum breadth of the boat, measured outside the boat shell, i.e.

$$GZ = GM \cdot \frac{2F}{B_{max}} \qquad (4)$$

The differences are not greater than the errors of numerical calculations.

From the above calculations it follows also that with the variation of displacement the righting arm changes to a higher degree in the opposite direction, i.e.

$$k \frac{\delta V}{V} = -\frac{\delta l}{l}$$

where $k > 1$, $l \equiv GZ$ and δ means here a difference. This means that the boat righting moment at the angle of deck immersion always decreases with an increase of the displacement. In other words, the stability safety of the boat always decreases when the freeboard of the boat decreases due to an increase of its loading. Thus it is very important that the boat should never be overloaded during operation. This agrees with a good shipping practice.

It is possible now to establish a very simple stability criterion for the small fishing boats. Namely, the stability of the boat it is considered as satisfactory if the boat at the design condition can withstand the shifting respectively large weight p from the plane of symmetry to the edge of the boat side, i.e. if the edge of the side will not immerse or if the angle of heel will not be larger than a stated value, say 15 degrees. Applying formula (4) we get

$$\frac{p}{\Delta} = 4 \cdot \frac{GM}{B_{max}} \cdot \frac{F}{B_{max}}$$

where

Δ - displacement of the boat at the design draught

F - freeboard understood as the distance of the lowest point of the edge of side from the deepest waterplane.

Table 2.

Boat		A	B	C	D	E
L	m	5.97	6.83	8.40	9.60	9.12
B_{max}	m	2.22	2.58	3.46	3.90	4.00
B	m	2.15	2.46	3.31	3.81	3.90
D	m	0.83	1.06	1.40	1.40	1.60
d	m	0.55	0.60	1.00	1.00	0.80
F	m	0.28	0.46	0.40	0.40	0.80
KG	m	0.46	0.58	0.77	0.77	0.96
L/B		2.78	2.78	2.54	2.52	2.34
B/d		3.91	4.10	3.31	3.81	4.88
B_{max}/D		2.68	2.43	2.47	2.79	2.50
F/B_{max}		0.126	0.178	0.116	0.103	0.200
C_{VP}		0.574	0.585	0.665	0.666	0.721
C_W		0.679	0.679	0.754	0.766	0.785
C_B		0.390	0.398	0.501	0.510	0.566

On Fig. 3 there are shown body plans of boat A and D.

Numerical calculations have shown that trim has a negligible effect on the hydrostatic magnitudes of the boat, except of LCB - what is self-explanatory.

In order to calculate the initial stability of the boat it is necessary to know the vertical distance of the metacentre above the base plane, i.e.

$$KM = KB + BM$$

If the curve of waterplane area was a parabola then the ordinate of the centre of buoyancy would be given by a formula:

$$KB = \frac{d}{1 + C_{VP}} \qquad (1).$$

If the moulded waterplane was a parabola then the initial metacentric radius

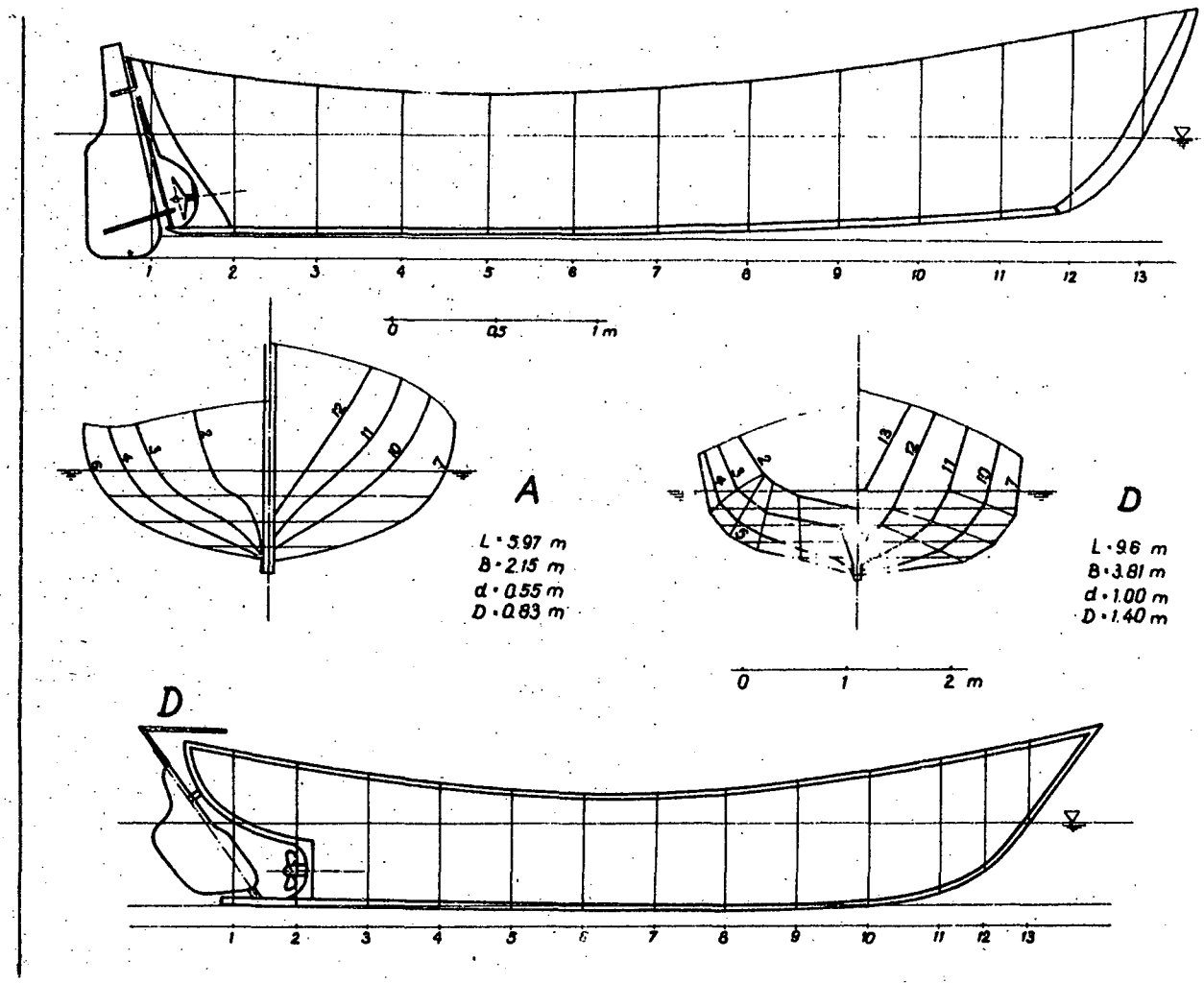

Fig. 3. Body plans of boat A and D.

projects were still the existing boats. During next years this percentage will be growing up.

There are various materials used for building the boats. Table 1 complies the Polish fishing boats according to the stuff from which the boats are made of.

Table 1.

Material	oak	steel	laminate	aluminium	laminate + oak	total
No of boats	1008	81	48	7	5	1149
%	87.7	7.1	4.2	0.6	0.4	100

As can be seen a considerable majority of boats in Poland, i.e. 87.7% is made of oak. It is necessary to expect, however, that in the nearest future the percentage of boats made of steel or laminate will be growing up.

Generally speaking, the boats can be regarded as safe. During the 5 recent years there have been no reports on the loss of boats or lives. It can be noticed that boat casualties have in practice disappeared at all when the sail was replaced by the engine. There are many reasons for this. Firstly - no sail, no heeling moment due to wind, secondly - due to engine the boat can hurry back to its haven in case of bad weather, thridly -the proper shape and proportions of the boats developed by the aged tradition.

On Fig. 1 and Fig. 2 there are presented distributions of lengths and breadths both for motor-boats and row-boats.

As far as the power of engine is concerned 86% of motor-boats are fitted with the engine of power up to 30HP.

There were carried out linear regressions of L_{OA}/B_{max} versus L_{OA} and B_{max} versus L_{OA} for 1149 Polish boats. They are as follows:

$$\frac{L_{OA}}{B_{max}} = 2.85 + 0.03 \cdot L_{OA}$$

$$B_{max} = 0.13 + 0.31 \cdot L_{OA}$$

with the coefficient of correlation r=0.82.

Quotient B_{max}/D appears to be not dependent statistically on L_{OA} what agrees with a basic stability criterion for small fishing boats. The average value of B_{max}/D is equal to 2.52.

Below at Table 2 there are given particulars of 5 Polish fishing boats. It is worthwhile emphasing that quotient L/B is less than 3. Boat A and B are made of oak, whereas three other boats - of steel.

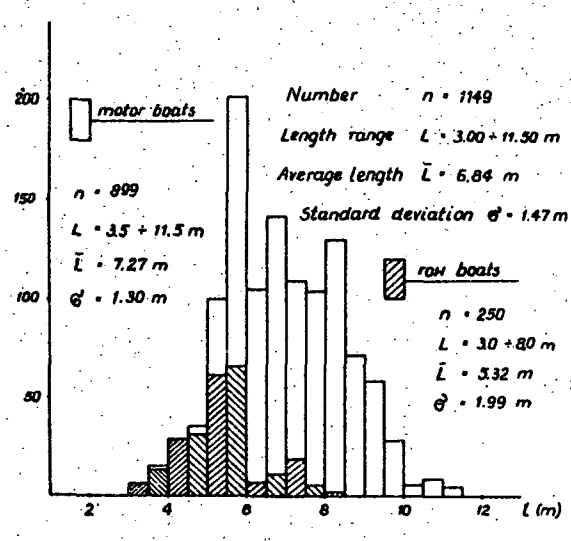

Fig. 1 - Histogram of lengths for fishing boats.

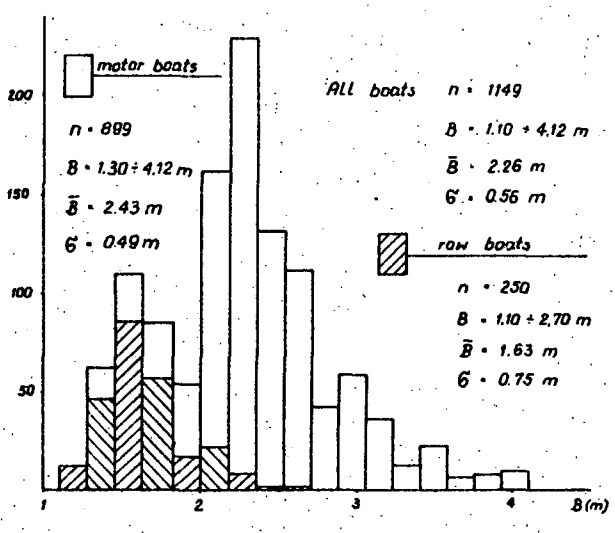

Fig. 2 - Histogram of breadths for fishing boats.

Third International Conference on Stability of Ships and Ocean Vehicles, Gdańsk, Sept. 1986 STAB'86

THE SAFETY OF SMALL OPEN DECK FISHING BOATS

M. Frąckowiak, M. Pawłowski

ABSTRACT

The paper is based on statistical data concerning the fishing boat being in service in Poland. There are given some geometrical characteristics of these boats, their propulsion power and the stuff used for their construction. The stability calculations have been carried out and a method for their safety assessment has been proposed. There has been proposed also magnitudes of freeboard at bow and midships based on shipping of water calculations in irregular head seas.
It is pointed out that the boats are safe due to their shapes created by agelong tradition.

1. INTRODUCTION

There are tremendous amount of small open deck fishing boats all over the world and their catches are significant when compared with the whole fisheries. In some countries such boats are the only crafts which supply the fish market. They operate quite often in heavy weather conditions. In addition to this their safety depends also on dimensions and shape, on load conditions and navigating skill of fishermen. Notwithstanding the above these small coastal fishing crafts are beyond the rules and regulations of classification societies. The only exception known to the authors are the Rules of Det Norske Veritas [1] wherein however, the wooden boats are not included. Even in these days the boats are built according to the agelong tradition related to a specific region and existing conditions. Very often they are built without any drawings and calculations. Also in Poland the open deck fishing boats are apart from the rules of the Polish Register of Shipping.

Besides the description of such boats being in service in Poland with the stability and seaworthy features the paper is going to give an answer whether such rules not being in use for ages are necessary now or not. When the boats came under the inspection there would be a question what kind of perameters of the boat were the most important to ensure the sufficient safety at sea. On the basis of these investigations it is possible to establish some criteria related to stability and floating capabilities.

The Norwegian rules consider the minimum freeboard and the stability for a particular heeling moment. The boats under 5,5 m in length and desired freeboard should be fitted out with the buoyancy elements. It means that for larger boats the buoyancy tanks are not necessary but here is a contradiction because there is also a requirement that all boats fully outfitted with additional load and completely flooded are not to sink and have positive righting arms up to 60°. For steel and laminate boat without additional buoyancy elements such requirements cannot be fullfilled.

2. GENERAL CHARACTERISTIC OF THE POLISH SMALL OPEN DECK FISHING BOATS

In the past, even not long ago, the boats were built by singular craftsmen or even fishermen mostly without any technical drawings according to the existing agelong tradition. These days the boats are built more often by not large workshops and the individual craftsmen are vanishing. Up today 37% of boats in service have been built in workshops according to technical drawings but the pattern of such

surface condition $\left[K\Phi + \frac{\partial \Phi}{\partial z}\right]_{z=0} = 0$. $G(P, Q)$ is given by,

$$G(P, Q)e^{i\omega t} = -2 \lim_{\mu \to 0} \int_0^\infty \frac{e^{-kz'} \cos k(y - y')}{k - K + i\mu} \, dk \, e^{i\omega t}$$

$\sigma_m(Q)$ is the density of source distribution along the section's contour C_h; when m=2, 3 and 4, the velocity potential provides radiation waves generated by the oscillation of the section; m=7 denotes the velocity potential of diffraction waves.

$\sigma_m(Q)$ in this equation has to be determined such that the velocity potential satisfies the following boundary conditions on the contour in its equilibrium.

For radiation problem:

$$\frac{\partial}{\partial n} \Phi_2 = -i\omega X_2 \frac{\partial y}{\partial n} e^{i\omega t}$$

$$\frac{\partial}{\partial n} \Phi_3 = -i\omega X_3 \frac{\partial z}{\partial n} e^{i\omega t}$$

$$\frac{\partial}{\partial n} \Phi_4 = i\omega X_4 \left(z\frac{\partial y}{\partial n} - y\frac{\partial z}{\partial n}\right) e^{i\omega t}$$

For diffraction problem:

$$\frac{\partial}{\partial n} \Phi_7 = -\frac{ig}{\omega} \zeta_a \frac{\partial}{\partial n}\left(e^{-Kz + iKy}\right) e^{i\omega t}$$

where n is the outward normal to the contour.

Actually (A-1) is rewritten in the form of the stream function instead of the velocity potential for computational convenience; the section contour is approximated by a polygon with 30 sides on each of which $\sigma_m(Q)$ is assumed to be constant.

With $\sigma_m(Q)$ thus determined, the dynamic swell-up, that is, the wave elevation due to both the radiation and diffraction is expressed by

$$\zeta_{RD}(y, 0, t) = Re\left\{\int_{C_h} [2KX_m\sigma_R(Q) + \zeta_a\sigma_D(Q)]2[\pi i e^{-Kz' - iK(y-y')} - \int_0^\infty \frac{k \cos kz' - K \sin kz'}{k^2 + K^2} e^{-K(y-y')} dk] \times ds \, e^{i\omega t}\right\} \quad \text{(A-2)}$$

We have the dynamic swell-up on the weather or lee side of the ship with substituting $y=+B/2$ or $y=-B/2$ into the equation (A-2).

deck with deck wetting occured only once to let the ship capsize (Fig.15).

Thus critical wave amplitude of capsize for those models, generally supposed to be different from that of deck wetness, is determined for each frequency of the incident waves. Dotted lines in Fig.3 ∿ 6 are such critical wave amplitude of capsize which agree fairly well with the experimental results particularly around the rolling natural period.

5. CONCLUDING REMARKS

We gave a correct prediction of critical wave height of deck wetness for ship models having simple configuration in regular beam seas. In this prediction our approach is computation of relative motion of the free surface to the ship in frequency domain in which are incorporated accurately effects of radiation and diffraction waves particularly including local waves prominent in the vicinity of the hull surface.

Frequency domain analysis provides us only with informations whether deck wetting occurs or not. Time domain analysis is required to predict how it happens, once or repeatedly and how much, which we know from observations, is crucial to investigate effects of deck wetting on fatal condition of a ship.

A rather simplified time domain analysis clarified dynamics of the ship that deck wetting does not occur in some cases repeatedly even in regular waves; however, in other, it is possible that rapid accumulation of shipping water on deck caused by repeated deck wetting leads to capsize.

REFERENCES

1. Caglayan, I. and Storch, R.: "Stability of Fishing Vessels with Water on Deck : A Review" Journal of Ship Research, Vol. 26, No.2, June 1982, pp.106 - 116.
2. Rakhmanin, N.N.: "Constant Heeling Forces and Their Effect upon the Stability of a Low-built Vessel in Waves" Second International Conference on Stability of Ships and Ocean Vehicles, Tokyo, 1982, pp.19 - 28.
3. Tamiya, S.: "On the Dynamical Effect of Free Water Surface" The Society of Naval Architects of Japan, Vol.103, June 1958, pp.59 - 67.
4. Dillingham, J.: "Motion Studies of a Vessel with Water on Deck" Marine Technology, Vol.18, No.1, Jan. 1981, pp.38 - 50.
5. Adee, B.H. and Caglayan, I.: "The Effects of Free Water on Deck on the Motions and Stability of Vessels" Second International Conference on Stability of Ships and Ocean Vehicles, Tokyo, Oct. 1982, pp.413 - 426.
6. Gonno, M.: "A Calculation on Deck Wetness in Regular Oblique Waves" Journal of the Kansai Society of Naval Architects, No.145, September 1972, pp.75 - 81.
7. Shin, C.: "On the Critical Wave Height of Deck Wetness for Two-dimensional Body" Trans. of the West-Japan Society of Naval Architects, No.56, August 1978, pp.207 - 228.
8. Shin, C.: "On the Critical Wave Height of Deck Wetness for Inclined Ships in Transverse Waves" Trans. of the West-Japan Society of Naval Architects, No. 64, August 1982, pp.135 - 143.
9. Grochowalski, S.: "The Prediction of Deck Wetting in Beam Seas in the Light of Results of Model Tests" Second International Conference on Stability of Ships and Ocean Vehicles, Tokyo, 1982, pp.433 - 447.
10. Shin, C.: "On the Shipping Water Due to Orbital Motion of the Wave" The Bulletin of Nagasaki Institute of Applied Science, Vol.21, No.1, June 1980, pp.13 - 24.
11. Shin, C.: "On the Unsymmetrical Rolling of Ships" The Bulletin of the College of Naval Architecture of Nagasaki" Vol. 15, No.2, Oct. 1974, pp.1 - 11.
12. Kobayashi, M.: "Hydrodynamic Forces and Moments Acting on Two-dimensional Asymmetrical Bodies" Mitsui Zosen Technical Review, No.87, July 1974, pp.1 - 14.

APPENDIX

2-D flow field around a section of the ship, forced to oscillate in the m-th mode of motion (m=2: swaying, 3: heaving, 4: rolling) of amplitude x_m and frequency ω, or fixed (m=7) in the incident waves

$$\zeta = \zeta_a \cos(Ky + \omega t)$$

coming abeam as shown in Fig.7, is expressed by the velocity potential:

$$\Phi_m(y, z, t) = R_e\{i\omega X_m \int_{C_h} \sigma_m(Q) \times G(P, Q)ds\, e^{i\omega t}\} \qquad (A\text{-}1)$$

where $G(P, Q)e^{i\omega t}$ is the velocity potential at $P(x, y)$ of a pulsating source located at $Q(x', y')$, which satisfies the linear free

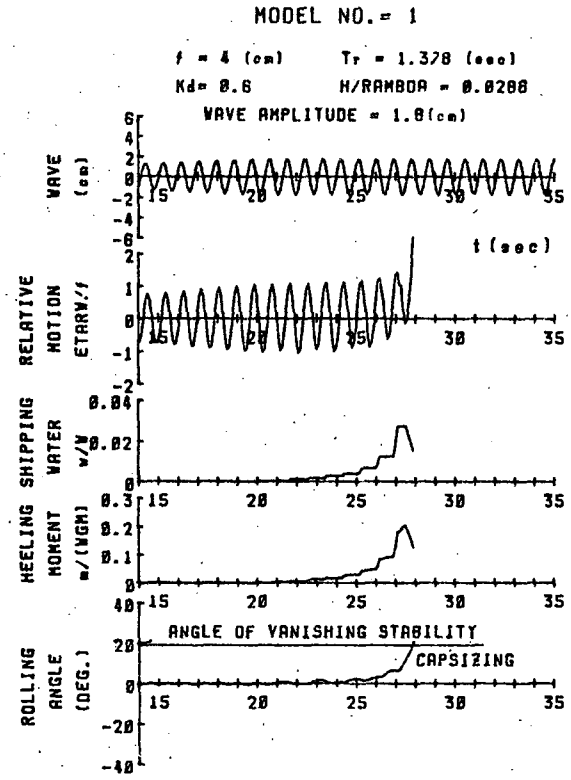

Fig.13 Transient responses under deck wetting

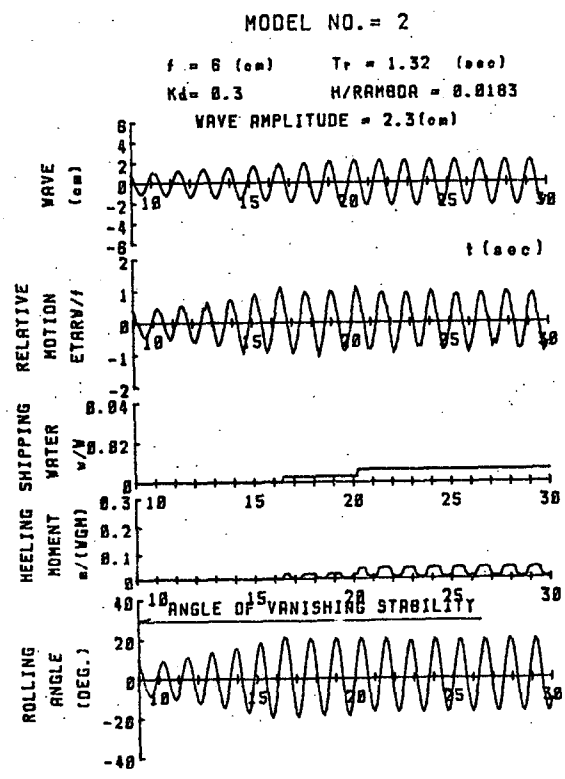

Fig.14 Transient responses under deck wetting

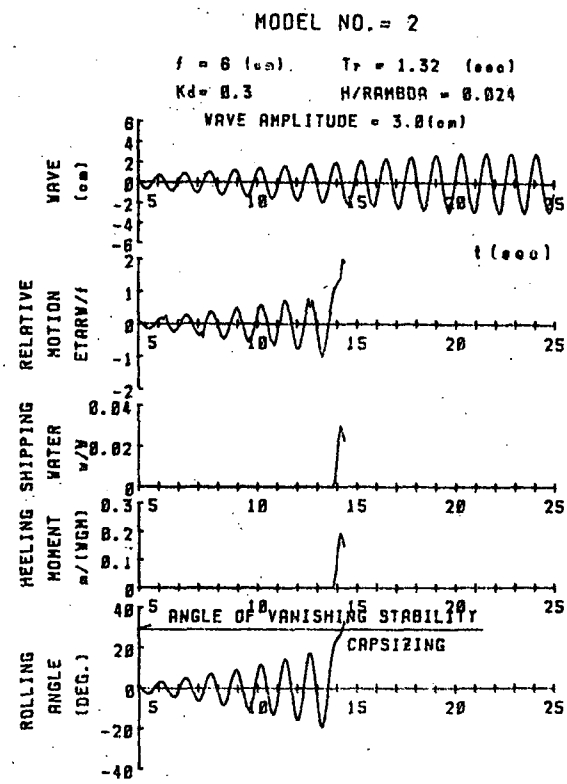

Fig.15 Transient responses under deck wetting

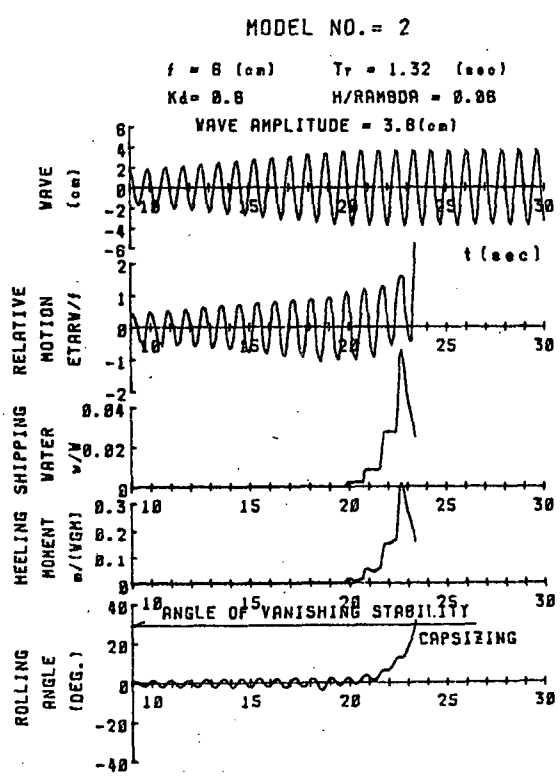

Fig.16 Transient responses under deck wetting

have similar results as shown in Fig.14 and 15. Shipping water as a result of deck wetting occured two times reduces the rolling angle to make the relative water surface lower than the bulwark even if waves are a little higher than the critical of deck wetness (Fig.14). However much higher wave pours sufficient amount of water on

some coefficients of the equations of motion due to the shipping water and also the rate of variation in the mass of the ship. Heeling angle newly computed gives a sectional form under the water leading to new wave exciting forces and moment. Then return to the equations of motion at the next step.

Several results of the simulation under the influence of shipping water are presented in Fig.10 ∿ 16: wave elevation at the center of the ship, relative motion/freeboard f, amount of shipping water/the ship's displacement W, heeling moment due to the shipping water/$W\overline{GM}$, and rolling angle.

Results for Model 1 are shown in Fig. 10 ∿ 13 at a frequncy very close to the natural rolling period but three different amplitudes of the incident waves. Wet deck does not occur with waves not sufficiently high in Fig.10; waves a little higher than the critical induce deck wetting once, but rolling angle decreases as the natural rolling period is away from that of the incident waves (Fig.11); waves much higher than the critical are able to make the ship capsize even after deck wetting occured only a few times as shown in Fig.12.

When wave period is short and far away from the natural rolling period, deck wetting occurs repeatedly even for small rolling angle. Then the ship capsizes under the effect of accumulated shipping water (Fig.13).

With different condition (Model 2), we

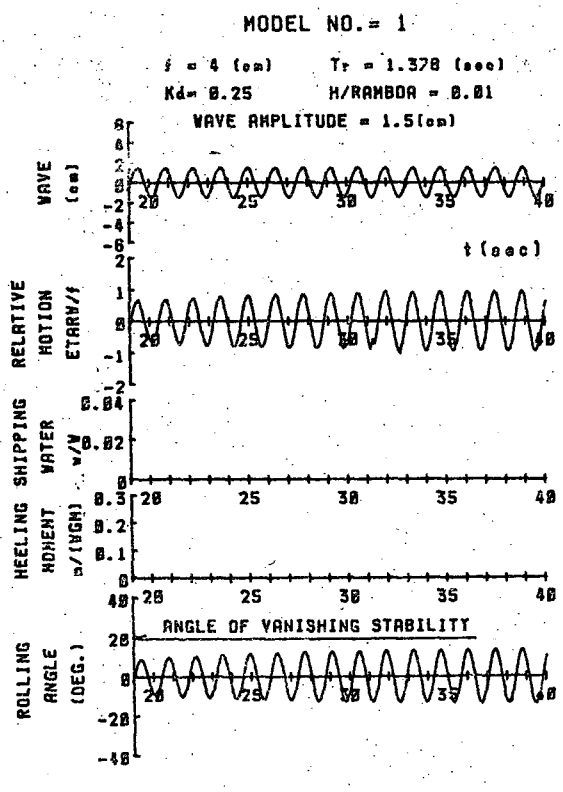

Fig.10 Transient Responses under deck wetting

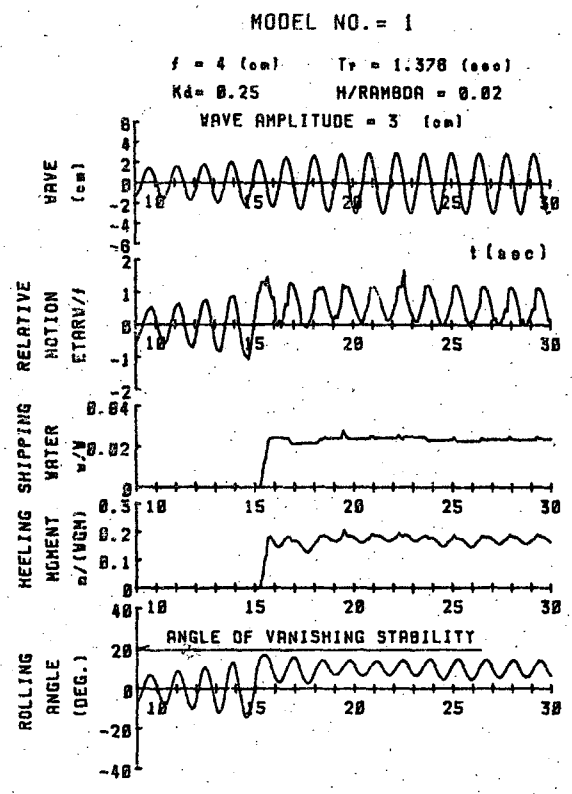

Fig.11 Transient responses under deck wetting

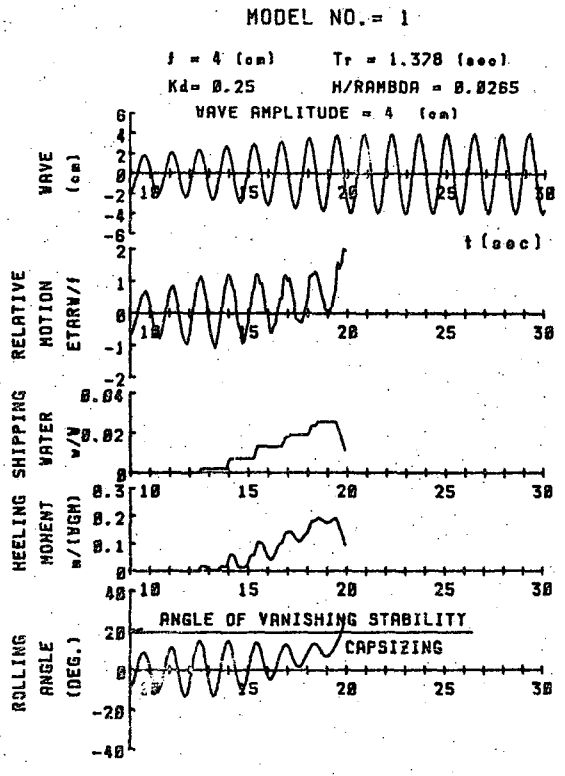

Fig.12 Transient responses under deck wetting

forces are considered to remain to be constant through the transition.

As already stated, shipping water gets on deck if the relative motion of water surface exceeds the bulwark top height; if the deck has already been filled up with shipping water, it overflows as a result of a large rolling angle. Then a portion of the momentum variation rate with time of the ship is proportional to a product of the variation rate in the mass or the moment of inertia and the motion velocity. Therefore such increase or decrease of the shipping water produces the variations in the damping forces as well as in the mass and the moment of inertia.

We have the equations of motion for the ship in the regular beam seas, based on considerations described so far, as follows:

$$M_{HH}\ddot{z} + N_{HH}\dot{z} + \rho g A_w z = F_{ze}(t) \qquad (11)$$

$$\left.\begin{aligned} &M_{SS}\ddot{y} + N_{SS}\dot{y} + A_{24}\ddot{\varphi} + B_{24}\dot{\varphi} = F_{ye}(t) \\ &I_{RR}\ddot{\varphi} + N_{RR}\dot{\varphi} + W\overline{GZ}(\varphi) + A_{42}\ddot{y} + B_{42}\dot{y} \\ &= M_{\varphi e}(t) + m(w, t) \end{aligned}\right\} \qquad (12)$$

where

$$M_{HH} = M + A_{33} + w(t)/g$$

$$N_{HH} = B_{33} - \frac{d}{dt}\{w(t)/g\}$$

$$M_{SS} = M + A_{22} + w(t)/g$$

$$N_{SS} = B_{22} - \frac{d}{dt}\{w(t)/g\}$$

$$I_{RR} = I + A_{44} + \Delta I$$

$$N_{RR} = B_{44} - \frac{d}{dt}(\Delta I)$$

The amount of shipping water $w(t)$ staying on deck is computed by equation (8); increment or decrement of $w(t)$ is determined according to equation (9) for the rolling angle at each time instant.

Increment of the mass moment of inertia ΔI due to shipping water is approximately $\Delta I = w(t)/g \times (\ell_y^2 + \ell_z^2)$ where ℓ_y and ℓ_z are horizontal and vertical distance between the center of gravity of the shipping water and the ship. Hydrodynamic coefficients A_{ij}, B_{ij} $(i, j = 2, 3, 4)$ are to be computed on the sectional form immersed under the water in its mean position even though we assume the frequency of motions is constant. In another words, the hydrodynamic coefficients might be different for each heeling angle of the ship. Shin [11] and Kobayashi [12] concluded that there is no considerable change in the hydrodynamic coefficient from the upright condition to the heeling angle less than 20°, unless the bulwark top is immersed under the free surface. In our computation, we employ the hydrodynamic coefficients at the upright condition, if the bulwark top is above the water and otherwise those at the actual heel angle.

In our ship models whose $\overline{GM}$ is not so high, the horizontal displacement of the center of gravity is not considerable as to induce the coupling between the heaving motion and other lateral motions. So we ignored the coupling to formulate the equation of heaving motion separately from the other motions.

$\overline{GZ}(\varphi)$ on the left hand side of equation (12) is given in Fig.2 and the heeling moment $m(w, t)$ on the right hand side is determined considering the free surface effect due to the rolling angle and the accumulated shipping water on deck.

Damping coefficient B_{44} determined in the free rolling test of the models at upright condition is substituted.

Gradual increase or decrease of heeling angle affects the wave exciting force through not only different exciting force on the inclined ship but also change in the vertical and horizontal distance between the point O and the center of gravity G (Fig.9). Wave exciting force is computed for every inclined position of the ship with Haskind-Newman formula as used in the derivation of the equation (5). $\bar{A}$ and ε must be different for right and left side of the inclined ship. Those on the waves coming side, of course, should be substituted into the equation (5) to have the wave exciting force on the inclined ship.

The equations of motion (11) and (12) are integrated step by step by the 4-th Runge-Kutta method. Initial condition of this integration is very gradual increase, say, 20 seconds for the model, of the wave amplitude from zero level to the stationary one; size of the time step in the integration is 0.1 second.

The relative motion of water surface $\eta_{RW}(t)$ is computed by equation (7) with substituting the instantaneous values of ship motions $y(t)$, $z(t)$ and $\varphi(t)$ at each step of the integration. With the relative motion lower than the critical value to cause deck wetting, computation proceeds to the next step. Otherwise, first compute $w(t)$, the shipping water accumulated during Δt, then $\ell_y'(w, \varphi)$ and $\overline{OG}$. We get the variation in

to estimate the amount of accumulated shipping water w on deck during the time t_1 and t_2 on the analogy of the flow over a dam with the equation,

$$w = \frac{2}{3}\sqrt{2g}\int_{t_1}^{t_2}\sqrt{0.6\{\eta_{RW}(t) - f\}}\,dt \qquad (8)$$

where the integrand is naturally zero if $\eta_{RW}(t) \leq f$. w given by equation (8) must not be beyond a limit even though we assume no free ports on deck, since more water overflows the bulwark. The limit of the amount of shipping water $w_{max}(t)$ to be able to stay instantaneously on deck is dependent on the rolling angle $\varphi(t)$ (see Fig.8). That is given by,

$$\left.\begin{aligned} w_{max}(t) &= f'b_0 - \frac{b_0}{2}\tan\varphi(t) \\ &\qquad 0 < |\varphi(t)| \leq \tan^{-1}(f'/b_0) \\ w_{max}(t) &= f'^2/\{2\tan\varphi(t)\} \\ &\qquad |\varphi(t)| > \tan^{-1}(f'/b_0) \end{aligned}\right\} \qquad (9)$$

No dynamical effect is included in this formula. It implies that we assume the over flow happens instantaneously if the amount of the shipping water exceeds the limit. But this assumption hardly af fects results of simulation in time domain of the ship behaviours.

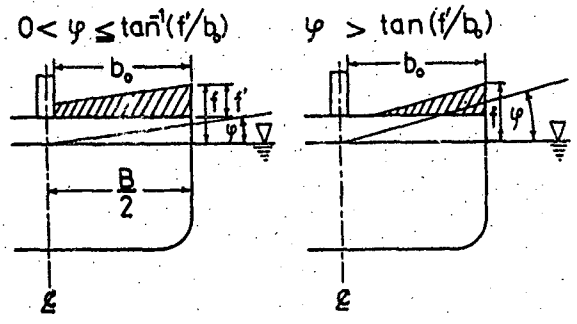

Fig.8 Skech of shipping water on deck

4.2 Effect of Shipping Water on the Ship Motions

The shipping water has various dynamical effects on the ship motions as well as statical ones. The latter, well known as the free water effect, has been studied in detail even including effect of the finite rolling angle by several authors. Tamiya [3] discussed on the former of shipping water deep enough on deck to conclude that it has a big influence on the ship motions when the natural rolling period of the ship is very close to that of the shipping water surface. Dillingham [4] and Adee and Caglayan [5] studied also the dynamical effects of very shallow shipping water on deck with numerical approaches. Dillingham analyzed the behaviours of shipping water on deck in time domain to find that the shipping water's motion works sometimes as damping of the ship motions.

In our mathematical model to simulate the ship's behaviour when some amount of shipping water gets on deck, the statical effect computed instantaneously is considered on the center of gravity, the mass and the moment of inertia of the ship.

In Fig.9 is illustrated shipping water staying on deck at the rolling angle of $\varphi(t)$. Heeling moment due to the shipping water, then is given by

$$m(w, t) = w(t) \times \ell'_y(w, \varphi) \qquad (10)$$

where $\ell'_y(w, \varphi)$ is the horizontal distance between the centers of gravity of the ship and the shipping water $w(t)$ when the rolling angle is $\varphi(t)$. When wet deck occurs and shipping water gets on deck repeatedly, then the position of the center of gravity of the whole body including both the mass of the ship and the shipping water change gradually. This effect is taken into the equations of motions in time domain.

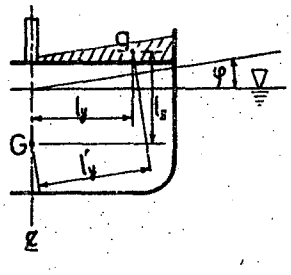

Fig.9 Definition of ℓ_y and ℓ_z

4.3 Time Domain Analysis of the Ship Motions

We simulate the gradual variation of the ship's natural rolling period and the development of large rolling motion leading to its capsize as shipping water is accumulated. We need convolution technique to analyze the ship's motion in time domain even with the linear assumption, since the hydrodynamic force on the ship is generally dependent upon the frequency.

However we are concerned with very slow transition of sinusoidal motion of the ship in regular waves; consequently it is possible to consider the characteristics of the ship's motion vary very gradually. So we assume that the coefficients of hydrodynamic

$$\left.\begin{aligned} F_{ye} &= -\frac{\rho g}{K}\zeta_a \bar{A}_S \sin(\omega t + \varepsilon_S) \\ F_{ze} &= -\frac{\rho g}{K}\zeta_a \bar{A}_H \sin(\omega t + \varepsilon_H) \\ M_{\varphi e} &= -\frac{\rho g}{K}\zeta_a (\bar{A}_S \overline{OG} \sin(\omega t + \varepsilon_S) \\ &\quad + \bar{A}_R d \sin(\omega t + \varepsilon_R)) \end{aligned}\right\} \quad (5)$$

$\bar{A}_S e^{i(\omega t - Ky + \varepsilon_S)}$, $\bar{A}_H e^{i(\omega t - Ky + \varepsilon_H)}$ and $\bar{A}_R d \times e^{i(\omega t - Ky + \varepsilon_R)}$ are waves propagating into the y direction when the cylinder's section is forced to oscillate in sway, heave and roll modes of unit amplitude on otherwise calm water surface with the frequency ω.

3.2 Computation of Relative Motion

We assumed hydrodynamic flow field around the cylinder to be 2-D ignoring end-effects in formulating the equations of motion.

Radiation ploblem of every section for the velocity potential to determine A_{ij}, B_{ij}, $\bar{A}$, ε and so on was solved by the close-fit method [3] that singularity distribution $\sigma(Q)$ on the section's contour, satisfying the linear free surface condition, is determined such that the boundary condition on the section is satisfied (see Appendix).

Diffraction problem is also solved in a similar way to find the singularity distribution giving the normal fluid velocity on the section with the same magnitude but the negative sign as that of the incident waves.

Dynamic swell-up, then, is expressed with making use of the solutions of equation (4) as follows:

$$\zeta_{RD}(\pm\frac{B}{2}, 0, t) = R_e\left\{\int_{C_h} [2KX_m\sigma_R(y', z') + \zeta_a\sigma_D(y', z')]2[\pi i e^{-Kz'-iK(\pm\frac{B}{2}-y')} - \int_0^\infty \frac{k\cos kz' - K\sin kz'}{k^2+K^2} e^{-K(\pm\frac{B}{2}-y')} dk] \times ds\, e^{i\omega t}\right\} \quad (6)$$

where, X_m : amplitude of the m-th mode motion

σ_R : density of the source distribution giving the radiation potential

σ_D : density of the source distribution giving the diffraction potential

The relative motion of the water surface η_{RW}, at weather side and η_{RL} at lee side, then, are

$$\left.\begin{aligned} \eta_{RW} &= z + \frac{B}{2}\varphi - \zeta(y=\tfrac{B}{2}) - \zeta_{RD}(y=\tfrac{B}{2}) \\ \eta_{RL} &= z - \frac{B}{2}\varphi - \zeta(y=\tfrac{B}{2}) - \zeta_{RD}(y=-\tfrac{B}{2}) \end{aligned}\right\} \quad (7)$$

In these equations z and φ are the heaving and rolling motion given as the solutions of equation (4); ζ is elevation of the incident waves (3); ζ_{RD} is the dynamic swell-up given by equations (6).

Solid lines in Figs.3, 4, 5 and 6 show theoretically predicted critical wave height of deck wetness obtained with equation (7). Agreement between the predicted and the observed critical wave height is almost complete. This is achieved by the inclusion of the dynamic swell-up computed accurately even within the limit of the linear theory.

4. TIME DOMAIN ANALYSIS OF SHIP MOTION UNDER THE EFFECT OF REPEATED DECK WETTING

4.1 Amount of Shipping Water

As already stated in section 2, it seems that once shipping water gets on deck it suppresses wet deck occur repeatedly particularly around rolling natural period. This might be accounted for by the reduced rolling motion resulting from the reduction of the GZ due to shipping water. We can not describe this transient phenomenon with the frequency domain analysis as given in section 3. We need time domain simulation.

In order to simulate the ship motion, incorporating the effects of shipping water accumulation on deck caused by repeatedly occured wet deck, it is crucial to have a mathematical model describing the flux of shipping water over the bulwark. We know we can predict accurately whether the wave surface exceeds the bulwark top or not with a procedure shown in the previous section. However we have no theoretical methods to give how high the water surface goes above the bulwark top. It is because we do not know how the wave field is, when the wave crest is away from the body boundary in such case as the water surface rises up above the bulwark top, with the linear theory assuming infinitely small wave motion.

Shin [10] proposed an empirical formula giving the relationship between the actual thickness of fluid flow above the bulwark top due to wave elevation higher than it particularly at weather side of the ship and the excess of the theoretically predicted relative motion over the freeboard.

With this empirical formula we are able

capsize. This is why the critical wave heights of deck wetness coincides with that of capsize in regular waves at most frequencies of the incident waves. However wave high enough to cause wet deck is not necessarily able to cause it in succession even in regular waves when the wave period is close to the natural rolling period, since shipping water reduces $\overline{GM}$, lengthens the natural rolling period to lead to reduction of the rolling motion and stops wet deck occur repeatedly. Of course very high waves can cause wet deck in succession and the model capsizes even after the reduction of the rolling motion resulting from the shipping water.

3. THEORETICAL PREDICTION OF CRITICAL WAVE HEIGHT OF DECK WETNESS

3.1 Critical Wave Height

Condition for sea water to get on deck is that motion of water surface relative to the ship is larger than actual freeboard (here we define it as the bulwark top height from the level of calm water surface in equilibrium). So in regular waves,

$$\left.\begin{matrix}\eta_{RW}\\ \eta_{RL}\end{matrix}\right\} \geq f \qquad (1)$$

is the condition of wet deck. $\eta_{RW,\ RL}$ are amplitudes of the relative motion of water surface at weather or lee side of the ship; f the freeboard. This condition also defines critical wave height of deck wetness in regular waves as follows:

$$\frac{H}{\lambda} = \frac{1}{\bar{\eta}_{RW,\ RL}} \frac{f}{\lambda} \qquad (2)$$

where H denotes height of the regular incident waves; λ the wave length; $\bar{\eta}_{RW,\ RL} = \eta_{RW,\ RL}/H$ whose values are independent of H, since we assumes the linearity of the relative motion.

The relative motion is a sum of all the effects, assuming the linear superposition principle, due to the elevation of the incident waves, the ship motions, the radiation waves generated by the ship motions and the diffraction of the incident waves on the hull.

Theoretical prediction of the latter two effects, which are called dynamic swell-up, needs a rather lengthy computation.

Ganno [6] took the effects of dynamic swell-up into the computation of the relative motion; however diffraction waves he included in his computation were approximate ones in which the diffraction waves are expressed in the same form as the radiation waves but with the ship section's velocity and acceleration replaced by the relative motions of the incident waves. Shin [7], [8] concluded that unless the diffraction waves are computed correctly, the relative motion prediction in beam seas is not accurate even when the wave length is as five times long as the ship's breadth. With inclusion of the diffraction waves computed exactly as well as the radiation waves, the prediction of the relative motion in beam seas becomes accurate enough to be available for the prediction of deck wetness.

Restricting our attention to the cylindrical body moving in beam seas,

$$\zeta = \zeta_a \cos(Ky + \omega t) \qquad (3)$$

where ζ_a is the amplitude, K the wave number and ω the frequency, we have the equations of motion (Fig.7):

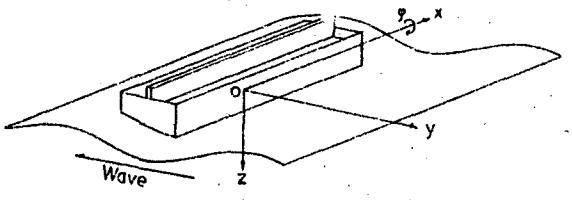

Fig.7 Coordinate system

$$\left.\begin{aligned}&(M + A_{33})\ddot{z} + B_{33}\dot{z} + \rho g A_W z = F_{ze}\\ &(M + A_{22})\ddot{y} + B_{22}\dot{y} + A_{24}\ddot{\varphi} + B_{24}\dot{\varphi} = F_{ye}\\ &(I + A_{44})\ddot{\varphi} + B_{44}\dot{\varphi} + W\overline{GZ} + A_{42}\ddot{y} + B_{42}\dot{y} = M_{\varphi e}\end{aligned}\right\} \qquad (4)$$

where, M, I : mass and moment of inertia of the ship

A_{ij}, B_{ij} : hydrodynamic coefficients of the section oscillating on otherwise calm water

ρ : specific density of water

g : acceleration of gravity

A_W : waterplane area

W : displacement

GZ : righting moment arm

The subscripts 2, 3 and 4 denote sway, heave and roll motion respectively; F_{ze}, F_{ye} and $M_{\varphi e}$ on the right hand side the wave exciting forces and moment. Haskind-Newman's relation gives their exact expression as follows:

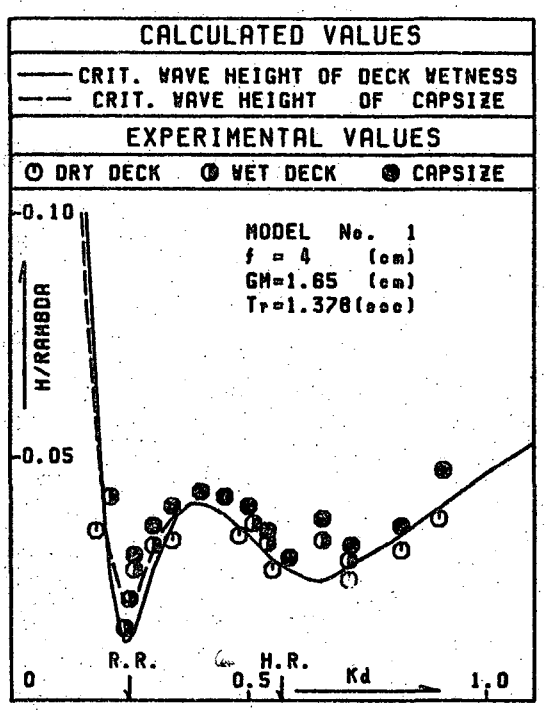

Fig.3 Critical wave height of deck wetness and capsize

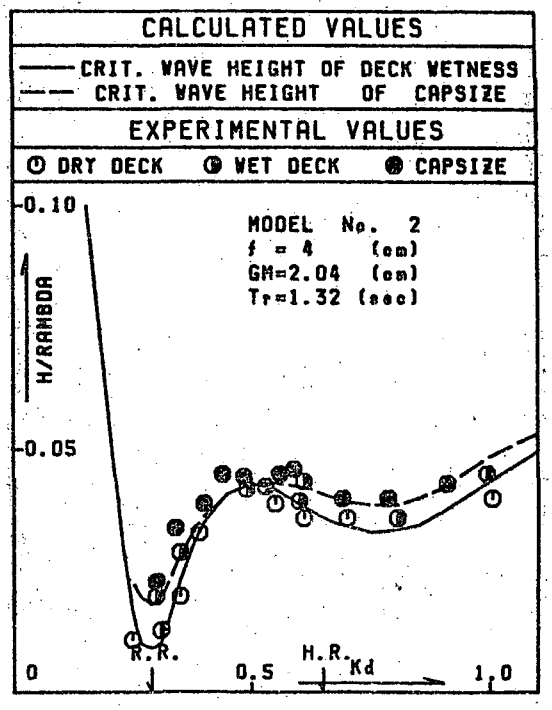

Fig.5 Critical wave height of deck wetness and capsize

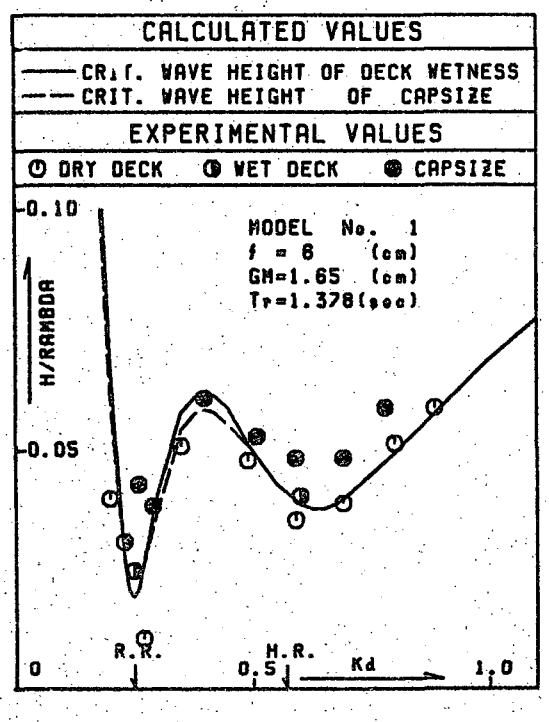

Fig.4 Critical wave height of deck wetness and capsize

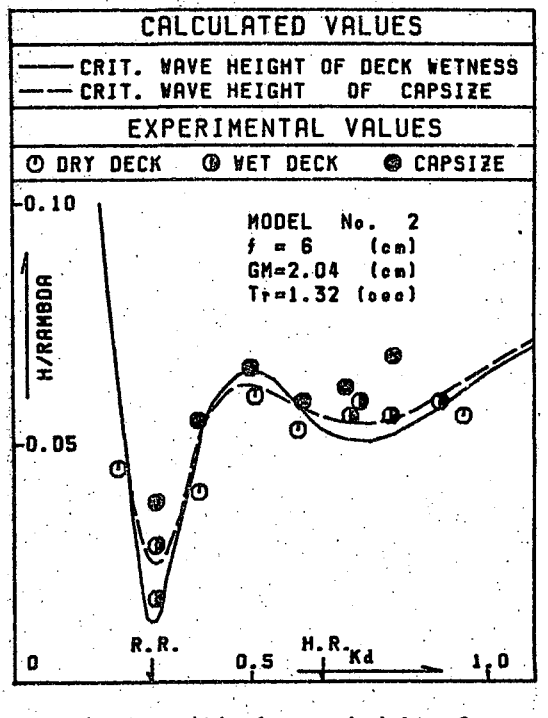

Fig.6 Critical wave height of deck wetness and capsize

the model does not capsize; black circles show the model capsizes after the shipping water is accumulated on the deck and under the influence of the vertical plate.

It is to be noticed that the critical wave height of wet deck is almost coincident with the critical wave height of capsize except at the frequencies of the incident waves close to natural rolling period indicated as R.R.; at this frequency the critical wave height of capsize is not so low as expected from the very low critical wave height of deck wetness which is attributable to large rolling angle.

Wet deck occurs in succession naturally in regular waves when the wave height is higher than the critical of deck wetness. Accumulated shipping water due to the wet deck occuring in succession reduces significantly stability of the model and makes it

to the reduction of the rolling angle and stops wet deck occur repeatedly. In order to understand this rather transient process we propose a simplified time domain simulation of the ship motion in waves exceeding the critical height of deck wetness. In the formulation of the time domain simulation, we use an empirical formula proposed by Shin [10] relating the amount of water, flowing into on deck every time deck wetness occurs, to the excess of wave height over the predicted critical wave height of deck wetness.

Results of the simulation describe well the observed process on the model tests from the start of deck wetness to capsize or to suppression of the deck wetness.

2. EXPERIMENT ON CRITICAL WAVE HEIGHT OF DECK WETNESS

Wet deck occurs on a ship in beam seas when amplitude of incident waves exceeds a critical magnitude. The magnitude is dependent on the period of the incident waves as well as the ship motion characteristics.

We conducted experiments on two models of cylindrical configuration; they are of an identical cross section through their fore to aft ends. The experiments are to find out the critical wave height of deck wetness ——the lowest wave height to cause wet deck ——for various frequencies of the incident waves. Model 1 is of rectangular cross section like a ship's midship section; Model 2 of elliptical cross section similar to the fore or aft section of a fishing boat (Fig.1 and Table 1). We provided each of them with two different bulwark heights above the water line; different bulwark heights correspond to different $\overline{GZ}$ vs. heel-angle curves as shown in Fig.2. Those $\overline{GZ}$ curves are supposed to be those of fishing boats at overloaded condition often possible to happen. We attached a vertical plate to the model deck on the center line through the fore to aft ends. This is to provide them with a substitute for deck house which might make shipping water not

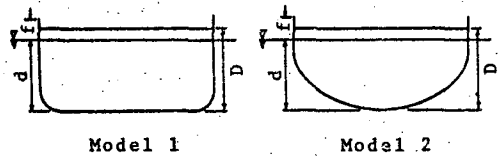

Model 1 Model 2

Fig.1 Cross sectional forms of models

Table 1

	MODEL 1	MODEL 2
L (cm)	160	150
B (cm)	30	30
D (cm)	15 14	15 14
d (cm)	12	12
f (cm)	6 4	6 4
W (kg)	54.23	44.33
GM(cm)	1.65	2.04
Tr(sec)	1.378	1.32

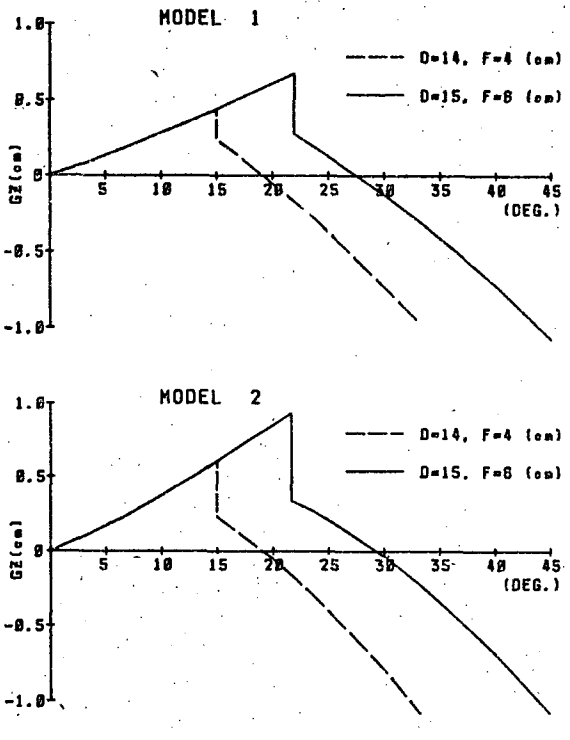

Fig.2 GZ-curves

movable laterally from one side to another of the deck. No freeing port openings through the bulwark to let shipping water flow out are provided on purpose to investigates effect of the accumulated water on ship's behaviour in waves.

We observed the models' motions in beam seas for several different wave heights at every frequency of the tested incident waves. Less wave height does not raise water up to the deck as marked by open circles in Figs.3, 4, 5 and 6 where H/RAMBDA denotes wave height-to-length ratio, Kd wave number non-dimensionarized with the model's draft; half-black circles indicate that shipping water gets on the deck but

Third International Conference on Stability of Ships and Ocean Vehicles, Gdańsk, Sept. 1986

STAB'86

THE EFFECTS OF DECK WETTING ON THE STABILITY OF SHIPS IN BEAM SEAS

C. Shin, M. Ohkusu

ABSTRACT

We show that accurate prediction is possible of critical wave height of deck wetness for ship models of cylindrical configuration in regular beam seas, in which are incorporated effects of diffraction waves including local waves predominant in the vicinity of the ship as well as radiation waves. The predicted critical wave height agrees with the measured in experiments. Although we are able to predict with frequency domain analysis whether deck wetness occurs or not at given frequency of waves, we are neither able to know how it does, once or repeatedly, nor how it leads to more fatal condition such as capsize.

We clarify with a simplified time domain simulation why deck wetness causes capsize at some frequencies or not at other.

1. INTRODUCTION

Considerable attention has been given to the problem of the effect of shipping water on the stability of a ship in waves. A simplified assumption of great use is that the effect is a statical one well known as the free water effect. An extensive review is given in Caglayan and Storch [1] of recent studies on the dynamical effect of the shipping water as well as statical one; it is also studied by Rakhmanin [2].

Tamiya [3] investigated on dynamical behaviour of the water on deck deep enough to conclude that it has a considerable effect on the ship motions when the natural rolling period of the ship is very close to that of the motion of the shipping water. Dillingham [4] and Adee and Caglayan [5] studied dynamics of very shallow water on deck and its effect on the ship stability with numerical approach. Dillingham found that the shipping water's motion works sometimes as damping of the ship motions.

To see whether deck wetness occurs or not to cause shipping water, we need to predict correctly the relative motion of the water surface to the ship. Ganno [6] pointed out that dynamic swell-up, namely water surface elevation due to the radiation and the diffraction of incident waves should not be ignored to have correct prediction of the relative motion. Shin[7],[8] and Grochowalski [9] gave theoretical predictions of the relative motion.

To know really the ship's behaviour in waves under the influence of deck wetness and shipping water as a result, it is not sufficient to predict whether the deck wetness occurs or not. It is crucial to see how the deck wetness occurs, once or progressively. Moreover we have to know how much amount of water flows into on deck. We need to predict how the shipping water, due to the deck wetness occured once or repeatedly, changes the ship motions to lead to more fatal condition like capsize. In another words we need to know a transient process through from the start of deck wetness to capsize.

We give in this paper a prediction of critical wave height of deck wetness, which agrees well with the experimental one, for ship models having simple configulation in regular beam seas. Experimental observations teach us that wave high enough to cause wet deck is not able to cause it repeatedly even in regular waves when the wave period is close to the natural rolling period. We guess that the shipping water caused by first one or two waves exceeding the critical wave height of deck wetness reduces GM, lengthens the natural rolling period to lead

- multihull ships or ocean vehicles
high speed (greater than 20 knots) in any ship
- zero speed and no manuevering while at sea
submerging portions of the ships.

When the new shipping modes became popular, there was no official reminder of the degree of safety provided and the shipping industry went into the new multi-mode shipping without including the previous safety levels. This situation needs to be reversed, particularly when rapid sinking, increased danger to life and increased damage to the environment are considered.

This conference could outline steps to be taken toward the goal and invite physical oceanographers to comment on such a program. It could jointly improve both research areas and could foster stronger professional cooperation between both groups.

6. Acknowledgment

6.1 The authors state that the opinions expressed in this paper are their own and are not necessarily the views of the U.S. Coast Guard.

6.2. The authors wish to acknowledge Mr. H. A. Chatterton and LT R. Gilbert for their valuable assistance in critiquing the paper and for assistance in the Tables & Figures.

Also combinations of stability hazards may occur. A few, such as rudder heeling occur routinely in conjunction with other hazards, much as following sea, steep wave slope stability reduction etc.

Accurate determination of stability hazards in a seaway requires better knowledge of the seaway itself but much more is required. The seaway spectrum is not enough. In order to accurately explore the instantaneous variation in stability, the exact sea slope, velocity, momentum, direction relative to a ships course and the exact ship attitude at each moment in time is necessary.

Alternatively, it needs to be proven that instantaneous differentials are not large enough to cause capsize either directly or through sequences of increasing roll velocity, acceleration or greater roll angles.

4.7 For several years during the 1960's, one of the committees of the World Meterological Organization regularly offered seaway data to the IMCO-SubCommittee on Subdivision and Stability, but finally announced that until the naval architects started to use seaway information more, there did not appear to be a need to continue the interaction. This friendly challenge also pinpointed the weak link in stability analysis. There are several steps between pure seaway information and pure ship design by which both sets of experts must interact in a manner that will assist each other.

The interaction steps between oceanographers and ship designers can be categorized as follows in Table 3.

Both groups are presently in step 1 or the early activity in step 2. At present, the interaction between physical oceanographers and ship designers is less than adequate.

Table 3

Oceanographer/Naval Architect Interaction

Step 1 - Oceanographer

Study physical characteristics of waves, wave spectra, wave groups, rogue waves, - all oceans.
Provide spectra, seasonal variations, extreme wave characteristics.

Step 1 - Naval Architect

Balance ship form in individual waves; head-beam and following seas;
Determine restoring moment; Determine rate of change of restoring moment;
Determine spectral ship motions, probability of immersion and emersion

Step 2 - Oceanographer

Provide actual wave sequences in regular and irregular seas.
Provide data on rogue wave occurences; size, velocity, number of occurrences.

Step 2 - Naval Architect

Study changing stability from wave to wave, establish limits of roll motion, roll velocity, roll acceleration.
Determine rate of change of restoring moment.
Establish maximum variance between statical moment curves from wave top to trough

Step 3 - Oceanographer

Provide size, steepness, period, velocity, frequency and location of occurrence, of specific waves and wave groups.

Step 3 - Naval Architects

Study stability variations in all types of waves, wave systems, wave groups, wave spectra.
Identify good and poor stability reactions.
Establish maximum permissible variances by limiting accelerations, velocities, and motions.

5. SUMMARY

5.1 In summary, since there is an obvious lack of adequate stability standards to cope with all stability accidents, there must be more stability research. Research should be undertaken to understand the limits of both static and dynamic stability changes that a specific hull form may undergo. With a full understanding of the limits of stability the tasks of selecting a standard and deciding how to provide information to the crew become more logical and possibly simpler.

5.2 The research can be undertaken on specific hull forms but must assume operational loading conditions. The research must include seakeeping analysis. The research on ship stability must include parallel research in physical oceanography. Specific seakeeping problems or geographically similar seaway conditions may be jointly studied.

5.3 Since administrations are responsible for selection of stability standards, they should consider requiring basic seakeeping analyses by designers for all ship designs which have unique features such as:

- cargo distribution on deck or outside of hull
- mono hulls with blunt ends
- unequal disoritation of superstructure along hull bulk.
Transfer of large weights

been explored thoroughly, even for monohulls. Indeed the offshore industry has done more toward discovering the interaction of a single MODU design with various waves, wave groups and wave spectra than the monohull ship designer. The same wave which will not bother a very large vessel may overturn or founder a smaller one.

Referring to Figure 3, the differential curve marked "Large Seaway" may also be the result of a poor hull form for the seaway or of excessive gyradius due to poor loading or a combination of similar factors. To our knowledge little ship research has been comprehensive in this regard.

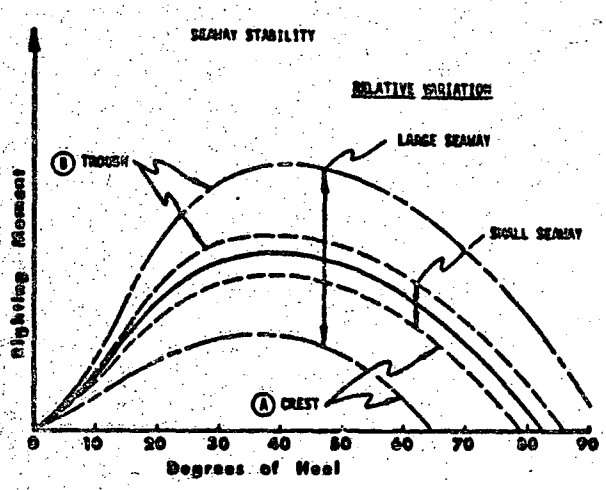

FIG 3

The seaway related stability accidents in Table 1 are:
a-Single Broadside wave
b-Resonant rolling
c-Following or Quartering Sea
d-Steep wave Systems
e-Wave groups

Of these, resonant rolling (b) is covered in standard naval architectural literature and is perhaps the least likely accident to occur because of the random nature of the seaway and because it takes several rolls to capsize which gives the master time, in most cases, to take corrective action.

The following sea situation (c) has been described and examined in model tests but has not yet been reduced to easily used design mathematics for the designer.

Steep wave systems (d) are also capable of causing a capsize in head seas. This phenomenon has been examined in model tanks but has not yet been quantified enough to provide the naval architect with design guidelines to prevent it.

Wave groups (e) which could cause an extra large roll, series of rolls, or direct capsize is possibly a more likely occurence than resonant rolling because of the random seas which predominate.

4.6 Stability by gravity (center of gravity below the center of buoyancy) is enjoyed by very few floating structures. Form stability of every floating object changes continuously: Cargo loading for each voyage, Fuel and Ballast changes daily, and the seaway changes Moment by Moment. This is not fully appreciated by many of those involved in marine transportation.

The establishment of stability standards include:

(a) a recognition of a stability hazard
(b) calculation of the effect of the hazard
(c) selection of a reserve to offset the hazard
(d) instructions to the crew on maintaining the stability reserve

For research purposes, the effect of each stability change is a valid subject for review and discussion; for regulatory purposes, the list must be limited to the larger changes of stability. The Administration issuing the safety certification must be assured that all but a minor percentage of possible casualties are either prevented or mitigated to small magnitude. It is possible (and often the case) that the regulatory standard used may not actually relate directly to the hazard; yet if the reserve included in the standard is large enough, the standard may considered valid for each ship for the particular hazard. One objective of all maritime persons and agencies should be to acquaint the general public with the fact that the stability standards that exist are supposed to be conservative enough to cover all similar hazards.

Since so many stability accidents are possible (per TABLE 1) and the amount of reserve stability necessary to save the ship from a particular hazard varies with each ship in each hazard occurrence, it often occurs that a Ship may have a greater reserve than necessary for the accident that is about to occur. However, it may also occur that less than enough reserve is available.

The principal benefit of research is it will show which hazards require the largest reserve.

Since the stability curve changes constantly in a seaway, there may be newer ship hull forms or ship loading arrangements which have a wide, seaway induced differential righting moment curve such that excessive rolling, pitching, and heaving moments may be created. (Fig 2).

a shape coefficient of 1.25 and assuming the wind acts over 60% of the leg area. No credit is given for any shielding effect of the legs. Many in industry feel this approach is overly conservative and have gone so far as to conduct wind tunnel tests on specific leg section designs.

For both independent leg and mat-type units, there is also a feeling that the 1.4 area ratio is too severe. The criteria for barges is cited as being sufficient and note that submersible heavy-lift vessels need only meet a modified Rahola criterion when carrying MODUs on deck. A time domain simulation type of analysis with supporting model testing would help clarify the adequacy of the current criteria.

Damage stability standards for self-elevating units are another area that should be included in research. The current standards assume minor damage from side penetration only and not bottom damage or flooding from over the top, resulting from damaged ventilators or improperly secured openings. They require that a transverse extent of damage of 5 feet be assumed between main transverse bulkheads. This has resulted in a virtual re-design of these units so that pre-load tanks are now located around the periphery of the unit and extend 5 feet into the hull, as assumed in the damage penetration. There are also now larger compartments inboard of this 5 foot penetration, the flooding of which has not been accounted for in many designs. Yet, the world wide casualties indicate that flooding from over the top is a major factor in the loss of these units. Research is needed to determine the extent to which flooding from over the top is responsible for casualties and propose revised standards where necessary.

4. NEXT GENERATION STABILITY STANDARD

4.1 Relating each stability hazard to the righting curve picture (whether arm or Moment) is necessary to quantify stability and is the best mathematical way to provide similar levels of safety assurance from each accident. There may exist some types of ship, among the many new ones in evidence in 1986, which are vulnerable to specific stability accidents because of the fact that stability regulations were developed for different types of ships.

The mathematics necessary to evaluate have been available for many years. They are the statical righting moment curve and the dynamical moment curve. Yet only the statical arm (not moment) curve is presently in general use.

We naval architects are quick to explain that the statical arm curve is identical to the statical moment curve but we have not yet begun to appreciate for our own professional needs, the difference between two ships of greatly different size having the same STATICAL ARM curve but perhaps vastly different reaction to the same seaway.

The 34 potential stability hazards in table 1 can be grouped into four (4) general categories:

a. Internal changes-VCG,free surface, cargo shift etc.

b. Cargo Stowage and Security

c. Wind and other direct external forces

d. Seaway action

4.2 Internal Changes

The internal change most requiring research is the effect of the shift in gyradius on roll and roll dynamics, on particular, to establish limits for various hull forms (containerships, RO/RO, RO/RO Pontoons) in order to help avoid excessive roll accelerations.

4.3 Cargo Security

The cargo stowage problem most requiring research attention is the physical/chemical problem of examining bulk cargo materials for the tendency to liquify and become a fluid or semi-viscous cargo under specific ranges of temperature and humidity.

4.4 External Forces

External forces such as wind, anchor lines, mooring forces, wind gusts, towing hawsers, nets or trawls, hauling blocks, and wave impact at relatively high speeds, are also known accidents causes, capable of capsizing the ship. However these are not well defined in the mathematical sense so that the same degree of confidence exists for the designer in producing a ship that is equally resistant to capsize in all the situations named.

4.5 Seaway Evaluation

Not all seaway stability accidents can be evaluated or prevented by either GM or the shape of the stability curve. The ship changes stability with every wave in the sea, as well as daily with changes in consumables, per voyage with different cargoes, etc. Also the size relationship of every ship to every wave has not yet

research should be performed to discover the threshold of minimum stability for this type of ship.

3.5 Offshore Ocean Vehicles

3.5.1 The OFFSHORE industry, developed over the past 25 years, includes many new types of ocean vehicles which fit awkwardly into regulations derived for the more traditional ship. Since the major types of offshore equipment (i.e.-oil drilling units, pipeline installation barges, deep sea mooring/towing craft) are subject to all of the ICLL 66 regulations and various codes (ie MODU), they must meet a freeboard concept, a hull integrity and strength concept, and must provide for safety of personnel working in open weather conditions.

The freeboard concept of mobile drilling units has no direct relation to the concept of approx 20% intact reserve buoyancy which is the foundation of the load line rules.

3.5.2 Self-elevating Mobile Offshore Drilling Units

There are two basic types of self-elevating units, the independent leg type and the mat type. The former typically has a triangular shaped hull with three legs on which the hull moves up and down. The leg length ranges between 75m' for older units and 130m. for the newest units. The legs are usually a truss arrangement and have spud cans at the end of the legs to support the unit on the sea bottom. The spud cans are normally free flooding to prevent implosion and thus contribute no buoyant volume to the unit. The stability of these units is readily improved by lowering the legs. Surprisingly, the most vulnerable state of these units with regard to stability is during the inclining test. The absence of any liquids below deck and any variable load on deck means that the vertical center of gravity (VCG) is at its highest point. The VCG is typically above the deck house because of the effect of the legs.

Mat-type rigs have a mat which supports the unit on the bottom. These units are favored in areas where the bottom bearing pressures are limited. The mat has several compartments which are permanently ballasted and others that are permanently empty to provide buoyancy. The legs are attached to the mat. The platform is positioned up or down on the legs depending on the water depth in which the unit is drilling and the desired air gap. The stability of the unit is greatest when the separation of the mat and platform is at a minimum. Stability is reduced as the separation between mat and platform is increased. These units are sometimes operated in this fashion when completing a field move, that is, a short move of less than 12 hours duration. Although the VCG is reduced, the position of the center of buoyancy is also changed. The net effect is a reduction in the righting arm. As the mat and platform are separated the wind heeling arm is also affected. Although the wind force is reduced, there is an offsetting increase in the moment arm because the center of underwater resistance has changed.

The stability criteria applied to both of these types of self-elevating units is the familiar 1.4 area ratio of the righting arm curve to the heeling arm curve. The legs contribute upwards of 80% of the total heeling moment.

Stability research is needed in several jack-up MODU areas. One area is to determine loading and seaway combinations which cause roll and pitch motions of these units which impose high roll accelerations. These can cause severe stresses on both the legs and cantilever securing arrangements. One casualty in the U.S. has been attributed to high rolling accelerations which caused the securing devices on the cantilever beam to fail.

Another area is the accurate determination of lightship data. The current use of the inclining experiment has led to known differences in vertical center of gravity of 2 meters for identical rigs. One explanation for this is that most units have a transverse height of metacenter (KM) close to an order of magnitude greater than the vertical center of gravity. Thus, there is a great sensitivity of the transverse and longitudinal KM to changes in draft and trim. The triangular shape of the independent leg units often means they have transverse KM values nearly equal to the longitudinal KM values. Some are inclined in the longitudinal direction using the cantilever beam as the inclining weight. The cantilever is weighed prior to the inclining experiment using jacks and evaluating the pressure readings.

One alternative to the inclining experiment has been a detailed weight summary and deadweight survey to verify the calculated displacement and longitudinal center of gravity. Another suggestion has been to induce a free surface during the inclining experiment to reduce the transverse or longitudinal metacentric height. This may not be desirable because of the already tender condition during the inclining.

Research is also needed to determine more realistic shape coefficients, particularly for legs since they make the largest contribution to the total wind heeling moment. At present, the wind force on the legs is derived by assuming

Statistically, the accidents to RO-RO ships are not much more numerous or frequent than other types of shipping. However, the RO-RO has several features which make it more vulnerable to total loss. In the intact stability mode, such ships have the disadvantages of:

..Most cargo carried above the freeboard deck which automatically causes a significant reduction in static stability.
..Cargo carried on wheels or carriages which make secure lashing a major difficulty.
..Heavy cargo weights carried on wheels are higher than ordinary container cargo and take much more storage room. Thus the opportunity to stow such cargo low in the ship is less when on multiple port voyages than the dedicated containership.

.. After Hull Form and Stern Door configuration may cause following sea instabilities

The damage considerations which ought to be covered by present design practices are largely absent and not required in regulation. However, design practice in flooding protection of dry cargo vessels has actually retreated from safety considerations since 1960. At that time, both design practice and the rules of the major classification societies required watertight bulkheads up to the weather deck spaced evenly throughout the ship.

3.4.4 Heavy Lift Ships

Heavy lift ships are another unique variation of dry cargo ships which have developed mostly in the past 10 years. These ships also have possibilities for unique stability problems. In the intact stability conditions the several possible problems are:

1. the lifting operation itself

2. the vertical variations in cargo

3. carrying cargo on deck

4. removing hatch covers in order to carry large single pieces of cargo.

5. the possibility of captured sea water in the well or holds when encountering a severe storm.

6. The effect of pendulum motions of a suspended weight on the roll motion of the ship.

The lifting operation has always been one to be carefully controlled. Thus far, there are few known instances of capsize by mishandling of the load or of ballast shifting while a load was suspended. This we attribute to the fact that the heavy lift is a special, carefully managed operation.

There is one particular heavy lift operation which may catch even the most careful management by surprise because it involves small ocean swells rather than seaway. This accident would occur either because the roll characteristics of a ship with a suspended load are much different from the same load stowed in or on the ship; or because a swell which causes a minor angle of heel also causes an instantaneous major pendulum change in the heeling moment due to the suspended load.

To defend against this accident the ship design should include model tests to discover the limits or threshold of roll movement at which catastrophic capsize would be inevitable.

It is not as likely to occur in a harbor as in an estuary or open sea situation. Still it seems possible that the propeller wash from one vessel might be enough to cause such an accident.

There is both research and operational control needed to prevent such an accident. With regard to research, the ship form and lifting geometry should be modeled in roll due to a single low amplitude, long period swell. The object of the research should be to establish the maximum pendulum weight (heavy lift) as a percentage of the ships displacement which can be lifted without danger of capsize by a small swell. Various restraining tackle on the pendulum will of course assist the ship to handle the heavy lift safely but should not be counted on to permit a heavier lift.

Unpublished engineering studies done in the USA have indicated that if the heavy lift is more than 10% of the total displacement of ship and heavy lift, the system may be subject to a sudden capsize by a single long period swell.

3.4.5 Semi-Submersible Heavy Lift Ships

Semi-submersible heavy lift ships are perhaps the most recent design innovation which have been only slightly affected by regulations. The International Convention of Load Lines 1966 states that the load line shall not be submerged. It has been accepted by most parties to the convention that these ships must be given an International Exemption Certificate because of this regulation. All Exemption certificates are reported to the International Maritime Organization noting efforts to achieve an equivalency with load line regulations. The presumption is that this will encourage a continuous international review which should lead to modifications or new load line standards.

Semi-Submersible Heavy Lifts Ships may also be vulnerable to a very small specific wave occurrence during the lifting operation. Model tests or other

The specialized combination ship type called OBO - (Oil, Bulk, Ore) might suffer an intact stability accident in those ships which cargo free surface across the full beam of the ship.

Additionally, those specialized ships carrying liquids of specific gravity greater than 1.0 might suffer a larger than usual loss of intact stability when some cargo tanks are only partially filled.

The naval architectural calculations necessary to show free surface correction do not require difficult research or model studies. Only straightforward engineering evaluations using known methodology are needed. Such calculations are only necessary to show that, with the full free surface of cargo taken into consideration, the stability evaluation meets a given standard. At this time there is no international agreement on what that standard should be, especially for large ships.

Each tank ship will respond differently to seaway motions depending it relative size compared ship to the seaway. Many nations use as a governing stability standard for tankships up to 100 meters in length IMO Res. 167 even though most Tanker ar much larger than 100 meters and may be penalized for using this standard

In selecting a criteria for very large Tankships, the righting arm curve required areas may be modified depending on size of tanks and the influence of the free surface on the overall ship motions.

3.4 Dry Cargo Ships

Three decades ago, dry cargo ships were almost all of the mixed cargo, break bulk type carrying barrels, crates, sacks and palletized cargo. The single major specialty ship was the bulk cargo ship carrying ore, coal, or grain.

Now much of the palletized, boxed, crated cargo is placed in "containers" and carried intermodally on ships of several distinct types. These are the very large long distance containership, the combination RO/RO containership and the vehicular RO/RO for short international voyages.

3.4.1 Containerships

The evolution of containerships has included several significant stability variations. The earliest containerships were tankships which carried containers on deck and corrected for the high center of gravity of cargo by carrying high density ballast in the cargo tanks. Although this corrected the vertical center of gravity, it created a larger vertical gyradius. Some of these ships had difficulty keeping containers on board due to high roll velocity (and roll accelerations).

When the 'purpose built' containership became popular the shipping system evolved permanently into a shipping system including cargo carried on deck. Thus the stability of the containership can potentially be varied much more than the older system with the cargo inside. To the author's knowledge, the stability limits of these loading variations in a seaway have not been researched. Several stability problem areas need to be researched. Some of these are:

*Stability limits based on size relative to the seaway. 60m - 250m should include an examination of roll characteristics, roll velocity, and acceleration.

*The effect of the variation of gyradius (vertical and longitudinal on rolling and pitching motions due to possible variations of cargo loading and centers of gravity.

Because the loading patterns can vary so much ships may have a VCG which meets current stability standards but the cargo distribution may cause a variation of gyradius (vertical and longitudinal) sufficient to cause wide variances in rolling, and pitching motions.

One advantage of the containership is that it can easily be designed to meet future flooding resistance standards.

3.4.2 Combination Ro/Ro-Containership

The combination containership/RO-RO has much the same possibilities for stability variation as the single purpose containership. However, it is quite likely that it will have different limits of roll, roll velocity and roll acceleration because of the greater difficulty in providing efficient cargo lashings for wheeled cargo. This possibility provides a completely different need for stability research than the purpose built containership, because the same ship hullform, tested in a model tank, will have closer limits of acceleration and roll velocity than the purpose built ship.

With regard to subdivision, this type of vessel will be subject to some modifications when meeting an international standard. The lack of any design standard at this time has permitted existing ships to have a completely unknown degree of safety against flooding. A very few have been required by owners to be designed to the one compartment standards of flooding resistance. The designers had little difficulty including flooding resistance when considered early in design.

3.4.3 Ro/Ro ships

The Ro/Ro ship is the most maligned of the newer types of ships from both intact and damaged stability points of view.

2.5 Table 2 Damage Stability Causes

Flooding may occur through;
1. Lack of or loss of weathertight integrity of topsides.
2. Loss of watertight integrity of the main hull.

Flooding may lead to loss through;
1. Foundering
2. Plunging (loss of buoyancy at bow or stern only)
3. Capsize (when form stability is low)

3. SHIP-SPECIFIC STABILITY CONSIDERATIONS

3.1 The three principle ocean ship types of previous decades (passenger, tanker, and dry cargo ship) have evolved in the past 30 years into more than a dozen specialized ship types. Additionally the offshore industry has become a new category of ocean endeavor with many special ship types for exploring the raw materials in the ocean bottom. Fig. 2 names the most prevalent of these types and approximates their date of introduction into world commerce.

FIG 2

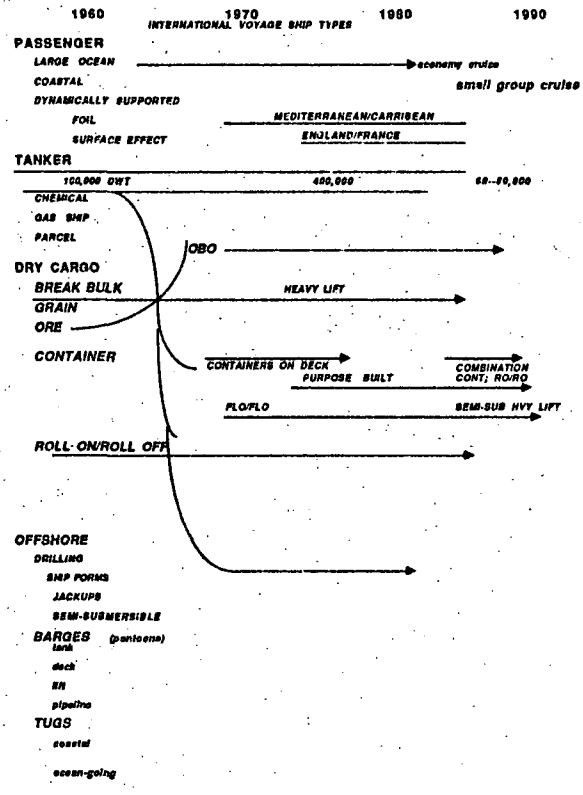

In the following paragraphs, the more obvious stability design features of each type are noted and briefly discussed with a view to whether or not naval architectural development should be undertaken to uncover possible design limitations.

It should be noted at the outset of this exercise that this proliferation of different types of ocean vehicles has occurred before the naval architecture community had fully evaluated the stability limits of the original three ship types, especially with regard to actions in a seaway.

3.2 Passenger Ships

Although passenger ships have changed less in the past few decades than the other types, there have been several unique developments which may affect their stability evaluation.

The first development is the change in large passenger ships from luxury liners to much higher passenger numbers carried on a relatively shorter cruises . The large size of such ships permits them to retain the ability to withstand wind and sea. However, the greater number of passengers makes the handling of passengers more difficult in damage situations and the designer must allow much greater stability reserves for their evacuation. How much stability reserve is necessary when several thousands of passengers are moving toward safety or being evacuated has not yet been discussed at IMO.

Another development is a, change in route which appears to be affecting the safety of some large passenger ships. Instead of maintaining a specific route, these ships change routes with seasons and tourist desires. Some are now venturing into floating ice to glimpse glaciers which offers greater possibility for another "TITANIC" type casualty. Others have followed special sea routes because of astronomical happenings or to observe the migrations of whales. Such voyages may lead the ship into unfamiliar waters.

Large passenger ferry boats on short international routes have increased in size, speed, number of passengers.

The need for research in passenger ships lies principally in damage situations wherein it is necessary to handle much larger numbers of people and maintain protection from capsizing in new route situations such as floating ice and in new designs with open vehicle decks.

3.3 Tankships

The class of ships dedicated to liquid cargoes or liquified gases has not historically had intact stability problems nor intact stability casualties. Yet, it is not that such ship designs are immune to stability accidents. Serious intact stability accidents might occur if the free surface reduction of stability by the liquid cargoes were ever to become large enough to adversely affect roll motion in a seaway.

mally it is based on the principles of cybernetic circulation of information, in substance however, it is reduced to reconciliation of the so-called long-and-short-term predictions. From utylitarian point of view its aim is to obtain the maximum economical effects for a specified ship. It seems that the above general features of the presented concept potentially where to a number of other problems related to designing and service of ships. In other words the features are present everywhere there where "the human factor" is indispensable element of an efficient an effective activity of a definite system. The factor for which, as a ship of a closed system with feedback, is identified with the activity of the elements: comparing and correcting. The factor, by nature difficult to be measured can however, be more effective, depending on the quantity of information it is supported by.

4. REFERENCES

1. Ochi M. "On Prediction of Extreme Values"; Journal of Ship Research vol. 17, March 1973;
2. Stasiak J. "Methods for Long-Term Prediction of Accelerations Affecting Ship's Hull and Cargo in the Seaway"; Ship Research Institute - Technical University of Gdańsk, Rep. No. 1586, 1982 in Polish.

ABOUT THE AUTHOR

Janusz Stasiak, graduated in marine engineering from the Technical University of Gdańsk.

Next he joined the Ship Research Institute of this University and have been working as a researcher at the Ship Hydromechanics Division. In 1982 he completed his Ph. D. thesis.

ZPPG/229/2/86/250

the lashing system is referred to. To a certain degree some relations are denoted by means of diagrams in Fig. 1; They will be given further detailed attention, here.

2.4.1. Stowage operations.

These operations are based on the information included in diagrams as shown in Figs. 3. and 4. They can proceed in the following way:

a/ At first there is assumed to be a state of completed loading on the ship /$\overline{MG}$/ and the worst waving conditions during the voyage are anticipated resulting in determined value of the permissible transverse acceleration. It should be the lowest value which with the adopted sea state, will not be exceeded at each relative heading angle. This estimation is made on the base of Fig. 4.

b/ Defined at point a/ the value of acceleration determines the admissible mass of the lashed container stack depending on its position/ IN or OUT/ and its configuration. Advantage is taken here of diagrams presented in Fig. 3.

c/ Having a ready plan of loading both containers and the whole ship, the current values of $\overline{MG}$ and the admissible transverse acceleration magnitudes are determined. These values as resultant may vary from the assumed ones at point a/ due to many reasons.
Defined in such a way they are the fundamental and obligatory information for the ship's command about the load condition.

2.4.2. Navigational procedures.

The navigational procedures are mainly connected with the selection and maintenance of such ship's velocity that the occuring transverse accelerations do not exceed the admissible ones defined by the information of the ship's load condition. The basic tools are here the diagrams as in Fig. 4. on the basis of which one can determine the range of the admissible relative angles. It would be extremely good if the ship's command had moreover a possibility of making a direct measurement or estimating the value of the real transverse accelerations. In such a situation the diagrams as in Fig. 4. could only be used as a base for choosing another heading angle, in case if for the current one the measured accelerations exceeded the permissible level. However, if there is not an appropriate apparatus at the ship's disposal for measuring accelerations it is always possible at least to estimate the transverse accelerations by measuring the angle of roll motions. It would be indispensable in this case a graphic information with regard to relation $a_t = f(\phi_A, \overline{MG})$, which would perfectly be complementary to the lashing system. In this way its usability will be the more profitable, the more accurate calculation model is applied. Thus this relation may have been prepared by the shipyard in the some way, as for example, diagrams in Fig. 4.

The document entitled "Lashing system ..." of the outlined here structure enables to include the ship's operation in the broad meaning of the word into the rational activities for the benefit of the safety of the load itself and the whole ship. The nature of the short-term prediction, which characterizes the information it contains makes it possible to increase the economical effectiveness of the ship and the whole shipping line. One can "adapt" the mass of the transported cargo to the weather conditions at least by differentiating the seasons of the year, e.g. for North Atlantic - summer and winter, on the base of rational - measurable premises. The stimulated approach by the current regulations does not provide such a possibility. Therefore one can say that it eliminates the whole sphere of the ship's operation from the activities not only connected with a tendency to cargo shipping maximization, but it does not enable to undertake rational operations to secure the cargo safety either. The ship's command not knowing explicitly the values of accelerations for which the admissible masses have been, according to the present requirements, determined, it can be suggested that lashing is absolutely safe. Fortunately, the practice of the ship's operation is such, that there are almost always undertaken activities aimed at minimization of the external loadings, but the master is doomed to its own experience in view of the lack od some rational information.

3. CONCLUSION

The presented in chapter 2 concept of the lashing system of containers transported on the weather decks by ships is, as has been indicated in the introduction, both an example and an authentic solution of a problem of optimum reconciliation of economics and the cargo ships safety. For-